UNIVERSITÀ DEGLI STUDI DI MILANO

DIPARTIMENTO DI CHIMICA

PhD COURSE IN CHEMISTRY, XXX CYCLE

Synthesis of integrin-targeting pro-drugs for the selective release of anti-tumor agents

CHIM/06 Organic Chemistry

Paula López Rivas

R11168

Tutor: Prof. Dr. Cesare GENNARI (University of Milan)

Co-Tutor UNIMI: Dr. Luca PIGNATARO (University of Milan)

Co-Tutor MAGICBULLET: Prof. Dr. Gábor Mező (Eötvös Loránd University, Budapest)

PhD course co-ordinator: Prof. Dr. Emanuela LICANDRO

A.Y. 2017/2018

A meus pais,
sen eles nunca tería chegado ata aquí.

A mis padres,
sin ellos nunca hubiera llegado hasta aquí.

To my parents,
without them I would have never arrived here.

Table of contents

Abbreviations

ADC	Antibody-Drug Conjugate
Akt	Protein kinase B (PKB)
Aoa	2-(aminooxy)acetic acid
ATP	Adenosine triphosphate
CAIX	Carbonic anhydrase IX
CPP	Cell penetrating peptides
CPT	Camptothecin
Dau	Daunorubicin
DBU	1,8-Diazabicyclo[5.4.0]undec-7-ene
DIC	*N,N'*-diisopropylcarbodiimide
DKP	Diketopiperazine
DMAP	4-dimethylaminopyridine
DMF	*N,N*-dimethylformamide
Doxo	Doxorubicin
DUPA	2-[3-(1,3-dicarboxypropyl)ureido]pentanedioic acid
ECM	Extracellular matrix
EDC	1-Ethyl-3-(3-dimethylaminopropyl)carbodiimide
EEDQ	*N*-Ethoxycarbonyl-2-ethoxy-1,2-dihydroquinoline.
EPR	Enhanced Permeability and Retention
FACS	Fluorescence-activated cell sorting
FAK	Focal adhesion kinase
FITC	Fluorescein-5-isothiocyanate
FR	Folate receptor
GnRH	Gonadortropin-releasing hormone
GnRHR	Gonadortropin-releasing hormone receptor
HATU	O-(7-azabenzotriazol-1-yl)-tetramethyl-uronium hexafluorophosphate
HOAt	1-Hydroxy-7-azabenzotriazole
HPLC	High-performance liquid chromatography
*iso*DGR	*iso*Asp-Gly-Arg
mAb	Monoclonal antibody
MED	Minimum Effective Dose
MMAE	Monomethyl auristatin E
MMF	Monomethyl auristatin F
MMP	Matrix metalloproteinase
MTD	Maximum Tolerated Dose
NHS	*N*-hydroxysuccinimide
NMR	Nuclear magnetic resonance
NP	Nanoparticle

PABC	*p*-aminobenzylcarbamate
PEG	Polyethylene glycol
PBS	Phosphate-buffered saline
PSMA	Prostate specific membrane antigen
PTX	Paclitaxel
RCC	Renal cell carcinoma
RGD	Arg-Gly-Asp
RP	Relative potency
r.t.	Room temperature
SAR	Structure-activity relationship
SMDC	Small Molecule-Drug Conjugate
SPPS	Solid phase peptide synthesis
SSTR	Somatostatin receptor
TI	Targeting index
TIS	Triisopropylsilane
TFA	Trifluoroacetic acid
t_R	Retention time

Amino acid*	One-letter code	Three-letter code
Alanine	A	Ala
Arginine	R	Arg
Asparagine	N	Asn
Aspartic	D	Asp
Cysteine	C	Cys
Glutamine	Q	Gln
Glutamic acid	E	Glu
Glycine	G	Gly
Histidine	H	His
Isoleucine	I	Ile
Leucine	L	Leu
Lysine	K	Lys
Methionine	M	Met
Phenylalanine	F	Phe
Proline	P	Pro
Serine	S	Ser
Threonine	T	Thr
Tryptophan	W	Trp
Tyrosine	Y	Tyr
Valine	V	Val

* D-amino acids are described by D-Xaa in the three-letter code and with the small letter in the one-letter code.

General introduction

In the last decades, anticancer therapy has raised as one of the most studied topics on pharmaceutical and medicinal science. However, despite the efforts made on this field, it is widely known that the main limitation of traditional chemotherapeutics is the lack of selectivity of the cytotoxic agents. Anticancer drugs act by interfering with different cell growth and replication mechanisms but, unfortunately, this occurs non-exclusively in tumor cells, but also on the healthy cells.

To overcome this limitation, different drug-delivery technologies have been developed so far, including nanoparticles, liposomes, Antibody-Drug Conjugates (ADCs), etc. Among them, the so called Small Molecule-Drug Conjugates (SMDCs) are based on the covalent conjugation of cytotoxic agents to different ligands (able to bind to a protein or other receptors overexpressed on tumor cells), by means of a variety of linkers.

This PhD thesis describes the synthesis, characterization and biological evaluation of several new SMDCs targeting the $\alpha_V\beta_3$ integrin receptor, a transmembrane receptor that recognizes the Arg-Gly-Asp (RGD) tripeptide sequence and it is overexpressed in many human cancers (such as breast cancer, glioblastoma, pancreatic tumor and prostate carcinoma). The conjugates described in this work are based on three fundamental parts (i.e., ligand, linker and cytotoxic payload), which have been manipulated in order to improve the potency and *in vitro* selectivity of the resulting construct towards $\alpha_V\beta_3$–expressing cancer cells)

The present work is structured as follows: Chapter 1 describes the traditional and most recent targeting technologies for drug delivery and introduces the targeted integrin receptor. Chapter 2 shows the synthesis and biological evaluation of the conjugates containing peptide linkers prone to cleavage in intracellular vesicles, such as the lysosomes. The second part of this Chapter ("Synthesis and biological evaluation of *cyclo*[DKP-RGD]-α-amanitin conjugates") was carried out in collaboration with the German company Heidelberg Pharma (HDP), within the frame of the Marie Sklodowska–Curie Innovative Training Network (ITN-ETN) "Peptide Drug Conjugates for Targeted Delivery in Tumor Therapy" (MAGICBULLET). In view of the *in vitro* results obtained with these first set of compounds, the research moved towards the study of peptide linkers susceptible to proteolysis in the extracellular environment, which was carried out in Eötvös Loránd University (ELTE) of Budapest (Hungary), under the supervision of Prof. Gábor Mező between October 2016 - March 2017 and is discussed in Chapter 3. As last,

Chapter 4 describes two new conjugates that may be activated both in intracellular compartments and in extracellular milieu, by means of ubiquitous tumor-associated enzymes. This part of the thesis was carried out in Heidelberg Pharma (Germany) under the supervision of Dr. Müller, between January and March 2018.

Chapter 1: Tumor targeting prodrugs

1.1. Introduction

Chemotherapy still represents the predominant strategy for cancer treatment, either alone or in combination with surgery and/or radiotherapy.[1] Most of traditional anticancer drugs are able to prominently kill fast-dividing cancer cells, and to induce apoptosis, either by targeting important proteins involved on the division of cells or by interacting with the DNA replication and transcription machinery.[2] A historical family of cytotoxic agents (used since as early as 1940s) are nitrogen mustards (including cyclophosphamide and chlorambucil), which provoke cell death by alkylation of DNA bases. During the same period, S. Farber and coworkers discovered that folic acid prompted the proliferation of some leukemia cells and, in collaboration with Y. Subbarao, they developed methotrexate (an antifolate agent), capable of blocking folic acid receptors and thus avoiding the formation of abnormal bone marrow. Later on, with the advances on the elucidation of DNA structure, thioguanine, 5-fluorouracil and cytosine arabinoside (ara-C) emerged as anticancer drugs, which compete with natural nucleosides, interfering with DNA synthesis. These compounds, together with methotrexate, represent early examples of "rational drug design", being developed considering the target, as opposed to serendipitous discovery.[3] Another example of DNA-interacting compound is cisplatin, which is known to crosslink the purine bases of DNA and interfere with the repair mechanisms.[4] Furthermore, there are some antitumor agents inhibiting either topoisomerase I and II, which are enzymes involved in different arrangements of DNA structure. Some examples are camptothecin (inhibitor of topoisomerase I) and anthracyclines (doxorubicin and daunorubicin) and etoposide for topoisomerase II.

Besides the development of drugs capable of interacting with folate receptors and the DNA machinery, another important target for cancer therapy is tubulin, a protein playing major role in different cellular processes, such as mitosis. For instance, the Vinca alkaloids family (among them, vincristine and vinblastine) bind to the monomeric tubulin and inteferes in the polymerization of the microtubules avoiding the formation of the mitotic spindle. Instead, taxanes (such as paclitaxel and docetaxel) produce the microtubule stabilization preventing the depolymerization.[5]

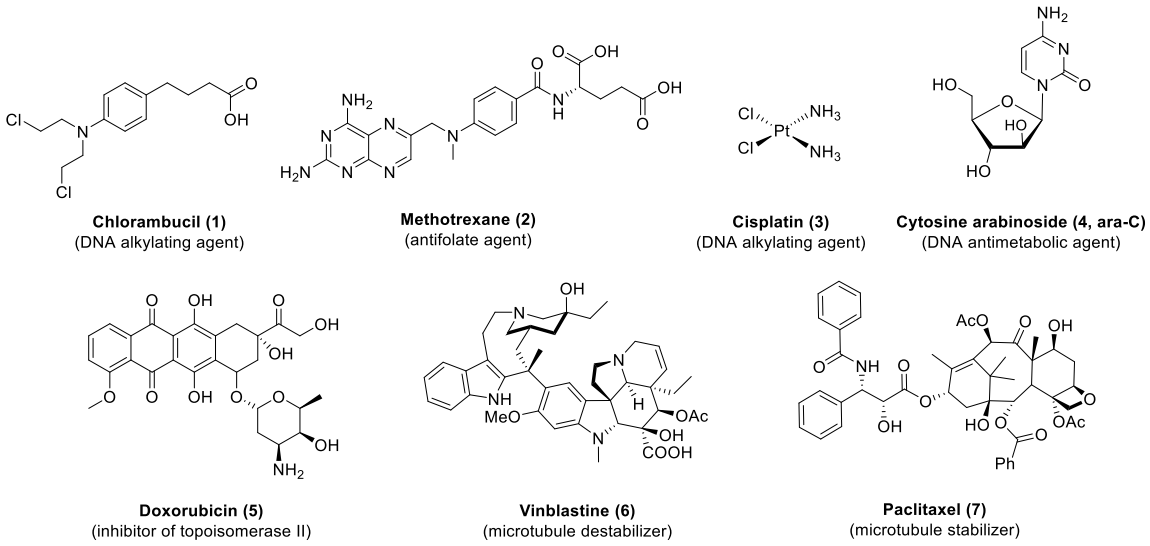

Figure 1. Molecular structures and mechanism of action of some antitumor agents.

Despite the variety of anticancer drugs that have been developed, these pharmaceutical products are characterized by a small therapeutic window, which means that the dose required to display therapeutic benefits (i.e., Minimum Effective Dose, MED), is not significantly lower than doses associated to side-effects (i.e. Maximum Tolerable Dose, MTD).

In order to improve the clinical effect of cancer therapy, multidrug treatment was introduced combining cytotoxic agents with different mechanisms of action and different toxicity profiles. However, a high systemic toxicity was observed with this approach, making clear the necessity of finding more potent anticancer compounds that decrease the Minimum Effective Dose (MED). For this reason, researchers have focused on the discovery of new natural products, since plants and other living organisms have been usually the main source of antitumor agents. This led to the discovery of new inhibitors of tubulin polymerization, with cell antiproliferative activity in the picomolar range. Maytansine, the dolastatins family (among them dolastatin 10 and 15) and cryptophycins form part of these newly discovered compounds. However, the increase of potency of the cytotoxic agents did not lead to better clinical performances, and the clinical evaluations of these new class of ultrapotent cytotoxic agents had to be discontinued at early stages.[2a] A successful exception is eribulin mesylate (an analogue of halichondrin) that shows easier to handle side effects and has been approved by the U.S. Food and Drug Administration in 2010, for the treatment of metastatic breast cancer refractory to anthracyclines and taxanes.[6]

Alternatively to traditional cytotoxic agents, inhibitors of tyrosine kinase enzymes have also found widespread applications in oncology. It has been demonstrated that the activity of a variety of tyrosine kinases is upregulated in tumor cells, causing altered phosphorylation cascades and abnormal activation of target proteins. Furthermore, the overexpression of tyrosine kinases in cancer cells or the presence of aberrant forms of these enzymes prompts the tumor cell growth. For these reasons, various inhibitors aiming to compete with ATP for binding to the catalytic site of protein kinases have been developed. Among this class of compounds, Imanitib mesylate has been approved by the FDA in 2001 for the treatment of chronic myelogenous leukemia (CML). Furthermore, Sunitinib has been approved for the treatment of metastatic renal cell carcinoma (RCC) and gastrointestinal stromal tumour (GIST)[7] and Sorafenib for hepatocellular carcinoma and for clear-cell renal-cell carcinoma (CCRCC).[8]

Although tyrosine kinase inhibitors have often grouped as “targeted” therapeutics, they show the same pharmacokinetic limitations as traditional chemotherapeutics. In particular, these small molecules do not accumulate efficiently in the mass of solid tumors, which are normally characterized by a high interstitial fluid pressure. Moreover, due to their low molecular weight and the high lipophilicity, these compounds are cleared rapidly from systemic circulation and they accumulate preferentially into healthy organs (mainly liver and kidneys) and excreted.

Overall, the limitations of cytotoxic agents emerged and these findings strongly suggested the necessity to develop more effective drugs, which could target cancer cells selectively and overcome the side-toxicity issues.

1.2. Targeted Cytotoxic Agents

The improvement of the selectivity of anticancer drugs (which leads to the increase of the Maximum Tolerated Dose, MTD) without affecting the potency of these agents (i.e. same Minimum Effective Dose, MED) could ideally lead to the increase of the therapeutic window and the decrease of the undesired side effects generally observed in cancer patients (Figure 2).[2a]

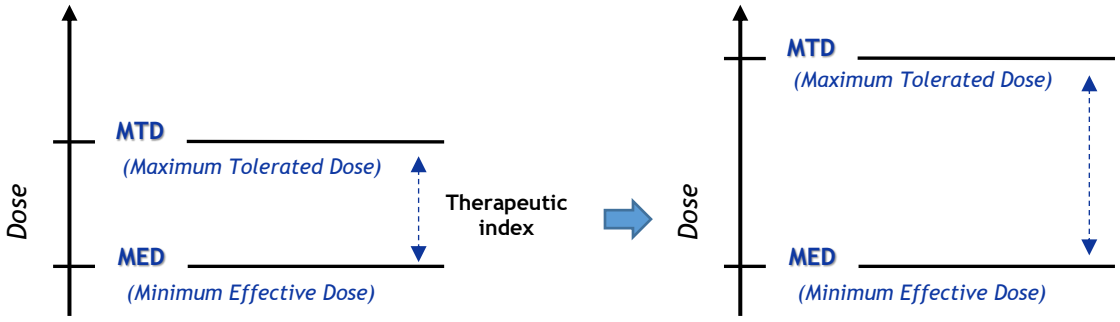

Figure 2. Increase of the Therapeutic index when the MTD is improved (due to the improvement of the selectivity).

Following this unmet medical need, many drug delivery systems have been developed for the selective release of antitumor drugs: antibodies, liposomes, polymers, micelles, iron oxide, gold or dendrimer nanoparticles (NPs), carbon nanotubes, etc.[9] All these drug delivery systems are based on one of the following targeting approaches:

- *Passive targeting*: it is based on the Enhanced Permeability and Retention (EPR) effect. Tumors are often characterized by leaky, tortuous and poorly differentiated vasculature that allows the extravasation of molecules with larger sizes (up to hundreds of nanometers). At the same time, the lymphatic system is normally affected in the tumor mass, decreasing the clearance of extravasated nanomaterials from the diseased site. Nanoparticles such as liposomes, polymers and micelles rely on this type of targeting approach.

- *Triggered drug delivery*: these systems are able to release their drug content upon exposure to different external stimuli (such as light, heat, ultrasound and magnetic field).

- *Active targeting to cancer cells:* this strategy relies on the binding of ligands to specific proteins (i.e. receptors or antigens) that are expressed in larger amounts by cancer cells, compared to normal tissues The so-called antibody-drug conjugates (ADCs) and small molecule-drug conjugates (SMDCs) belong to this class of therapeutic agents, and they will be described in more details in the following chapters.

- *Active targeting to endothelial cells:* delivery systems based on interacting with the endothelial cells (blood vessels cells) have been developed and they kill by depriving the tumor mass from oxygen and nutrients.

The development of targeted chemotherapies has been a field of increasingly interest during the last years and many efforts have been made to produce delivery systems able to improve the clinical efficacy of cancer treatment. Nowadays some of these technologies have reached the market, while many others are being investigated.

1.3. Antibody-Drug Conjugates (ADCs)

1.3.1. Monoclonal antibodies

Monoclonal antibodies (mAbs) can be considered as the most exploited biopharmaceutical tools for the treatment of cancer and many other indications. High-affinity mAbs selective for any kind of antigen can be now generated and, in the oncology field, they are normally exploited to target antigens that are present in cancer cells in mutated forms or that are overexpressed on tumor cells (in comparison with healthy tissues).[2a,10] The advent of monoclonal antibodies and their widespread application derives from the development of the hybridoma technology in 1975 by Köhler and Milstein, which allowed to produce single purified antibodies able to target a specific epitope of the antigen of interest.[11] In some cases, mAbs are pharmaceutically used to bind with high affinity proteins that may be fundamental for the disease progress, thus blocking their pathologic activity. Moreover, specific types of mAbs are able to induce cell death by different mechanisms, such as antibody-dependent cellular cytotoxicity (ADCC), antibody-dependent phagocytosis, receptor blockage which leads to apoptosis or interferes with other cell pathways, etc.

In 1980, the first human clinical trial with a murine monoclonal antibody was conducted in a patient with lymphoma using AB 89 antibody.[12] After this, many other murine mAbs were tested and, in many of these trials, an immune response to the antibody was observed, resulting in the detection of human anti-mouse antibodies (HAMA) in patients. In order to overcome the limitations of this first generation of monoclonal antibodies, chimeric and humanized mAbs were prepared by means of the recombinant DNA technology (see Figure 3). In both cases, the murine constant sequences are replaced by the human analogues. However, the chimeric mAbs retain the murine sequences in both the Variable domains (Fv) and the Complementary determining regions (CDR), while in the humanized mAbs the Fv are replaced with human sequences, maintaining the mouse CDR, which are the essential antigen recognition residues.

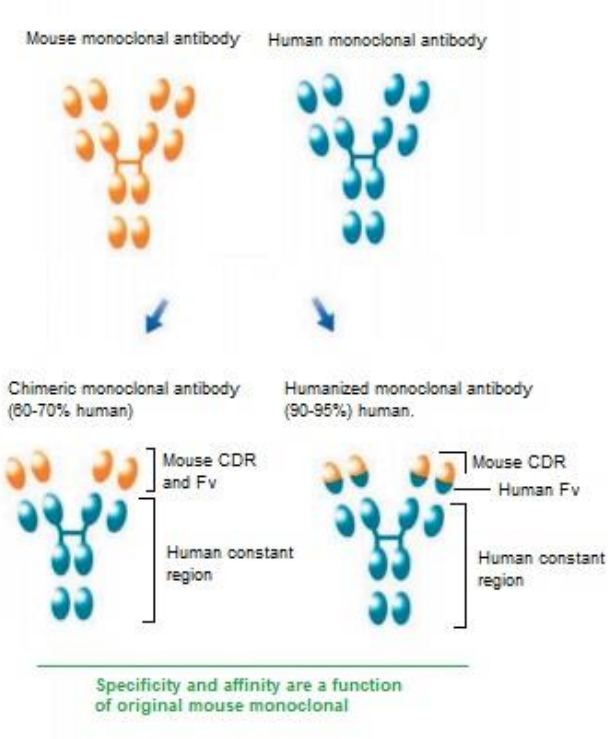

Figure 3. Representation of mouse, human, chimeric and humanized monoclonal antibodies; CDR= complementary determining regions; Fv= Variable domains.[13]

The increasing presence of human sequences in the mAb structure were found to significantly reduce or even eliminate the immune response observed with the murine mAbs, and to extend the half-life in circulation. Rituximab (Rituxan™) was the first mAb brought on the market in 1997 for the treatment of non-Hodgkin's lymphoma. After that, many others have gained marketing authorization, such as bevacizumab (Avastatin™) and trastuzumab (Herceptin™). Nowadays, mAbs have become the most studied

approach for the treatment of cancer and Rituxan™ and Avastatin™ are still the best-selling anticancer drug in the current year 2018.[14]

Unfortunately, most of these anticancer mAbs often fail to cure patients when used as single agents and they are often combined with chemotherapeutic drugs. However, given the outstanding binding specificity of monoclonal antibodies and the lack of selectivity of the antitumor medicines, mAbs started to be considered as possible vehicles for selective tumor-targeted release of anticancer drugs.[15]

1.3.2. Antibody-Drug Conjugates (ADCs)

ADCs are based on the conjugation of a monoclonal antibody with a cytotoxic agent through a smart linker, which should be ideally stable in circulation (to avoid systemic toxicity) and, at the same time, it should release the drug selectively at the tumor site. According to an ideal mechanism of action, the Antibody-Drug conjugate, upon binding to cell antigen, is internalized by a receptor-mediated endocytosis and, once inside the cell, the linker is cleaved through different mode of action, releasing the cytotoxic payload. Following this mechanism, first-generation ADC products relied on intracellular cleavable linkers, such as acid-labile linkers (which release the drug at the tumor acidic pH) or specific peptide sequences (which are preferentially cleaved by lysosomal enzymes, such as peptidases or esterases).[2a] However, in the last years, it has become clear that non-internalizing ADCs relying on extracellular drug release mechanisms could also be an efficient pharmacological approach.[15]

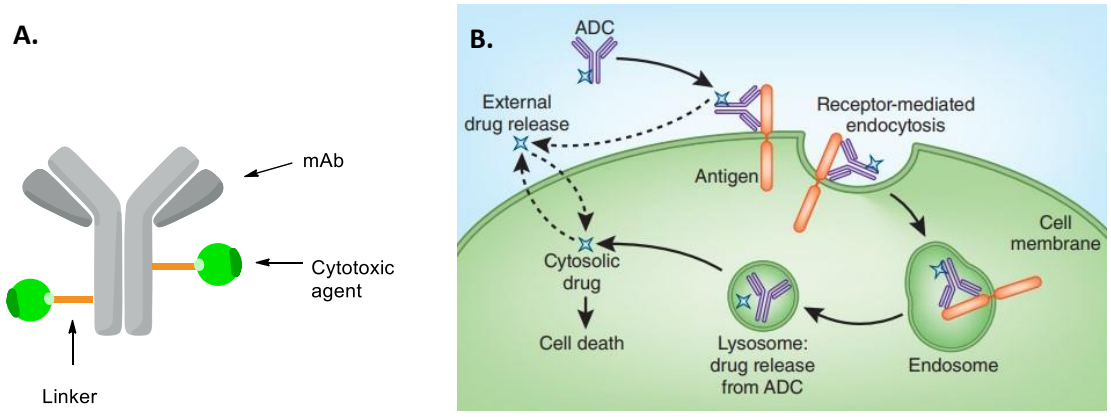

Figure 4. A) General structure of an Antibody-Drug Conjugate. B) Different mechanisms of ADC drug delivery: external drug release and receptor-mediated endocytosis.[16]

With this strategy, ADCs would release their anticancer payload in the tumor interstitium (through, for instance extracellular proteins, such as matrix metalloproteinases) and then the free drug would be free to diffuse through the tumor mass, and enter cancer cells by passive diffusion through the cell membrane. (Figure 4B).[15] The choice of the correct payload was found to be crucial since the birth of the ADC technology. First-generation ADCs were equipped with traditional chemotherapeutic drugs, such as methotrexate, doxorubicin or vinblastine. From the *in vitro* evaluation of most part of these conjugates emerged that the drug release from the targeting vehicle was not efficient, and the ADCs proved less potent than the free drug. Also, despite the significant ADC accumulation at the tumor site, the low therapeutic activity *in vitro* of these products suggested that different drug and linker modules should be considered.

The second generation of ADCs focused on the use of more potent anticancer drugs such as calicheamicins, maytansinoids (emtansine, mertansine), auristatins (monomethyl auristatin E – MMAE - and monomethyl auristatin F - MMAF) or SN38 (a derivative of camptothecin). These modifications led to the market authorization of the first ADC products. In particular, Mylotarg™ (gemtuzumab-ozogamycin) targeting CD33 (receptor expressed of myeloid cells) reached the market in 2000. While initial toxicity issues led to the ADC withdrawal in 2010, this product was reintroduced in 2017 after revising the dosage. This product is currently being used for the treatment of acute myeloid leukemia (AML).[10] Later on, Adcetris™ (brentuximab vedotin, approved in 2011 for the treatment of Hodgkin lymphoma and anaplasic large cell lymphoma), Kadcyla™ (ado-trastuzumab emtansine, approved in 2013 for the treatment of metastatic breast cancer expressing receptor HER2) also found FDA approval, together with the recently introduced Besponsa™ (inotuzumab ozogamicin, approved in 2017 for the treatment of CD22-positive acute lymphoblastic leukemia).[17]

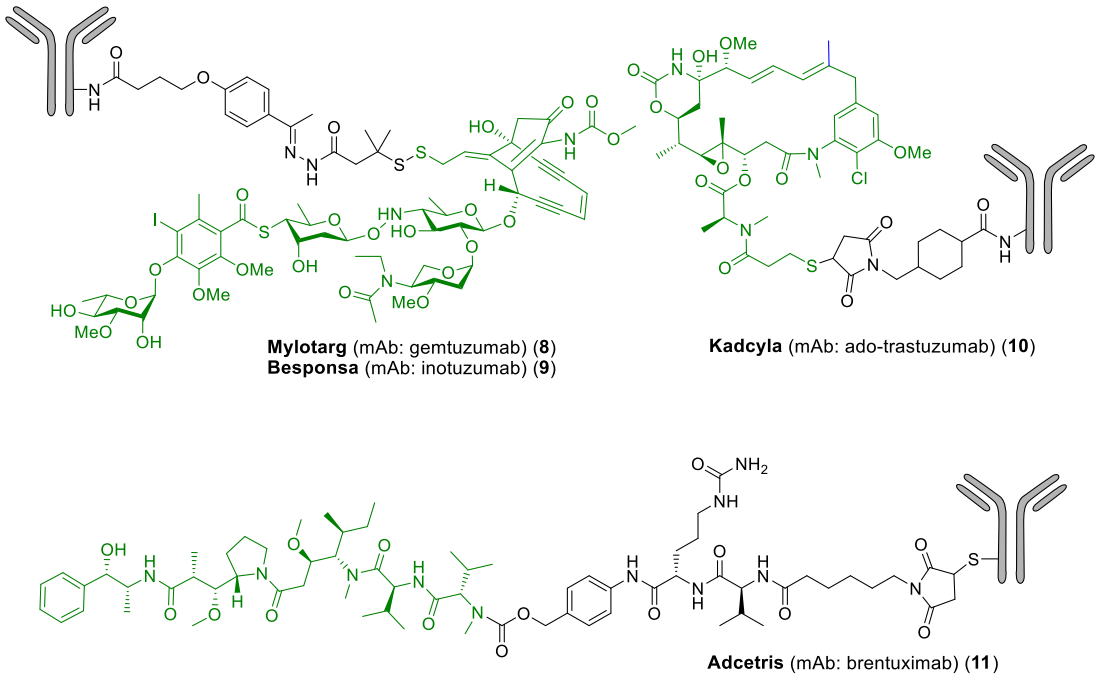

Figure 5. Structures of the ADCs available in the market.

Considering the high antigen affinity and the exquisite selectivity displayed by antibodies, ADCs represent the most promising platform for the targeted delivery of cytotoxic agents. However, it became increasingly clear that the success of ADC product may be limited by a number of factors: [2a,18]

- *Suboptimal Pharmacokinetic*: the slow extravasation of large-size macromolecules (such as antibodies) has been extensively described, and it limits the ADC accumulation in the tumor mass. Furthermore, upon extravasation, antibodies are often trapped by antigens situated on the perivascular tumor cells, preventing the binding to tumor cells that may not be adjacent to the blood vessels.

- *Possible immune system induce alterations:* the development of undesired immunogenicity caused by ADCs (even those bearing chimeric or humanized antibodies) may limit the efficiency of the ADC treatment.[19]

- *High manufacturing costs:* the production of large-scale ADCs is an expensive process, requiring the clinical-grade production of three components (i.e. mAb, toxin and final conjugate) as single entities.

Nowadays, many efforts are being made to improve the therapeutic performances of ADCs. The current approaches are based on the development of new antibody structures,such as miniantibodies, small immune proteins –SIP-, single-chain variable fragment –scFv-, etc.[2a,20]

1.4. Small Molecule-Drug Conjugates (SMDCs)

1.4.1. General structure and background

An alternative to overcome some of the limitations associated with ADCs is the use of smaller devices to target tumors, which could also bind to tumor-associated antigens, while exhibiting a better pharmacokinetic profile. These new class of compounds consists in the so called Small Molecule-Drug Conjugates (SMDCs) and they should ideally display better pharmacokinetic properties than ADCs (e.g., easier extravasation and deeper penetration of the tumor tissue, and little or no antigenicity) as well as reduced manufacturing costs.

The general structure of SMDCs (Figure 6) is reminiscent of ADCs and it is based on a small targeting moiety (such as a small ligand, a peptide or a peptidomimetic) linked to a cytotoxic agent via a smart linker, able to selectively release the cargo in the tumor mass. Similarly to ADCs, the choice of the correct combination of ligand-linker and drug is an important issue for the design of successful SMDCs, and they will be further discussed in the following sections (sections 1.4.2, 1.4.3 and 1.4.4).

Figure 6. General structure of the SMDCs.[21]

In addition to the Ligand, Linker and Drug moieties, SMDCs (but also ADCs) are normally equipped with spacers between the Ligand and the Linker, or between the Linker and the Drug portions. These moieties feature suitable functional groups for the chemical conjugation of each individual fragment of the drug delivery system. Furthermore, a

chemical structure between Ligand and Linker (i.e., *Spacer 1* in Figure 6) is often added to improve the pharmacokinetic properties of the conjugate. For example, polyethylene glycol (PEG) chains or short peptide sequences bearing hydrophilic residues are often included to improve water solubility.[22] Also, PEG spacers increase the size of the prodrug (which may impact on the circulation half-life) and provide a better flexibility, with a potential effect on the binding affinity.[23] Another type of spacer (i.e. *Spacer 2* in Figure 6) is included between the Linker and the cytotoxic agent to improve the kinetics of drug release. These linkers are often referred to as "self-immolative" and, upon cleavage of the linker, they undergo a series of elimination and/or cyclization processes that lead to the delivery of the free drug (Scheme 1).[24] The self-immolation process of electronic cascade spacers is known to proceed more quickly than the cyclization spacers.

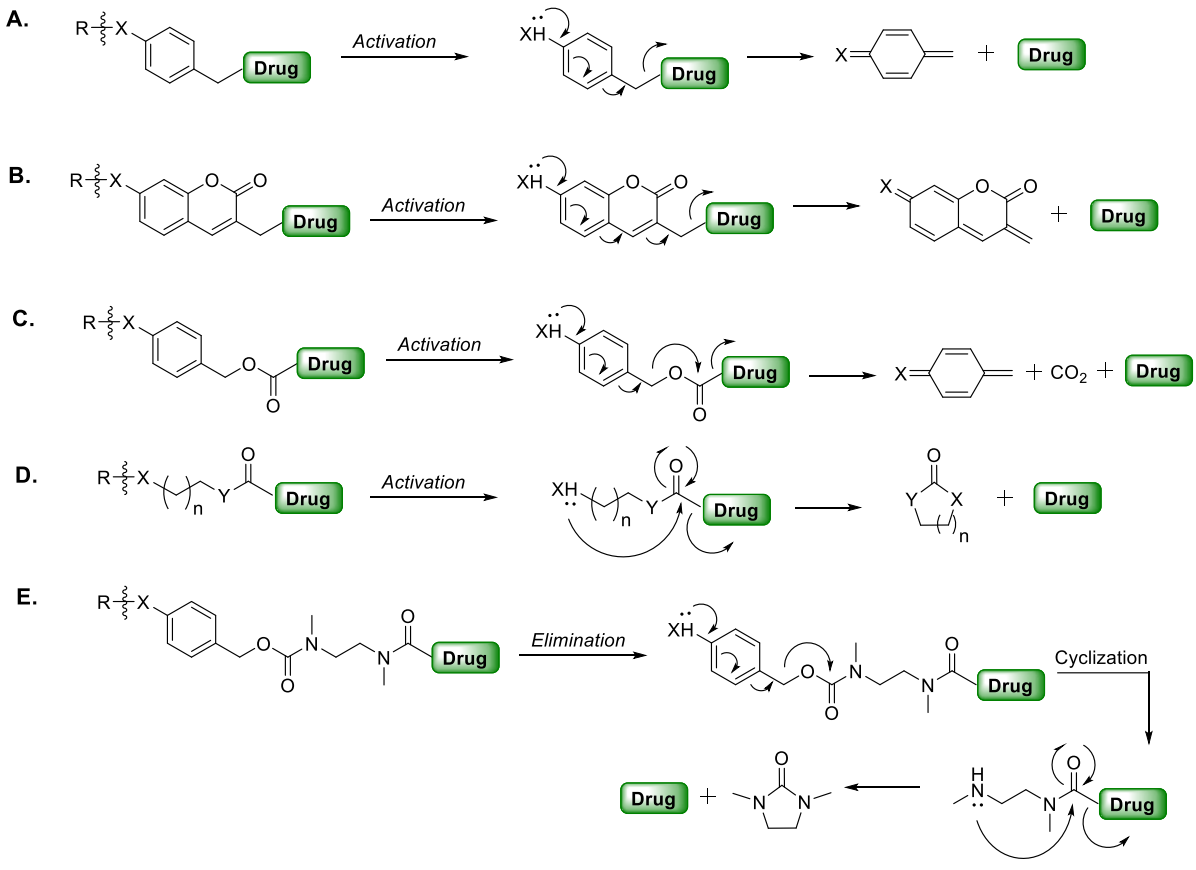

Scheme 1. Some of the most common self-immolative linkers.

1.4.2. The selection of the ligand

While up-to-date biotechnological methods allow the fast isolation of high-affinity antibodies against any type of protein antigen, the development of small organic molecules as ligands for a given tumor antigen is more problematic. The most used ligands are the natural-occurring ones, such as vitamins or hormones, whose receptors are often up-regulated by fast-growing tumors. However, it is conceivable that new technologies for hit identification (e.g. high-throughput screening, phage display and DNA-encoded chemical libraries) will be increasingly exploited to raise new ligands for SMDC applications.[18,25] As far as the receptor is concerned, it is possible to claim that some tumor antigens may represent more promising receptors for SMDCs than other proteins, and some important biological features (e.g. levels of expression, rate and pathway of internalization, tissue and cellular localization, etc.) must be taken into account during the SMDC design.

The most common examples of "druggable" antigen that have been investigated for SMDC development are the Folate Receptor (FR), the Hormone receptors (somatostatin and gonadotropin receptors), the prostate specific membrane antigen (PSMA) and the carbonic anhydrase IX (CAIX) enzyme.

Folic acid is a vitamin associated to different metabolic pathways (such as nucleotide biosynthesis), showing a high affinity for its receptor and that can be easily coupled to cytotoxic drugs. FR (an endocytic glycopolypeptide membrane protein) is upregulated in cancer cells and activated macrophages, but it has a limited distribution on normal cells. Indeed, this receptor is overexpressed in ovary, breast, lung, colon, kidney and brain tumors and on the hematopoietic cells of myelogenous origin.[15,26] Folic acid is considered the first small molecule to be used as ligand in SMDCs and the research in the field of folate-drug conjugates is a milestone in the development of tumor-targeting cytotoxic agents. The combination of this vitamin with the microtubule-interferring desacetylvinblastine hydrazide through a disulfide linker was the first folate-based SMDC to enter clinical investigation. This conjugate, known as Vintafolide or EC145 (Figure 7), showed some potential when administered in combination with other approved anticancer agents. Indeed, the combination of this folate-vinblastine conjugate with pegylated lysosomal doxorubicin (PDL) showed a 2 months extension of the progression-free survival in platinum-resistant ovarian cancer.[15,27]

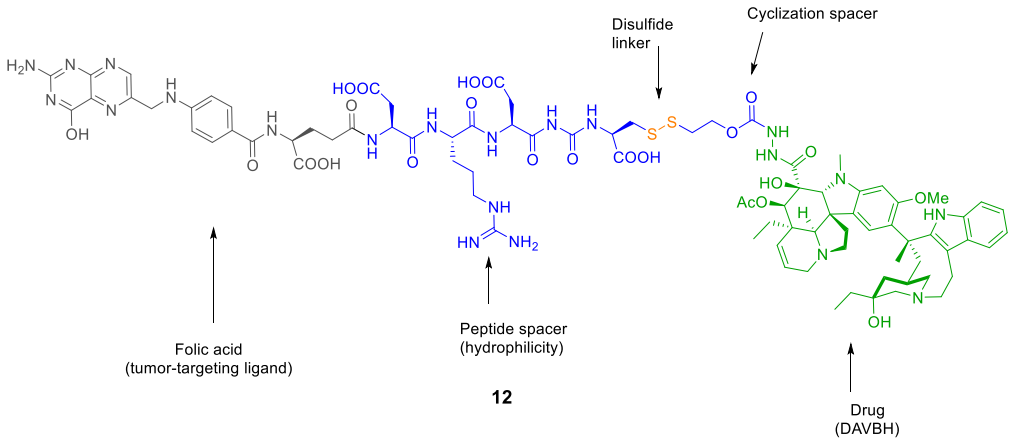

Figure 7. Structure of Vintafolide (**12**).

These first results prompted the development of other FR-targeted conjugates (with the folic acid combined to different cytotoxic agents such as paclitaxel, protein kinase inhibitors, tubulysin, etc.)[28] and also other vitamin-conjugates using biotin or vitamin B12 as ligands.[29]

Furthermore, Hormone Receptors have also been widely studied and, among them, the **Somatostatin (SSTRs) and Gonadotropin-releasing hormone (GnRHR) Receptors**. The first ones (especially subtypes 2, 3 and 5) are widely expressed in cancer cells, in particular neuroendocrine tumors[30] and SSTR-2 also in Renal cell carcinoma (RCC) and the corresponding metastases in thyroid, adrenal, and pancreatic glands.[31] Instead, GnRH receptors are known to be expressed on urogenital tumors, such as bladder, prostate, ovary and endometrium cancers, but also in breast and pancreatic tumors and glioblastomas.[32] Both somatostatin analogues and GnRH-targeting peptides have been conjugated to different cytotoxic agents such as paclitaxel[33] or camptothecin.[34] In the case of GnRHR binding peptides, they have also been coupled to daunorubicin[35] and doxorubicin. Indeed, it is worth to mention one of the examples involving this last cytotoxic agent, since this [D-Lys^6]GnRH analogue-doxorubicin (known as Zoptarelin Doxorubicin, AEZS-108 or AN-152) has shown low toxicity and good effectivity in phase II trials in women with GnRH receptor-positive endometrial cancer and with platinum refractory or resistant ovarian cancers. Currently, phase III clinical trials are being performed on patients with ovarian and endometrial cancer.[36] Furthermore, somatostatin has been used in nuclear medicine for diagnosis purposes. Analogues of this hormone have been conjugated to contrast agents, such as the chelator DOTA[37] or radiolabeled with ^{111}In.[38] This latter, in conjugation with octreotide ([^{111}In-diethylene-

triaminepentaacetic acid[0]]octreotide) is now available on the market for imaging of somatostatin receptor-positive tumors.

As mentioned previously, enzymes are also usual targets for the treatment of tumors. **Prostate-specific membrane antigen (PSMA)** is a well-known marker for prostate cancer, in which it is highly overexpressed, while it is not detectable in other tissues such as kidneys, small intestine or salivary gland. PSMA is a transmembrane glycoprotein that possess important functions in the prostate carcinogenesis and progression. It also displays folate hydrolase activity at the small intestine and *N*-acetylaspartylglutamate peptidase activity in the nervous system.[39] A variety of analogues of *N*-acetylaspartylglutamate have been prepared[40] and the ligand 2-[3-(1,3-dicarboxypropyl)ureido]pentanedioic acid (DUPA) is the most well-known PSMA ligand, due to its high binding affinity, synthetic accessibility and the presence of a free carboxylic acid which does not interfere with the binding event and it is therefore a suitable anchoring point for derivatization with different payloads. [41] Indeed, DUPA was conjugated to different imaging agents such as ^{99m}Tc, FITC (fluorescein isothiocyanate) and Rhodamine B isothiocyanate (Figure 8). The DUPA-^{99m}Tc was tested *in vivo*, in preclinical models, where the conjugate was found to target tumor cells selectively, albeit with a significant accumulation in the kidneys (due to the high expression of PSMA in murine kidneys).[41a] Interestingly, DUPA conjugates with Rhodamine B isothiocyanate were proved to bind selectively malignant cells in fresh peripherial blood samples from patients with prostate carcinoma, while no fluorescence was detected in the blood of healthy patients.[41a] This good results suggest that this imaging-conjugates could be applied for the detection and localization of tumors during surgery.

Due to the great selectivity showed by DUPA, also many cytotoxic agents were conjugated to this ligands, like tubulysin hydrazide (TubH),[41a] paclitaxel[42] or indenoisoquindoline (a topoisomerase I inhibitor).[43] In all cases, a cessation of the tumor growth in xenografted mice was observed, with no obvious toxicity and/or loss of body weight.

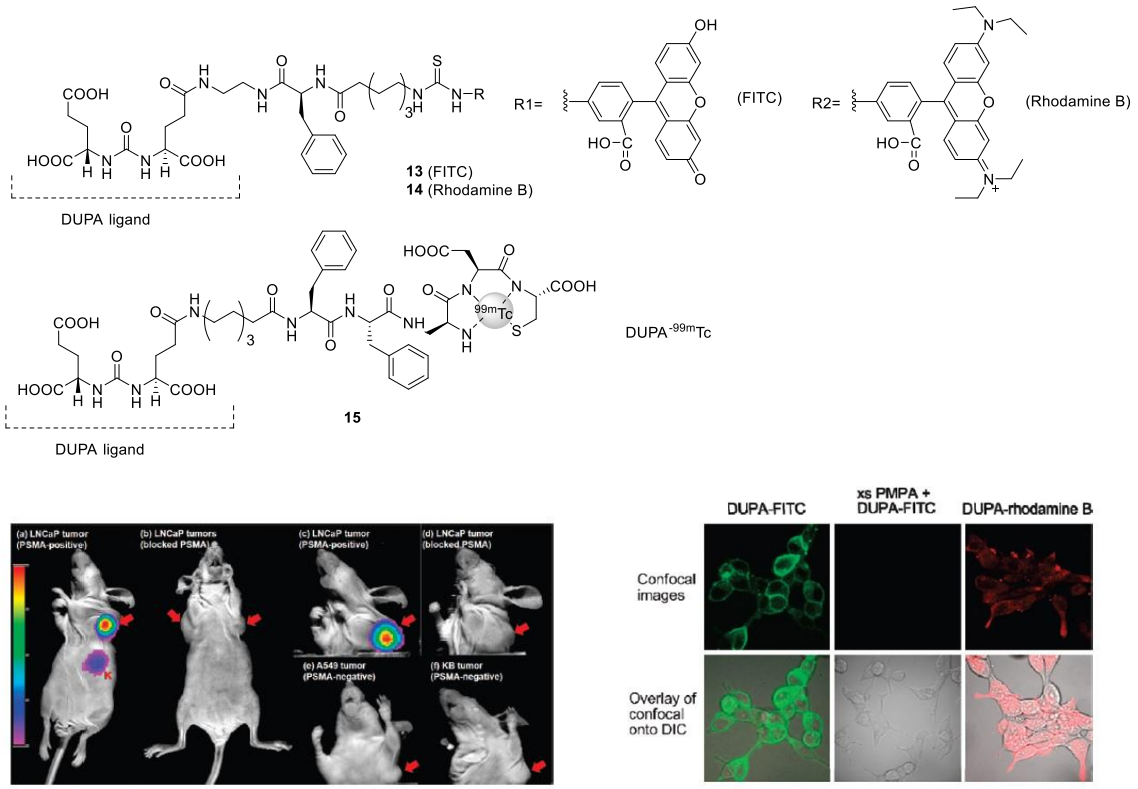

Figure 8. *Up*: Structure of DUPA conjugates containing different imaging agents (**13**, **14** and **15**). *Left image*: body radioimages of mice bearing LNCaP, A549 (PSMA negative) and KB (PSMA negative) tumors after 4h after administration of DUPA-^{99m}Tc conjugates. (K= kidney; red arrows= tumors).[41a] *Right ima*ge: confocal images and confocal differential interference contrast (DIC) images of DUPA-fluorescent conjugates (with FITC and rhodamine B) in LNCaP (prostate adenocarcinoma cells, PSMA positive) in the presence and absence of PMPA (PSMA inhibitor)

Besides PSMA, another enzyme investigated for SMDC applications is the **carbonic anhydrase IX (CAIX).** Human carbonic anhydrases are zinc-containing enzymes that catalyzes the reversible hydration of CO_2 to hydrogen carbonate and H^+ ($CO_2 + H_2O \leftrightarrows HCO_3^- + H^+$). Among the known 15 isoforms of this enzyme, the CAIX (a transmembrane protein) has gained much interest due to its overexpression in many solid tumors (e.g. glioblastoma, colorectal, breast cancer), being considered as a tumor-associated antigen and a marker of hypoxia.[44] Highly selective inhibitors belonging to the sulfonamide, sulfamate, coumarin and sulfocoumarin classes were developed as CAIX ligands. The sulfonamide SLC-0111 (for the treatment of advanced tumors) and the monoclonal antibody RENCAREX® (for the treatment of renal carcinoma) have already reached clinical trials (Phase I and phase III respectively).[45] In 2014, Neri et al.[46] developed the first SMDCs targeting the CAIX enzyme reporting therapeutic effects in preclinical models of human cancer. The conjugation of a high-affinity acetazolamide derivative with the maytansinoid DM1 via disulfide linkers showed a strong reduction of tumor volume *in vivo* (compounds **16** and **17**, Figure 9). Later on, CAIX inhibitors have been conjugated to a large number of payloads, such as tubulysin and MMAE.[47]

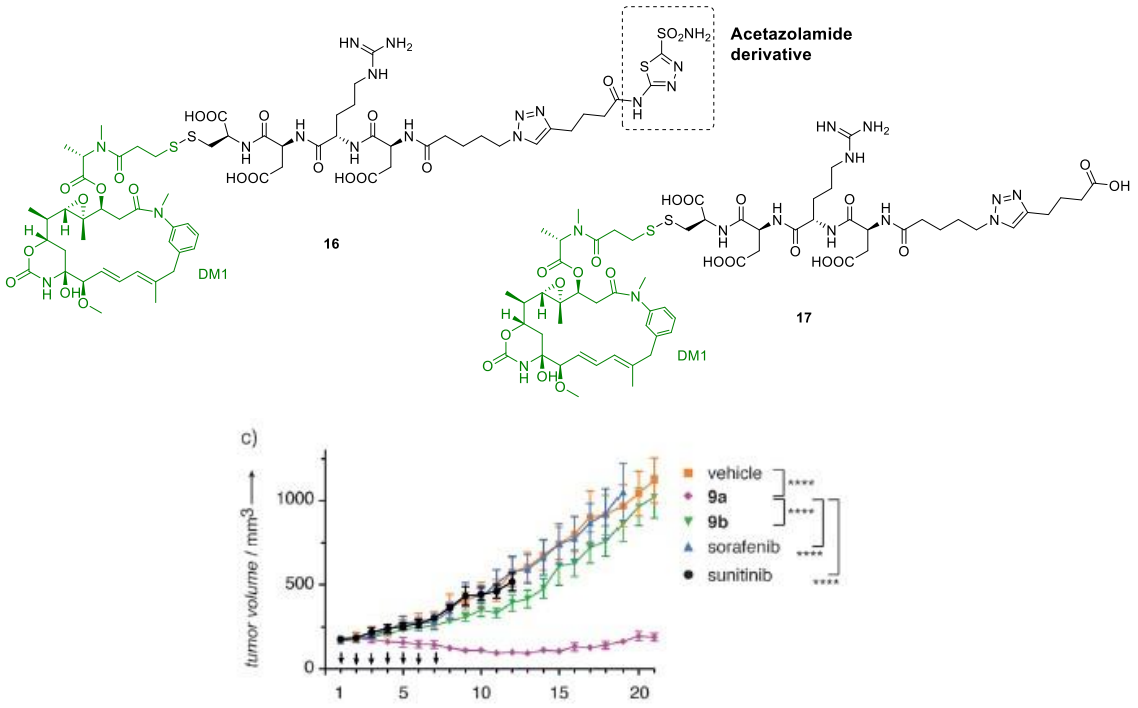

Figure 9. Tumor growth of in mice xenografted with SKRC52 (renal carcinoma). Treatment: 7 times on 7 consecutive days with 70 nmol of **16** (name 9a in the graphic), **17** (named 9b in the graphic), or vehicle (5% DMSO in PBS pH 7.4). Untargeted conjugate **17** was administered with equimolar amounts of acetazolamide.

1.4.3. The importance of the linker in the design of SMDCs

According to the physiological features of the targeted receptors, a variety of linkers have been used to promote drug release from SMDCs. They can be classified as follows:

- *Uncleavable linkers:* functional groups that are degradated neither in circulation nor at the tumor site (e.g. amides, triazoles, carbamates). These linkers are often used for imaging purposes by conjugation of the desired ligand with fluorescent probes or contrast agents.[37,38,48] Furthemore, uncleavable linkers have been often used in internalizing ADCs where they were proven to release efficiently the cytotoxic payloads. It is now widely accepted that, in these ADC products, the entire mAb structure is proteolytically degraded inside the targeted cell, eventually releasing the cytotoxic agent. On the other hand, no significant anticancer activities have been reported so far using non-cleavable SMDC products.

- *Hydrolytically labile linkers:* functional groups prone to hydrolysis, such as *N*-Mannich base-linker, esters or hydrazones. This class of functional groups has been used as linkers for drug release under the acidic conditions of lysosomes (pH 4.5 – 5.5), endosomes (pH 6.0 - 6.8) and in the extracellular environment of tumor masses.

- *Enzimatically-cleavable linkers:* these are short peptide sequences or carbohydrate moieties (like the β-glucuronide linker)[49] that are cleaved by proteases or glycoside hydrolases. Different sequences have been reported in the literature to target both intracellular and extracellular enzymes. For example, many dipeptide (Val-Cit, Phe-Lys, Val-Ala, etc)[50] and tetrapeptide squences (Gly-Phe-Leu-Gly)[51] have been used to target intracellular proteasese, such as Cathepsin B. Furthermore, the tripeptide sequence Ala-Ala-Asn has been used to target the lysosomally cleavable legumain enzyme (asparaginyl endopeptidase)[52] and longer sequences, such as as Gly-Pro-Leu-Gly-Ile-Ala-Gly-Gln[53] or Pro-Val-Gly-Leu-Ile-Gly[54] were used to target certain matrix metalloproteinase (MMP) isoforms, such as MMP2 and MMP9. Generally, these peptide sequences show high stability in circulation

- *Reducible linkers:* this group is formed by disulfides and metal complexes (that are cleaved as a result of the highly reducing environment of the intracellular compartment, which is due to the increased presence of antioxidants in cancer cells (like cysteine, reduced glutathione, peroxiredoxins, etc.).

1.4.4. The cytotoxic agent

Finally, since the therapeutic effect is given only by the biological activity of the cytotoxic payload, the drug impacts substantially on the activity and toxicity profile of the resulting SMDC. Moreover, it has been often reported that highly lipophilic payloads (e.g. MMAE, taxanes, maytansinoids, etc.) can elicit therapeutic effects also when incorporated in non- or poorly internalizing ADCs and SMDCs, as a result of the so-called “bystander effect”. This means that these devices are able to kill not only the antigen-positive tumor cells, but also the adjacent antigen-negative cancer cells.[55] On the other hand, highly hydrophilic payloads (e.g. MMAF, amanitin, etc.) do not efficiently diffuse through the cell membrane, while they show high anticancer activity when incorporated into internalizing therapeutics.

1.5. $\alpha_V\beta_3$ integrin targeting ligands for the delivery of chemotherapeutics.

1.5.1. Integrins

Integrins are a family of transmembrane receptors that are expressed in all cell types, with the exception of red blood cells (erythrocites). They are heterodimeric glycoproteins formed by two subunits non-covanlently associated, namely α and β. In total, 24 different heterodimers can be formed in vertebrates by combining the 18 α and the 8 β existing subunits and the resulting structure determines the substrate specificity, signaling properties and tissue expression.[56]

Integrins constitute a physical anchor for the cell and they are the principal adhesion receptors for the extracellular matrix (ECM) proteins, growth factors, inmunoglobulins, matrix-degrading proteases and cytokines. Receptor-ligand interaction promotes different intracellular signaling cascades that can include tyrosine phosphorylation of focal adhesion kinases (FAK).[57]

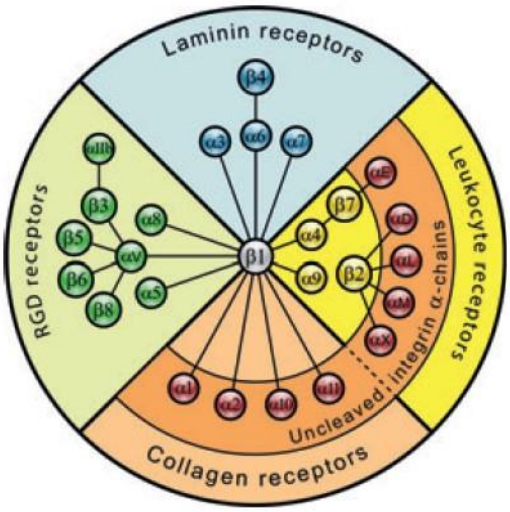

Figure 10. Schematic representation of the vertebrate integrin family.[58]

This kinase plays an essential role in cell motility, survival, and proliferation. Furthermore, integrins collaborate with other receptors (such as the growth factor receptors –GFRs) for the regulation of many cellular events, such as cell migration, invasion and cytokinesis.[59] Besides their physiological role, integrins are involved in different processes of tumor development, such as invasion, angiogenesis and metastasis. In

particular, the β_3 subunit is associated with the capacity of cancer to metastasize and the $\alpha_V\beta_3$ receptor is strongly associated with the regulation of angiogenesis.[55b] For these reasons, this particular integrin heterodimer has been widely investigated as tumor antigen and several pharmaceutical activities focused on $\alpha_V\beta_3$-targeted therapies.

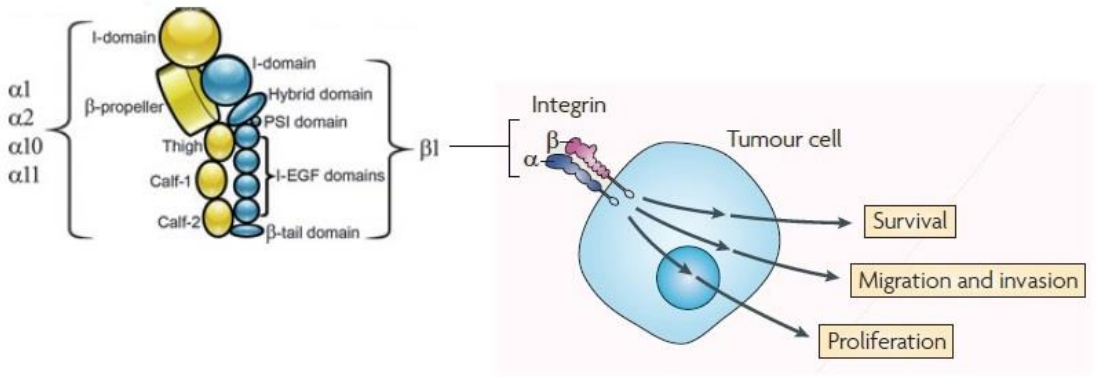

Figure 11. Schematic representation of the function of integrins in cancer cells and representation of the two subunits.[59]

1.5.2. $\alpha_V\beta_3$ as tumor-targeting receptor

$\alpha_V\beta_3$ has been widely investigated for drug delivery purposes, due to its high expression on several human cancers but not in the healthy tissues. [56,58] $\alpha_V\beta_3$ is involved in ECM remodeling and degradation, which are the key processes for tumor invasion and metastasis. The overexpression of $\alpha_V\beta_3$ in prostate carcinoma and breast cancer has been associated with bone metastasis while, in glioblastoma, the increased levels of the receptor are associated with enhanced cell motility and resistance to apoptosis.[60]

The complex “cross-talk” networks involving $\alpha_V\beta_3$ and different growth factor receptors seem to regulate the angiogenesis on tumors. For example, the coordination between the integrin receptor and the fibroblast growth factor (FGF) has been reported to inhibit pro-angiogenic signaling, while the interaction between $\alpha_V\beta_3$ and VEGFR (vascular endothelial growth factor receptor) triggers angiogenesis. This process has been described to proceed through the activation of enzyme matrix metalloproteinase-2 (MMP-2), that degrades the collagen matrix, therefore enabling the ECM rearrangement.[57]

In 1984, Ruoslahti and coworkers discovered that many integrin receptors recognize the Arg-Gly-Asp (RGD) sequence, which is present in fibronectin and many other ECM proteins[61] and this tripeptide was identified as specific binding motif.

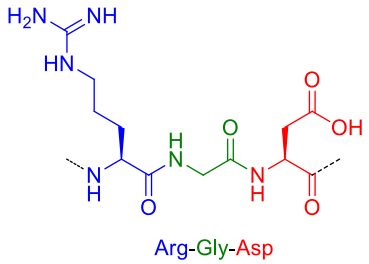

Figure 12. Structure of the RGD (Arg-Gly-Asp) sequence.

This discovery led to the development of many RGD-bearing compounds which showed low nanomolar affinity for $\alpha_V\beta_3$, especially those constrained into cyclic structures.[62] A well-known example of this series of compounds is the integrin ligand cilengitide (compound **18**, Fig. 13), which was developed by Kessler and coworkers.[63] The understanding of the X-ray analysis of the co-crystals obtained from $\alpha_v\beta_3$ and cilengitide was an important milestone in the development of this research area. In this crystal structure, an extended conformation of the RGD sequence in the integrin binding pocket was observed, with a 9-Å distance between C-β atoms of the Arg and Asp residues: this arrangement allows the interaction of the arginine side chain with two anionic aspartic acid residues in the α-subunit, whereas the aspartic acid binds to divalent metal cation in the metal ion-dependent adhesion site (MIDAS) region of the β-subunit.[64]

The deep understanding of the structural features of the $\alpha_v\beta_3$-cilengitide complex prompted the development of many peptides and peptidomimetics targeting the $\alpha_v\beta_3$ integrin.[65] One interesting example is MK-0429 (**19**), which have been evaluated in clinical trials as anticancer drugs.[66]

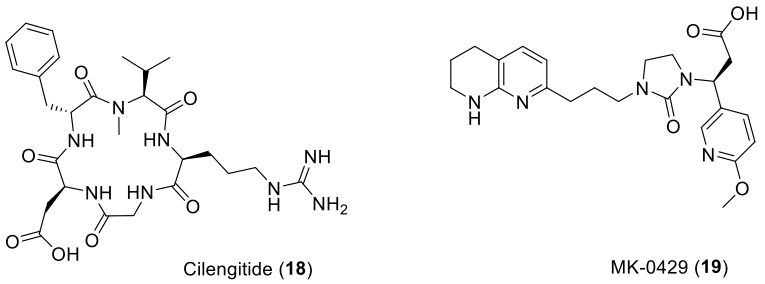

Figure 13. Structures of cilengitide and MK-0429.

Both cilengitide and MK-0429 were demonstrated to be non-toxic and well-tolerated, the compounds did not display significant therapeutic benefits. Moreover, it has been described that cilengitide, under specific experimental conditions, may possess pro-angiogenic activity.[67] After this clinical failure, the clinical evaluation of cilengitide was discontinued. However, although the efficacy of $\alpha_V\beta_3$ integrin ligands as anti-angiogenic agents may be controversial, their use as tumor targeting agents still represents a promising strategy.

1.5.3. RGD ligands for tumor imaging and therapy

Many of the RGD-peptides and peptidomimetics developed in the recent years have been conjugated to imaging agents. [^{18}F]Galacto-RGD was the first example of radiotracer bearing the RGD sequence used for the study and visualization of $\alpha_V\beta_3$ expression in cancer. In this conjugate, the *cyclo*[RGDfK] was used as ligand for tumor targeting.[68] Another example using this ligand is the DOTA-*cyclo*[RGDfK] labelled with ^{111}In or ^{90}Y, which has been subjected to biodistribution studies in mice with SKOV-3 human ovarian carcinoma.[69] Furthermore, the ^{99m}Tc-NC100692 (NC100692: RGD bearing cyclic peptide) has been evaluated in clinical trials as probe for single photon emission computed tomography (SPECT). Besides showing good tolerability, these experiments showed that ^{99m}Tc-NC100692 can be used to detect persistent angiogenesis in patients with remote myocardial infarction.[70]

In addition to their use on the field of imaging, the RGD peptides and peptidomimetics have been also investigated as possible vehicles for the selective delivery of cytotoxic agents to tumors, not only when incorporated into SMDC products, but also when coupled to lyposomes, nanoparticles, etc. Integrins are commonly considered as internalizing receptors[71] and specific proteins (i.e. caveolin and clathrin) are known to interact with the intracellular domain of $\alpha_v\beta_3$ integrin and promote the receptor folding into membrane vesicles that travel to early endosomes. Later on, $\alpha_v\beta_3$ integrin can be either driven to intracellular compartments responsible for protein degradation (e.g. endosomes and lysosomes), or recycled to the plasma membrane.[72]

Doxorubicin was the first cytotoxic agent to be coupled with an integrin ligand. It was coupled to RGD-4C (**20**, Figure 14) and tested in mice bearing the MDA-MB-435 human breast cancer, which is known to express α_V integrins. The results showed an increased volume tumor growth inhibition and lower toxicity compared to the free drug.[73]

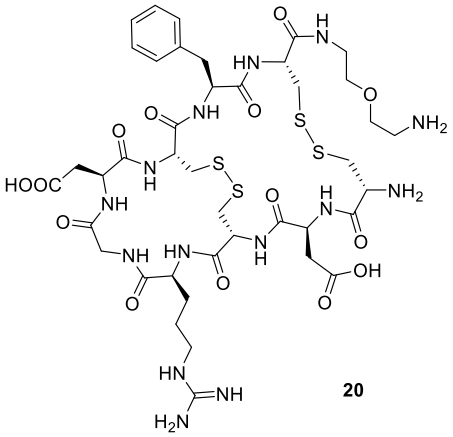

Figure 14. Structure of RGD-4C.

Later on, a variety of cytotoxic agents have been conjugated to RGD-bearing ligands using different release mechanisms. For example, Manzoni *et al.* have designed nine paclitaxel-containing conjugates bearing either Azabicycloalkane-RGD or Aminoproline-RGD as ligand. All of them showed good *in vitro* growth inhibition in different cell lines [U2-OS (human osteosarcoma), IGROV-1(human ovarian carcinoma), IGROV-1/Pt1 (cisplatin-resistant human ovarian carcinoma) and H460 (human large cell lung carcinoma)]. Among these conjugates, compound **21** bearing a triazole linker was tested in mice xenografted with an ovarian carcinoma and a better tumor volume inhibition was observed when compared with the free drug.[74]

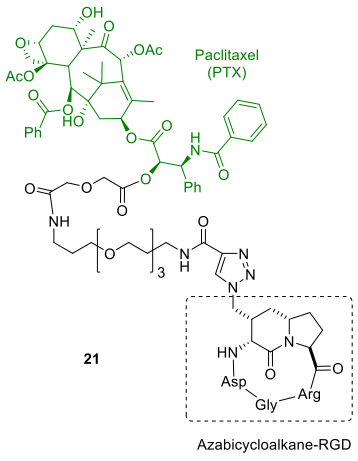

Compound	TVI %[a]	BWL[b]	TOX[c]
21	98	7	0/5
PTX	81	5	0/5

a) Tumor volume inhibition % in treated over control mice assessed 7 days after last treatment; b) body weight loss % induce by treatment; the highest change is reported; c) dead/treated mice.

Figure 15. Structure of the Azabicycloalkane-RGD conjugate (**21**) tested *in vivo* and table with the efficacy of *i.v.* of 21 and Paclitaxel (PTX) (36 mg/kg q4dx4) on IGROV-1/Pt1 xenografted mice.

Moreover, more potent drugs were used in conjugation with RGD-bearing compounds. For example, MMAE has been conjugated to a non-peptidic $\alpha_V\beta_3$ ligand through the peptide linker Ala-Ala-Asn. This sequence acts as specific substrate of legumain, an intracellular protease.

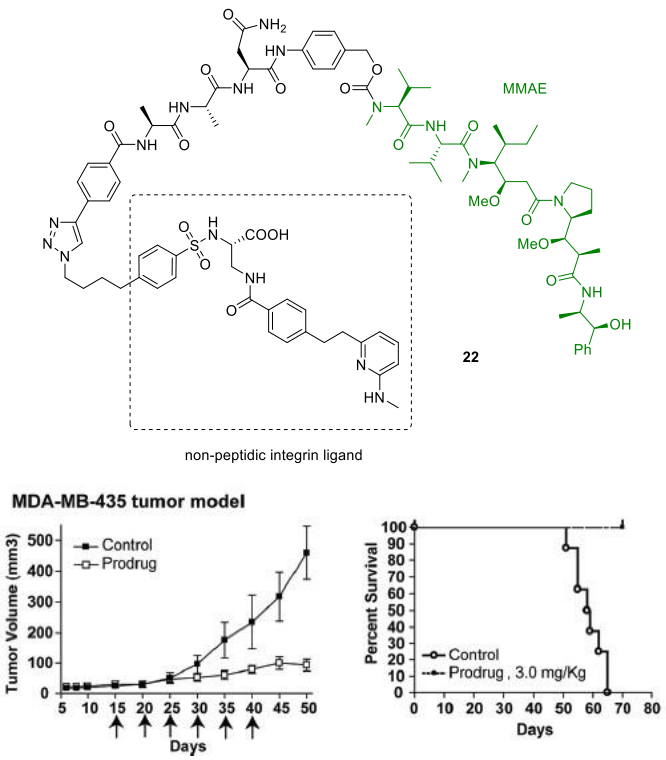

Figure 16. Structure of conjugate **22** and results of *in vivo* experiments. Left graphic: *in vivo* effect of conjugate **22.** When the experiment started, the diameter was around 5 mm. Control= saline alone. Dose of conjugate **22**= 3 mg/kg. Right graphic: Survival based on the primary tumor diameter (>1.5 cm) and natural death.

Due to its targeting properties, the resulting SMDC (compound **22**, Fig. 16) was administered to MDA-MB-435 tumor-bearing mice at 30-fold higher molar dose than the maximum tolerated dose of free MMAE. This resulted in improved antitumor response and much lower toxicity compared to the free MMAE.[75]

1.5.4. Previous work of our group

In 2009, the Gennari and Piarulli group developed a series of new integrin ligands in which the RGD sequence is constrained into a cycle by the bifunctional 2,5-diketopiperazine (DKP) scaffold. The DKP ring constrains the nitrogen atom of an α-amino amide: this modification of the two peptide bonds is known to reduce the susceptibility of peptide bonds to metabolic cleavage and it confers conformational rigidity.

These changes in structural and physical properties, as well as the presence of functional groups that can act as donors (amide proton) and acceptors (carbonyl groups) of hydrogen bonds were found to be sources of favorable interactions with the biological target.

Eight different diketopiperazines were prepared starting from combination of L- and D-amino acids, bearing carboxy (derived from aspartic and glutamic acids) or amino groups (derived from an amino-serine residue) in their side chains. Furthermore, the amide nitrogen atoms of the DKP ring were differently functionalized with benzylic moieties. The DKPs were used to join N and C termini of the Arg-Gly-Asp sequence, resulting in a library of 8 peptidomimetics (Figure 17).[65 d-e]

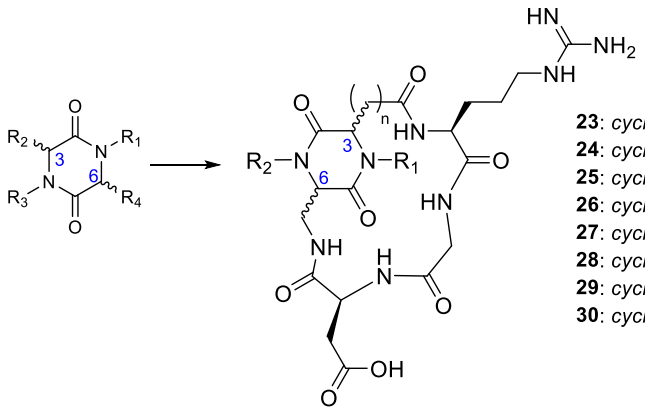

23: *cyclo*[DKP-1-RGD]= 3*S*, 6*S*, R_1=H, R_2=CH_2Ph, n=1
24: *cyclo*[DKP-2-RGD]= 3*R*, 6*S*, R_1=H, R_2=CH_2Ph, n=1
25: *cyclo*[DKP-3-RGD]= 3*S*, 6*R*, R_1=H, R_2=CH_2Ph, n=1
26: *cyclo*[DKP-4-RGD]= 3*R*, 6*S*, R_1=CH_2Ph, R_2=H, n=1
27: *cyclo*[DKP-5-RGD]= 3*R*, 6*S*, R_1=CH_2Ph, R_2=CH_2Ph, n=1
28: *cyclo*[DKP-6-RGD]= 3*S*, 6*R*, R_1=CH_2Ph, R_2=H, n=1
29: *cyclo*[DKP-7-RGD]= 3*S*, 6*R*, R_1=CH_2Ph, R_2=CH_2Ph, n=1
30: *cyclo*[DKP-7-RGD]= 3*S*, 6*R*, R_1=H, R_2=CH_2Ph, n=2

Figure 17. Structure of the 8 peptidomimetic RGD ligands developed by Gennari and Piarulli group.

The library members were tested *in vitro* for their ability to compete with fibronectin for the binding to the purified $\alpha_v\beta_3$ and $\alpha_v\beta_5$ receptors: IC_{50} values in the 10^{-10}-10^{-6} molar range demonstrated that the DKP ring strongly influences the ligand affinity for the receptor. NMR and *in silico* conformational studies completed the panel of SAR studies, providing the structural basis of the affinity observed *in vitro*. Due to its low-nanomolar affinity for the $\alpha_v\beta_3$ receptor and to its synthetic accessibility, the *cyclo*[DKP- 3-RGD] (that will be named "*cyclo*[DKP-RGD]" in the following Chapters) was selected among the

library members as hit compound for further biological evaluations. While this compound was found to inhibit the capillary network formation in human umbilical vein endothelial cells (HUVEC), it did not interfere with the production of mRNA for the α_v, β_3, and β_5 subunits.[76] Moreover, due to its inhibitory effect on integrin-mediated FAK/Akt transduction pathways and cell infiltration processes, ligand **25** has been recently classified as a pure $\alpha_v\beta_3$ antagonist.[65f] These results highlighted the differences between the *cyclo*[DKP-RGD] ligand and the well-known cilengitide (**18**), whose controversial agonist-like activity has been mentioned in Paragraph 1.5.1.

Cyclo[DKP-3-RGD] was functionalized with an amino-methyl group (-CH_2NH_2) as a conjugation site to cytotoxic drugs [77] and it was used for the synthesis of conjugates with different cytotoxic agents (such as paclitaxel and camptothecin)[50, 78]

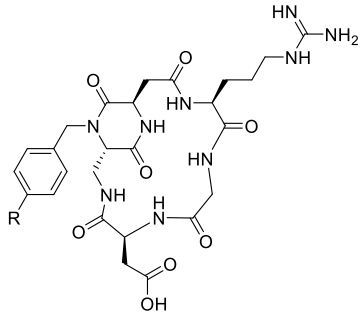

cyclo[DKP-3-RGD] | R = H (**31**) / R = CH_2NH_2 (**32**)

Figure 18. Structure of both the *cyclo*[DKP-3-RGD] (**31**) and the amino-methyl functionalized *cyclo*[DKP-3-RGD] (**32**).

In particular, the ligand *cyclo*[DKP-3-RGD]-CH_2NH_2 (**32**) was conjugated to paclitaxel through the Phe-Lys and Val-Ala linkers (Figure 19, **33** and **34**) and the tumor-targeting ability of the resulting SMDC compounds was evaluated in cell viability assays, against isogenic cell lines expressing $\alpha_V\beta_3$ at different levels. Similarly to other several targeted prodrugs, the conjugates showed lower cytotoxicity than the free drug. However, the use of cell lines with different target expression was useful to determine the selectivity displayed by theses conjugates towards $\alpha_V\beta_3$-positive cells. As reported in Table 1, compound **33** showed a more selective anticancer activity, which was compared to the potency displayed by the free PTX and quantified in terms of selectivity (S) and Targeting Index (TI).

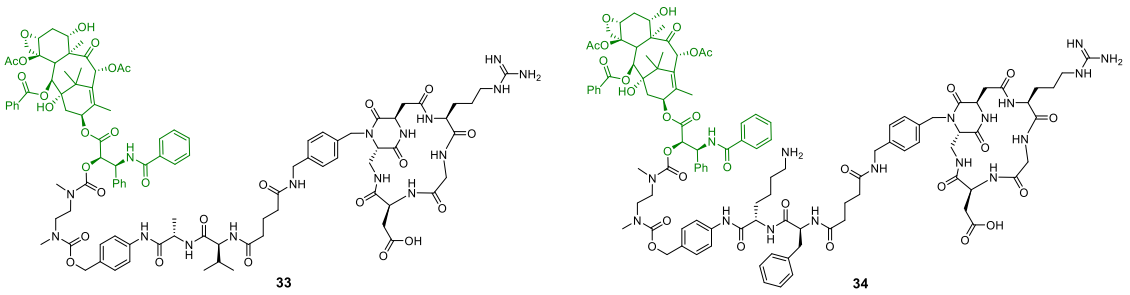

Figure 19. Structures of *cyclo*[DKP-RGD]-Val-Ala-PTX (**33**) and *cyclo*[DKP-RGD]-Phe-Lys-PTX (**34**).

Table 1. Antiproliferative activity of conjugates **33** and **34** on the isogenic cell lines CCRF-CEM after 6 hours of treatment followed by compound washout and 138 h of growth in fresh medium.

Compound	IC_{50} (nM)		S[a]	TI[b]
	CCRF-CEM ($\alpha_V\beta_3$ -)	CCRF-CEM ($\alpha_V\beta_3$ +)		
Paclitaxel	155 ± 55	21 ± 2	7.4	1
33	5153 ± 977	77 ± 20	66.9	9.0
34	535 ± 70	34 ± 2	15.7	2.1

[a] Selectivity (*S*): $IC_{50}(\alpha_v\beta_3 -)$ / $IC_{50}(\alpha_v\beta_3 +)$. [b] Targeting Index (T.I.): Selectivity / Selectivity observed with free paclitaxel.

Furthermore, our group has recently conjugated the functionalized ligand **32** with camptothecin through a disulfide linker (**35**, Figure 20).[79] Unfortunately, this compound was found to be poorly stable in the cell culture medium, resulting in a fast extracellular release of the camptothecin (CPT) payload and hampering the selectivity.

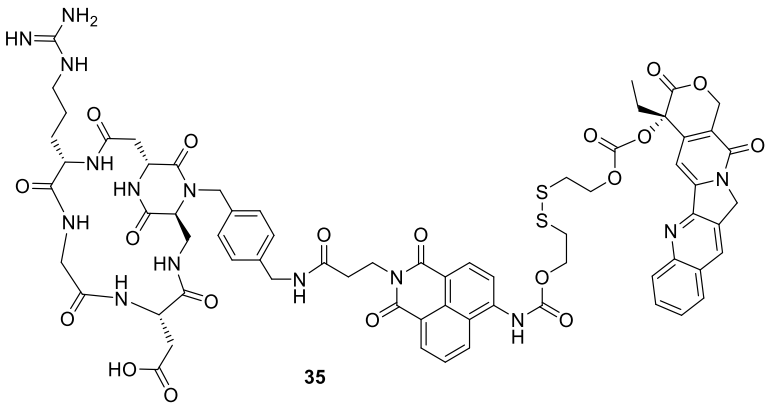

Figure 20. Structure of cyclo[DKP-RGD]-Naph-SS-CPT.

As observed in the previous examples, the linker proved to be very important for the selectivity and for the overall pharmaceutical outcome of the conjugates. For this reason, my PhD work focused on the development of SMDCs containing different linkers, which can be either cleaved by lysosomal or extracellular enzymes. Moreover, we evaluated the SMDC activation by ubiquitous enzymes, potentially expressed both in intracellular compartments and in extracellular milieu.

Chapter 2: Conjugates bearing lysosomally cleavable linkers.

Part of the work described in this Chapter was published in the following articles:

- P. López Rivas, L. Bodero, B. Korsak, T. Hechler, A. Pahl, C. Müller, D. Arosio, L. Pignataro, C. Gennari, U. Piarulli, *Beilstein J. Org. Chem*. **2018**, *14*, 407-415.

- P. López Rivas, I. Ranđelović, A. R. M. Dias, A. Pina, D. Arosio, J. Tóvári, G. Mező, A. Dal Corso, L. Pignataro, C. Gennari, *Eur. J. Org. Chem.* **2018**, 2902-2909. DOI: 10.1002/ejoc.201800447

2.1. Synthesis and biological evaluation of RGD-peptidomimetic-paclitaxel conjugates bearing the Gly-Phe-Leu-Gly linker.

In this section, a deeper study of RGD conjugates bearing lysosomally-cleavable linkers is reported. Starting from the promising data obtained with compound *cyclo*[DKP-RGD]-Val-Ala-PTX (**33**), the design of new SMDC products was carried out with the aim of evaluating the influence of each individual moiety of the conjugate on the integrin affinity and selective cell toxicity . Taking the structure of conjugate **33** as a reference, modifications were introduced at three different points (Figure **21**): the peptide linker, the spacer connecting the linker to the ligand and the integrin ligand.

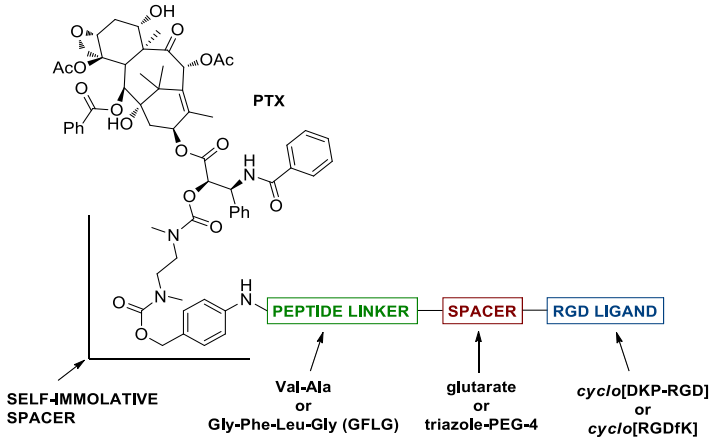

Figure 21. Summary of the changes introduced in the SMDCs structure.

Both the cytotoxic drug paclitaxel and the self-immolative spacer remained unchanged. The mechanism of drug release is explained in Scheme 1 (mechanism E, section 1.4.1 of the Introduction). In this self-immolative fragment, a dimethylethylenediamino chain is connected to a *p*-aminobenzylcarbamate (PABC) spacer through a physiologically-stable carbamate bond.[24a,79] Furthemore, another carbamate bond connects the dimethylethylenediamino structure to the 2'-OH bond of paclitaxel (Figure 22).

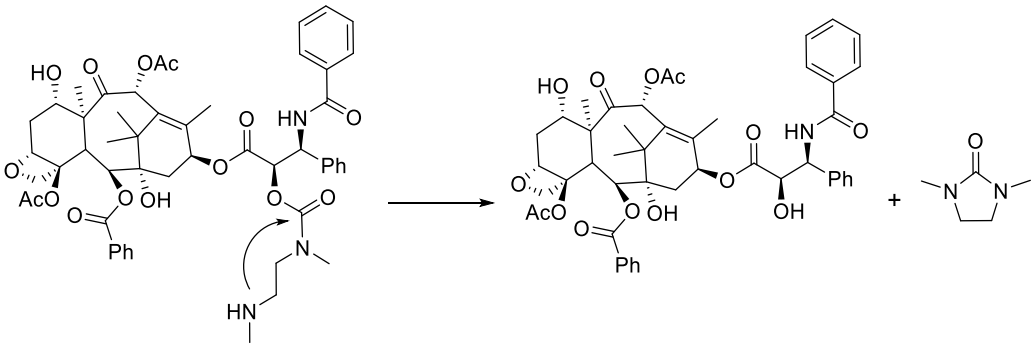

Figure 22. Structure and mechanism of cyclization of the *N,N'*-dimethylethylenediamino spacer to release free PTX.

This particular combination of 1,6-elimination and cyclization spacers has been often used for the preparation of prodrugs and, in the case of PTX, the two carbamate bonds improve the poor stability in murine and human plasma observed for previous conjugates (e.g., compound **36,** Figure 23), bearing an ester bond.[77] The two methyl groups introduced at both nitrogen atoms of the dimethylethylenediamino chain are used both to accelerate the cyclization process (i.e. more nucleophilic N atom) and to prevent the rearrangement of the 2'-carbamate bond and subsequent degradation of the paclitaxel's structure.[80]

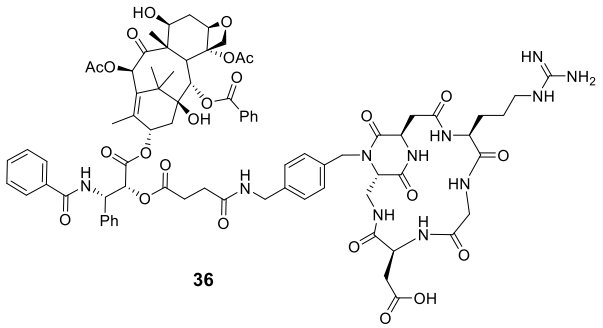

36

Figure 23. Structure of *cyclo*[DKP-RGD]-PTX bearing an ester bond.

On the other hand, the glutarate spacer introduced between the Linker and Ligand (present in conjugate **33**) was compared to a hydrophilic tetraethylene glycol (PEG-4), connected to the linker-drug module through a triazole ring. The polyethylene glycol chains are known to improve the hydrophilicity and flexibility of the SMDC constructs as well as their bioavailability. [81] In this work, a short PEG-4 spacer was selected in order to avoid the formation of bulky loops that can impair the binding to the receptor.[82] Connected to this spacer, the Gly-Phe-Leu-Gly (GFLG) linker was selected as an alternative to Val-Ala: this tetrapeptide is a widely known lysosomally-cleavable linker possessing good plasma and serum stability.[51c] Specifically, this linker is known to be cleaved by Cathepsin B at the C-terminal glycine.[83] One of the first examples of the use of GFLG as smart linker for tumor-targeting was introduced by Omelyanenko *et al*. in 1998. In this work, the linker was used to conjugate doxorubicin and meso chlorin e6 mono(*N*-2-aminoethylamide) (Mce_6) to the HMPA copolymer [(N-(2-hydroxypropyl)methacrylamide]. The resulting polymer-drug conjugate was also labelled with the OV-TL16 antibody, which was used to target ovarian carcinoma cell lines. The resulting Antibody-polymer-Drug conjugate showed 2 orders of magnitude improvement of the *in vitro* cytotoxicy against OVCAR-3 cell line when compared with the non-targeted HPMA copolymer conjugates.[84] More recently, the GFLG linker has been used in different delivery systems such as dendrimers[51c], nanoparticles[85] and SMDCs bearing gonadotropin-releasing hormones (GnRH)[51a,51d] or cell-penetration peptides (CPP).[51b]

Beside the linker and spacer fragments, we devised the replacement of the *cyclo*[DKP-RGD] ligand with the *cyclo*[RGDfK] cyclopeptide. The latter is a widely used and synthetically accessible integrin ligand[86] and its inclusion in the tested compounds would provide insights into the effects of the different ligand structures in the biological output. As a result of this modular design, four GFLG-bearing conjugates were designed and their structures are depicted in Figure 24. The prepared compounds were evaluated *in vitro* for their integrin receptor binding and their antiproliferative activity and compared with *cyclo*[DKP-RGD]-Val-Ala-PTX **33** and its PEG-4 analogue *cyclo*[DKP-RGD]-PEG-4-Val-Ala-PTX **41** (Figure 24) synthesized in our group.[50,81b]

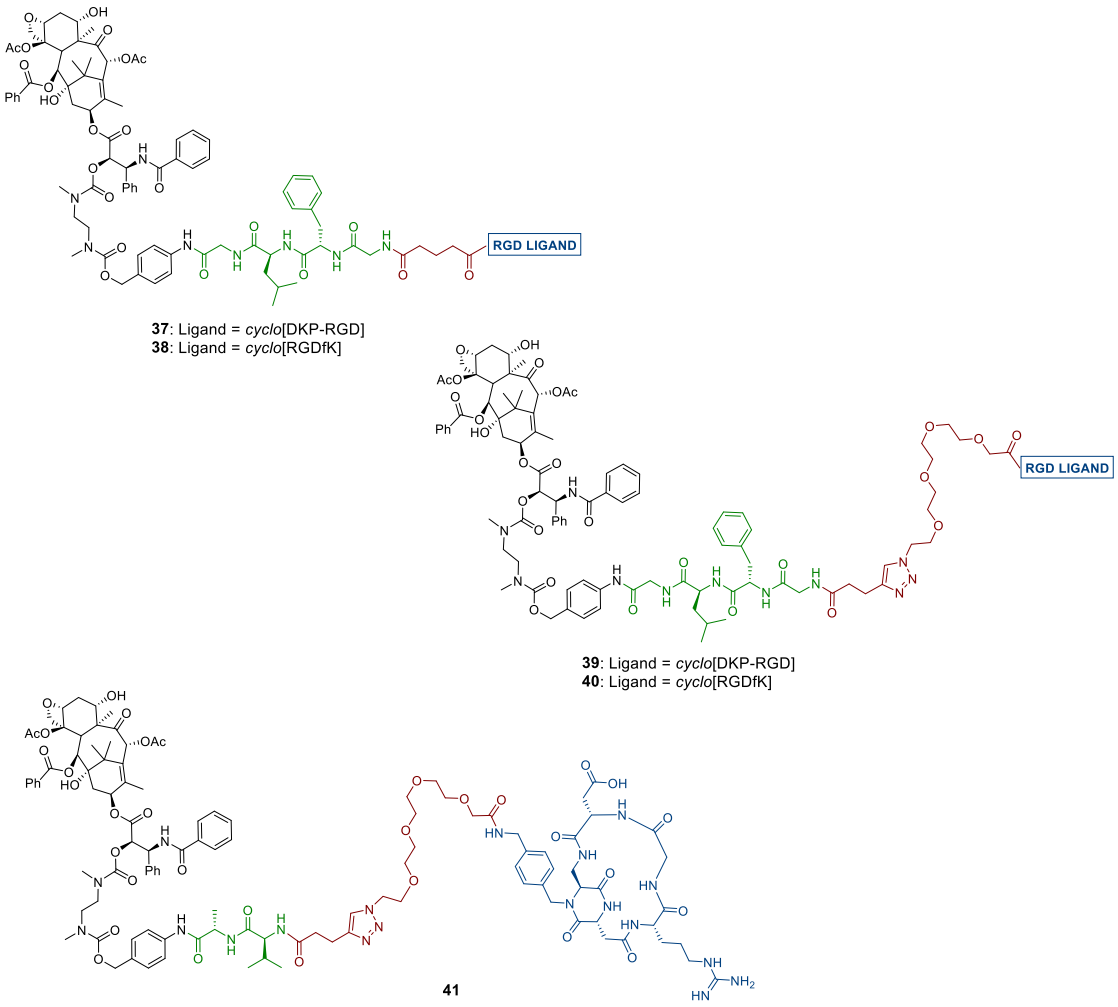

Figure 24. Structures of *cyclo*[DKP-RGD]-GFLG-PTX (**37**), *cyclo*[RGDfK]-GFLG-PTX (**38**), *cyclo*[DKP-RGD]-PEG-4-GFLG-PTX (**39**), *cyclo*[RGDfK]-PEG-4-GFLG-PTX (**40**) and *cyclo*[DKP-RGD]-PEG-4-Val-Ala-PTX (**41**).

2.1.1. Synthesis

A) Synthesis of cyclo[RGDfK], cyclo[RGDfK]-PEG-4-azide and Fmoc-GFLG-OH

The RGD ligand *cyclo*[RGDfK] and the GFLG linker were both synthesized by solid phase peptide synthesis (SPPS). In particular, the linear protected Fmoc-Asp(O*t*Bu)-D-Phe-Lys(Boc)-Arg(Pbf)-Gly-OH (**43**, Scheme 2.A) and Fmoc-Gly-Phe-Leu-Gly-OH (**48**, scheme 2.B) were synthesized on 2-chlorotrityl resin (0.87 mmol/g loading capacity) using the Fmoc protocol. Upon loading of the C-terminal amino acid (Fmoc-Gly-OH in both cases) sequences of amino acid coupling and deprotections led to the final sequences **42** and **47,** still bound to the resin.

The peptide sequences, protected at the Lys, Asp and Arg side chains with acid-labile protecting groups (respectively, Boc, O*t*Bu and Pbf) were cleaved from the resin with a mildly acidic mixture (i.e. 8:1:1 CH_2Cl_2/MeOH/AcOH) and the oily crudes were precipitated with water, leading to compounds **43** and **48**. Both compounds were used without further purification and the latter one was used as starting point for the synthesis of the four final conjugates. The formation of the peptide cycle was performed upon Fmoc removal from compound **43,** and the resulting amine **44** was reacted with a 6:4:4 *i*Pr_2NEt/BOP/HOBt mixture, in a highly diluted (1 mM) DMF solution. Remarkably, the efficacy of the peptide cyclization was found to be dependent on the reaction scale, with results worsening when the starting material was higher than 150 mg.
Final deprotection of **45** was performed with a cocktail of TFA/thioanisole/EDT/phenol/TIS and the crude was precipitated in cold diethyl ether. The centrifuged pellet was purified by preparative HPLC yielding pure *cyclo*[RGDfK] **46**. This compound was either coupled to glutarate-based linkers or to a PEG-4 spacer (following a procedure reported previously[81b] and shown in Scheme 3) resulting in the corresponding *cyclo*[RGDfK]-PEG-4-azide (**51a**) compound. *Cyclo*[DKP-RGD]-PEG-4-azide (**51b**) was synthesized following the same methodology.

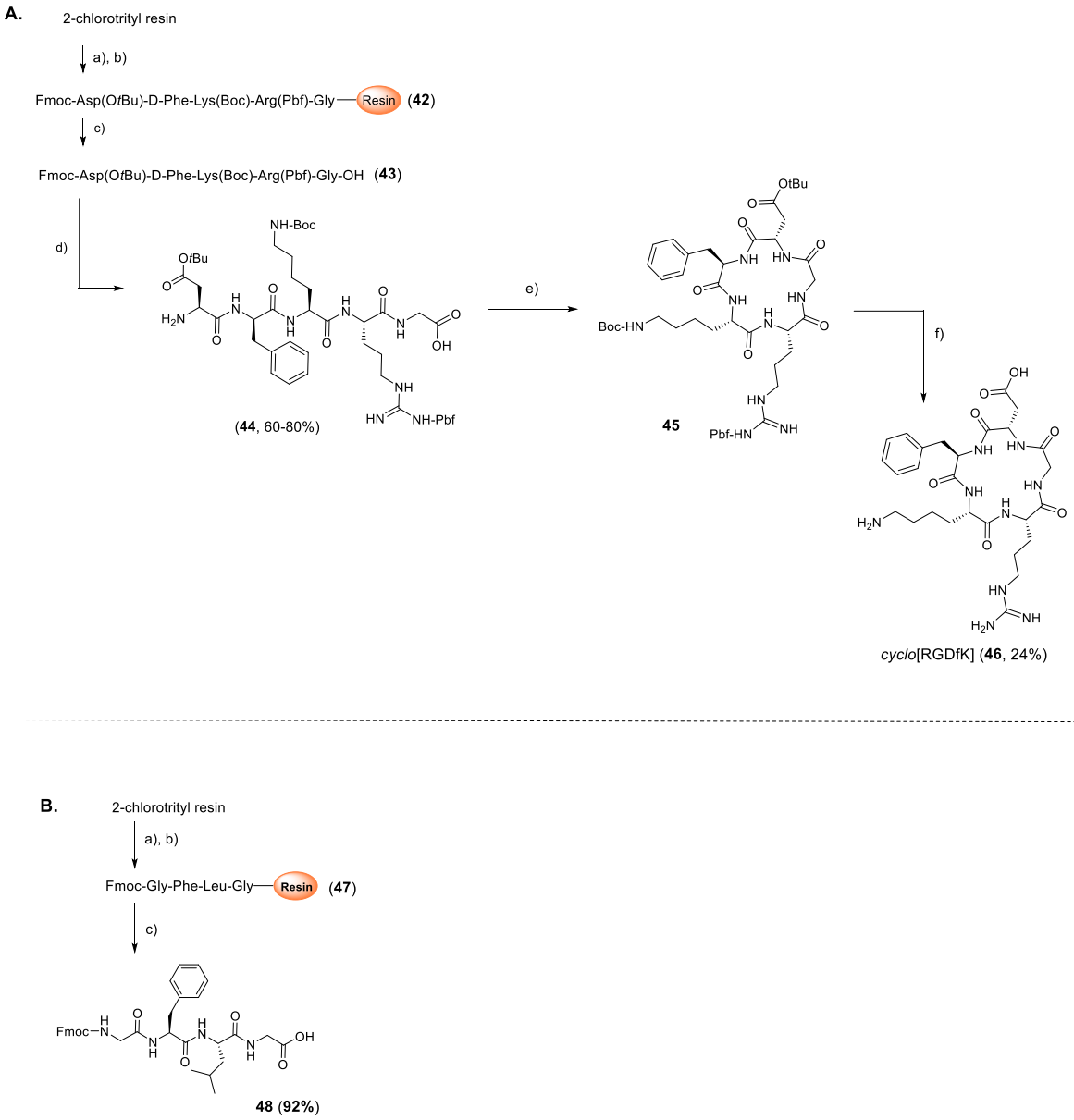

Scheme 2. Synthesis of *cyclo*[RGDfK] (**46**) and Fmoc-GFLG-OH (**48**). Reagents and conditions: a) i. Fmoc-Gly-OH (1 equiv.), *i*Pr_2NEt (3 equiv.), 1:1 CH_2Cl_2/DMF, 2 h, r.t.; ii. Capping with 7:2:1 CH_2Cl_2/MeOH/*i*Pr_2NEt; b) i. Fmoc-deprotection: 2% DBU, 2% piperidine, DMF, 1 h; ii. Fmoc-AA-OH (3 equiv.), HOBt (4 equiv.), DIC (4 equiv.), 2 h; conditions (b) are repeated for the coupling of every amino acid of the sequence; c) 8:1:1 CH_2Cl_2/MeOH/AcOH, 2 h, precipitation in water; d) DMF, 20% piperidine, 2 h; e) 6:4:4 *i*Pr_2NEt/BOP/HOBt, 1 mM concentration in DMF, 24 h, precipitation in 5% $NaHCO_3$; f) TFA/thioanisole/EDT/phenol/TIS (14.25 mL / 375 µL / 375 µL /1.125 g / 375 µL), 3 h. DBU = 1,8-Diazabicyclo[5.4.0]undec-7-ene; AA = amino acid; BOP = (benzotriazol-1-yloxy)tris(dimethylamino)phosphonium hexafluorophosphate; DIC = *N,N'*-diisopropylcarbodiimide; EDT = 1,2-ethanedithiol; TIS = triisopropylsilane.

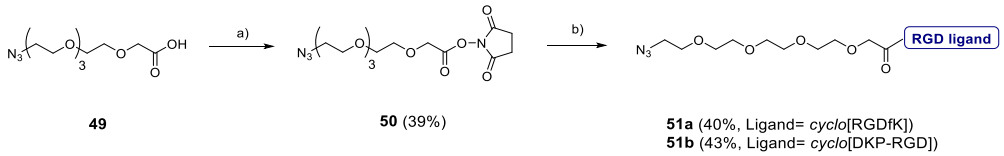

Scheme 3. Synthesis of *cyclo*[RGDfK]-PEG-4-azide (**51a**) and *cyclo*[DKP-RGD]-PEG-4-azide (**51b**). Reagents and conditions: a) EDC • HCl, NHS, THF; b) *Cyclo*[RGDfK] (**46**) or *cyclo*[DKP-RGD]-CH_2NH_2 (**32**), CH_3CN/PBS (pH 7.3-7.6), overnight. PBS = phosphate-buffered saline.

*B) Synthesis of conjugates **37**- **40***

Conjugates **37**- **40** were synthesized as described in Scheme 4.

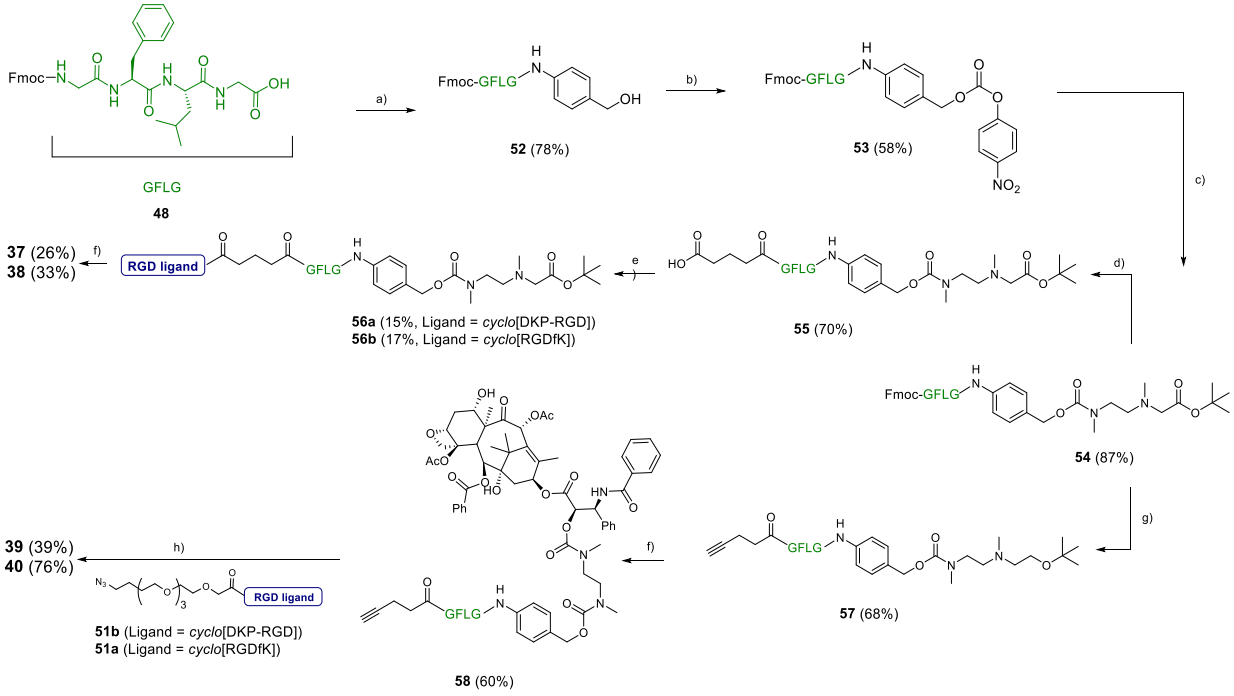

Scheme 4. Synthesis of conjugates **37**-**40**. Reagents and conditions: a) HOBt, DIC, 4-aminobenzyl alcohol, DMF, overnight; b) 4-nitrophenylchloroformate, pyridine, 4:1 THF/DMF, 2 h; c) *N*-Boc-*N,N'*-dimethylethylenediamine **60**, *i*Pr_2NEt, THF, overnight; d) i. piperidine, DMF, 4 h; ii. glutaric anhydride, DMAP, *i*Pr_2NEt, DMF, overnight; e) i. DIC, NHS, DMF; ii. *Cyclo*[DKP-RGD]-CH_2NH_2 **32** (for **56a**) or *cyclo*[RGDfK] **46** (for **56b**), 1:1 DMF/PBS (phosphate-buffered saline, pH 7.3-7.6), overnight; f) i. TFA, CH_2Cl_2; ii. 2'-(4-nitrophenoxycarbonyl)PTX **60**, *i*Pr_2NEt, DMF, overnight; g) i. piperidine, DMF, 4 h; ii. 4-pentynoic acid, HATU, HOAt, *i*Pr_2NEt, DMF, overnight; h) *cyclo*[DKP-RGD]-PEG-4-azide (**51b**) or *cyclo*[RGDfK]-PEG-4-azide (**51a**), $CuSO_4$ • 5 H_2O, sodium ascorbate, DMF/H_2O. DIC = *N,N'*-diisopropylcarbodiimide; DMAP = 4-dimethylaminopyridine; NHS = *N*-hydroxysuccinimide; PTX = paclitaxel.

The preparation of compounds **37**-**40** started with the installation of the self-immolative spacer to the protected tetrapeptide Fmoc-GFLG-OH (**48**), produced by SPPS. This compound was treated with 4-aminobenzyl alcohol in the presence of HOBt and DIC coupling agents, to yield amide **52**. The hydroxyl group was reacted with *p*-nitrophenyl chloroformate and elongated with *N*-Boc-*N,N'*-dimethylethylenediamine **59**[87] (scheme 5), affording carbamate **54**. The latter was used as a common intermediate for the synthesis of all RGD-PTX conjugates, bearing either the PEG-4 or the glutarate spacers. In particular, for the synthesis of compounds **37** and **38**, the Fmoc protecting group was removed in solution and, after removal of DMF and piperidine from the reaction mixture, the crude amine was treated with glutaric anhydride. Flash chromatography afforded the resulting hemigluatarate **55** in high yield (up to 70% in two steps). This carboxylic acid was activated with *N*-hydroxysuccinimide (NHS) and coupled either to the functionalized *cyclo*[DKP-RGD] (**32**) or to *cyclo*[RGDfK] (**46**). This conjugation was run at controlled pH, since the reaction is inhibited at pH < 7.0, due to amine protonation, whereas at pH > 7.6 the hydrolysis of the NHS ester competes significantly with the desired coupling. Due to the presence of *cyclo*[DKP-RGD] (which is routinely isolated as a TFA salt, upon HPLC purification), the pH of the reaction mixture was adjusted in the 7.3-7.6 range by adding aliquots of base (0.2 M aqueous solution of NaOH). The crude residue was purified by semipreparative HPLC affording intermediates **56a** and **56b**. As last step, compounds **56a** and **56b** were Boc-deprotected and reacted with 2'-(4-nitrophenoxycarbonyl)paclitaxel (**60**, scheme 5) affording the final *cyclo*[DKP-RGD]-GFLG-PTX (**37**) and *cyclo*[RGDfK]-GFLG-PTX (**38**).

For the PEG-4 containing conjugates, intermediate **54** was Fmoc-deprotected as described above and treated with 4-pentynoic acid in the presence of HATU, HOAt and *i*Pr_2NEt, affording compound **57.** The latter was Boc-deprotected and coupled with 2'-(4-nitrophenoxycarbonyl)paclitaxel (**60**, scheme 5) to yield alkyne **58**. The latter was subjected to copper-catalyzed azide-alkyne cycloaddition with either *cyc*lo[RGDfK]-PEG-4-azide (**51a**) or *cyclo*[DKP-RGD]-PEG-4-azide (**51b**).[81b] The final conjugates **39** and **40** were obtained after purification through semipreparative HPLC.

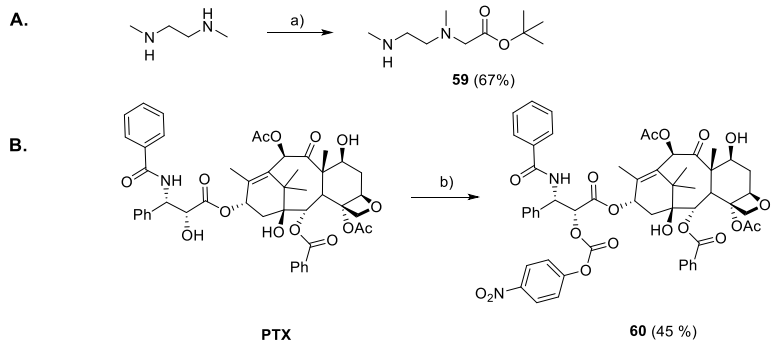

Scheme 5. A) Synthesis of *N*-Boc-*N,N'*-dimethylethylenediamine **59**. Reagents and conditons: a) *N,N'*-dimethylethylenediamine, Di-tert-butyl dicarbonate, CH_2Cl_2, overnight; B) Synthesis of 2'-(4-nitrophenoxycarbonyl)paclitaxel **60**. Reagents and conditions: b) PTX, 4-nitrophenyl chloroformate, pyridine, -50º C to -20 ºC, 4 h.

2.1.2. *In vitro* biological evaluation

A) Integrin receptor competitive binding assays

The new GFLG conjugates **37**-**40** were examined *in vitro* for their ability to inhibit biotinylated vitronectin binding to the purified $\alpha_V\beta_3$ and $\alpha_V\beta_5$ receptors and compared with the values obtained for the free ligands *cyclo*[RGDfK] **46** and *cyclo*[DKP-RGD] ligand **31**. The calculated IC_{50} values are shown in Table 2, together with the data reported for compound *cyclo*[DKP-RGD]-Val-Ala-PTX **33** (Figure 19) and its PEG-bearing analogue *cyclo*[DKP-RGD]-PEG-4-Val-Ala-PTX **41** (Figure 24), as previously published by our group. [50,77,81b]

Screening assays were carried out through incubation of the immobilized integrin receptors with solutions of the tested compounds at different concentrations (10^{-12}-10^{-5} M) in the presence of biotinylated vitronectin, and measuring the concentration of bound vitronectin.

As reported in Table 2, *cyclo*[DKP-RGD] **31** and *cyclo*[RGDfK] **46** showed a similar affinity for the $\alpha_V\beta_3$, with IC_{50} values in the low nanomolar range. However, *cyclo*[RGDfK] **46** proved more selective towards the $\alpha_V\beta_3$ (in comparison with $\alpha_V\beta_5$) than *cyclo*[DKP-RGD] **31**. However, the respective SMDC products did not reflect the observed selectivity, since a more pronounced selectivity for $\alpha_V\beta_3$ integrin was exhibited by SMDC products containing the *cyclo*[DKP-RGD]. In general, all synthesized compounds showed high binding affinity and selectivity for $\alpha_V\beta_3$, with IC_{50} values in the low nanomolar range, comparable with those obtained for the free ligands (**31** and **46**).

Table 2. Inhibition of biotinylated vitronectin binding to the isolated $\alpha_V\beta_3$ and $\alpha_V\beta_5$ receptors.

Compound	Structure	IC_{50} (nM)[a] $\alpha_V\beta_3$	IC_{50} (nM)[a] $\alpha_V\beta_5$
31	*cyclo*[DKP-RGD]	4.5 ± 1.1	149 ± 25
46	*cyclo*[RGDfK]	1.4 ± 0.2	117.5 ± 7.8
37	*cyclo*[DKP-RGD]-GFLG-PTX	54.8 ± 14.0	> 1000[b]
38	*cyclo*[RGDfK]-GFLG-PTX	62.6 ± 10.9	649 ± 136
39	*cyclo*[DKP-RGD]-PEG-4-GFLG-PTX	42.4 ± 7.4	> 1000[b]
40	*cyclo*[RGDfK]-PEG-4-GFLG-PTX	12.1 ± 2.0	473 ± 25
33	*cyclo*[DKP-RGD]-Val-Ala-PTX	13.3 ± 3.6	924 ± 290
41	*cyclo*[DKP-RGD]-PEG-4-Val-Ala-PTX	14.8 ± 3.9	>1000[b]

[a] IC_{50} values were calculated as the concentration of compound required for 50% inhibition of biotinylated vitronectin binding as estimated by GraphPad Prism software. All values are the arithmetic mean ± the standard deviation (SD) of duplicate determinations. [b] Biotinylated vitronectin binding was not completely inhibited in the concentration range tested.

B) Cell viability assays

In order to evaluate the antitumor properties of the new conjugates and to assess the ability of the synthesized compounds to selectively target $\alpha_V\beta_3$ integrin in human cancer cells, antiproliferative assays were carried out using two cell lines with different levels of expression of integrin $\alpha_V\beta_3$. These experiments were performed in collaboration with the National Institute of Oncology (OOI) of Budapest.

U87 cells (human glioblastoma) were chosen as $\alpha_V\beta_3$ expressing cell line and HT29 cells (human colorectal adenocarcinoma) were selected as $\alpha_V\beta_3$ negative. The different $\alpha_V\beta_3$ expression on the cell membrane of the two cell lines was confirmed by flow cytometry (see the Experimental Section) and the results were in keeping with literature data.[88] Both U87 and HT29 cell lines were treated with free PTX and with conjugates **33** and **37-41** and incubated for 96 hours. The choice of this incubation time was made by taking into account the cyclization of the self-immolative *N,N'*-dimethylethylenediamino spacer, which is known to be a slow transformation.
The data emerged from this in vitro assay are shown in Table 3.

Table 3. *In vitro* antiproliferative activity of free PTX and conjugates **33** and **37**-**41** in U87 and HT29 cell lines for 96 hours.

	IC_{50} (nM)[a]				
Comp.	U87 ($\alpha_V\beta_3$+)	HT29 ($\alpha_V\beta_3$–)	RP_{U87}[b]	RP_{HT29}[c]	TI[d]
PTX	32.66 ± 21.81	1.82 ± 1.85	1	1	1
37	2031 ± 454	3413 ± 983	0.01608	0.00053	30
38	1250 ± 293.6	2692 ± 676	0.02613	0.000692	38
39	854.7 ± 165.1	1979 ± 252	0.03821	0.0009196	42
40	506.2 ± 113.6	1272 ± 156	0.06452	0.001431	45
33	2686 ± 589	6452 ± 1723	0.01216	0.0002821	43
41	432.6 ± 129.3	12840 ± 2730	0.07550	0.0001417	533

[a] IC_{50} values were calculated as the concentration of compound required for 50% inhibition of cell viability. Both cell lines were treated with different concentrations of PTX and compounds **33** and **37**-**41** during 96 hours. The samples were measured in triplicate; [b] Relative Potency in U87 cell line (RP_{U87}): IC_{50} PTX in U87/ IC_{50} Conjugate in U87; [c] Relative Potency in HT29 cell line (RP_{HT29}): IC_{50} PTX in HT29/ IC_{50} Conjugate in HT29; [d] Targeting Index (TI): RP_{U87}/RP_{HT29}.

All tested conjugates proved to be less potent than free paclitaxel against both cell lines. However, it has been reported by our group that the use of a RGD-PTX conjugate devoid of peptide linkers and chemically "uncleavable" is normally much less active against cancer cells (i.e. IC_{50} > 10 μM).[50] Furthemore, conjugates bearing the PEG-4 spacer (**39-41**) proved more potent (2.4-6.2 times) against the U87 cell line than the analogs containing the glutarate spacer (**33**, **37** and **38**), which may be ascribed to the enhanced hydrophilicity and flexibility provided by the PEG-4 spacer, which may assist the binding to the receptor.[81a]

In order to quantify the loss of potency of each conjugate with respect to paclitaxel a new parameter was introduced: the Relative Potency (RP), consisting in the ratio IC_{50} PTX/IC_{50} Conjugate calculated for each cell line. It was observed that for all the conjugates, the RP in the HT29 cell line ($\alpha_V\beta_3$-) was 1-2 orders of magnitude lower than in U87 ($\alpha_V\beta_3$+). This indicated that the loss of potency of the conjugates with respect to PTX increases when there is no $\alpha_V\beta_3$ receptor in the cell line, which highlights the selectivity displayed by the RGD conjugates.

Subsequently, RP values of the conjugates were normalized in terms of Targeting Index (TI), which provided a direct evaluation of the ability of these new conjugates to target the $\alpha_V\beta_3$ expressing cell lines (TI= RP_{U87}/RP_{HT29}). Good Targeting Indexes were observed through the whole series, with values between 30-45 (for conjugates **33** and **37-40**).To

our delight, conjugate **41** displayed excellent selectivity, with the highest TI value (TI=533) of the series.

To assess if the observed targeting was ascribable to an integrin-mediated binding and cell internalization process, conjugate **41** was added to the $\alpha_V\beta_3$+ cell line U87 in the presence of 50-fold excess of free ligand *cyclo*[DKP-RGD] (**31**). In this competition experiment, binding site of surface-expressed integrin receptors should be blocked by the excess of free ligand, thus preventing the binding of the conjugates and the following receptor-mediated endocytosis. For this reason, an increase in the IC_{50} values of the conjugates should be observed. The results of this experiment are shown in Table 4.

Table 4. Competition experiments of conjugate **41** in the presence of a 50-fold excess of *cyclo*[DKP-RGD] (**31**) in U87 for 96 hours.

Compound(s)	IC_{50} (nM)[a] U87 ($\alpha_V\beta_3$+)	Inhibition Ratio[b]	Corrected Inhibition Ratio[c]
cyclo[DKP-RGD] (**31**)	$342.8 \cdot 10^3 \pm 94.7 \cdot 10^3$	-	-
PTX	32.66 ± 21.81	-	-
PTX + 50-fold excess *cyclo*[DKP-RGD] (**31**)	10.66 ± 4.8	0.33	1
41	432.6 ± 129.3	-	-
41 + 50-fold excess *cyclo*[DKP-RGD] (**31**)	717.5 ± 216.3	1.66	5.03

[a] IC_{50} values were calculated as the concentration of compound required for 50% inhibition of cell viability. U87 cells were treated with different concentrations compound **41** in the presence of 50-fold excess *cyclo*[DKP-RGD] (**31**) during 96 hours. The samples were measured in triplicates; [b] Inhibition Ratio = (IC_{50} Compound + 50-fold excess **31**) / IC_{50} Compound; [c] Corrected Inhibition Ratio = Inhibition Ratio PTX/Inhibition Ratio **41**.

As foreseen, *cyclo*[DKP-RGD] (**31**) was barely toxic for the U87 cells, with an IC_{50} in the µM range (343 µM), but the treatment was associated to cell morphology changes and cell detachment, which is in line with the physiological nature of integrins as cell adhesion mediators. However, treatment with free ligand was found to enhance the cell sensitivity to paclitaxel, as revealed by the unexpected 3-fold decrease of PTX IC_{50} values. On the contrary, the presence of free ligand resulted in a loss of potency displayed by compound **41**. Taking in consideration the observed synergy between free *cyclo*[DKP-RGD] **31** and PTX, a Corrected Inhibition Ratio was calculated, showing a 5-fold decrease of the cytotoxicity of conjugate **41** in the presence of the free ligand. These results suggest that the internalization process is mediated, at least in part, by the $\alpha_V\beta_3$ receptor.

2.1.3. Conclusions

In this section, four new conjugates bearing the GFLG linker were successfully synthesized (**37**-**40**) and evaluated *in vitro* for their integrin binding and their cell antiproliferative activity. These compounds were evalutated together with two other conjugates containing the Val-Ala linker, previously synthesized in our research group (**33** and **41**). All conjugates exhibited good binding affinity (IC_{50} values in the low nanomolar range) and selectivity towards the $\alpha_V\beta_3$ receptor. In the cell viability assays against U87 ($\alpha_V\beta_3$+) and HT29 ($\alpha_V\beta_3$-), all conjugates were less active than the free PTX payload, with conjugates containing the PEG-4 spacer (**39-41**) showing the highest potency. Furthermore, the RPs values were considerably smaller in HT29 than in U87, indicating the correlation between the cytotoxic activity and the integrin expression.

From this series, *cyclo*[DKP-RGD]-PEG-4-Val-Ala-PTX (**41**) proved the best one, showing TI=533. A competition experiment with this conjugate in the presence of *cyclo*[DKP-RGD] (**31**) demonstrated a 5-fold decreased cytotoxicity, supporting the hypothesis that the RGD-PTX conjugate interacts with the $\alpha_V\beta_3$ receptor and selectively releases the cytotoxic cargo inside integrin-expressing cells. Due to all mentioned before, we consider that conjugate **41** is a good candidate to proceed for *in vivo* experiments in the future.

2.2. Synthesis and biological evaluation of *cyclo*[DKP-RGD]-α-amanitin conjugates.

The selective drug delivery to diseased tissues has been successfully carried out with the use of particular types of cytotoxic agents, which were found to be too potent to be used as “non-targeted” drugs. This approach overcomes the observed physiological decrease of drug potency resulting from the covalent conjugation to a targeting vehicle and it can be considered the key to the marketing success of ADC products. From the pharmacological point of view, the increased drug potency impacts on the therapeutic window of targeted prodrugs by decreasing the minimum effective dose (MED).

Among the variety of cytotoxic agents that have been investigated as anticancer drugs, the amatoxin family is found mostly in the death cap mushroom (*Amanita Phalloides*) and it is known to cause fatal poisoning in humans. As one of the most toxic member of this family, α-amanitin has been isolated around 60 years ago and it has been investigated for therapeutic purposes. From the structural point of view, this toxin consists of a bicyclic octapeptide featuring an intra-annular tryptathionine (highlighted in green in Figure 25). While the extraction from natural source has been the only source of α-amanitin,[89] its total synthesis has been recently published by Mathinkoo *et al*.[90] . It has been reported that α-amanitin mediates cell death by blocking the RNA Polymerase II. This enzyme mediates the cellular transcription of DNA to mRNA and its susceptibility for α-amanitin depends on the species of eukaryotic cell.[91] In most mammalian cells, α-amanitin exhibits low cellular uptake and μM cytotoxicity, since it is a strongly polar and poorly membrane permeable compound.[92] Howerer, the toxin is highly active against mammalians’ hepatocytes , since they express the OATP1B3 transporter on their surface, which is responsible for the internalization of amatoxins and, as a result, for the related hepatic failure.[93]

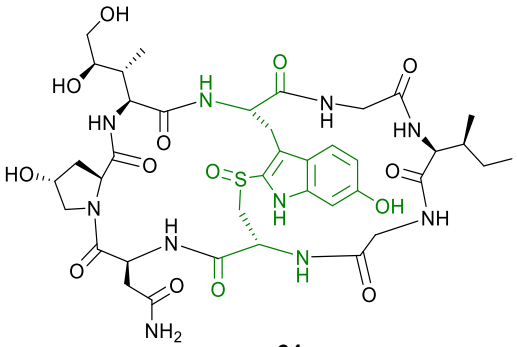

61

Figure 25. Structure of α-amanitin**.**

This transporter-mediated mechanism of internalization suggests that the conjugation of α-amanitin to devices able to bind internalizing tumor antigens might be a successful approach for cancer therapy. One of the first antibody-drug conjugates bearing α-amanitin was developed in 1981.[94] This product, raised against protein Thy-1.2 (a transmembrane murine receptor, expressed on murine T cells) was featured α-amanitin as payload and it was evaluated *in vitro* against the T lymphoma S49.1 cell line. In this test, the ADC product showed higher toxicity than the free α-amanitin. More recently, Moldenhauer and coworkers synthesized an anti-EpCAM-α-amanitin conjugate (i.e. a chimerized monoclonal antibody targeting the epithelial cell-adhesion molecule EpCAM). After two injections of this ADC (at 100 μg/kg dose), complete tumor regression in 90% of the mice bearing BxPc-3 pancreatic xenograft tumors was observed.[95] Besides the ADC application, α-amanitin has been also conjugated to a pH low insertion peptide (pHLIP), capable of improving the internalization of the peptide payload through a pH-mediated translocation across the membrane, followed by intracellular cleavage of a disulfide linker.[96] Finally, in 2015, Perrin and co-workers conjugated the *cyclo*[RGDfK] integrin ligand to an amanitin analog through a triazole ring.[97] The conjugate was tested *in vitro* against the U87 glioblastoma cell line, but the conjugate was found to be only slightly more potent than the free α-amanitin.

Inspired by this literature data, and in collaboration with Heidelberg Pharma (HDP) we developed two SMDCs containing the α-amanitin toxin conjugated and the functionalized *cyclo*[DKP-RGD] **32** through both a lysosomally-cleavable Val-Ala and an uncleavable, nonpeptide linker (Figure 26). The latter was prepared to be used as control compound for the biological assays.

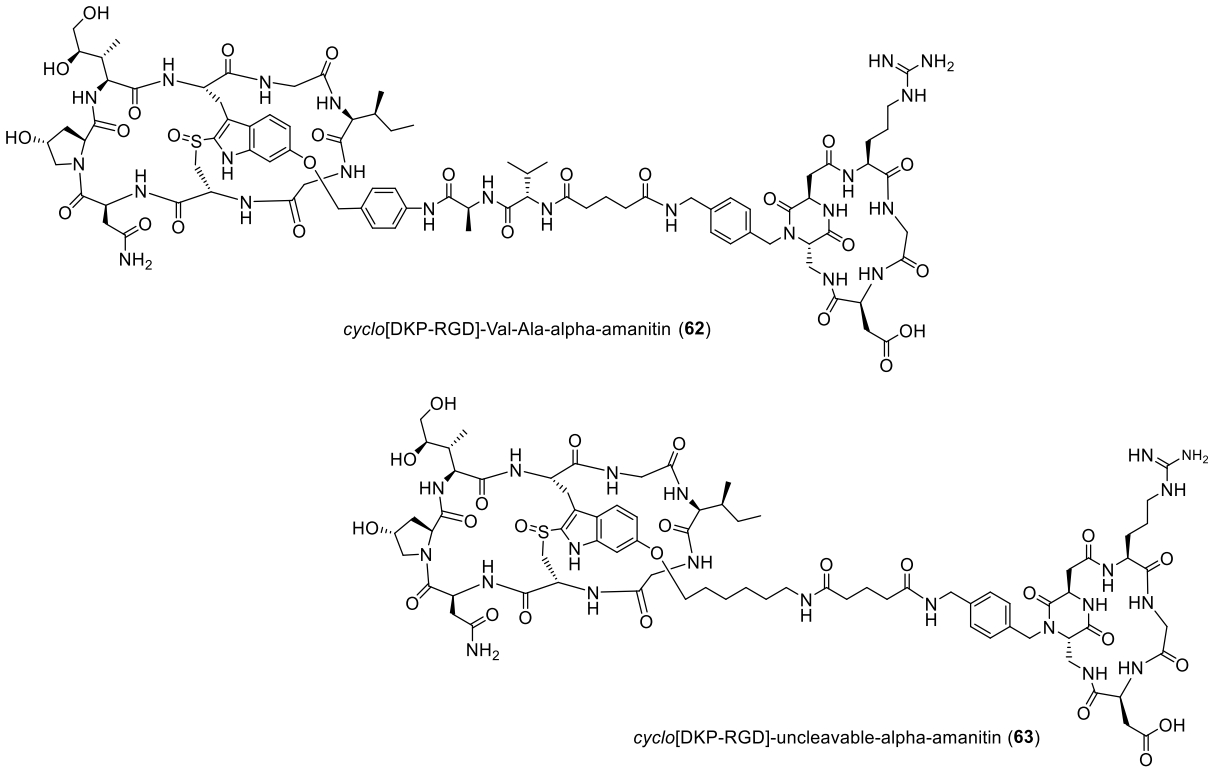

Figure 26. Structures of *cyclo*[DKP-RGD]-Val-Ala-α-amanitin (**62**) and *cyclo*[DKP-RGD]-uncleavable- α-amanitin (**63**).

2.2.1. Synthesis

Compounds **62** and **63** were prepared following similar synthetic strategies as described in Scheme 6.

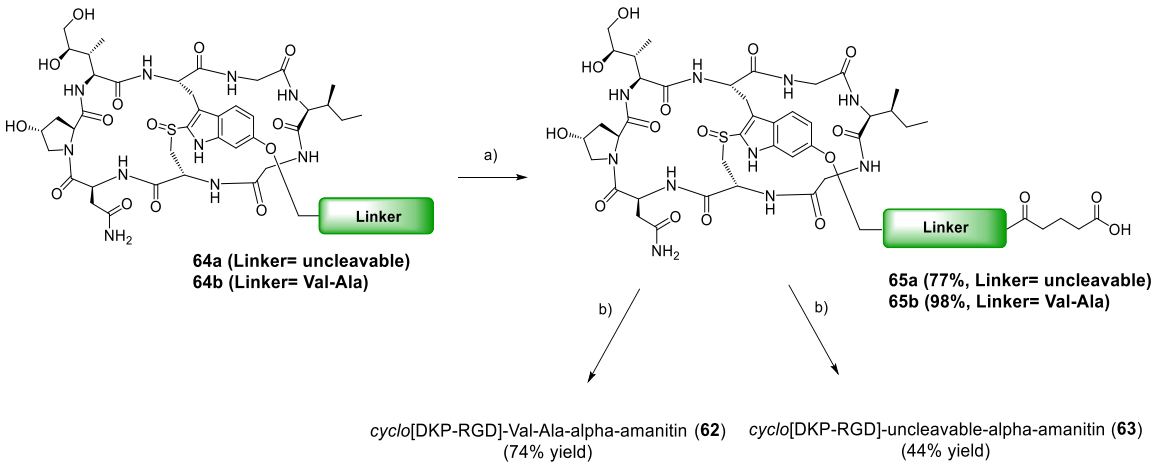

Scheme 6. General synthesis of α-amanitin-RGD derivatives. Reagents and conditions: a) glutaric anhydride, DMAP, *i*Pr$_2$NEt, DMF, overnight, b) i. DIC, *N*-hydroxysuccinimide (NHS), DMF, overnight; ii. *cyclo*[DKP-RGD]-CH$_2$NH$_2$ (**32**), PBS/DMF (for conjugate **62**) or PBS/CH$_3$CN (for conjugate **63**) (pH 7.5), overnight. DMAP: 4-dimethylaminopyridine; DIC: *N,N'*-diisopropylcarbodiimide; PBS: phosphate-buffered saline.

The α-amanitin compounds containing either the uncleavable (**64a**) or the Val-Ala (**64b**) linker were provided by HDP and directly reacted with glutaric anhydride to form compounds **65a** and **65b**, respectively. Initially, low yield was observed for **65a** (41%), as the reaction proceeded with the formation of a side product. The modulation of the stoichiometry improved the yield of the reaction up to 77% for **65a** and 98% for **65b**. Both compounds were activated as *N*-hydroxysuccimidyl esters and directly coupled to the functionalized *cyclo*[DKP-RGD] (**32**) affording final compounds **62** and **63**.

2.2.2. *In vitro* biological evaluation

A) Integrin receptor competitive binding assays

Analogously to the SMDC products bearing the GFLG linker (section 2.1.), the two new *cyclo*[DKP-RGD]-α-amanitin conjugates were evaluated by their ability to inhibit biotinylated vitronectin binding to the purified $\alpha_V\beta_3$ receptor. The calculated IC_{50} values are shown in Table 5. This analysis was carried out in parallel with other three conjugates synthesized in the research group of Prof. Umberto Piarulli (University of Insubria), bearing the integrin ligand *cyclo*[DKP-*iso*DGR] (compound **66** and its amine-bearing derivative **67**, depicted in Figure 27). This compound was developed as analogue of the most well-known RGD-bearing peptidomimetics, in which the RGD sequence is substituted with an *iso*aspartate-glycine-arginine tripeptide. The latter is also recognized by integrins and the *cyclo*[DKP-*iso*DGR] was found to bind $\alpha_V\beta_3$ receptor with low nanomolar affinity.[98] The resulting *cyclo*[DKP-*iso*DGR]-α-amanitin conjugates were structurally similar to the RGD-bearing analogs **62** and **63**. In particular, the ligand and the α-amanitin were connected through either a Val-Ala dipeptide or an uncleavable nonpeptide linker (in compound **68** and **69**, respectively). Furthermore, a third structure containing the PEG-4 spacer was also included (**70**).

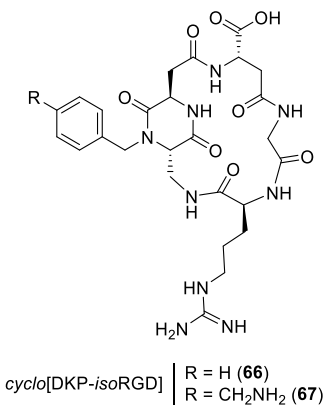

Figure 27. Structure of both the *cyclo*[DKP-*iso*DGR] (**66**) and the aminomethyl functionalized *cyclo*[DKP-*iso*DGR] (**67**).

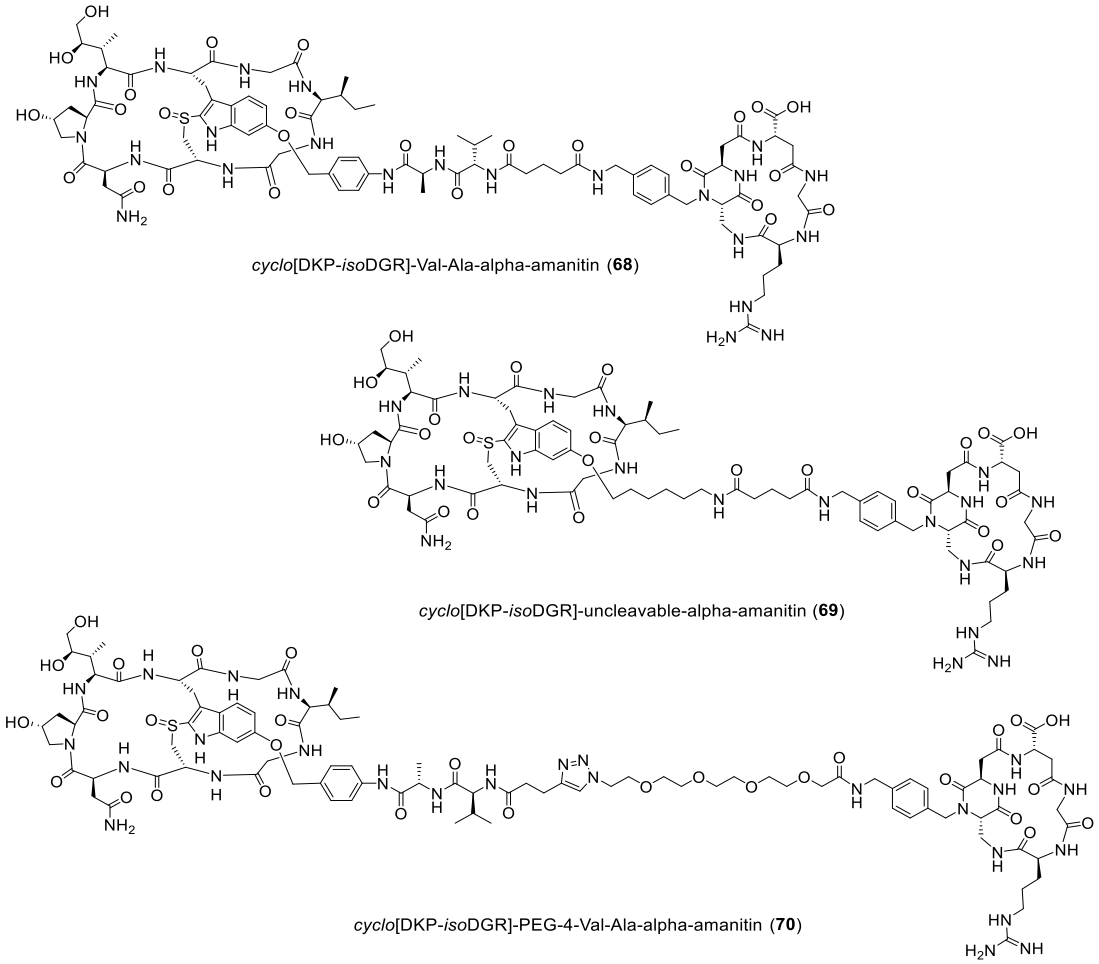

Figure 28. Structures of *cyclo*[DKP-*iso*DGR]-Val-Ala-α-amanitin (**68**), *cyclo*[DKP-*iso*DGR]-uncleavable-α-amanitin (**69**), and *cyclo*[DKP-*iso*DGR]-PEG-4-Val-Ala-α-amanitin (**70**).

Table 5. Inhibition of biotinylated vitronectin binding to the isolated $\alpha_V\beta_3$ receptor

Compound	Structure	IC_{50} (nM)[a] $\alpha_V\beta_3$
31	*cyclo*[DKP-RGD]	4.5 ± 1.1
66	*cyclo*[DKP-*iso*DGR]	9.2 ± 1.1
63	*cyclo*[DKP-RGD]-uncleavable-α-amanitin	11.6 ± 2.4
69	*cyclo*[DKP-*iso*DGR]-uncleavable-α-amanitin	6.8 ± 4.3
62	*cyclo*[DKP-RGD]-Val-Ala-α-amanitin	14.7 ± 6.6
68	*cyclo*[DKP-*iso*DGR]-Val-Ala-α-amanitin	6.4 ± 1.9
70	*cyclo*[DKP-*iso*DGR]-PEG-4-Val-Ala-α-amanitin	3.8 ± 0.3

[a] IC_{50} values were calculated as the concentration of compound required for 50% inhibition of biotinylated vitronectin binding as estimated by GraphPad Prism software. All values are the arithmetic mean ± the standard deviation (SD) of duplicate determinations.

The results showed that both *cyclo*[DKP-RGD]-α-amanitin and *cyclo*[DKP-*iso*DGR]-α-amanitin conjugates (**62**-**63 and 68-70**) bind to the purified $\alpha_v\beta_3$ receptor at low nanomolar ranges despite the presence of the bulky α-amanitin drug. The IC_{50} values where found to be in the same range of the one of free ligands *cyclo*[DKP-RGD] **31** and *cyclo*[DKP-*iso*DGR] **66**.

B) Cell viability assays

With the aim to evaluate the selective release of α-amanitin to human cancer cells expressing $\alpha_V\beta_3$ integrin, antiproliferative assays were carried out as described in Section 2.1. U87 glioblastoma cells were selected as $\alpha_V\beta_3$ positive cell line, while MDA-MB-468 (breast adenocarcinoma) and A549 (human lung carcinoma) were selected as $\alpha_V\beta_3$ negative cells. Even though literature data about the presence of the β_3 subunit in MDA-MB-468 are often contradictory,[88a, 99] we performed FACS analysis revealing no $\alpha_V\beta_3$ expression in our experimental conditions.

The two *cyclo*[DKP-RGD]-α-amanitin and the three *cyclo*[DKP-*iso*DGR]-α-amanitin conjugates were added to the cell lines at different concentrations, in parallel with free α-amanitin, and incubated for 96 hours. Cell viability was evaluated with the CellTiterGlo 2.0 assay and the results are shown in Table 6.

Table 6. Antiproliferative activity of free α-amanitin and conjugates **62-63** and **68-70** in U87, MDA-MB-468 and A549 cell lines for 96 hours.

Comp.	Structure	IC_{50} (nM)[a]		
		U87 ($\alpha_V\beta_3$+)	MDA-MB-468 ($\alpha_V\beta_3$-)	A549 ($\alpha_V\beta_3$-)
61	α-amanitin	347 ± 132.5[b]	185 ± 49.6[b]	518 ± 305[b]
63	*cyclo*[DKP-RGD]-uncleavable-α-amanitin	2552 ± 37.6	1111 ± 228.4	n.d.[c]
69	*cyclo*[DKP-*iso*DGR]-uncleavable-α-amanitin	3355 ± 19.1	2200 ± 96.2	n.d.[c]
62	*cyclo*[DKP-RGD]-Val-Ala-α-amanitin	1446 ± 83.9	202 ± 10.3	2160 ± 23.3
68	*cyclo*[DKP-*iso*DGR]-Val-Ala-α-amanitin	143 ± 33.8	59 ± 23.4	217 ± 98.3
70	*cyclo*[DKP-*iso*DGR]-PEG-4-Val-Ala-α-amanitin	165 ± 4.0	66 ± 24.1	720 ± 98.1

[a] IC_{50} values were calculated as the concentration of compound required for 50% inhibition of cell viability. All cell lines were treated with different concentrations of α-amanitin and compounds **62-63** and **68-70** for 96 hours. The samples were measured in triplicate; [b] Average values from three independent experiments; [c] n.d.: these data could not be determined.

As reported for the previous paclitaxel-bearing conjugates, *cyclo*[DKP-RGD]-uncleavable-α-amanitin (**63**) and *cyclo*[DKP-*iso*DGR]-uncleavable α-amanitin (**69**), proved less potent than the free toxin, against all treated cell lines. However, while the *cyclo*[DKP-RGD]-α-amanitin conjugate bearing Val-Ala (**62**) showed also decreased potency against all cells, IC_{50} values were much lower than the uncleavable analogs. Interestingly, *cyclo*[DKP-*iso*DGR]-Val-Ala-α-amanitin (**68**) proved moderately more potent than α-amanitin in the three cell lines (2.4-3.1 times), while *cyclo*[DKP-*iso*DGR]-PEG-4-Val-Ala-α-amanitin (**70**) proved more potent only against U87 and MDA-MB-468 (2.1-2.8 times). In general, these data seemed to indicate that the *iso*DGR ligand may mediate a better internalization of the cytotoxic payloads, albeit with no significant correlation with the expression of $\alpha_V\beta_3$ on the cell surface.

This observation may be ascribed to the fact that both U87 and MDA-MB-468 cell lines express other integrin receptors different from $\alpha_V\beta_3$. For this reason, competition experiments of ligand-drug conjugates in the presence of free integrin ligand were carried out in order to determine if the observed cytotoxicity is given by non-specific interactions with the targeted cells or by an integrin-mediated process. *Cyclo*[DKP-*iso*DGR]-Val-Ala-α-amanitin (**68**) and *cyclo*[DKP-*iso*DGR-PEG-4-Val-Ala-α-amanitin (**70**) were tested against U87 ($\alpha_V\beta_3$ +, $\alpha_V\beta_5$ +, $\alpha_V\beta_6$ -, $\alpha_5\beta_1$ +) and MDA-MB-468 ($\alpha_V\beta_3$ -, $\alpha_V\beta_5$ +, $\alpha_V\beta_6$ +, $\alpha_5\beta_1$ -) cells, in the presence of 50-fold molar excess of cilengitide (Table 7).[88b,99,100] The latter

was chosen considering its high affinity for a panel of integrin heterodimers, such as $\alpha_V\beta_3$, $\alpha_V\beta_5$, $\alpha_V\beta_6$ and $\alpha_5\beta_1$.[101]

In vitro test against U87 cells showed that the excess of free ligand did not influence the biological activity of compound *cyclo*[DKP-*iso*DGR]-PEG-4-Val-Ala-α-amanitin (**70**), as observed from the non-significant increase of IC_{50} values, from 91 nM (in the absence of cilengitide) to 143 nM (with cilengitide). On the other hand, a more significant increase of IC_{50} values was observed for both compounds against MDA-MB-468 cells: from 47 nM (in the absence of cilengitide) to 259 nM (with cilengitide) for conjugate **68** and from 65 nM to 340 nM for conjugate **70**.

These results suggest that this two conjugates can, at least partially, bind and be internalized by integrins different from $\alpha_V\beta_3$ (e.g. $\alpha_V\beta_5$). However, the exact nature of this process is not clearly defined yet and further studies are needed.

Table 7. Competition experiments of conjugate **68** and **70** in the presence of a 50-fold excess of cilengitide in U87 for 96 hours.

Structure	IC_{50} (nM)[a]	
	U87 ($\alpha_V\beta_3$+, $\alpha_V\beta_5$+, $\alpha_V\beta_6$-, $\alpha_5\beta_1$+)	MDA-MB-468 ($\alpha_V\beta_3$-, $\alpha_V\beta_5$+, $\alpha_V\beta_6$+, $\alpha_5\beta_1$-)
cyclo[DKP-*iso*DGR]-Val-Ala-α-amanitin (**68**)	107 ± 26.8	47 ± 21.1
cyclo[DKP-*iso*DGR]-Val-Ala-α-amanitin (**68**) + 50-fold excess of cilengitide	106 ± 11.6	259 ± 55.2
cyclo[DKP-*iso*DGR]-PEG-4-Val-Ala-α-amanitin (**70**)	91 ± 30.6	65 ± 17.6
cyclo[DKP-*iso*DGR]-PEG-4-Val-Ala-α-amanitin (**70**) + 50-fold excess of cilengitide	143 ± 59.3	340 ± 210.3

[a] IC_{50} values were calculated as the concentration of compound required for 50% inhibition of cell viability. Both cell lines were treated with different concentrations of compounds **68** and **70** in the presence of a 50 fold excess of cilengitide during 96 hours. The samples were measured in triplicates.

2.2.3. Conclusions

In this section, two new *cyclo*[DKP-RGD]-α-amanitin conjugates (**62** and **63**) were synthesized and evaluated *in vitro* for their integrin receptor binding affinity and their antiproliferative activity. These compounds were evaluated together with three other conjugates containing the *cyclo*[DKP-*iso*DGR] ligand (**68**-**70**). Despite the presence of the bulky α-amanitin drug, the conjugates bound the $\alpha_V\beta_3$ receptor in the low nanomolar

range, with IC_{50} values comparable to those of the free ligands. In cell viability assays, a loss of potency was observed for *cyclo*[DKP-RGD]-Val-Ala-α-amanitin (**62**) and the two conjugates bearing the uncleavable linker (**63** and **69**). On the other hand, *cyclo*[DKP-*iso*DGR]-Val-Ala-α-amanitin (**68**) and *cyclo*[DKP-*iso*DGR]-PEG-4-Val-Ala-α-amanitin (**70**) showed better IC_{50} against all tested cell lines, proving that the *iso*DGR motif can display higher potency against cancer cell lines, even though no direct correlation was observed between the $\alpha_V\beta_3$ expression and the observed cytotoxic activity. Competition experiments carried out with the two latter compounds (**68** and **70**) demonstrated that a more marked increase of the IC_{50} values in the presence of cilengitide occurred when the MDA-MB-468 cell line ($\alpha_V\beta_3$ -, $\alpha_V\beta_5$ +, $\alpha_V\beta_6$ +, $\alpha_5\beta_1$ -) were studied, suggesting that this two conjugates are possibly bound and internalized by integrins different from $\alpha_V\beta_3$ (e.g. $\alpha_V\beta_5$).

Chapter 3: Conjugates containing extracellular MMP-2 cleavable linkers

While the antigen internalization has been often indicated as a key requirement for the efficacy of targeted therapeutics, the development of new drug delivery platforms, capable of releasing the payload in the extracellular environment, is an emerging approach for drug delivery.[102] This strategy relies on the accumulation of ADCs or SMDCs at the tumor site, mediated by the binding to non- or poorly internalizing proteins. Here, the release of the free drug takes place extracellularly, upon action of specific extracellular effectors (e.g., extracellular reducing agents, pH, enzymes, etc.). Once released in the extracellular milieu, the free drug should enter the cancer cells by passive diffusion, causing localized damage (Figure 29) and, potentially, kill cancer cells that may not express the targeted antigen.[103] Considering this mechanism of action, the success of these conjugates is determined by different features, such as the efficacy of the ligand or antibody to accumulate in the tumor mass, the kinetic of drug release or the presence of a suitable linker-payload tandem (e.g., highly lipophilic and membrane-permeable drugs should be preferable). This approach proved effective in several mouse models of cancer, and it has been proposed as a valid approach, especially against certain types of solid tumors. In this Chapter, new Small Molecule-Drug Conjugates have been developed to target $\alpha_V\beta_3$ integrin and, assuming the slow internalization process of the transmembrane antigen, these conjugates were designed to be activated by the extracellular Matrix Metalloproteinase 2 (MMP-2, also known as gelatinase A).

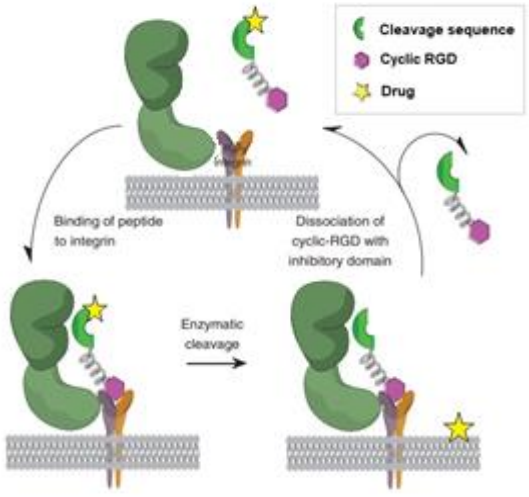

Figure 29. Mechanism of extracellular drug release of conjugates.[104]

MMP-2 is one of the 25 members of the MMP family (also called matrixins), which are zinc-dependent endopeptidases that play important roles in the degradation of collagen, elastin, fibronectin, laminin and other proteins, such as cell adhesion molecules and growth factor receptors. MMP-2 and other MMPs (MMP-1, MMP-14, MMP-18, etc.) unwind and cleave the triple helix of interstitial collagens, which constitutes the first step in the degradation of extracellular matrix compounds.[105] The MMPs are classified on the basis of the substrate recognition (MMP-2 is known to recognize collagens IV, V, VII, X and gelatin). It is now widely accepted that the ECM remodeling mediated by these proteins sustains significantly tumor growth and development.[106] For this reason, these proteins are overexpressed in many human tumors and, specifically, the expression of MMP-2 is elevated in breast, prostate, colorectal, ovary, bladder and gastric cancer.[107] MMP-2 is formed by three fundamental domains (propeptide, catalytic and hemopexin/vitronectin like domain) and it is initially secreted as an inactive zymogen (proenzyme). After proteolytic cleavage, the soluble active form is produced and trapped by cancer cell surface receptors.[107b]

In particular, MMP-2 was found to colocalize with $\alpha_V\beta_3$ *in vivo* in angiogenic blood vessels and melanoma tumors.[108] The presence of the $\alpha_V\beta_3$-MMP-2 complex on the cell surface of tumors has been described as a marker of aggressive tumors, as the interaction of the hemopexin C domain of MMP-2 and $\alpha_V\beta_3$ is necessary for cell invasion and angiogenesis.[109]

The MMP-2 enzyme is able to recognize and cleave several peptides of different lengths.[110] Most part of the substrates described in the literature vary from 6 to 9 amino acids and they have been used as linkers in different drug delivery systems, such as dendrimers, nanoparticles and peptide-drug conjugates.[111] It has been observed that sequences starting with the Gly-Pro-Leu-Gly (GPLG) tetrapeptide are cleaved at the C-terminal Gly residue with high proteolytic rates.[112] For this reason, many peptides containing either GPLG or the shortened PLG sequence have been used for imaging of MMP-2 activity and for the extracellular delivery of cytotoxic agents.[113] Among them, Gly-Pro-Leu-Gly-Val-Arg-Gly (GPLGVRG) has been widely studied.[114] For instance, the peptide was derivatized by Bremer *et al.* in 2001 with a C-terminal lysine (resulting in the peptide GPLGVRGK), which was coupled to the fluorophore FITC (fluorescein-5-isothiocyanate). Furthemore, this structure was attached to a copolymer (methoxy-polyethylene-glycol-derivatized poly-L-lysine), labeled with a near-infrared dye (Figure 30). As long as the peptide is intact, the NIR fluorophore is quenched by proximity with FITC. By contrast, after cleavage of the MMP-2 linker, the increased dye fluorescence can be used to monitor MMP-2 activity.

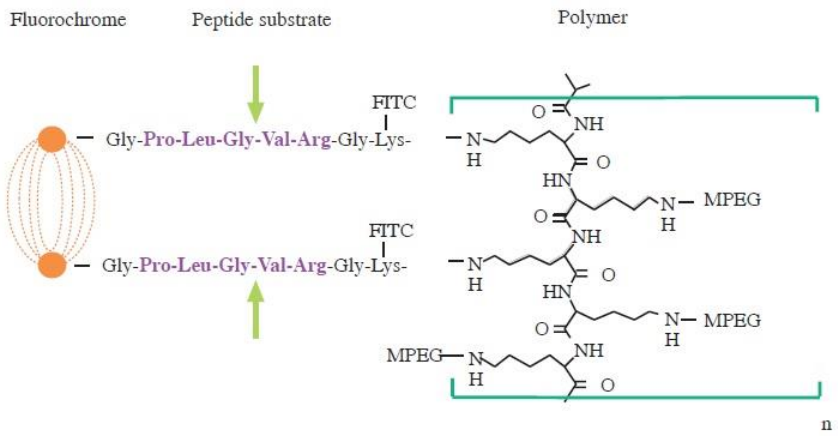

Figure 30. Structure of the MMP-2 cleavable probe bearing two fluorophores and a copolymer developed by Bremer *et al.* [115]

This construct was tested *in vivo* in mice bearing the BT20 tumor (which had been indicated as low MMP-2-expressing cells) and HT1080 (which was reported to produce high amounts of MMP-2). It was observed that, in the first case, a lower fluorescence signal was observed in comparison with the HT1080 tumors (31.0 ± 6.6 versus 85.0 ± 5.1 AU).[115]

Inspired by these applications and by the observation of the MMP-2/$\alpha_V\beta_3$ colocalization, we designed two conjugates containing MMP-2 cleavable linkers. In the first case, *cyclo*[RGDfK] **46** was connected to the anthracycline daunorubicin (Dau) through the GPLGVRG linker (Figure 31, compound **71**). In this case, daunorubicin was connected via the *N*-terminus of the linker. Furthemore, Dau was connected to the GPLGVRG linker through an aminoxy acetate spacer, taking advantage of its high chemoselectivity for the ketone group of Dau. It is known that functionalizations of this C-13 ketone group do not affect dramatically the antitumor effect.[51a] Furthemore, the oxyme bond is known to be highly hydrolitycally and chemically stable (at pH values between 3 and 8), avoiding premature drug release in circulation.[116] For this reason, SMDC **71** was designed to be activated by MMP-2, leading to the release of active metabolite **72.**

Following an alternative approach, *cyclo*[RGDfK] **46** was connected to paclitaxel (PTX) through the GPLG sequence. The resulting conjugate **73** was designed as structural

analogue of RGD-PTX compounds described in the previous Chapters, featuring the same payload and "two-step" self-immolative spacer.

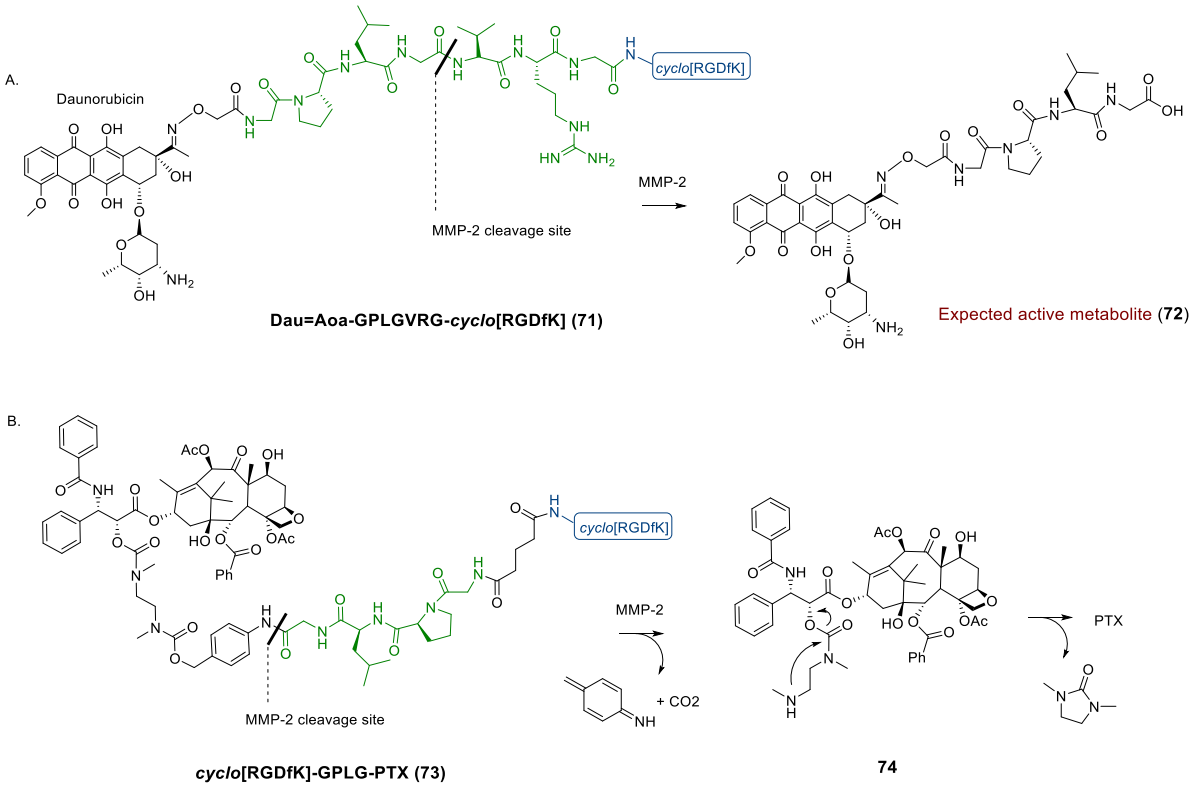

Figure 31. A. Molecular structure of Dau=Aoa-GPLGVRG-*cyclo*[RGDfK] (**71**); **B.** Molecular structure of *cyclo*[RGDfK]-GPLG-PTX (**73**) and mechanism of PTX release.

3.1. Synthesis

*A) Synthesis of Dau=Aoa-GPLGVRG-cyclo[RGDfK] (**71**)*

Compound **71** was synthesized as depicted in Scheme 7. The peptide linker of compound **71** was synthesized on 2-chlorotrityl resin following the Fmoc protocol, as described in section 2.1.1. In the initial steps of the SPPS, a clear detection of proline loading with traditional colorimetric tests was not possible, which made necessary the cleavage of small portions of resin, followed by LC-MS analysis of the detached material.

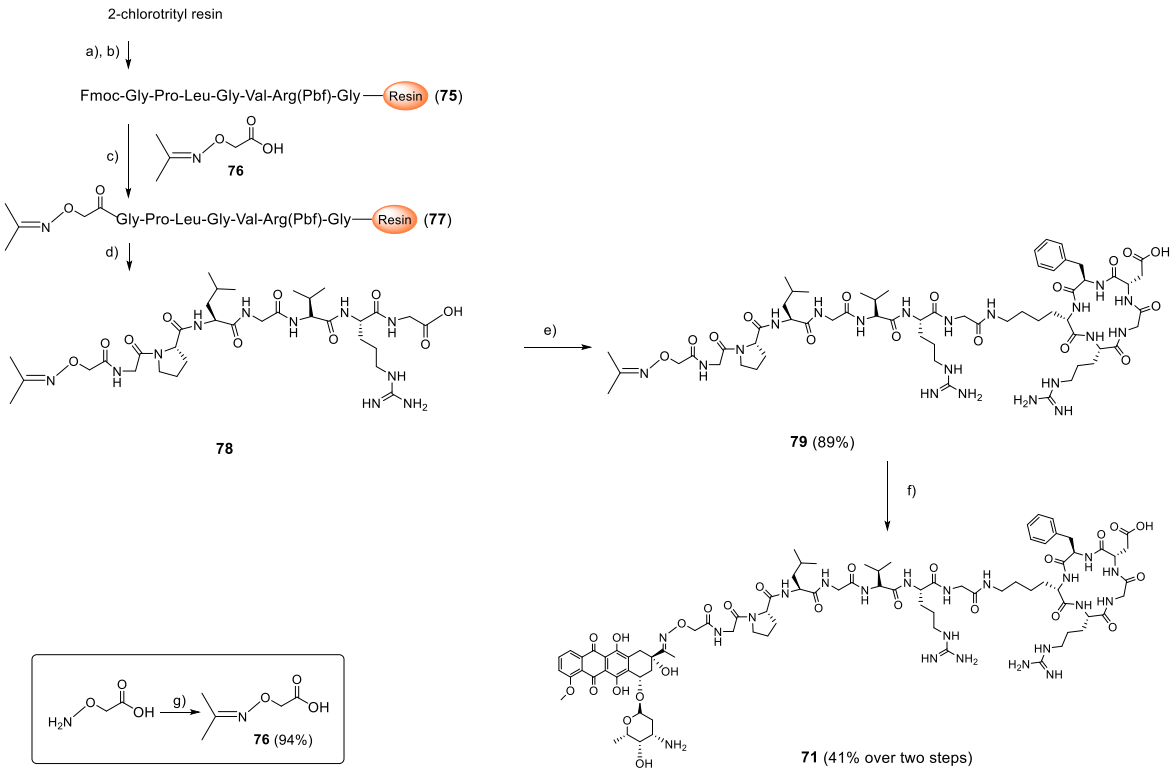

Scheme 7. a) i. Fmoc-Gly-OH (1 equiv.), *i*Pr$_2$NEt (3 equiv.), 1:1 CH_2Cl_2/DMF, 2 h, r.t.; ii. Capping with 7:2:1 CH_2Cl_2/MeOH/*i*Pr$_2$NEt; b) i. Fmoc-deprotection: 2% DBU, 2% piperidine, DMF, 1 h; ii. Fmoc-AA-OH (3 equiv.), HOBt (4 equiv.), DIC (4 equiv.), 2 h; conditions (b) are repeated for the coupling of every amino acid of the sequence; c) i. Fmoc-deprotection: 2% DBU, 2% piperidine, DMF; ii. 2-((propan-2-ylideneamino)oxy)acetic acid **76** (1 equiv.), HOBt (4 equiv.), DIC (4 equiv.), 2 h; d) 95/2.5/2.5 TFA/TIS/H_2O, 3 h., precipitation in diethyl ether; e) i.Pre-activation: BOP (0.9 equiv.), *i*Pr$_2$NEt (2.7 equiv.), DMF, 20 mins; ii. *Cyclo*[RGDfK] (**46**); f) i. *O*-methyloxylamine hydrochloride, NH_4OAc buffer; 2h.; ii. Daunorubicin, NH_4OAc buffer, 2 days; g) acetone, r.t., 45 mins. DBU = 1,8-Diazabicyclo[5.4.0]undec-7-ene; AA = amino acid; BOP = (benzotriazol-1-yloxy)tris(dimethylamino)phosphonium hexafluorophosphate; DIC = *N,N'*-diisopropylcarbodiimide.

After the synthesis of the peptide sequence, the protected 2-((propan-2-ylideneamino)oxy)acetic acid **76** was coupled on resin, following the same protocol described for the amino acids coupling. This compound was previously synthesized by protection of the commercially available 2-(aminooxy)acetic acid (Aoa) with acetone for 45 minutes, affording the protected compound **76** in 94% of yield.

Finally, the peptide sequence was cleaved from the resin with 95/2.5/2.5 TFA/TIS/H_2O mixture. These highly acidic conditions were chosen in order to isolate the peptide devoid of the Pbf group on the arginine side chain. Later on, compound **78** was successfully coupled to the *cyclo*[RGDfK] integrin ligand: after several trials of unsuccessful activation of **78** with either *N*-hydroxysuccinimide or *N*-hydroxyphthalimide, the compound was pre-

activated with BOP and *i*Pr_2NEt and then coupled with *cyclo*[RGDfK] **46**, leading to compound **79** in high yields. As last step, the aminooxy acetate was deprotected and coupled directly with daunorubicin, affording the final Dau=Aoa-GPLGVRG-*cyclo*[RGDfK] (**71**).

*B) Synthesis of cyclo[RDGfK]-GPLG-PTX (**73**)*

Compound **73** was synthesized as described in Scheme 8. The Fmoc-GPLG-OH sequence was produced following the same SPPS protocol described in the previous section for Dau=Aoa-GPLGVRG-*cyclo*[RGDfK] (**71**). Since this peptide sequence did not show any acid-labile groups on the amino acid side chains, a milder cleavage cocktail was tested. In particular, treatment of the resin with a 8:1:1 CH_2Cl_2/MeOH/AcOH mixture led successively to compound **81**, which was later treated with 4-aminobenzyl alcohol and EEDQ, to yield compound **82**. The following steps leading to compound **85** were carried out as described before (section 2.1.1., synthesis B). Also in this case, pre-activation of **85** with BOP and *i*Pr_2NEt and coupling with *cyclo*[RGDfK[(**46**), led to the isolation of compound **86**. Upon Boc removal, the resulting amine was reacted with 2'-(4-nitrophenoxycarbonyl)paclitaxel (**60**). The crude residue was purified by semipreparative HPLC affording **73**.

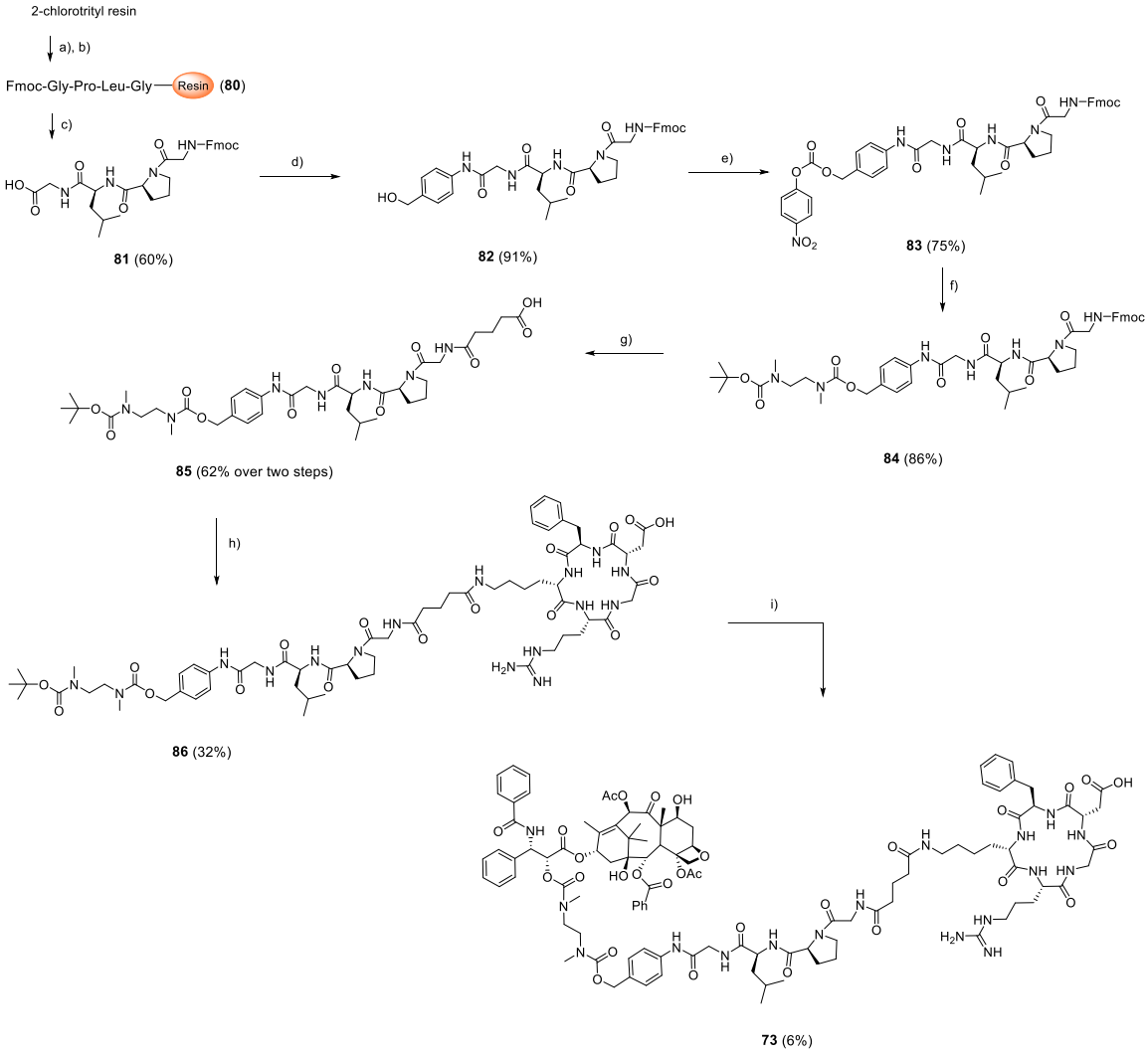

Scheme 8. a) i. Fmoc-Gly-OH (1 equiv.), *i*Pr$_2$NEt (3 equiv.), 1:1 CH_2Cl_2/DMF, 2 h, r.t.; ii. Capping with 7:2:1 CH_2Cl_2/MeOH/*i*Pr$_2$NEt; b) i. Fmoc-deprotection: 2% DBU, 2% piperidine, DMF; ii. Fmoc-AA-OH (3 equiv.), HOBt (4 equiv.), DIC (4 equiv.), 2 h; conditions (b) are repeated for the coupling of every amino acid of the sequence; c) 8:1:1 CH_2Cl_2/MeOH/AcOH, 2 h, precipitation in water; d) EEDQ, 4-aminobenzyl alcohol, CH_2Cl_2, overnight; e) 4-nitrophenylchloroformate, pyridine, CH_2Cl_2, overnight; f) *N*-Boc-*N,N'*-dimethylethylenediamine **59**, *i*Pr$_2$NEt, CH_2Cl_2, overnight; g) i. Piperidine (5 equiv.), CH_2Cl_2, 3 h; ii. glutaric anhydride, DMAP, *i*Pr$_2$NEt, CH_2Cl_2, overnight; h) i.Pre-activation: BOP (0.9 equiv.), *i*Pr$_2$NEt (2.7 equiv.), DMF, 20 min; ii. *Cyclo*[RGDfK] (**46**); i) i. TFA, CH_2Cl_2, 1h.; ii. 2'-(4-nitrophenoxycarbonyl)PTX **60**, *i*Pr$_2$NEt, DMF, overnight. DBU = 1,8-Diazabicyclo[5.4.0]undec-7-ene; AA = amino acid; BOP = (benzotriazol-1-yloxy)tris(dimethylamino)phosphonium hexafluorophosphate; DIC = *N,N'*-diisopropylcarbodiimide; EEDQ= *N*-Ethoxycarbonyl-2-ethoxy-1,2-dihydroquinoline.

3.2. Cleavage experiments in the presence of MMP-2

The effective cleavage of the peptide linker of Dau=Aoa-GPLGVRG-*cyclo*[RGDfK] (**71**) was evaluated in the presence of recombinant Human MMP-2 in TCNB-buffer (pH=7.5)

and the metabolites assessed by HPLC-MS analysis. The peptide:enzyme rate was 100:1. Unfortunately, *cyclo*[RGDfK]-GPLG-PTX (**73**) was not soluble under the experimental conditions, and its kinetics of drug release are still under investigation.

The results are shown below:

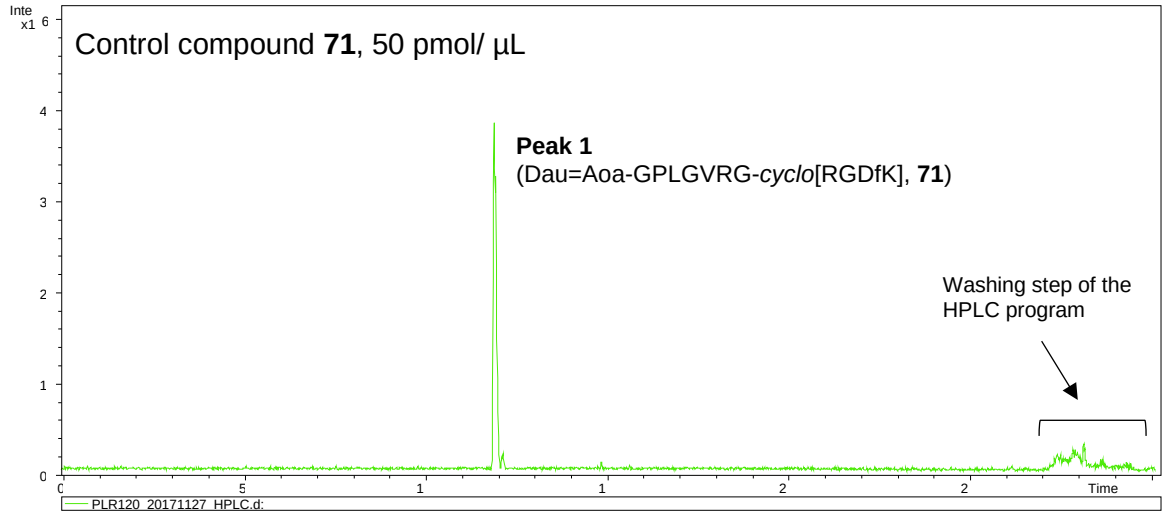

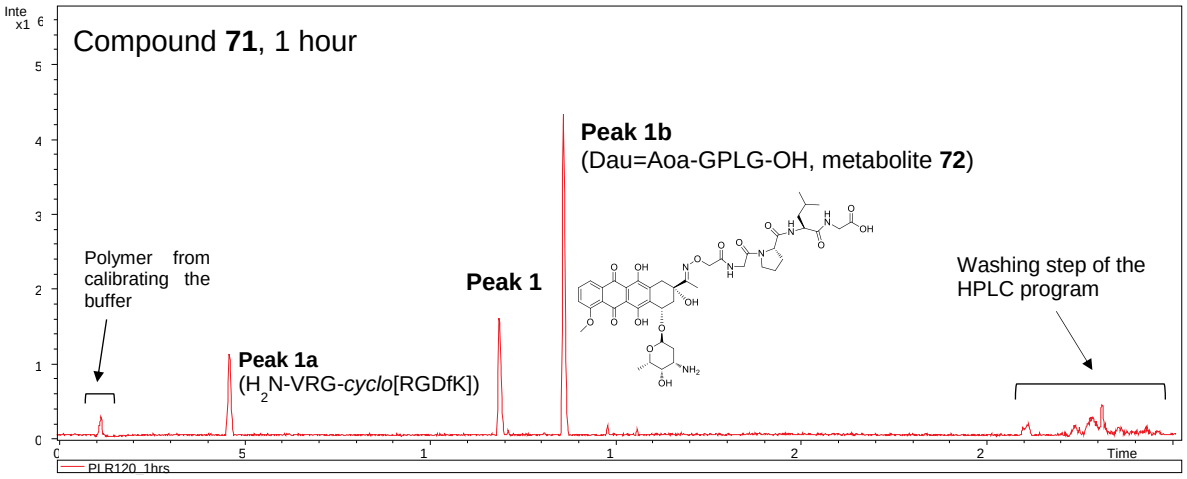

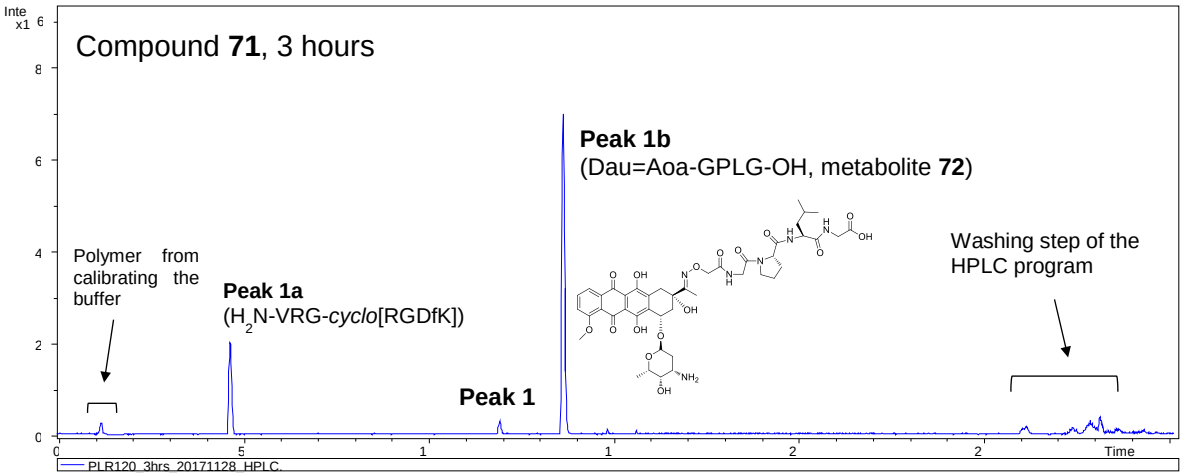

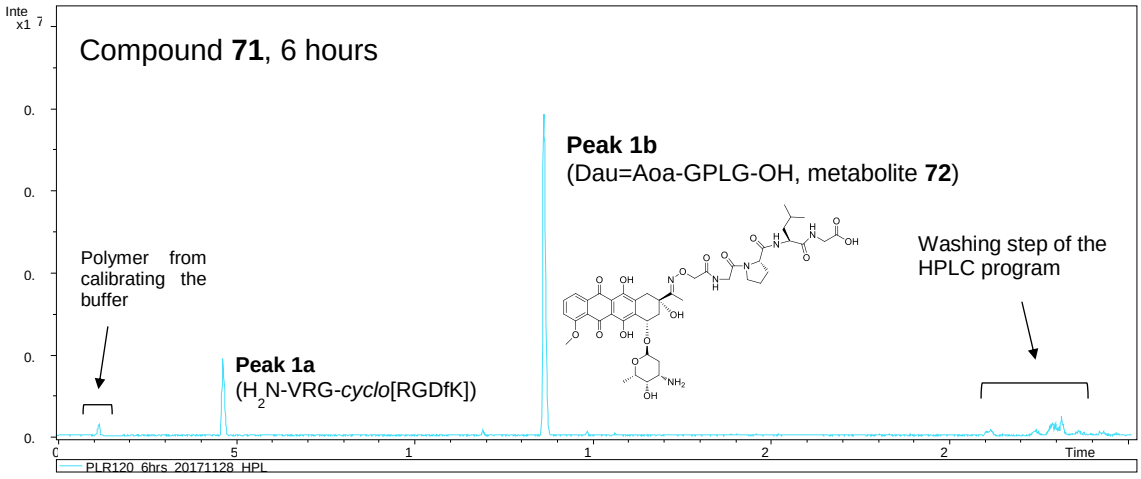

As expected, the preferred cleavage site is between Gly and Val. It was observed that the formation of the active metabolite **72** started after 1 hour and the complete formation was achieved after 6 hours of incubation with the MMP-2 enzyme

3.3. *In vitro* biological evaluation

Integrin receptor competitive binding assays

Analogously to the conjugates bearing lysosomally cleavable linkers (Chapter 2) the two new conjugates were evaluated by their ability to inhibit biotinylated vitronectin binding to the purified $\alpha_V\beta_3$ receptor. The calculated IC_{50} values are shown in Table 8, together with the free ligand *cyclo*[RGDfK] (**46**).

As highlighted by the Table, compounds **71** and **73** showed good binding affinity, with IC_{50} values in the low nanomolar range, comparable with the affinity reported for the free ligand *cyclo*[RGDfK] **46**. These results prompted us to proceed with further *in vitro* antiproliferative assays, which are currently ongoing.

Table 8. Inhibition of biotinylated vitronectin binding to the isolated $\alpha_v\beta_3$ and $\alpha_v\beta_5$ receptors.

Compound	Structure	IC_{50} (nM)[a] $\alpha_V\beta_3$
46	*cyclo*[RGDfK]	1.4 ± 0.2
71	Dau=Aoa-GPLGVRG-*cyclo*[RGDfK]	2.04 ± 0.86
73	*cyclo*[RGDfK]-GPLG-PTX	1.75 ± 1.10

[a] IC_{50} values were calculated as the concentration of compound required for 50% inhibition of biotinylated vitronectin binding as estimated by GraphPad Prism software. All values are the arithmetic mean ± the standard deviation (SD) of duplicate determinations.

3.4. Conclusions

In this section, two new conjugates bearing extracellular cleavable linkers were synthesized: Dau=Aoa-GPLGVRG-*cyclo*[RGDfK] (**71**) and *cyclo*[RDGfK]-GPLG-PTX (**73**). For compound **71**, linker cleavage by MMP-2 was evaluated, showing that the peptide bond between Gly and Val is the preferential site of the enzymatic cleavage, and that the formation of the active metabolite **72** (Dau=Aoa-GPLG-OH) was completed within 6 hours. Furthermore, both conjugates were evaluated *in vitro* for their integrin

receptor binding, which revealed that both compounds retained good binding affinity (in the low nanomolar range). At the moment, cell viability assays are being performed.

Chapter 4: Conjugates containing the β-glucuronide linker

β-Glucuronidase is a well-known tumor-associated enzyme, present both in intracellular compartments (i.e. lysosomes) and in the extracellular environment of tumors. The high expression of this enzyme in the tumor interstitium has been linked to the extracellular liberation of lysosomal β-glucuronidase from apoptotic or necrotic cancer cells.[105,117] Furthermore, the accumulation in the extracellular matrix was found to significantly increase upon inflammation, which is one of the hallmarks of cancer. In particular, the activation of tumor-infiltrating macrophages and neutrophils was found to result in the extracellular release of β-glucuronidase.[116b,118]

This enzyme is a tetrameric glycoprotein with four identical subunits (77 kDa each) and its active site comprises three amino acid residues: Glu^{540}, Glu^{451} and Tyr^{504}. The role of the latter one is still unclear. However, as observed in the proposed mechanism of Figure 32, Glu^{540} acts as a nucleophile and Glu^{451} has the role of an acid-base catalyst or proton donor. The substrate specificity of this enzyme is wide: almost any aglycone in a β-linkage can be hydrolyze to glucuronic acid. In particular, β-glucuronidase is responsible for the cleavage of glucuronosyl-O bonds of glucuronic acid moieties in glucosaminoglycans (e.g. heparan sulfate, chondroitin sulfate and dermatan sulfate) and its deficiency is known to provoke a rare lysosomal storage disease, known as mucopolysaccharidosis type VII (Sly syndrome).[105, 117a, 118a] Compared to normal tissues, β-glucuronidase is highly expressed in breast, lung, melanomas and gastrointestinal tract carcinomas.[105,119] Due to this high tumor expression and specific enzymatic activity, glucuronide-containing prodrugs have been developed with the aim to target the cancer tissues avoiding systemic toxicity (since the enzyme is not present in the general circulation).[105, 118a] For instance, glucuronide triggers have been applied to the so-called field of antibody-directed enzyme prodrug therapy (ADEPT), which aims at increasing the enzyme concentration at the tumor site, as well as in gene-directed enzyme prodrug therapy (GDEPT), in which a gene encoding the enzyme is targeted to the tumour.[118,119] Moreover, β-glucuronide-containing prodrugs[120] and imaging agents[121] have been developed, showing high stability in circulation and a high hydrophilicity, which limits the cell permeability of the intact prodrug, and the resulting off-target toxicity.[117b,122] Furthermore, these prodrugs may take advantage of the presence of dying cells (and necrotic areas) in the tumor mass, which results in a significant initial expression of β-glucuronidase. This improves the penetration of the

prodrug into the tumor and the resulting cytotoxic activity prompts the cancer cells to shed more enzyme, leading to an amplification of the cleavage cascade.[117a]

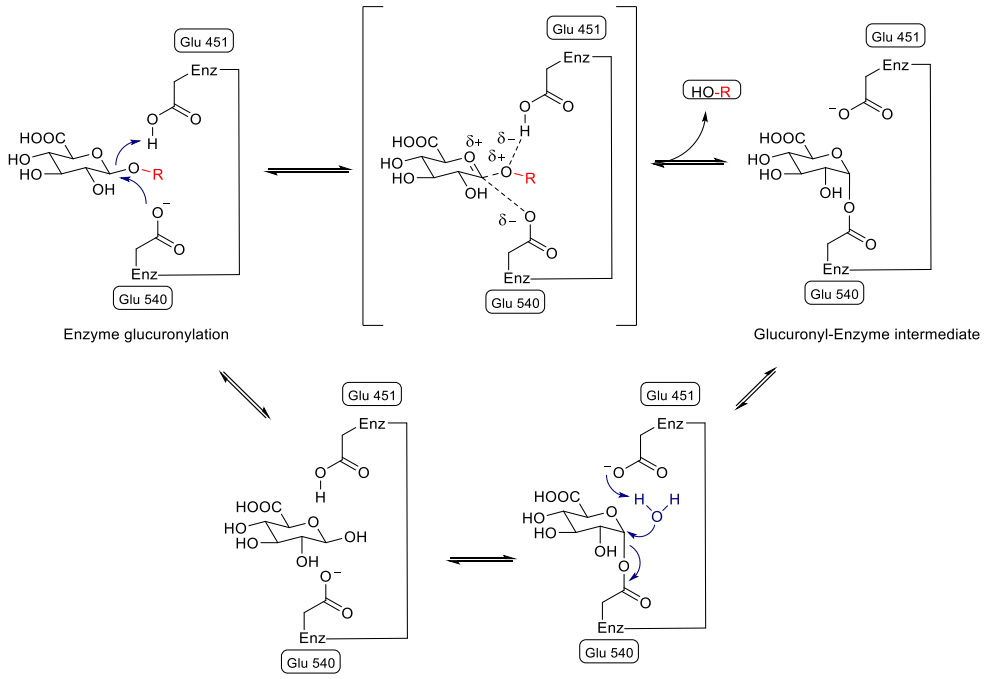

Figure 32. Proposed mechanism of β-glucuronidase-mediated hydrolysis.

One example of prodrug cleaved by β-glucuronidase is the conjugate containing cyclopamine (an inhibitor of the Hedgehog signalling pathway of cancer cells) and β-glucuronide (compound **87**, Figure 33, developed by Renoux *et al*. in 2011.[123]

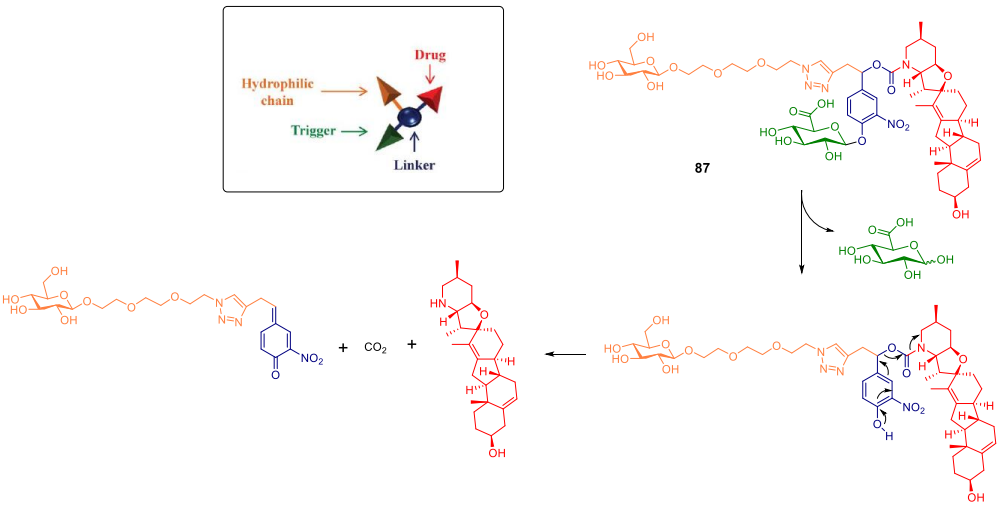

Figure 33. Structure of compound **87** and mechanism of release.

This compound was incubated with U87 cells for 5 days: after addition of β-glucuronidase in culture media, a good antiproliferative effect was observed, with prodrug **87** showing an IC_{50} value of 24.5 μM, which was comparable to the activity reported for the free drug (IC_{50}= 16.5 μM). On the other hand, in the absence of the enzyme, prodrug **87** did not affect the viability of the cells.

Furthermore, the β-glucuronide linker has been widely used in ADC products.[124] For example, mAbs cAC10 (anti-CD30) and h1F6 (anti-CD70) have been conjugated to doxorubicin using this linker as shown in Figure 34.[125]

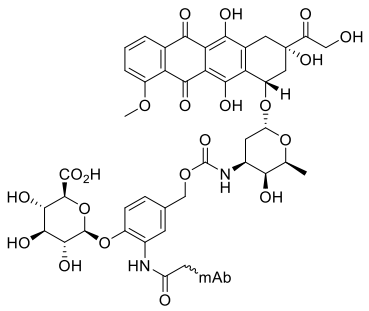

Figure 34. Structure of the mAbs conjugated to doxorubicin (Doxo) through the β-glucuronide linker.

These ADC products have been subjected to *in vitro* cytotoxicity studies against a panel of cell lines and the results are reported in Table 9. It was observed that both conjugates were selective for the corresponding antigen-positive cell lines and that the potency was comparable with that of the free drug. This observation seems to indicate that the ADC products used are internalized by the parent antigens, following receptor-mediated endocytosis and intracellular cleavage of the glucuronide linker.

Table 9. *In vitro* cytotoxicity of cAC10-β-glucuronide-Doxo and h1F6-β-glucuronide-Doxo in different cell lines

		IC_{50} (nM)				
Compound	Antigen	Karpas 299[a] (CD30+)	L428[a] (CD30+, CD70-)	L540 Cy[a] (CD30 +)	WSU-NHL[a] (CD30-)	Caki-1[a] (CD70 +)
Doxo	-	1.2	0.1	0.5	-	0.7
cAC10-β-glucuronide-Doxo	CD30	0.4	0.4	0.9	>32[b]	-
h1F6-β-glucuronide-Doxo	CD70	-	>29[b]	-	-	0.6

[a] The free drug and the Antibody-drug conjugates were incubated for 96 h; [b] No activity at highest concentration tested.

Inspired by all these data, two *cyclo*[DKP-RGD]-MMAE (monomethyl auristatin E) conjugates bearing β-glucuronide as linker were developed, containing both a glutarate (**88**) and a PEG-4 spacer (**89**). In these conjugates, the drug release occurs through the same 1,6-elimination triggered by enzymatic cleavage of the glycosidic bond, mentioned in Figure 33. The use of the MMAE payload, possessing a secondary amine group, allows the direct formation of a carbamate bond with the *p*-aminobenzyl alcohol fragment, avoiding the use of diamine-based cyclization spacer (i.e. unlike PTX and other payload that are normally functionalized at hydroxyl groups).

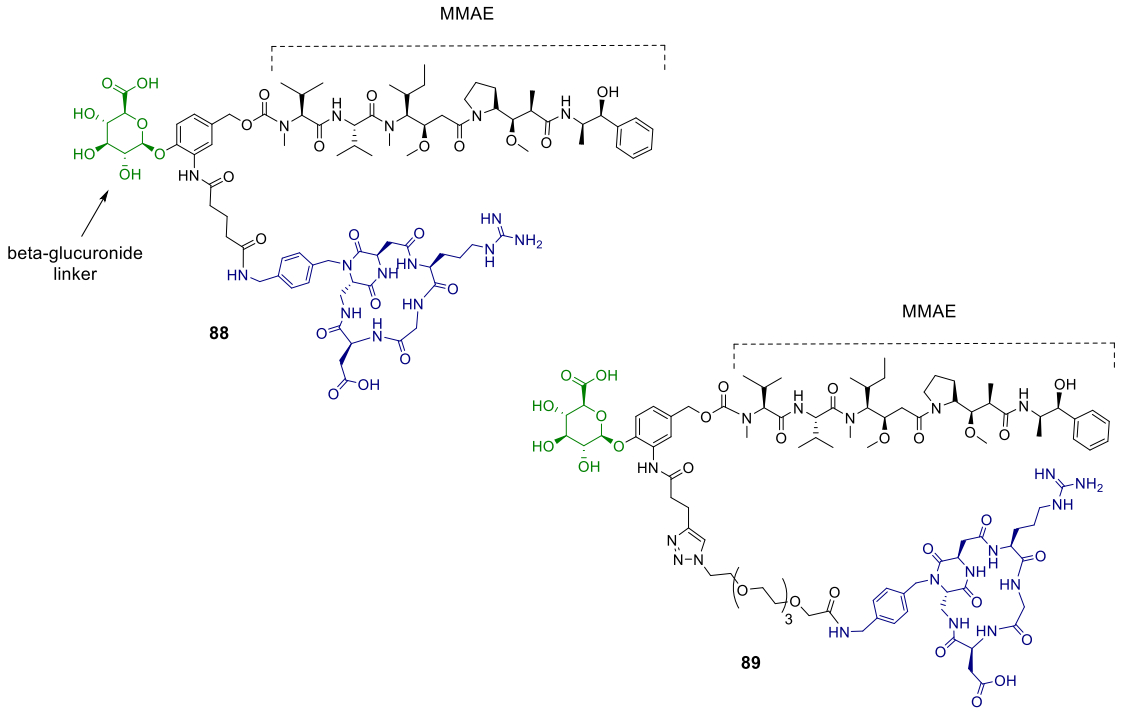

Figure 35. Structures of *cyclo*[DKP-RGD]-glucuronide-MMAE (**88**) and *cyclo*[DKP-RGD]-PEG-4-glucuronide-MMAE (**89**).

4.1. Synthesis

The synthetic methodology of both final conjugates is described in Scheme 9. Compounds **90** and **91** were linked through a glycosidic bond, giving intermediate **92**. The aldehyde group of this compound was reduced with sodium borohydride to give alcohol **93** followed by hydrogenation of the nitro group, yielding **94**. The latter was a common intermediate for the formation of both final conjugates. For the synthesis of *cyclo*[DKP-RGD]-β-glucuronide-MMAE **88**, compound **94** was Fmoc-protected and reacted with 4-nitrophenylchloroformate, affording carbonate **95**. The latter was reacted

with the secondary amine moiety of MMAE in the presence of HOBt under basic conditions. Upon deprotection of both sugar and aniline moieties, the resulting compound **96** was coupled to di(succinimidyl) glutarate with a disappointing 15% yield, due to both the low reactivity of the aniline nitrogen atom and the partial deprotection of compound **97** under the reaction and HPLC conditions. Later on, this *N*-hydroxysuccinimidyl ester was reacted with the *cyclo*[DKP-RGD] ligand, as described for previous conjugates, leading to the final compound **88** upon HPLC purification.

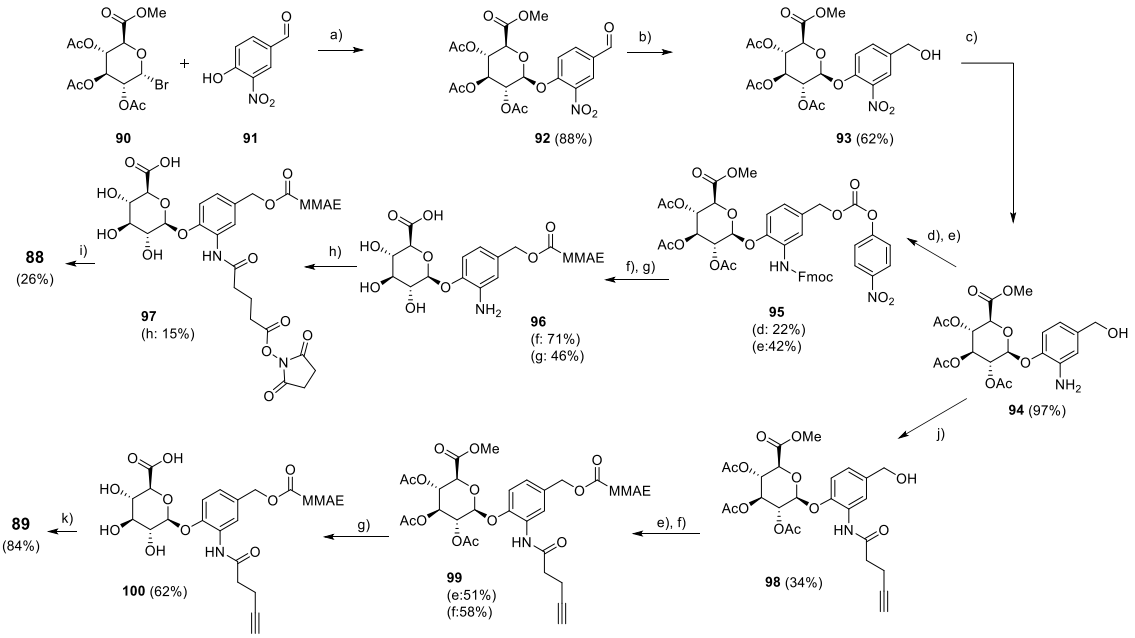

Scheme 9. Synthesis of conjugates **88** and **89**. Reagents and conditions: a) Ag_2O, molecular sieves, CH_3CN, overnight; b) Silica gel, $NaBH_4$, *i*PrOH/$CHCl_3$, 2.5 h; c) H_2/Pd, EtOAc, EtOH, MeOH, overnight; d) Fmoc-OSu, *i*Pr_2NEt, DMAP, CH_2Cl_2, 3 h; e) 4-nitrophenylchloroformate, pyridine, THF, 3 h; f) MMAE, HOBt, *i*Pr_2NEt, pyridine, DMF, 2 h: g) LiOH, 1:1 MeOH/H_2O, 2 h; h) Di(succinimidyl)glutarate, *i*Pr_2NEt, DMAP, DMF, 3 h; i) *cyclo*[DKP-RGD] **32**, PBS/DMF, 3 h; j) 4-pentynoic acid, HATU, HOBt, *i*Pr_2NEt, DMF, overnight; k) N_3-PEG-4-*cyclo*[DKP-RGD] **51b**, $CuSO_4 \cdot 5H_2O$, sodium ascorbate, DMF/H_2O.

For the synthesis of *cyclo*[DKP-RGD]-PEG-4-glucuronide-MMAE (**89**), compound **94** was coupled with 4-pentynoic acid, yielding the alkyne **98** in low yield. The latter was activated and coupled with MMAE, followed by deprotection of the sugar moiety, as described above. Finally, a copper-catalyzed azide-alkyne cycloaddition was performed using N_3-PEG-4-*cyclo*[DKP-RGD] **51b** and the terminal alkyne **100**, affording the final conjugate **89** in 84% yield after HPLC purification.

The evaluation of integrin binding affinity, enzymatic cleavage and antiproliferative activity of both *cyclo*[DKP-RGD]-glucuronide-MMAE (**88**) and *cyclo*[DKP-RGD]-PEG-4-glucuronide-MMAE (**89**) are still in progress.

4.2. *In vitro* biological evaluation

Integrin receptor competitive binding assays

Analogously to to the conjugates bearing lysosomally cleavable linkers (Chapter 2) and MMP-2 cleavable linkers (Chapter 3), *cyclo*[DKP-RGD]-glucuronide-MMAE (**88**) and *cyclo*[DKP-RGD]-PEG-4-glucuronide-MMAE (**89**) were evaluated by their ability to inhibit biotinylated vitronectin binding to the purified $\alpha_V\beta_3$ receptor and compared to the free ligand *cyclo*[DKP-RGD] (**31**). The calculated IC_{50} values are shown in Table 10.

Table 10. Inhibition of biotinylated vitronectin binding to the isolated $\alpha_V\beta_3$ receptor.

Compound	Structure	IC_{50} (nM)[a] $\alpha_V\beta_3$
31	*cyclo*[DKP-RGD]	4.5 ± 1.1
88	*cyclo*[DKP-RGD]-glucuronide-MMAE	20.0 ± 9.6
89	*cyclo*[DKP-RGD]-PEG-4-glucuronide-MMAE	76.7 ± 5.8

[a] IC_{50} values were calculated as the concentration of compound required for 50% inhibition of biotinylated vitronectin binding as estimated by GraphPad Prism software. All values are the arithmetic mean ± the standard deviation (SD) of duplicate determinations.

Both compounds showed high binding affinity, with IC_{50} values in the low nanomolar range, comparable with those obtained for the free ligands (**31**).

4.3. Conclusions

In this Chapter, two *cyclo*[DKP-RGD]-MMAE (monomethyl auristatin E) conjugates bearing β-glucuronide as linker, containing both a glutarate (**88**) and a PEG-4 spacer (**89**) were synthesized. The preparation of the latter proved to be more straightforward, carried out with generally higher yields. As a future work, a negative control for the cleavage experiments and antiproliferative assays will be synthesized. This compound was designed with a different distribution of the substituents in the aminobenzyl aromatic

ring, with the β-glucuronide linker in meta-position with respect to the MMAE (**101**, Figure 36). In particular, this structure should not lead to the release of the free drug upon enzymatic cleavage of the β-glucuronide linker, since the 1,6-elimination will not take place

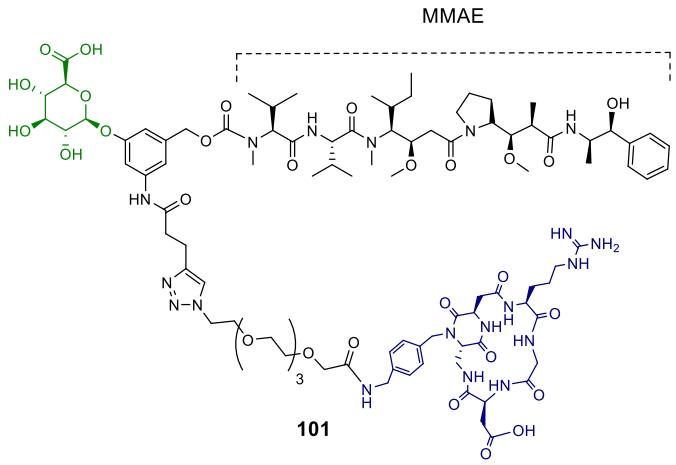

Figure 36. Structure of the negative control to be developed.

Overall, the *in vitro* evaluation of this group of RGD-MMAE conjugates bearing β-glucuronide linker will provide information about the integrin-targeting ability of the RGD ligand. Indeed, cancer cell lines with different levels of integrin expression will be used, following an experimental set similar to the one described by Senter and coworkers[125]

(Table 9). The ideal observation of high TI values would be consistent with the mechanism of integrin-mediated endocytosis of these SMDCs, with linker cleavage in intracellular compartments and subsequent release of MMAE. Importantly, the high potency of this payload makes these compounds attractive candidates for *in vivo* applications. The administration of these compounds to tumor-bearing mice would hopefully result in their high accumulation in the tumor xenograft. Here, the presence of dying cells and necrotic areas is likely to result in the high expression of β-glucuronidase in the tumor microenvironment. For this reason, it is conceivable that the linker cleavage may occur preferentially in extracellular areas, leading to the diffusion of MMAE in the tumor mass.

Conclusions and perspectives

In this PhD work, a variety of new SMDCs were designed and synthesized featuring different types of linkers and cytotoxic payloads. All of them were characterized and conjugated to peptidomimetic ligands bearing the RGD sequence (namely, the *cyclo*[DKP-RGD] and *cyclo*[RDGfK] compounds) aimed at targeting $\alpha_V\beta_3$ integrin receptor overexpressed in many human cancers.

In the first part of this thesis, different conjugates cleaved by lysosomal enzymes were synthesized. At first, taking the previously synthesized *cyclo*[DKP-RGD]-Val-Ala-PTX **33** as reference, the influence of each individual moiety of the conjugate on the integrin affinity and selective cell toxicity was evaluated. The newly synthesized conjugates (**37**-**40**), bearing the lysosomally cleavable GFLG linker and glutarate or PEG-4 spacer, were evaluated *in vitro* for their cell antiproliferative activity and compared with compounds **33** and **41** (bearing the lysosomally cleavable Val-Ala linker). In the cell viability assays against U87 ($\alpha_V\beta_3$+) and HT29 ($\alpha_V\beta_3$-), all conjugates proved less active than the free PTX payload, with conjugates containing the PEG-4 spacer (**39-41**) showing the highest potency in the series. In this part, we proposed the determination of the Relative Potency (RP), consisting in the ratio IC_{50} PTX/IC_{50} conjugate calculated for each cell line. This new parameter quantifies the loss of cytotoxic potency of each conjugate with respect to paclitaxel. Since higher RP values were observed for the U87 cell line we could conclude that the loss of potency was more evident when the cell does not express $\alpha_V\beta_3$. As reported in previous works of our group, the Targeting Index value was introduced to correlate the different RP values observed for a single compound for the two cell lines. Among all the tested compounds, *cyclo*[DKP-RGD]-PEG-4-Val-Ala-PTX **41** showed the best Targeting Index of the series (TI = 533). Competition experiments were carried out with this conjugate in the $\alpha_V\beta_3$+ cell line U87 in the presence of 50-fold excess free ligand *cyclo*[DKP-RGD] (**31**). The observed 5-fold decrease of conjugate toxicity demonstrated that conjugate **41** is, at least partially, internalized by the cancer cells through an integrin $\alpha_V\beta_3$-mediated process, which leads to the intracellular delivery of the cytotoxic cargo. Unfortunately, the use of α-amanitin as a more potent cytotoxic payload did not lead to a significant improvement of the targeting ability of these conjugates, nor to the development of more potent integrin-targeted conjugates.

For this reason, the study of extracellularly cleavable linkers was investigated. We focused on the GPLG and GPLGVRG peptide sequences, which are recognized and cleaved by MMP-2 enzyme. Two conjugates were synthesized: Dau=Aoa-GPLGVRG-

cyclo[RGDfK] (**71**) and *cyclo*[RDGfK]-GPLG-PTX (**73**). Cleavage experiments in the presence of the MMP-2 enzyme were carried out for **71**, confirming that the preferred cleavage site is between Gly and Val and that the formation of the active metabolite **72** (Dau=Aoa-GPLG-OH) is completed within 6 hours. Currently, further *in vitro* experiments (antiproliferative assays) are being performed.

In the last part of the thesis, two *cyclo*[DKP-RGD]-MMAE (monomethyl auristatin E) conjugates bearing β-glucuronide as linker, containing both a glutarate (**88**) and a PEG-4 spacer (**89**) were synthesized. These conjugates are recognized by β-glucuronidase, which is a well-known tumor-associated enzyme, present both intracellularly (in lysosomes) and extracellularly (in the interstitium of highly aggressive and necrotic tumors). These compounds will be subjected to cleavage experiments and cell viability assays.

In summary, the loss of potency generally displayed by the lysosomally cleavable conjugates in antiproliferative assays prompted us to the design of new SMDCs bearing extracellular cleavable linkers. This strategy has got credits from literature data and it has been proposed as a promising alternative to internalizing conjugates. While this approach will allow us to take the internalization out of the equation and to develop highly potent conjugates, it will be important to submit these compounds to *in vivo* therapy experiments, in order to understand the contribution to the selectivity given by the integrin ligand. Evidences of efficient drug release from non-internalizing prodrugs, brought at the diseased site by the RGD affinity for tumor-expressed integrins, will potentially support the clinical investigation of this anticancer devices.

Experimental section

General remarks and procedures

Materials and methods

All manipulations requiring anhydrous conditions were carried out in flame-dried glassware, with magnetic stirring and under a nitrogen atmosphere. All commercially available reagents were used as received. Anhydrous solvents were purchased from commercial sources and withdrawn from the container by syringe, under a slight positive pressure of nitrogen. The reactions were monitored by analytical thin-layer chromatography (TLC) using silica gel 60 F254 pre-coated glass plates (0.25 mm thickness) or Macherey-Nagel 0.20 mm silica gel 60 with fluorescent indicator pre-coated polyester sheets (40 × 80 mm). Visualization was accomplished by irradiation with a UV lamp and/or staining with Cerium/Molibdate reagent, ninhydrin or cynnamaldehyde. Automated chromatography was performed with Teledyne Isco CombiFlash Rf 150. HPLC purifications were performed on Dionex Ultimate 3000 equipped with Dionex RS Variable Wavelenght Detector (semipreparative column: Atlantis Prep T3 OBD^{TM} 5 µm 19 × 100 mm; flow 15 mL/min unless stated otherwise). Also, preparative HPLC LaPrep∑ equipped with autosampler AS3950 and a Phenomenex Luna C-18(2) column, 10 µm, 250 × 21.2 mm, with precolumn at 30 mL/min flow rate and KNAUER 2501 HPLC system (preparative column: Luna 10 µm C18 (2) 100A 250 × 21.2 mm) were used. HPLC traces of final products were performed on Hitachi Chromaster (column oven Chromaster 5310, pump Chromaster 5110, autosampler Chromaster 5210, DAD Chromaster 5430) equipped with a Phenomenex Luna C-18(2) column, 10 µm, 250 × 4.6 mm, with precolumn at 1.4 mL/min flow rate were used. The analysis of the integrals and the relative percentage of purity were performed with the software Chromeleon 6.80 SR11 Build 3161. Freeze-drying: the products were dissolved in water and frozen with dry ice. The freeze-drying was carried out at least for 48 h at -50 °C using the instrument 5Pascal Lio5P DGT.

Proton NMR spectra were recorded on a spectrometer operating at 400.16 MHz. or 500 MHz. Proton chemical shifts are reported in ppm (δ) with the solvent reference relative to tetramethylsilane (TMS) employed as the internal standard (DMSO δ = 2.5 ppm; D_2O

δ = 4.79 ppm; $CDCl_3$ δ = 7.26 ppm; CD_2Cl_2 δ = 5.32 ppm). The following abbreviations are used to describe spin multiplicity: s = singlet, d = doublet, t = triplet, q = quartet, m = multiplet, bs = broad signal, dd = doublet of doublet, ddd = doublet of doublet of doublet, ddt = doublet of doublet of triplet, td = triplet of doublet. Carbon NMR spectra were recorded on a spectrometer operating at 100.63 MHz or 126 MHz, with complete proton decoupling. Carbon chemical shifts are reported in ppm (δ) relative to TMS with the respective solvent resonance as the internal standard.

Low resolution mass spectra (MS) were recorded on Thermo Finnigan LCQ Advantage (ESI source), Bruker Daltonics Esquire 3000+ ion trap mass (ESI source), Micro Waters Q-Tof (ESI source) and Thermo Fisher linear ion trap LTQ XL mass spectrometer. The MALDI–TOF–MS spectra were recorded on a Bruker Microflex™ LT instrument, supporting the sample on α-cyano-4-hydroxycinnamic acid (HCCA) and sinapinic acid (SA) matrices. The peptide calibration standard (300–3000 Da range), which consisted of angiotensin II, angiotensin I, substance P, bombesin; ACTH clip 1-17, ACTH clip 18-39, somatostatin 28, was purchased from Bruker Daltonics® and used to calibrate the MALDI-TOF-MS instrument. High-resolution mass spectra (HRMS) were performed with a Fourier Transform Ion Cyclotron Resonance (FT-ICR) Mass Spectrometer APEX II & Xmass software (Bruker Daltonics) – 4.7 T Magnet (Magnex) equipped with ESI source, available at CIGA (Centro Interdipartimentale Grandi Apparecchiature) c/o Università degli Studi di Milano.

General procedure for SPPS

The compounds were synthesized manually on 2-chlorotrityl resin (0.87 mmol/g loading capacity) using the Fmoc protocol. The resin (1 g) was swollen in CH_2Cl_2 for 30 min. Then, the CH_2Cl_2 was removed and the resin was washed 3 times with DMF. After this, coupling of the amino acids was carried out.

The protocol is as follows:

1) Coupling of the first amino acid (Fmoc-glycine-OH):

(i) A solution of Fmoc-glycine-OH (300 mg, 1 equiv.) and *i*Pr_2NEt (700 µL, 3 equiv.) in 1:1 CH_2Cl_2/DMF (4 mL) was added to the swollen resin, and the mixture was stirred for 2 h; (ii) the resin was washed with DMF (2 ×) and CH_2Cl_2 (2 ×); (iii) capping in a 7:2:1 CH_2Cl_2/MeOH/*i*Pr_2NEt (3 times × 5 min, 20 mL); (iv) the resin was washed with CH_2Cl_2

(3 ×), DMF (2 ×) and CH_2Cl_2 again (3 ×); (v) the Kaiser test was performed as follows: a few drops of ninhydirin solution (0.28 M in ethanol), phenol solution (21 M in ethanol) and KCN solution (0.33 mM in pyridine)[a] were added over a bead of resin and then the mixture was heated (a yellow color was observed in the absence of free amines); (vi) the resin was washed with DMF (2 ×); (vii) Fmoc deprotection was performed: the resin was treated with 2% piperidine and 2% of DBU in DMF (3 × 7 min), then washed with DMF (3 ×) and CH_2Cl_2 (2 ×) before performing again the Kaiser test (a blue color was indicative of successful removal of the Fmoc protecting group).

2) Addition of the other amino acids

The following protocol was repeated for the addition of every single amino acid:
(i) a solution of the amino acid (3 equiv.), HOBt (540 mg, 4 equiv.) and DIC (540 µL, mmol, 4 equiv.) in 4 mL of DMF was added to the resin and the suspension was stirred for 2 h; (ii) the resin was washed with DMF (3 ×), CH_2Cl_2 (2 ×) and DMF (2 ×); (iii) Kaiser test was performed; (iv) Fmoc deprotection was performed as described in Paragraph 1, step (vii).

3) Cleavage from the resin

*Cleavage **A***

(i) The resin was dried under vacuum for 2 h and then dissolved in a 8:1:1 CH_2Cl_2/MeOH/AcOH mixture (25 mL) for 2 h; (ii) the resin was filtered, washed with other 25 mL of 8:1:1 CH_2Cl_2/MeOH/AcOH mixture and then the solution was evaporated obtaining an oil; (iii) distilled water was added to the crude and a white solid was formed, which was filtered and washed with additional water; (iv) the white solid was dried under vacuum for one day.

*Cleavage **B***

(i) The resin was dried under vacuum for 2 h and then dissolved in 95/2.5/2.5 TFA/TIS/H_2O mixture for 3 h; (ii) the resin was filtered, washed with more 95/2.5/2.5 TFA/TIS/H_2O mixture and then the solution was added to cold diethyl ether, observing the formation of a white solid (iii); The precipitate was centrifuged (3 × 5 mins), frozen-dried and used without further purificacion.

[a] This solution was prepared as follows: 16.5 mg of KCN were dissolved in 15 mL of distilled water. 1 mL of the previous solution was then diluted with 49 mL of pyridine.

4) Calculation of the yield for SPPS

The yield is calculated using the formula: [amount of peptide obtained/ (resin loading × amount of resin × MW peptide)] × 100.

Biological assays

Solid-phase binding receptor assay

Recombinant human integrin $\alpha_v\beta_3$ receptor (R&D Systems, Minneapolis, MN, USA) and (when also determined) purified $\alpha_v\beta_5$ receptor (Chemicon International, Inc., Temecula, CA, USA) were diluted to 0.5 μg/mL in coating buffer containing 20 mM Tris-HCl (pH 7.4), 150 mM NaCl, 1 mM $MnCl_2$, 2 mM $CaCl_2$, and 1 mM $MgCl_2$. An aliquot of diluted receptor (100 μL/well) was added to 96-well microtiter plates (Nunc MaxiSorp) and incubated overnight at 4 °C. The plates were then incubated with blocking solution (coating buffer plus 1% bovine serum albumin) for 2 h at r.t. to block nonspecific binding. After washing 2 times with blocking solution, plates were incubated shaking for 3 h at r.t., with various concentrations (10^{-5}-10^{-12} M) of test compounds in the presence of 1 μg/mL biotinylated vitronectin (Molecular Innovations, Novi, MI, USA). Biotinylation was performed using an EZ-Link Sulfo-NHS-Biotinylation kit (Pierce, Rockford, IL, USA). After washing 3 times, the plates were incubated shaking for 1 h at r.t., with streptavidin-biotinylated peroxidase complex (Amersham Biosciences, Uppsala, Sweden). After washing 3 times with blocking solution, plates were incubated with 100 μL/well of Substrate Reagent Solution (R&D Systems, Minneapolis, MN, USA) for 30 min with shaking. After stopping the reaction with the addition of 50 μL/well 2N H_2SO_4, absorbance at 415 nm was read in a SynergyTM HT Multi-Detection Microplate Reader (BioTek Instruments, Inc.). Each data point represents the average of triplicate wells; data analysis was carried out by nonlinear regression analysis with GraphPad Prism software (GraphPad Prism, San Diego, CA, USA). Each experiment was repeated in duplicate

Determination of integrin $\alpha_V\beta_3$ receptor expression of U87 and HT29 cell lines for the in vitro experiments of the conjugates bearing the Gly-Phe-Leu-Gly linker

U87 and HT29 cells were seeded in T25 flasks with ventilation cap and incubated at 37 °C in a humidified atmosphere with 5% CO_2 for 48 h. Cells were harvested and fixed with 4% PFA (Paraformaldehyde). With 3% BSA (Bovine Serum Albumin) were blocked all possible non-specific binding sites on the cell, and cells were exposure with LM609 anti Integrin $\alpha_V\beta_3$ antibody conjugated with FITC (Merck Millipore, Darmstadt, Germany). In control samples cells were not stained with antibody, and auto-fluorescence intensity of cells was measured. Fluorescent intensity of stained samples was measured by flow cytometer Beckman Coulter, and compared with auto-fluorescence intensity of control samples.

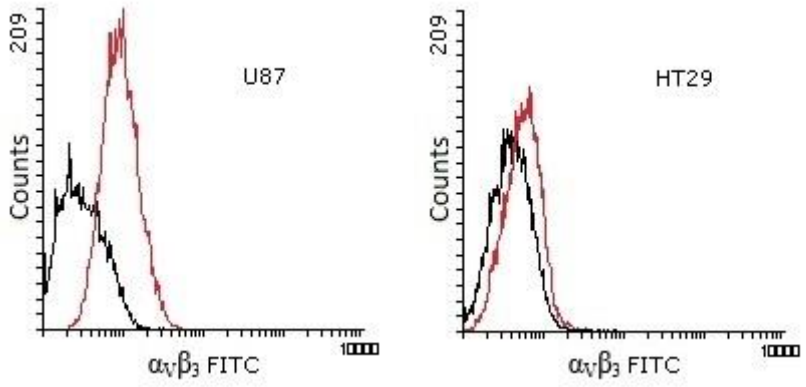

Figure 37. Flow cytometry analysis of integrin $\alpha_V\beta_3$ in U87 and HT29 cell lines. Black: auto-fluorescence of the cell; Red: fluorescence of $\alpha_V\beta_3$ integrin antibody.

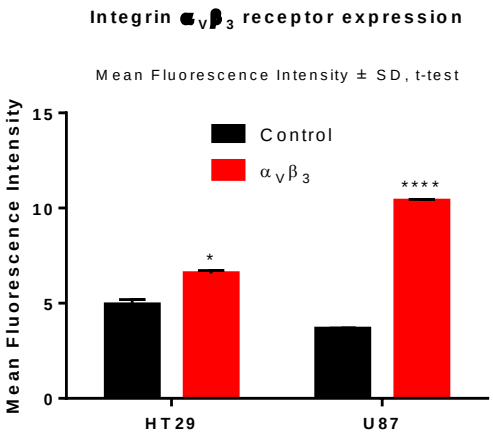

Figure 38. Mean fluorescence intensity of $\alpha_V\beta_3$ receptors expression in U87 and HT29 cell lines.

Determination of integrin $\alpha_V\beta_3$ receptor expression of U87, MDA-MB-468 and A549 cell lines for the in vitro experiments of the cyclo[DKP-RGD]-α-amanitin conjugates

The expression of integrin $\alpha_V\beta_3$ in U87-MG, A549 and MDA-MB 468 cells was determined by flow cytometry on a FACSCalibur device (Becton Dickinson). Before staining, cells were fixed with fixation solution (0.5% PFA in PBS). 5×10^5 cells per sample were stained in staining medium (PBS, 25 mM HEPES, 3% FCS, 0.02% Na-Azide) with an anti-human integrin $\alpha_V\beta_3$ antibody conjugated to Alexa Fluor 488 (R&D Systems) or isotype control conjugated to Alexa Fluor 488 (Thermo Fischer) at a concentration of 4 µg/mL for 45 min at room temperature. Cells were washed with PBS and the mean fluorescence intensity was measured for 10.000 gated events. Data were analyzed using flow cytometry and associated software (BD Biosciences) (Figure 39).

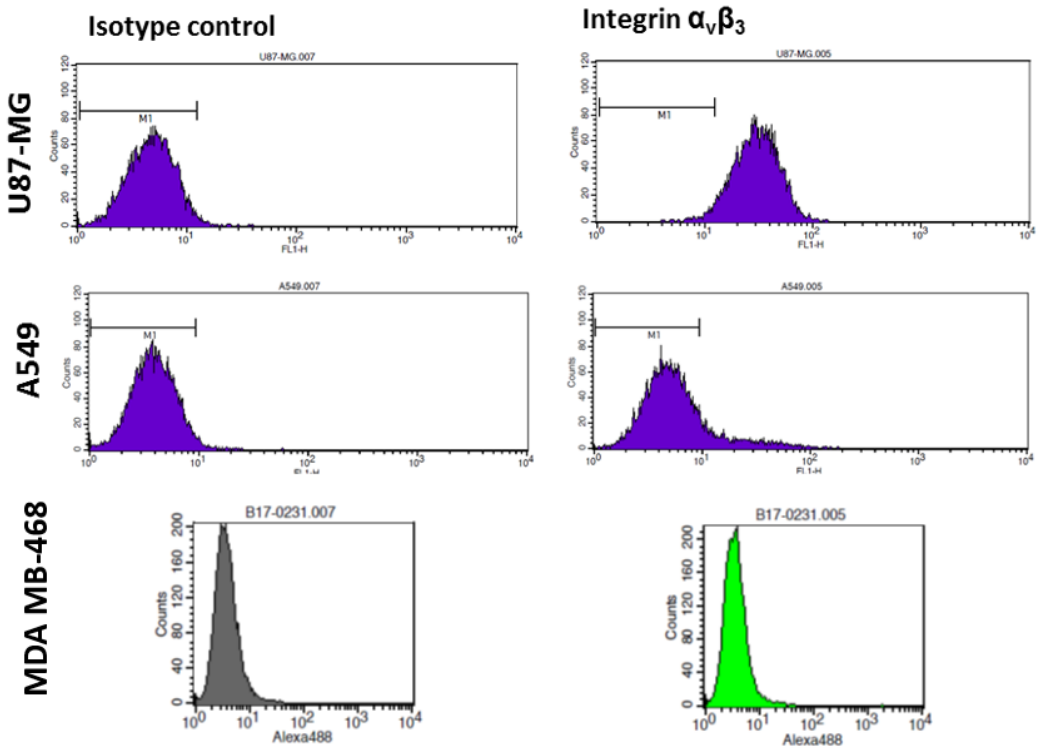

Figure 39. Flow cytometry analysis of integrin $\alpha_V\beta_3$ expression in cancer cell lines. U87-MG: integrin $\alpha_V\beta_3$ overexpressed; A549 and MDA-MB 468: integrin $\alpha_V\beta_3$ negative.

Cell culture of U87 and HT29 cell lines for the in vitro experiments of the conjugates bearing the Gly-Phe-Leu-Gly linker

U87 (human malignant glioma) and HT29 (human colorectal adenocarcinoma) cell lines obtained from ATCC were cultured in sterile T25 flasks with ventilation cap (Sarstedt, Nümbrecht, Germany) at 37 °C in a humidified atmosphere with 5% CO_2. For U87 cells, DMEM medium (Dulbecco's Modified Eagle's Medium) (Lonza, Basel, Switzerland) containing 4500 mg L^{-1} glucose and supplemented with 10% heat-inactivated and filtered FBS (Fetal Bovine Serum) (Lonza, Basel, Switzerland) and 1% Penicillin-Streptomycin (Lonza, Basel, Switzerland) was used. HT29 cells were grown in RPMI 1640 medium supplemented with 10% FBS and 1% Penicillin-Streptomycin.

Cell culture of U87, MDA-MB-468 and A549 cell lines for the in vitro experiments of the cyclo[DKP-RGD]-α-amanitin conjugates

All cell culture reagents were purchased at PAN-Biotech GmbH unless otherwise stated. Cell lines were obtained from CLS (U87-MG, MDA-MB 468 and A549). Cell lines were authenticated using Multiplex Cell Authentication by Multiplexion (Heidelberg, Germany) as described recently.[126] The SNP profiles matched known profiles or were unique. The purity of cell lines was validated using the Multiplex cell Contamination Test by Multiplexion (Heidelberg, Germany) as described recently.[127] No Mycoplasma, SMRV or interspecies contamination was detected. U87-MG, MDA-MB 468 and A549 cells were cultivated continuously for not more than 3 months in MEM Eagle´s, DMEM or Ham´s F12 medium, respectively supplemented with 10% heat inactivated fetus calf serum, L-glutamine and antibiotics. Cell lines were maintained at 37 ºC and 5% CO_2 in a high humidity atmosphere.

Cell therapy and viability assay of the conjugates bearing the Gly-Phe-Leu-Gly linker

Cell viability was determined by MTT assay (3-(4,5-dimethylthiazol-2-yl)-2,5-diphenyl-tetrazolium bromide) obtained from Sigma Aldrich (St. Louis, MO, USA). After standard trypsinization, cells were seeded at 3×10^3 cells (U87) and 4×10^3 cells (HT29) per well in a 96-well plates and incubated. After 24 h, cells were treated with various concentrations of conjugates **33** and **37-41** and free drug PTX (paclitaxel) and incubated

in appropriate serum-containing growth medium for 96 h under standard growth conditions. Control wells were untreated. Afterward, the MTT assay was performed by adding 20 µL of MTT solution (5 mg mL^{-1} in PBS) to each well and after 4 h of incubation at 37 °C, the supernatant was removed. The formazan crystals were dissolved in 100 µL of a 1:1 solution of DMSO (Sigma Aldrich, St. Louis, MO, USA) and EtOH (Molar Chemicals Kft. Hungary) and the absorbance was measured after 15 min at λ = 570 nm by using a microplate reader (BIO-RAD, model 550). Average background absorbance of DMSO-EtOH only, was subtracted from absorbance values of control and treated wells, and cell viability was determined relative to untreated (control) wells where cell viability was arbitrarily set to 100%. Absorbance values of treated samples were normalized versus untreated control samples and interpolated by nonlinear regression analysis with GraphPad Prism software to generate dose-response curves. The 50% inhibitory concentration (IC_{50}) was determined from the dose-response curves by using sigmoidal interpolation curve fitting. The experiments were done in triplicate.

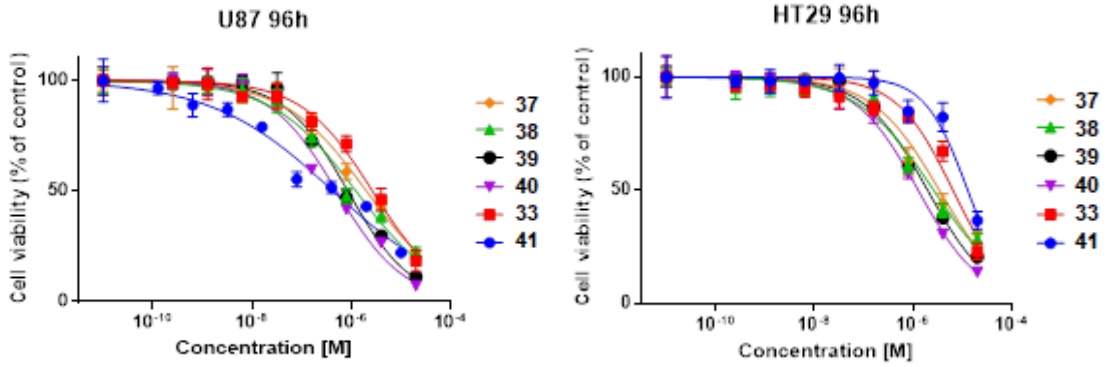

Figure 40. Dose-response curves of conjugates **33** and **37-41**.

Cell therapy and viability assay of the cyclo[DKP-RGD]-α-amanitin conjugates

Cell viability assays were performed in U87-MG, A549 and MDA-MB 468 cell lines according to the following procedure: 2 × 10^3 cells/well were plated in 96-well black clear bottom plates (Perkin Elmer) and incubated overnight. 1:5 serial dilutions of compounds **62, 63** and **68-70** were prepared in cell culture media. The compounds were added to the cell culture and incubated for additional 96 h. Starting concentration of compounds **62, 63** and **68-70** in the wells was 1 × 10^{-5} M and cell viability was determined with the

CellTiterGlo 2.0 assay (Promega) in accordance to manufacturer's instructions. The cell viability was calculated in relation to the non-treated controls for each cell line. All samples were measured in triplicate. Data analysis was carried out using software GraphPad Prism (GraphPad Software Inc., La Jolla, CA, USA).

Competition experiments of the conjugates bearing the Gly-Phe-Leu-Gly linker

Antiproliferative activity of compound **41** in the presence of free ligand was carried out as follows: U87 integrin $\alpha_V\beta_3$-expressing cells were seeded at 3×10^3 cells per well in 96-well plates and incubated. After 24 h, cells were treated simultaneously with conjugate **41** and with 50-fold molar excess of free RGD ligand (**31**, Figure 18) for 96 h. Cells were also treated with free Paclitaxel (PTX) in the presence of 50-fold molar excess of free RGD ligand (**31**) for 96 h. Control wells were untreated. Cell viability was determined by MTT assay. IC_{50} was calculated using GraphPad Prism software. The experiments were done in triplicate.

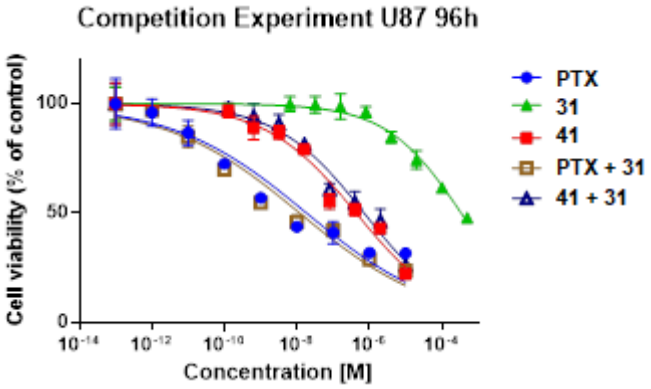

Figure 41. Dose-response curves of Paclitaxel and conjugate **41** in the presence of 50-fold excess *cyclo*[DKP-RGD] (**31**) in U87 cell line.

Competition experiments of the cyclo[DKP-RGD]-α-amanitin conjugates

The competition experiments were performed in U87-MG and MDA-MB 468 cell lines according to the following procedure: 2×10^3 cells/well were plated in 96-well black clear bottom plates (Perkin Elmer) and incubated overnight. A solution containing 1×10^{-4} M of the conjugate (**68** or **70**) and 5×10^{-3} M of Cilengitide **18** (Figure 13) (50 fold excess of ligand in comparison to the conjugate) was prepared in the growth medium and 1:5 serial

dilutions were prepared in cell culture media. The compounds were added to cell culture and incubated for 96 h. Starting concentration of the compounds in the wells was 0.01 mM whereas that of cilengitide was 0.5 mM. Cell viability was determined with the CellTiterGlo 2.0 assay (Promega) in accordance to manufacturer's instructions. Cell viability was calculated in relation to the non-treated controls for each cell line. All samples were measured in triplicate. Data analysis was carried out using software Graph Pad Prism (Graph Pad Software Inc., La Jolla, CA, USA).

Cleavage experiments with Dau=Aoa-GPLGVRG-*cyclo*[RGDfK] (71)

The conditions of the cleavage experiments are summarized as follow:

Injection Temperature	365 °C
Drying gas	12 L/min
Nebulizer gas pressure	70 psi
Target	900
Range	350-1900
Flow rate	1 mL/min
Program (t-B%)	2min 2% 25min 70% 26min 95% 28min 95% 29min 2%
Injected amount	7 µL (loop: 5 µL)
Guard Column	C4, Phenomenex
RP-HPLC Column	Phenomenex; Aeris 3,6 µm; Widepore XB-C8; 150x4.6 mm
Eluent A	Distilled H_2O + 0.1% CH_3COOH
Eluent B	CH_3CN/ distilled H_2O (80:20) + 0.1% CH_3COOH
Enzyme	Human MMP-2 Recombinant expressen in *E. Coli* (Sigma-Aldrich)
Peptides	Dau=Aoa-GPLGVRG-*cyclo*[RGDfK] (**71**) *Cyclo*[RGDfK]-GPLG-PTX (**73**) was not soluble under measurement conditions
Peptide:Enzyme rate	100:1
Peptide concentration	50 pmol/ µL
Buffer	TCNB-buffer; pH:7.5 (Tris-HCl buffer; 150mM NaCl; 5 mM $CaCl_2$, 1mM 4-aminophenylmercuric acetate)
Samples	1, 3, 6 h (enzymatic reactions were stopped by adding CH_3COOH)

Synthesis of RGD Peptidomimetic-paclitaxel conjugates bearing the Gly-Phe-Leu-Gly linker (37-40)

Synthesis of *cyclo*[RGDfK] (**46**)

*Fmoc-Asp(OtBu)-D-Phe-Lys(Boc)-Arg(Pbf)-Gly-OH (**43**)*

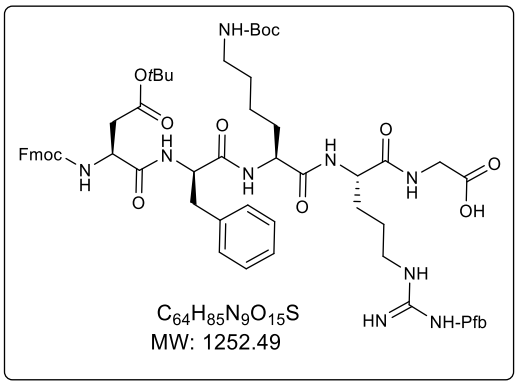

The experimental protocol is described in the general procedure for SPPS. Cleavage **A** was used in this case.

MS (ESI+): *m/z* calcd. for $[C_{64}H_{86}N_9O_{15}S]^+$: 1252.60 $[M + H]^+$; found: 1252.9.

*H_2N-Asp(OtBu)-D-Phe-Lys(Boc)-Arg(Pbf)-Gly-OH (**44**)*

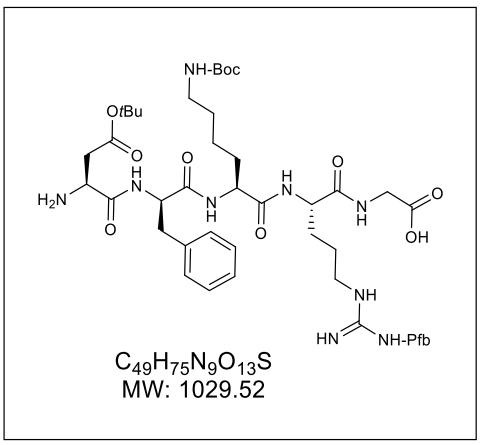

Compound **43** (2.2 g, 2.1 mmol) was dissolved in DMF and cooled at 0 ºC. A 20% solution of piperidine in DMF (20 mL) was then added and the resulting solution was stirred for 3 h at r.t. The suspension was then filtered, the liquid phase was evaporated and used in the following reaction without further purification. Yield: 1.13 g (60%). MS (ESI+): *m/z*

calcd. for $[C_{49}H_{76}N_9O_{13}S]^+$: 1030.56 $[M + H]^+$; found: 1030.5; *m/z* calcd. for $[C_{49}H_{77}N_9O_{13}S]^{2+}$: 515.77 $[M + 2H]^{2+}$; found: 515.9.

*Cyclized H_2N-Asp(OtBu)-D-Phe-Lys(Boc)-Arg(Pbf)-Gly-OH (**45**)*

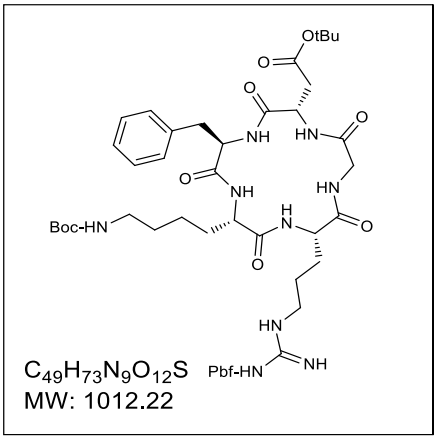

Compound **44** (100 mg,[b] 0.097 mmol, 1 equiv.) was dissolved in 100 mL of DMF (1 mM) and the pH adjusted to 8 by adding aliquots of NaOH 0.2 M. BOP (171 mg, 0.388 mmol, 4 equiv.) and HOBt (52.42 mg, 0.388 mmol, 4 equiv.) were added and the reaction was stirred at r.t. for 24 h. The solvent was evaporated and a 5% aqueous solution of $NaHCO_3$ was added. The precipitate formed was filtered, freeze-dried and used without further purification. MS (ESI+): *m/z* calcd. for $[C_{49}H_{74}N_9O_{12}S]^+$: 1012.52 $[M + H]^+$; found: 1012.6.

*Cyclo[RGDfK] (**46**)*

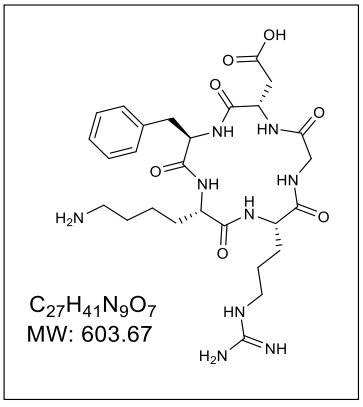

Compound **45** (132 mg) was dissolved in 15 mL of the cleavage cocktail TFA/thioanisol/EDT/phenol/TIS (14.25 mL / 375 µL / 375 µL /1.125 g / 375 µL) and the reaction was stirred at r.t. for 3 h. Cold Et_2O was added to the mixture and centrifuged. The obtained pellet was purified by preparative HPLC [Gradient: 95% (H_2O + 0.1%

[b] It was observed that with an amount of compound **44** larger than ca. 150 mg the performance of the cyclization reaction decreased drastically.

CF_3COOH) / 5% (CH_3CN + 0.1% CF_3COOH) to 50% (H_2O + 0.1% CF_3COOH) / 50% (CH_3CN + 0.1% CF_3COOH) in 45 min]. MS (ESI+): *m/z* calcd. for $[C_{27}H_{42}N_9O_7]^+$: 604.32 $[M + H]^+$; found: 604.4; *m/z* calcd. for $[C_{27}H_{43}N_9O_7]^{2+}$: 302.67 $[M + 2H]^{2+}$; found: 302.9.

Synthesis of Fmoc-Gly-Phe-Leu-Gly-*N*-[4-[[[(*N*-(Boc)-*N*,*N*′-dimethylethylenediamine)carbonyl]oxy]methyl]phenyl (**54**)

*Fmoc-Gly-Phe-Leu-Gly-OH (**48**)*

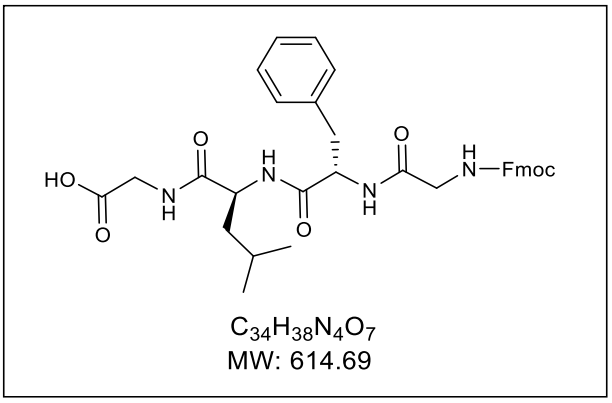

$C_{34}H_{38}N_4O_7$
MW: 614.69

The experimental protocol is described in the general procedure for SPPS.

^{1}H NMR (400 MHz, DMSO) *δ* 12.55 (s, 1H), 8.14-7.98 (m, 3H), 7.89 (d, *J* = 7.5 Hz, 2H), 7.70 (d, *J* = 7.4 Hz, 2H), 7.51 (t, *J* = 6.0 Hz, 1H), 7.41 (t, *J* = 7.3 Hz, 2H), 7.32 (t, *J* = 7.3 Hz, 2H), 7.24-7.18 (m, *J* = 4.0 Hz, 4H), 7.18-7.12 (m, 1H), 4.55 (td, *J* = 8.7, 4.5 Hz, 1H), 4.37-4.29 (m, 1H), 4.28-4.18 (m, 3H), 3.76-3.69 (m, 2H), 3.57 (ddd, *J* = 22.8, 17.2, 6.5 Hz, 2H), 3.02 (dd, *J* = 13.8, 4.4 Hz, 1H), 2.81-2.74 (m, 1H), 1.60 (td, *J* = 13.1, 6.5 Hz, 1H), 1.48 (t, *J* = 7.2 Hz, 2H), 0.85 (dd, *J* = 16.8, 6.5 Hz, 6H); MS (ESI+): *m/z* calcd. for $[C_{34}H_{39}N_4O_7]^+$: 615.28 $[M + H]^+$; found: 615.4.

*Fmoc-Gly-Phe-Leu-Gly-N-[4-(hydroxymethyl)phenyl] (**52**)*

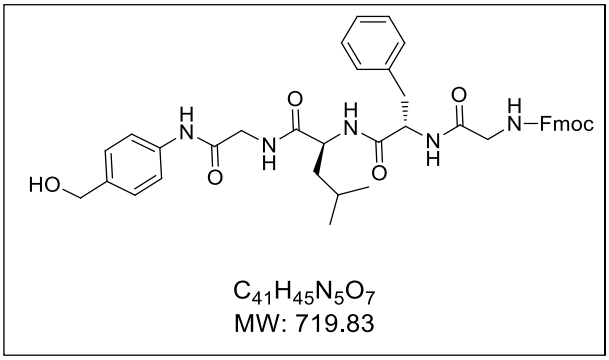

$C_{41}H_{45}N_5O_7$
MW: 719.83

Compound **48** (270 mg, 0.44 mmol, 1 equiv.), HOBt (119 mg, 0.88 mmol, 2 equiv.) and DIC (136 µL, 0.88 mmol, 2 equiv.) were dissolved in DMF (16 mL) under nitrogen and stirred for 5 min. 4-Aminobenzyl alcohol (108.4 mg, 0.88 mmol, 2 equiv.) dissolved in DMF (5 mL) was then added to the previous mixture and the reaction was stirred overnight under nitrogen. DMF was then evaporated and CH_2Cl_2 was added. A yellow precipitate was formed and the solid was separated by filtration. Yield: 249 mg (78%). ^{1}H NMR (400 MHz, DMSO) δ 9.78 (s, 1H), 8.17 (q, *J* = 11.9, 6.7 Hz, 2H), 8.04 (d, *J* = 8.0 Hz, 1H), 7.89 (d, *J* = 7.5 Hz, 2H), 7.70 (d, *J* = 7.4 Hz, 2H), 7.59-7.47 (m, 3H), 7.41 (t, *J* = 7.4 Hz, 2H), 7.32 (t, *J* = 7.4 Hz, 2H), 7.27-7.19(m, 6H), 7.18-7.11 (m, 1H), 5.09 (t, *J* = 5.6 Hz, 1H), 4.57 (td, *J* = 8.6, 4.7 Hz, 1H), 4.43 (d, *J* = 5.2 Hz, 2H), 4.33-4.19 (m, 4H), 3.94-3.80 (m, 2H), 3.59 (ddd, *J* = 46.2, 16.8, 6.1 Hz, 2H), 3.04 (dd, *J* = 13.9, 4.4 Hz, 1H), 2.79 (dd, *J* = 13.8, 9.2 Hz, 1H), 1.66-1.57 (dt, *J* = 13.1, 6.6 Hz, 1H), 1.51 (t, *J* = 7.2 Hz, 2H), 0.87 (dd, *J* = 18.0, 6.4 Hz, 6H) ^{13}C NMR (101 MHz, DMSO) δ 172.70, 171.57,169.46, 167.82, 156.93, 144.29, 141.17, 138.09, 137.89, 129.69, 128.47, 128.11, 127.55, 127.43, 126.70, 125.71, 120.58, 119.28, 66.24, 63.06, 54.19, 51.83, 47.06, 43.78, 42.96, 41.14, 37.89, 24.56, 23.46, 22.15.

*Fmoc-Gly-Phe-Leu-Gly-N-[4-[[[(4-nitrophenoxy)carbonyl]oxy]methyl]phenyl] (**53**)*

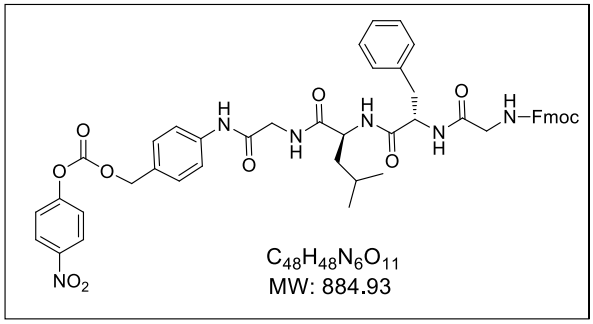

Compound **52** (97 mg, 0.134 mmol, 1 equiv.) was dissolved in a mixture of THF (3 mL) and DMF (1 mL) and the reaction was cooled to 0 ºC under nitrogen. Pyridine was added (27 µL, 0.335 mmol, 2.5 equiv.) followed by a solution of 4-nitrophenyl chloroformate (54 mg, 0.268 mmol, 2 equiv.) in DMF (710 µL). The reaction was stirred for 10 min at 0 ºC and then stirred for 2 h at r.t.. The solvent mixture was then removed and the crude was dissolved in CH_2Cl_2 and washed with 1 M aqueous $KHSO_4$ (2 ×). The organic phase was dried over Na_2SO_4, concentrated and purified by flash chromatography (eluent: 95:5 CH_2Cl_2/MeOH). Yield: 68.1 mg (58%). ^{1}H NMR (400 MHz, DMSO) δ 9.93 (s, 1H), 8.34-8.27 (m, 2H), 8.24-8.15 (m, 2H), 8.03 (d, *J* = 7.9 Hz, 1H), 7.88 (d, *J* = 7.5 Hz, 2H), 7.68 (dd, *J* = 12.0, 8.0 Hz, 4H), 7.59-7.49 (m, 3H), 7.41 (t, *J* = 8.1 Hz, 4H), 7.31 (t, *J* = 7.1 Hz, 2H), 7.22 (d, *J* = 4.3 Hz, 4H), 7.18-7.11 (m, 1H), 5.24 (s, 2H), 4.62-4.51 (m, 1H), 4.34-4.17 (m, 4H), 3.89 (d, *J* = 6.1 Hz, 2H), 3.72-3.48 (m, 2H), 3.04 (dd, *J* = 13.9, 4.4 Hz, 1H), 2.79 (dd, *J* = 13.9, 9.3 Hz, 1H), 1.61 (dt, *J* = 13.1, 6.5 Hz, 1H), 1.51 (t, *J* = 7.2 Hz, 2H), 0.87 (dd, *J* = 18.2, 6.4 Hz, 6H). ^{13}C NMR (101 MHz, DMSO) δ 172.76, 171.58, 169.47, 168.17, 156.93, 155.76, 152.43, 145.64, 144.29, 141.17, 139.74, 138.08, 129.98, 129.69, 128.47, 128.10, 127.54, 126.69, 125.87, 125.71, 123.07, 120.58, 119.46, 70.72, 66.24, 54.18, 51.82, 47.06, 43.78, 43.16, 41.13, 37.90, 24.55, 23.77, 23.45, 22.15; MS (ESI+): *m/z* calcd. for $[C_{48}H_{48}N_6NaO_{11}]^+$: 907.33 $[M + Na]^+$; found: 907.37.

*Fmoc-Gly-Phe-Leu-Gly-N-[4-[[[(N-(Boc)-N,N'-dimethylethylenediamine)carbonyl]oxy]methyl]phenyl] (**54**)*

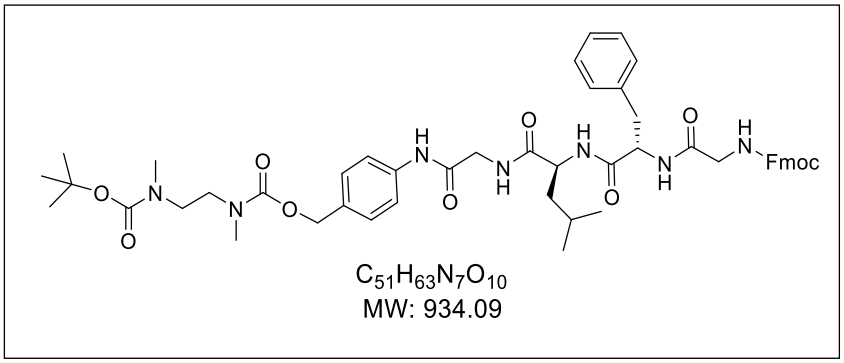

Compound **53** was dissolved in THF (1 mL) and the solution cooled to 0 ºC under nitrogen. A solution of *N*-Boc-*N*,*N'*-dimethylethylenediamine (13.9 µL, 0.068 mmol, 2 equiv.) and *i*Pr_2NEt (14.8 µL, 0.085 mmol, 2.5 equiv.) in THF (0.55 mL) was then added and the reaction was stirred overnight at r.t..The mixture was diluted with CH_2Cl_2 and washed with 1 M aqueous solution of $KHSO_4$ (2 ×), saturated aqueous solution of $NaHCO_3$ (2 ×) and brine (1 ×). The organic phase was dried over Na_2SO_4 and concentrated. The product was used without further purification. Yield: 27.6 mg (87%). ^{1}H NMR (400 MHz, DMSO) *δ* 9.86 (s, 1H), 8.21-8.14 (m, 2H), 8.03 (d, *J* = 8.0 Hz, 1H), 7.89 (d, *J* = 7.5 Hz, 2H), 7.68 (t, *J* = 14.0 Hz, 2H), 7.60 (d, *J* = 8.2 Hz, 2H), 7.52 (t, *J* = 5.9 Hz, 1H), 7.41 (t, *J* = 7.4 Hz, 2H), 7.36-7.25 (m, 4H), 7.21 (d, *J* = 4.2 Hz, 4H), 7.18-7.10 (m, 1H), 4.97 (s, 2H), 4.63-4.51 (m, 1H), 4.36-4.08 (m, 4H), 3.90 (d, *J* = 14.7 Hz, 2H), 3.73-3.49 (m, 2H), 3.03 (dd, *J* = 13.8, 4.3 Hz, 1H), 2.87-2.64 (m, 8H), 1.65-1.57 (m, 1H), 1.56-1.47 (m, = 2H), 1.43-1.31 (m, 12H), 0.86 (dd, *J* = 18.1, 6.4 Hz, 6H); ^{13}C NMR (101 MHz, DMSO) *δ* 172.25, 171.08, 168.99, 167.54, 156.46, 155.34, 154.65, 143.82, 140.70, 138.47, 137.61, 132.08, 131.60, 129.22, 128.93, 128.42, 128.27, 127.99, 127.62, 127.29, 127.07, 126.21, 125.24, 121.39, 120.10, 118.93, 78.45, 66.04, 65.77, 53.71, 51.33, 46.59, 45.89, 43.30, 42.65, 40.67, 37.43, 33.70, 28.02, 24.08, 22.98, 21.67; MS (ESI+) *m/z* calcd. for $[C_{51}H_{63}N_7NaO_{10}]^+$: 956.45 $[M + Na]^+$; found: 956.71.

Synthesis of *cyclo*[DKP-RGD]-GFLG-PTX (**37**) and *cyclo*[RGDfK]-GFLG-PTX (**38**)

*(Hemiglutarate)-Gly-Phe-Leu-Gly-N-[4-[[[(N-(Boc)-N,N'-dimethylethylenediamine)carbonyl]oxy]methyl]phenyl] (**55**)*

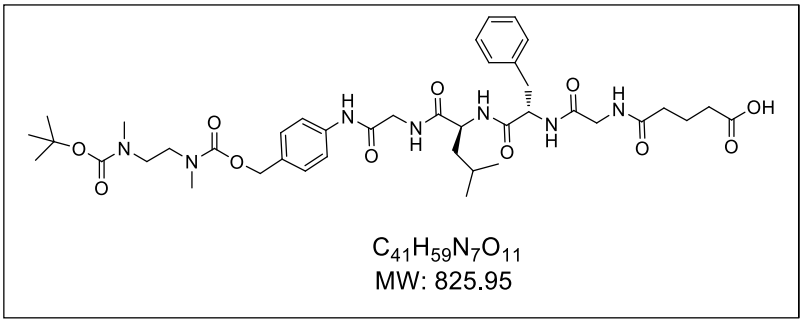

$C_{41}H_{59}N_7O_{11}$
MW: 825.95

Compound **54** (10 mg, 0.011 mmol, 1 equiv.) was dissolved in DMF (200 µL) and the mixture was cooled to 0 ºC under nitrogen. Piperidine (5.3 µL, 0.054 mmol, 5 equiv.) was added and the reaction was stirred for 5 h. The crude was diluted with CH_2Cl_2 and extracted with saturated aqueous solution of $NaHCO_3$ (3 ×). The organic phase was dried over Na_2SO_4, concentrated, dried under vacuum for 2 h and used in the following step without further purification. The crude free amine (0.011 mmol, 1 equiv.) was dissolved in DMF (120 µL) and cooled to 0 ºC under nitrogen atmosphere. *i*Pr_2NEt (7.1 µL, 0.041 mmol, 3.75 equiv.), DMAP (0.33 mg, 0.00275 mmol, 0.25 equiv.) and glutaric anhydride (3.1 mg, 0.0275 mmol, 2.5 equiv.) were then added and the reaction was stirred overnight at r.t.. The mixture was diluted in CH_2Cl_2 and washed with 1 M aqueous solution of $KHSO_4$ (2 ×) and brine (1 ×). The organic phase was dried over Na_2SO_4, concentrated and purified by flash chromatography (eluent: 9:1 CH_2Cl_2/MeOH + 0.2% AcOH). Yield: 6.4 mg (70%) over two steps. ^{1}H NMR (400 MHz, DMSO): δ 9.91 (s, 1H), 8.37 (s, 1H), 8.24-8.15 (t, *J* = 5.5 Hz, 2H), 8.06 (t, *J* = 5.4 Hz, 1H), 7.62 (d, *J* = 8.3 Hz, 2H), 7.28 (d, *J* = 8.3 Hz, 2H), 7.25-7.21 (m, 4H), 7.19-7.15 (m, 1H), 4.98 (s, 2H), 4.53 (td, *J* = 9.0, 4.6 Hz, 1H), 4.29 (td, *J* = 14.0, 8.4 Hz, 1H), 3.87 (d, *J* = 5.8 Hz, 2H), 3.70-3.53 (m, 3H), 3.32 (s, 6H), 3.04 (dd, *J* = 13.8, 4.4 Hz, 1H), 2.87-2.65 (m, 8H), 2.14 (dd, *J* = 16.7, 7.5 Hz, 4H), 1.89 (s, 2H), 1.74-1.67 (m, 2H), 1.64-1.48 (m, 4H), 1.35 (s, 9H), 0.87 (dd, *J* = 20.2, 6.3 Hz, 6H). ^{13}C NMR (101 MHz, DMSO) δ 172.86, 171.69, 169.53, 168.15, 155.82, 138.99, 138.23, 132.04, 129.66, 128.87, 128.73, 128.50, 126.69, 119.42, 78.88, 66.53, 66.32, 54.55, 51.89, 46.80, 46.42, 46.32, 46.08, 43.28, 42.52, 41.08, 37.73, 34.88, 34.41, 34.15, 28.42, 24.57, 23.50, 22.09, 21.22; MS (ESI+) *m/z* calcd. for $[C_{41}H_{59}N_7NaO_{11}]^+$: 848.42 $[M + Na]^+$; found: 848.64.

*Cyclo[DKP–RGD]–Gly-Phe-Leu-Gly-N-[4-[[[(N-(Boc)-N,N'-dimethylethylenediamine)carbonyl]oxy]methyl]phenyl] (**56a**).*

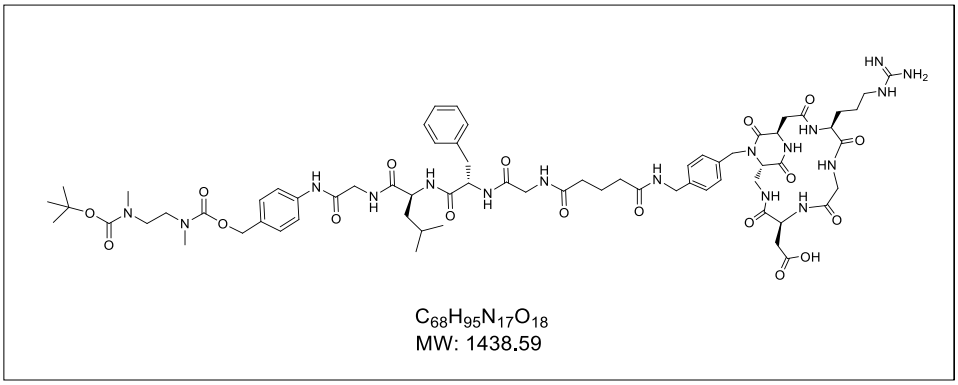

Compound **55** (11 mg, 0.0119 mmol, 2 equiv.) was dissolved in DMF (500 µL) and cooled to 0 ºC under nitrogen. *N*-Hydroxysuccinimide (NHS, 1.8 mg, 0.0155 mmol, 2.6 equiv.) and EDC·HCl (3.4 mg, 0.0179 mmol, 3 equiv.) were added and the reaction was stirred at 0 ºC for 5 min. The reaction was allowed to reach r.t. and stirred overnight under nitrogen. Volatiles were removed in vacuo and the crude was re-dissolved in DMF (375 µL). A solution of compound **32** (5.2 mg, 0.006 mmol, 1 equiv.) in phosphate buffer solution (375 µL, pH 7.5) was then added. During the first 3 h, the pH value was kept near 7.3-7.5 adding 0.2 M aqueous NaOH when necessary. The resulting solution was stirred overnight and then concentrated under vacuum. The crude residue was purified by semipreparative HPLC [Gradient: 100% (H_2O + 0.1% CF_3COOH) / 0% (CH_3CN + 0.1% CF_3COOH) to 25% (H_2O + 0.1% CF_3COOH) / 75% (CH_3CN + 0.1% CF_3COOH) in 15 min; t_R (product): 10.5 min]. Yield: 1.41 mg (15%) over 2 steps. HRMS (ESI+): *m/z* calcd. for $[C_{68}H_{96}N_{17}O_{18}]^+$:1438.712 $[M + H]^+$; found: 1438.710; *m/z* calcd. for $[C_{68}H_{96}N_{17}NaO_{18}]^+$: 730.856 $[M + H + Na]^{2+}$; found: 730.851; *m/z* calcd. for $[C_{68}H_{95}N_{17}Na_2O_{18}]^{2+}$: 741.840 $[M + 2Na]^{2+}$; found: 741.842.

*Cyclo[DKP-RGD]-GFLG-PTX (**37**)*

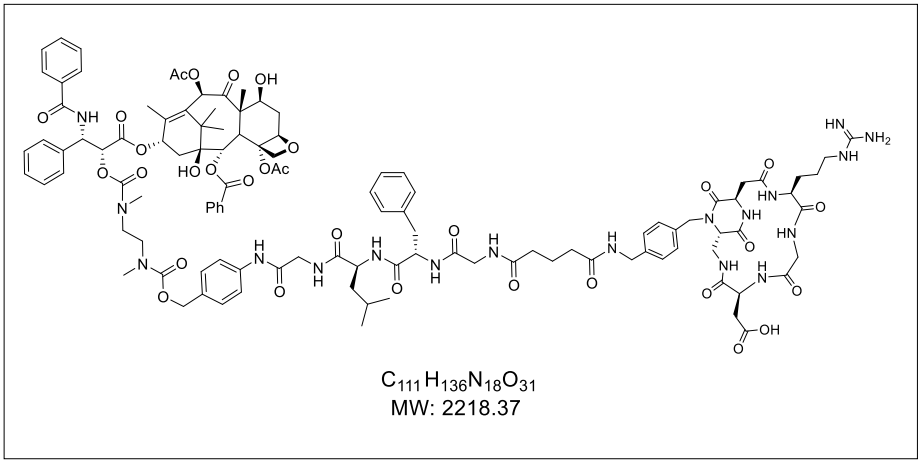

A half volume of TFA was added to a 0.03 M solution of intermediate **56a** in CH_2Cl_2 and the reaction was stirred at r.t. for 1 h. The solvent was evaporated under vacuum to afford the amine TFA salt. The crude was freeze-dried and used without further purification. The resulting TFA salt (6.4 mg, 0.0041 mmol, 1 equiv.) was dissolved in DMF (470 µL) and cooled to 0 ºC under nitrogen atmosphere. *i*Pr_2NEt (3.6 µL, 0.0205 mmol, 5 equiv.) and 2'-(4-nitrophenoxycarbonyl)paclitaxel (12.5 mg, 0.0123 mmol, 3.5 equiv.) were added and the mixture was allowed to reach r.t. and stirred overnight. The crude was concentrated, and the residue was purified by semipreparative HPLC [Gradient: 100% (H_2O + 0.1% CF_3COOH) / 0% (CH_3CN + 0.1% CF_3COOH) to 0% (H_2O + 0.1% CF_3COOH) / 100% (CH_3CN + 0.1% CF_3COOH) in 20 min; t_R (product): 12.5 min]. Yield: 2.09 mg (26%). MS (MALDI): *m/z* calcd. for $[C_{111}H_{137}N_{18}O_{31}]^+$: 2219.38 $[M + H]^+$; found: 2220.6 (HCCA matrix), 2219.1 (SA matrix); HRMS (ESI+): *m/z* calcd. for $[C_{111}H_{137}N_{18}O_{31}Na]^{2+}$: 1120.480 $[M + H + Na]^{2+}$; found: 1120.479; *m/z* calcd. for $[C_{111}H_{137}N_{18}O_{31}Na_2]^{3+}$: 754.650 $[M + H + 2Na]^{3+}$; found: 754.648.

*Cyclo[RGDfK]-Gly-Phe-Leu-Gly-N-[4-[[[(N-(Boc)-N,N'-dimethylethylenediamine)carbonyl]oxy]methyl]phenyl] (**56b**)*

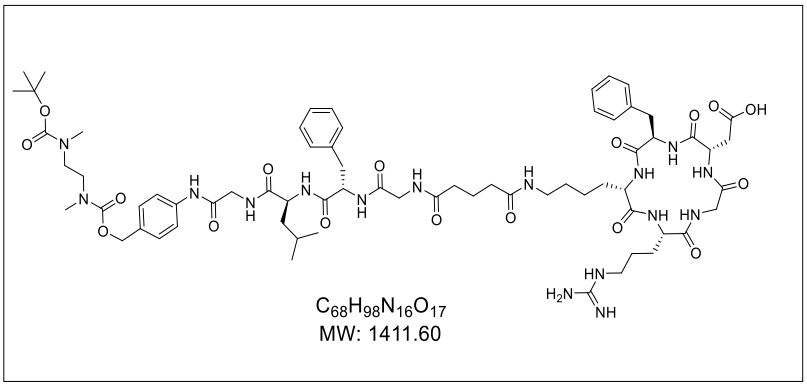

Compound **55** (13 mg, 0.016 mmol, 1.3 equiv.) was dissolved in DMF (350 µL) and cooled to 0 ºC under nitrogen. NHS (2.8 mg, 0.024 mmol, 2 equiv.) and DIC (3.7 µL, 0.024 mmol, 2 equiv.) were added and the reaction was stirred at 0 ºC for 5 min. The reaction was allowed to reach r.t. and stirred overnight under nitrogen. Volatiles were then removed in vacuo and the crude was re-dissolved in DMF (750 µL). A solution of *cyclo*[RGDfK] 1 (10 mg, 0.012 mmol, 1 equiv.) in phosphate buffer (750 µL, pH 7.5) was then added. In the initial part of the reaction (first 2-3 h), the pH was kept in the 7.3-7.6 range by adding small aliquots of 0.2 M NaOH. The resulting solution was stirred overnight and then concentrated under vacuum. The crude residue was purified by semipreparative HPLC [Gradient: 100% (H_2O + 0.1% CF_3COOH) / 0% (CH_3CN + 0.1% CF_3COOH) to 25% (H_2O + 0.1% CF_3COOH) / 75% (CH_3CN + 0.1% CF_3COOH) in 15 min; t_R (product): 11 min]. Yield: 3.15 mg (17%) over two steps. MS (MALDI): *m/z* calcd. for $[C_{68}H_{99}N_{16}O_{17}]^+$: 1412.61 $[M + H]^+$; found: 1412.2 (HCCA matrix); HRMS (ESI+): *m/z* calcd. for $[C_{68}H_{98}N_{16}NaO_{17}]^+$: 1433.719 $[M + Na]^+$; found: 1433.717; *m/z* calcd. for $[C_{68}H_{98}N_{16}Na_2O_{17}]^{2+}$ 728.360 $[M + 2Na]^{2+}$; found: 728.355.

*Cyclo[RGDfK]-GFLG-PTX (**38**)*

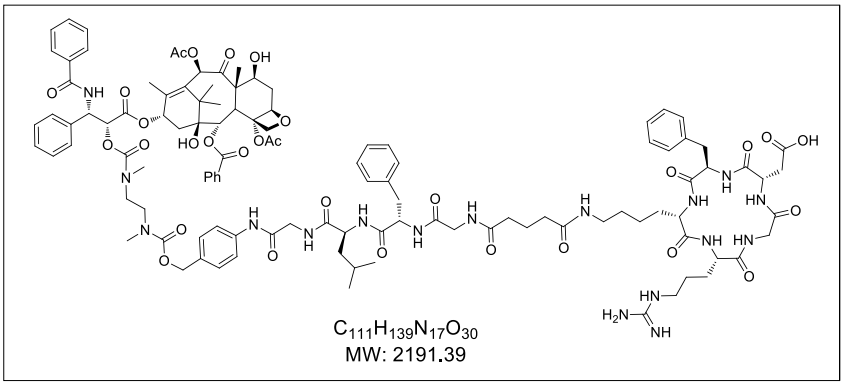

A half volume of TFA was added to a 0.03 M solution of intermediate **56b** in CH_2Cl_2 and the reaction was stirred at r.t. for 1 h. The solvent was evaporated to afford the free amine as TFA salt. The crude was freeze-dried and used without further purification. The resulting TFA salt (2.5 mg, 0.00163 mmol, 1 equiv.) was dissolved in DMF (190 µL) and cooled at 0 ºC under nitrogen atmosphere. *i*Pr_2NEt (2 µL, 0.0115 mmol, 7 equiv.) and 2'-(4-nitrophenoxycarbonyl)paclitaxel **60** (5.8 mg, 0.0057 mmol, 3.5 equiv.) were added and the mixture was stirred overnight at r.t.. The crude was concentrated, and the residue was purified by semipreparative HPLC [Gradient: 100% (H_2O + 0.1% CF_3COOH) / 0% (CH_3CN + 0.1% CF_3COOH) to 0% (H_2O + 0.1% CF_3COOH) / 100% (CH_3CN + 0.1% CF_3COOH) in 20 min; t_R (product): 13 min]. Yield: 1.22 mg (33%). MS (MALDI): *m/z* calcd. for $[C_{111}H_{140}N_{17}O_{30}]^+$: 2192.39 $[M + H]^+$; found: 2193.4 (HCCA matrix); 2194.1 (SA matrix); HRMS (ESI+): *m/z* calcd. for $[C_{111}H_{140}N_{17}O_{30}Na]^{2+}$: 1106.993 $[M + H + Na]^{2+}$; found: 1106.991.

Synthesis of *cyclo*[RGDfK]-PEG-4-azide **(51a**)

*Cyclo[RGDfK]-PEG-4-azide **(51a)*** [c]

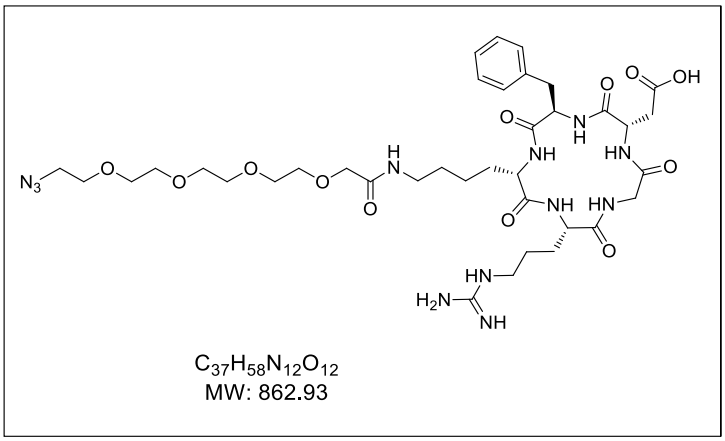

Compound **50** (6.52 mg, 0.018 mmol, 1.3 equiv.) was dissolved in CH_3CN (800 µL) and cooled to 0 ºC under nitrogen atmosphere. *Cyclo*[RDGfK] **46** (10 mg, 0.014 mmol, 1 equiv.) was dissolved in phosphate buffer solution (pH 7.5, 600 µL) and added to the previous solution. The reaction was allowed to reach r.t. and stirred overnight under nitrogen. During the first 3 h, the pH value was kept near 7.3-7.5 by adding 0.2 M aqueous NaOH when necessary. The mixture was then concentrated and the crude purified by semipreparative HPLC [gradient: 90% (H_2O + 0.1% CF_3COOH) / 10% (CH_3CN + 0.1% CF_3COOH) to 55% (H_2O + 0.1% CF_3COOH) / 45% (CH_3CN + 0.1% CF_3COOH) in 10 min]. ^{1}H NMR (400 MHz, D_2O) δ 7.39 (t, *J* = 7.2 Hz, 2H), 7.33 (d, *J* = 7.1 Hz, 1H), 7.27 (d, *J* = 7.2 Hz, 2H), 4.65 (dd, *J* = 9.6, 6.3 Hz, 1H), 4.36 (dd, *J* = 9.0, 5.6 Hz, 1H), 4.22 (d, *J* = 15.0 Hz, 1H), 4.09 (s, 2H), 3.89 (dd, *J* = 10.1, 4.7 Hz, 1H), 3.76 (s, 5H), 3.72 (t, *J* = 3.2 Hz, 10H), 3.53 (s, 1H), 3.50 (t, *J* = 4.8 Hz, 3H), 3.26-3.13 (m, 5H), 3.11-2.88 (m, 4H), 2.75 (dd, *J* = 16.8, 6.4 Hz, 1H), 1.88 (dt, *J* = 20.3, 6.8 Hz, 1H), 1.66 (dd, *J* = 17.2, 11.4 Hz, 3H), 1.58-1.46 (m, 4H), 1.04-0.94 (dd, *J* = 14.3, 7.1 Hz, 2H), 1.00 (s, 2H); ^{13}C NMR (101 MHz, D_2O) δ 174.53, 174.32, 173.02, 172.72, 172.26, 171.33, 171.27, 156.66, 135.97, 129.14, 128.79, 127.24, 70.30, 69.64, 69.56, 69.21, 55.41, 55.04, 52.38, 50.14, 49.61, 43.46, 40.46, 38.51, 36.96, 34.28, 29.90, 27.58, 27.30, 24.43, 22.55; MS (ESI+) *m/z* calcd. for $[C_{37}H_{59}N_{12}O_{12}]^+$: 863.44 $[M + H]^+$; found: 863.65; *m/z* calcd. for $[C_{37}H_{58}N_{12}NaO_{12}]^+$: 885.42 $[M + Na]^+$; found: 885.66; *m/z* calcd. for $[C_{37}H_{59}N_{12}NaO_{12}]^{2+}$: 443.22 $[M + Na + H]^{2+}$; found: 443.78.

[c] A. Raposo Moreira Dias, A. Pina, A. Dal Corso, D. Arosio, L. Belvisi, L. Pignataro, M. Caruso, C. Gennari, *Chem. Eur. J.* **2017**, *23*, 14410-14415.

Synthesis of *cyclo*[DKP-RGD]-PEG-4-GFLG-PTX (**39**) and *cyclo*[RGDfK]-PEG-4-GFLG-PTX (**40**)

*4-((5S,8S)-8-benzyl-5-isobutyl-4,7,10,13-tetraoxo-3,6,9,12-tetraazaheptadec-16-ynamido)benzyl tert-butyl ethane-1,2-diylbis(methylcarbamate) (**57**)*

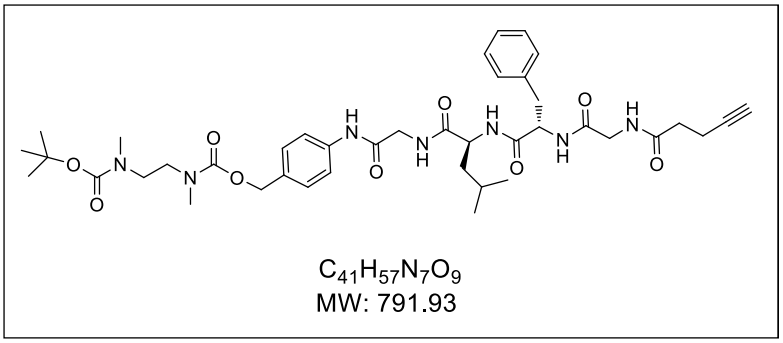

$C_{41}H_{57}N_7O_9$
MW: 791.93

Compound **54** (15 mg, 0.016 mmol, 1 equiv.) was dissolved in DMF (300 µL) and cooled to 0 ºC under nitrogen. Piperidine (7.9 µL, 0.08 mmol, 5 equiv.) was added and the reaction was stirred at r.t. overnight. The mixture was diluted with AcOEt and washed with saturated aqueous solution of $NaHCO_3$ (3 ×). The organic phase was dried over Na_2SO_4, concentrated and dried under vacuum. The resulting free amine was used in the next step without further purification. A solution of 4-pentynoic acid (2.35 mg, 0.024 mmol, 1.5 equiv.) in DMF (540 µL) was cooled to 0 ºC under nitrogen. HATU (10.3 mg, 0.0272 mmol, 1.7 equiv.), HOAt (3.7 mg, 0.0272 mmol, 1.7 equiv.) and *i*Pr_2NEt (11 µL, 0.064 mmol, 4 equiv.) were added and the mixture was stirred at 0 ºC for 20 min. A solution of the free amine in DMF (230 µL) was then added to the stirred mixture. The reaction was allowed to reach room temperature and stirred overnight. The mixture was diluted with a 4:1 AcOEt/CH_2Cl_2 mixture and washed with 1 M aqueous solution of $KHSO_4$ (2 ×), a saturated aqueous solution of $NaHCO_3$ (1 ×) and brine (1 ×). The organic phase was dried over Na_2SO_4 and concentrated. The solid was suspended in Et_2O and the product was collected. Yield: 6.9 mg (55%) over two steps. ^{1}H NMR (400 MHz, DMSO) δ 9.86 (s, 1H), 8.19-8.10 (m, 3H), 8.05 (d, *J* = 8.1 Hz, 1H), 7.60 (d, *J* = 8.4 Hz, 2H), 7.29 (d, *J* = 8.4 Hz, 2H), 7.25-7.21 (m, 4H), 7.19-7.13 (m, 1H), 4.98 (s, 2H), 4.54 (td, *J* = 9.0, 4.3 Hz, 1H), 4.29 (dd, *J* = 14.7, 7.9 Hz, 1H), 3.87 (dd, *J* = 5.5, 3.1 Hz, 2H), 3.76-3.54 (m, 2H), 3.04 (dd, *J* = 13.9, 4.2 Hz, 1H), 2.86-2.65 (m, 9H), 2.32 (s, 4H), 1.65-1.56 (m, 1H), 1.52 (t, *J* = 6.6 Hz, 2H), 1.35 (s, 12H), 0.88 (dd, *J* = 20.1, 6.4 Hz, 6H); MS (ESI+) *m/z* calcd. for $[C_{41}H_{57}N_7NaO_9]^+$: 814.41 $[M + Na]^+$; found: 814.66.

*Alkyne-Gly-Phe-Leu-Gly-PTX (**58**)*

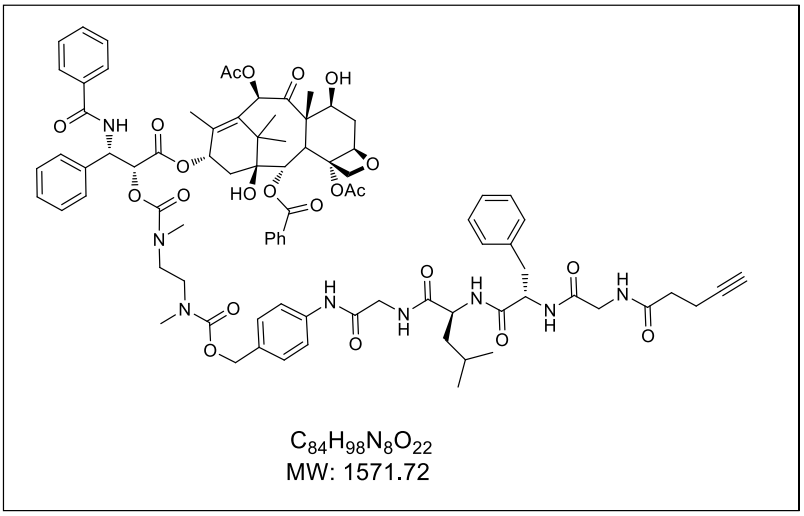

$C_{84}H_{98}N_8O_{22}$
MW: 1571.72

A half volume of TFA was added to a 0.03 M solution of compound **57** in CH_2Cl_2 and the reaction was stirred at r.t. for 1 h. The solvent was evaporated to afford the free amine as TFA salt. The crude was freeze-dried and used without further purification. The resulting TFA salt (7.5 mg, 0.0108 mmol, 1 equiv.) was dissolved in DMF (320 µL) and cooled at 0 ºC under nitrogen atmosphere. *i*Pr_2NEt (7.5 µL, 0.043 mmol, 4 equiv.) and 2'-(4-nitrophenoxycarbonyl)paclitaxel **60** (16.5 mg, 0.0162 mmol, 1.5 equiv.) were added and the mixture was stirred at r.t. overnight. The reaction mixture was diluted with AcOEt and washed with a 1 M aqueous solution of $KHSO_4$ (2 ×) and brine (1 ×). The organic phase was dried over Na_2SO_4, concentrated and purified by flash chromatography (eluent: 9:1 CH_2Cl_2/MeOH) to afford pure **58**. Yield: 10.18 mg (60%). HRMS (ESI+): *m/z* calcd. for $[C_{84}H_{98}N_8O_{22}Na]^+$: 1593.669 [M + Na]$^+$; found: 1593.667; *m/z* calcd. for $[C_{84}H_{98}N_8O_{22}Na_2]^{2+}$: 808.329 [M + 2Na]$^{2+}$; found: 808.328.

*Cyclo[DKP-RGD]-PEG-4-GFLG-PTX (**39**)*

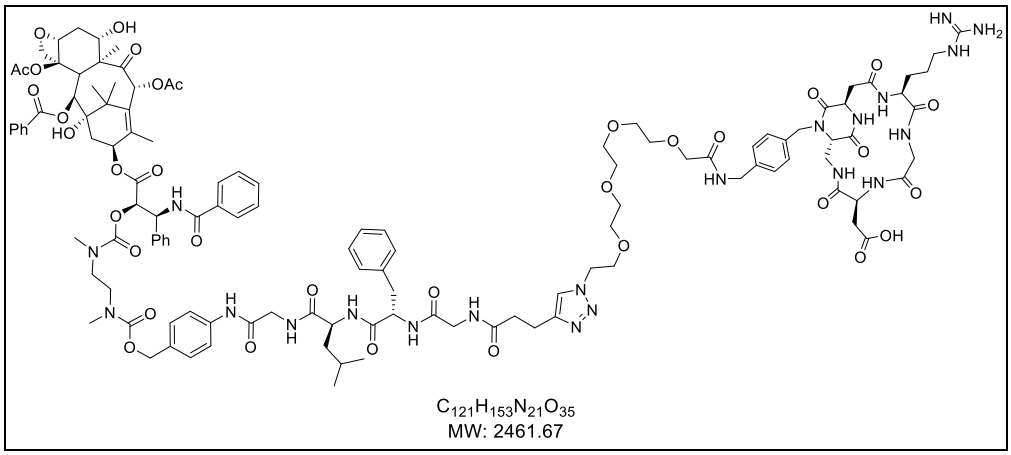

Compounds **58** (3.9 mg, 0.0025 mmol, 1.5 equiv.) and **51b** (1.7 mg, 0.0017 mmol, 1 equiv.) were dissolved in a degassed 1:1 water/DMF mixture (170 µL). Degassed aqueous solutions of $CuSO_4 \cdot 5H_2O$ (0.2 mg, 0.000835 mmol, 0.5 equiv.) and sodium ascorbate (0.198 mg, 0.001 mmol, 0.6 equiv.) were added at r.t. and the mixture was stirred overnight at 30 ºC. The solution was concentrated, and the crude residue was purified by semipreparative HPLC [Gradient: 100% (H_2O + 0.1% CF_3COOH) / 0% (CH_3CN + 0.1% CF_3COOH) to 0% (H_2O + 0.1% CF_3COOH) / 100% (CH_3CN + 0.1% CF_3COOH) in 20 min; t_R (product): 12.5 min]. Yield: 1.67mg (39%) over two steps. MS (ESI+): *m/z* calcd. for $[C_{121}H_{153}N_{21}O_{35}Na_2]^{2+}$: 1253.81 $[M + 2Na]^{2+}$, found 1254.06; MS (ESI-): *m/z* calcd. for $[C_{121}H_{151}N_{21}O_{35}]^{2-}$: 1229.8 $[M - 2H]^{2-}$, found 1230.0.

*Cyclo[RGDfK]-PEG-4-GFLG-PTX (**40**)*

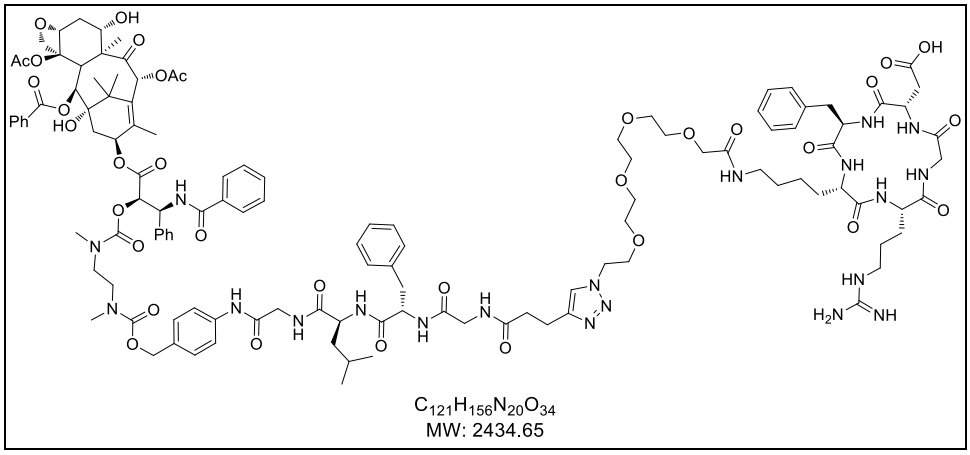

Compound **58** (5 mg, 0.0032 mmol, 1.5 equiv.) and **51a** (1.84 mg, 0.0022 mmol, 1 equiv.) were dissolved in a degassed 1:1 water/DMF mixture (220 µL). Degassed aqueous solutions of $CuSO_4 \cdot 5H_2O$ (0.28 mg, 0.0011 mmol, 0.5 equiv.) and sodium ascorbate (0.26 mg, 0.00132 mmol, 0.6 equiv.) were added at r.t. and the mixture was stirred overnight at 30 ºC. The solution was concentrated, and the crude residue was purified by semipreparative HPLC [Gradient: 100% (H_2O + 0.1% CF_3COOH) / 0% (CH_3CN + 0.1% CF_3COOH) to 0% (H_2O + 0.1% CF_3COOH) / 100% (CH_3CN + 0.1% CF_3COOH) in 20 min; t_R (product): 13 min]. Yield: 4.13 mg (76 %) over two steps. MS (MALDI): *m/z* calcd. for $[C_{121}H_{157}N_{20}O_{34}]^+$: 2434.65 $[M + H]^+$, found: 2436.0 (HCCA matrix); 2435.7 (SA matrix).

Synthesis of *cyclo*[DKP-RGD]-α-amanitin conjugates (62 and 63)

Synthesis of *cyclo*[DKP-RGD]-Val-Ala-α-amanitin (**62**)

Hemiglutarate-Val-Ala-α-amanitin (**65b**)

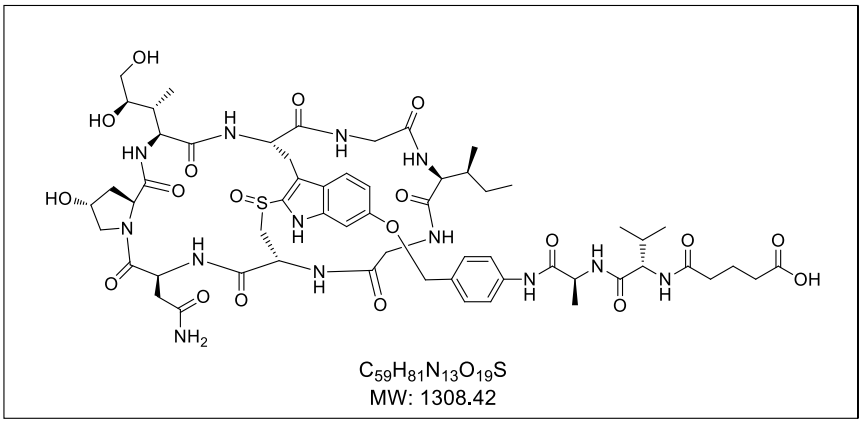

Compound **64b** (5 mg, 3.9 µmol, 1 equiv.) was cooled at 0 ºC under nitrogen atmosphere. Glutaric anhydride (0.65 mg, 5.7 µmol, 1.5 equiv.), DMAP (0.12 mg, 0.9 µmol, 0.25 equiv.) and *i*Pr_2NEt (1 µL, 5.7 µmol, 1.5 equiv.) were added as stock solutions in DMF and the reaction was stirred at 0 ºC for a few minutes. The mixture was then warmed to room temperature and stirred overnight under nitrogen atmosphere. The solvent was evaporated under high vacuum and the crude was purified by semipreparative HPLC [Waters Atlantis 21 mm × 10 cm column; gradient: 100% (H_2O + 0.1 % CF_3COOH)/0% (CH_3CN + 0.1% CF_3COOH) to 50% (H_2O + 0.1 % CF_3COOH)/50% (CH_3CN + 0.1% CF_3COOH) in 9 minutes; t_R: (product): 8.6 min]. The purified compound was then freeze-dried to allow compound **65b** as a white solid (4.92 mg, 98% yield). MS (MALDI-TOF): *m/z* calcd. for $[C_{59}H_{82}N_{13}O_{19}S]^+$: 1309.42 $[M + H]^+$; found: 1309 (SA matrix); *m/z* calcd. for $[C_{59}H_{81}N_{13}NaO_{19}S]^+$: 1331.40 $[M + Na]^+$; found: 1331.7 (HCCA matrix), 1331 (SA matrix); *m/z* calcd. for $[C_{59}H_{81}N_{13}Na_2O_{19}S_2]^{2+}$: 1354.39 $[M + 2\ Na]^{2+}$; found: 1353.7 (HCCA matrix), 1353 (SA matrix).

Cyclo[DKP-RGD]-Val-Ala-α-amanitin (**62**)

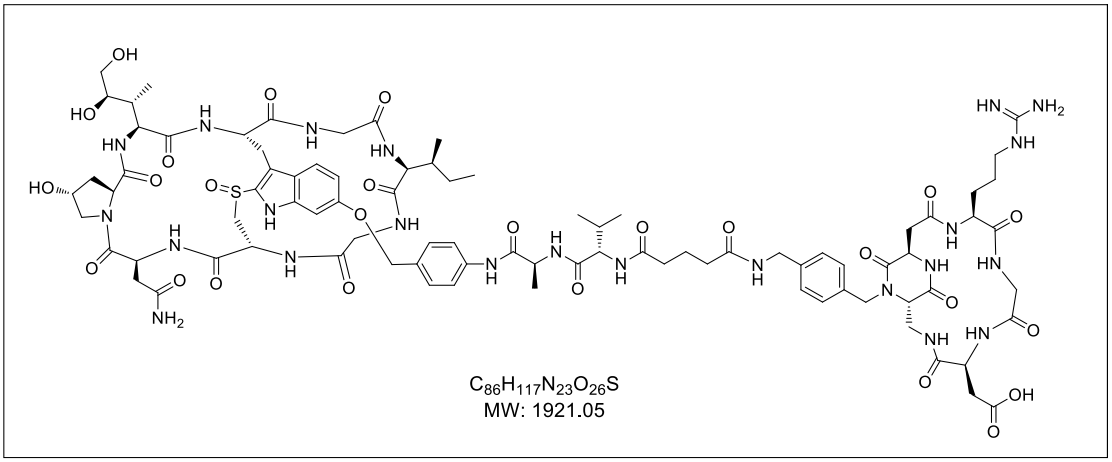

Compound **65b** (8.46 mg, 6.5 μmol, 1 equiv.) was dissolved in 80 μL of DMF and cooled at 0 ºC under nitrogen conditions. *N*-hydroxysuccinimide (1.11 mg, 9.7 μmol, 1.5 equiv.) and DIC (1.5 μL, 9.7 μmol, 1.5 equiv.) were added (the two incorporated reagents were prepared as stock solutions in DMF) and the reaction was stirred at 0 ºC for a few minutes. The mixture was then warmed to room temperature and stirred overnight under nitrogen atmosphere. Volatiles were then removed *in vacuo* to give a solid, which was re-dissolved in PBS (210 μL, pH 7.5) and DMF (30 μL) and cooled at 0 ºC. A solution of NH_2CH_2-*cyclo*[DKP-RGD] (**32**) (2.78 mg, 3.23 μL, 0.5 equiv.) in phosphate buffer (150 μL, pH 7.5) was then added to the previous solution, and the pH was adjusted to 7.3-7.6 by adding small aliquots of aqueous NaOH (0.2 M) during the first hours of reaction, until a stable value was observed. The solution was concentrated, and the crude residue was purified by semipreparative HPLC [Waters Atlantis 21 mm × 10 cm column; flow: 15 mL/min, gradient: 100% (H_2O + 0.1 % CF_3COOH)/0% (CH_3CN + 0.1% CF_3COOH) to 50% (H_2O + 0.1 % CF_3COOH)/50% (CH_3CN + 0.1% CF_3COOH) in 9 minutes; t_R: (product): 8.3 min]. The purified compound was then freeze-dried to allow compound **62** as a white solid (4.85 mg, 74% of yield).

MS (ESI+) *m/z* calcd. for $[C_{86}H_{119}N_{23}O_{26}S]^{2+}$: 960.92 $[M + 2H]^{2+}$; found: 960.76; *m/z* calcd. for $[C_{86}H_{118}N_{23}NaO_{26}S]^{2+}$: 971.91 $[M + Na + H]^{2+}$; found: 972.23; *m/z* calcd. for $[C_{86}H_{117}N_{23}Na_2O_{26}S]^{2+}$: 982.9 $[M + 2Na]^{2+}$; found: 982.74; HRMS (ESI+): *m/z* calcd. for $[C_{86}H_{118}N_{23}NaO_{26}S]^{2+}$: 971.91 $[M + Na + 1H]^{2+}$; found: 971.91; *m/z* calcd. for $[C_{86}H_{117}N_{23}Na_2O_{26}S]^{2+}$: 982.90 $[M + 2Na]^{2+}$; found: 982.90; *m/z* calcd. for $[C_{86}H_{116}N_{23}Na_3O_{26}S]^{2+}$: 993.89 $[M + 3Na - H]^{2+}$; found: 993.89; *m/z* calcd. for $[C_{86}H_{117}N_{23}Na_3O_{26}S]^{3+}$: 662.93 $[M + 3Na]^{3+}$; found: 662.93.

Synthesis of *cyclo*[DKP-RGD]-uncleavable-α-amanitin (**63**)

Hemiglutarate-aminohexyl-α-amanitin (**65a**)

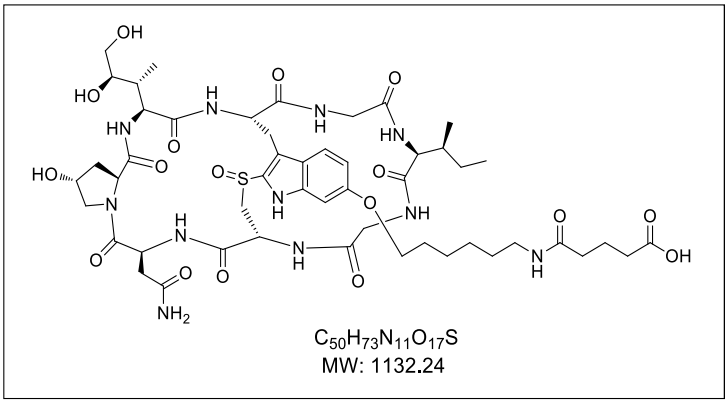

Compound **64a** (5 mg, 4.4 μmol, 1 equiv.) was dissolved in 10 μL of DMF and cooled at 0 ºC under nitrogen conditions. Glutaric anhydride (1.26 mg, 11 μmol, 2.5 equiv.), DMAP (0.13 mg, 1.1 μmol, 0.25 equiv.) and *i*Pr$_2$NEt (2.87 μL, 16.5 μmol, 3.75 equiv.) were added as stock solutions in DMF and the reaction was stirred at 0 ºC for a few minutes. The mixture was then warmed to room temperature and stirred overnight under nitrogen atmosphere. The solvent was evaporated under high vacuum and the crude was purified by semipreparative HPLC [Waters Atlantis 21 mm × 10 cm column; gradient: 100% (H_2O + 0.1 % CF_3COOH)/0% (CH_3CN + 0.1% CF_3COOH) to 55% (H_2O + 0.1 % CF_3COOH)/45% (CH_3CN + 0.1% CF_3COOH) in 10 minutes; t_R: (product): 8.8 min]. The purified compound was then freeze-dried to allow compound **65a** as a white solid (3.85 mg, 77% yield). ^{1}H NMR (400 MHz, D_2O) *δ* 8.70 (d, *J* = 9.8 Hz, 1H), 8.25 (d, *J* = 7.1 Hz, 1H), 7.77 (d, *J* = 8.9 Hz, 1H), 7.10 (d, *J* = 2.0 Hz, 1H), 6.96 (dd, *J* = 8.9, 2.1 Hz, 1H), 5.26 (td, *J* = 11.4, 8.1 Hz, 1H), 5.11 (dd, *J* = 12.8, 4.7 Hz, 1H), 5.00 (s, 1H), 4.74 (s, 1H), 4.67 – 4.61 (m, 2H), 4.26 – 4.09 (m, 5H), 3.88 (d, *J* = 13.7 Hz, 1H), 3.82 (d, *J* =18.8 Hz, 2H), 3.77 – 3.71 (m, 5H), 3.67 – 3.52 (m, 3H), 3.30 – 3.20 (m, 4H), 2.94 (dd, *J* = 14.6, 11.8 Hz, 1H), 2.58 – 2.50 (m, 1H), 2.49 – 2.41 (m, 1H), 2.34 – 2.28 (m, 2H), 2.27 – 2.14 (m, 3H), 1.89 – 1.79 (m, 4H), 1.78 – 1.70 (m, 1H), 1.61 – 1.48 (m, 5H), 1.47 – 1.38 (m, 2H), 1.29 – 1.19 (m, 1H), 1.03 (d, *J* = 7.0 Hz, 3H), 0.92 – 0.86 (m, 6H); ^{13}C NMR (101 MHz, D_2O) *δ* 174.86, 174.17, 173.79, 173.27, 171.88, 171.65, 170.91, 170.17, 168.65, 168.53, 157.00, 139.14, 127.40, 122.47, 121.38, 114.35, 111.87, 96.07, 72.73, 69.84, 68.81, 63.36, 62.08, 59.91, 56.63, 55.73, 52.89, 51.60, 50.64, 42.58, 41.68, 39.12, 37.87, 37.21, 34.85, 33.30, 32.69, 28.06, 25.44, 25.33, 24.76, 20.76, 14.12, 12.96, 9.80; MS (ESI+) *m/z* calcd. for $[C_{50}H_{74}N_{11}O_{17}S]^+$: 1132.50 $[M + H]^+$; found: 1132.87; *m/z* calcd. for $[C_{50}H_{73}N_{11}NaO_{17}S]^+$: 1154.48 $[M + Na]^+$; found: 1154.86; *m/z* calcd. for $[C_{50}H_{75}N_{11}O_{17}S]^{2+}$:

566.75 [M + 2H]$^{2+}$; found: 566.95; *m/z* calcd. for [$C_{50}H_{74}N_{11}NaO_{17}S$]$^{2+}$: 578.25 [M + 1H + Na]$^{2+}$; found: 577.94.

Cyclo[DKP-RGD]-uncleavable-α-amanitin (**63**)

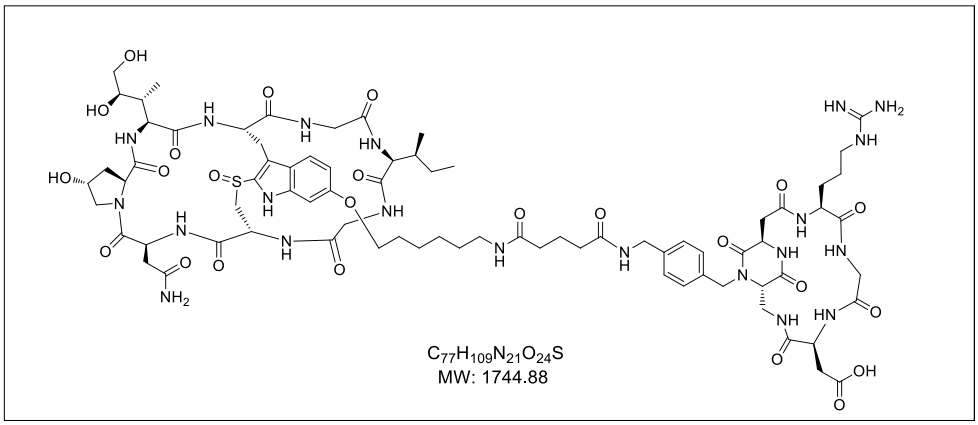

Compound **65a** (7.58 mg, 6.7 μmol, 1 equiv.) was dissolved in 175 μL of DMF and cooled at 0 ºC under nitrogen atmosphere. *N*-hydroxysuccinimide (1.15 mg, 10 μmol, 1.5 equiv.) and DIC (1.55 μL, 10 μmol, 1.5 equiv.) were added as stock solutions in DMF and the reaction was stirred at 0 ºC for a few minutes. The reaction was allowed to reach room temperature and stirred overnight under nitrogen atmosphere. Volatiles were then removed *in vacuo* to give a solid, which was redissolved in acetonitrile (176 μL) and cooled at 0 ºC. A solution of NH_2CH_2-*cyclo*[DKP-RGD] (**32**) (2.88 mg, 3.35 μmol, 0.5 equiv.) in phosphate buffer (211 μL, pH 7.5) was then added to the acetonitrile solution, and the pH value was adjust to 7.3–7.6 with NaOH (0.2 M). The resulting solution was warmed to room temperature and stirred overnight. During the first hours, the pH was adjusted between 7.3–7.6 with NaOH (0.2 M), until a stable value was observed. The solution was concentrated, and the crude residue was purified by semipreparative HPLC [Waters Atlantis 21 mm × 10 cm column; gradient: 100% (H_2O + 0.1 % CF_3COOH)/0% (CH_3CN + 0.1% CF_3COOH) to 50% (H_2O + 0.1 % CF_3COOH)/ 50% (CH_3CN + 0.1% CF_3COOH) in 9 minutes; t_R: (product): 8 min]. The purified compound was then freeze-dried to allow compound **63** as a white solid (2.87 mg, 46% yield). ^{1}H NMR (400 MHz, D_2O) δ 8.70 (s, 1H), 8.27 (d, *J* = 8.2 Hz, 1H), 7.68 (d, *J* = 8.9 Hz, 1H), 7.26 (m, 4H), 7.01 (d, *J* = 2.1 Hz, 1H), 6.88 (dd, *J* = 8.8, 2.1 Hz, 1H), 5.30 – 5.19 (m, 1H), 5.11 (dd, *J* = 9.5, 4.7 Hz, 1H), 5.03 – 4.97 (m, 2H), 4.88 (t, *J* = 7.1 Hz, 1H), 4.75 (s, 1H), 4.68 – 4.61 (m, 2H), 4.55 (dd, *J* = 7.9, 5.6 Hz, 1H), 4.39 – 4.04 (m, 11H), 4.00 – 3.79 (m, 3H), 3.79 – 3.48 (m, 10H), 3.31 – 3.14 (m, 6H), 2.99 – 2.74 (m, 2H), 2.66 – 2.43 (m, 1H), 2.34 – 2.12 (m, 4H), 2.05 – 1.87 (m, 2H), 1.85 – 1.70 (m, 3H), 1.71 – 1.60 (m, 1H), 1.57 – 1.44 (m, 4H), 1.43 – 1.33 (m, 2H), 1.26 – 1.20 (m, 2H), 1.15 (d, *J* = 6.5 Hz, 8H), 1.04 (d, *J* = 7.0

Hz, 3H), 0.95 – 0.85 (m, 6H). MS (MALDI-TOF): *m/z* calcd. for $[C_{77}H_{110}N_{21}O_{24}S]^+$: 1745.89 $[M + H]^+$; found: 1746.5 (HCCA matrix), 1747.9 (SA matrix).

Synthesis of Dau=Aoa-GPLGVRG-*cyclo*[RGDfK] (71) and *cyclo*[RGDfK]-GPLG- PTX (73) bearing extracellular cleavable linkers

Synthesis of Dau=Aoa-GPLGVRG-*cyclo*[RGDfK] (**71**)

*2-((propan-2-ylideamino)oxy)acetic-Gly-Pro-Leu-Gly-Val-Arg-Gly-OH (**78**)*

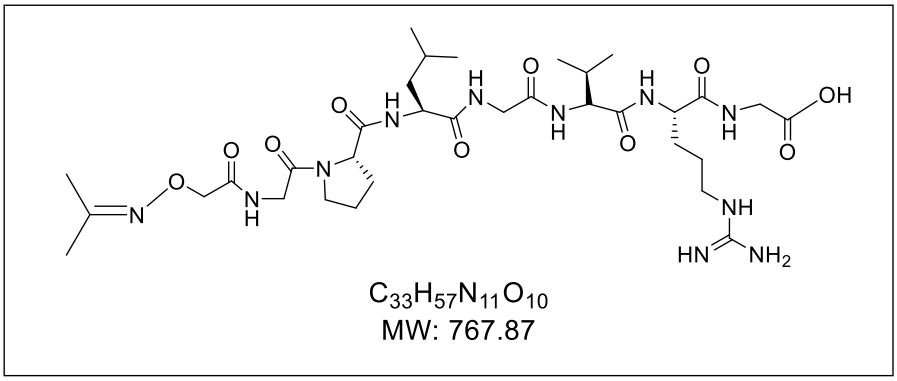

The experimental protocol is described in parts 1 (*Coupling of the first amino acid – Fmoc-glycine-OH*) and 2 (*Addition of other amino acids)* of the General procedure for SPPS.[d]

The resin was dried under vacuum for 2 h and then dissolved in a 9.5/0.5/0.5 TFA/TIS/H_2O mixture with magnetic stirring for 3 h. After this, the crude was added into a diethyl ether cold solution and a white solid was formed. The diethyl ether was centrifuged (3 x 5 mins) and the pellet obtained was frozen-dried. The compound was used without further purification. Yield: 200 mg (60%). MS (ESI+): *m/z* calcd. for $[C_{33}H_{58}N_{11}O_{10}]^+$: 768.44 $[M + H]^+$; found: 768.6.

[d] The addition of 2-((propan-2-ylideneamino)oxy)acetic acid was made also in SPPS following the experimental procedure described in Part 2 of the general procedure for the SPPS.

*2-((propan-2-ylideamino)oxy)acetic-Gly-Pro-Leu-Gly-Val-Arg-Gly-cyclo[RGDfK] (**79**)*

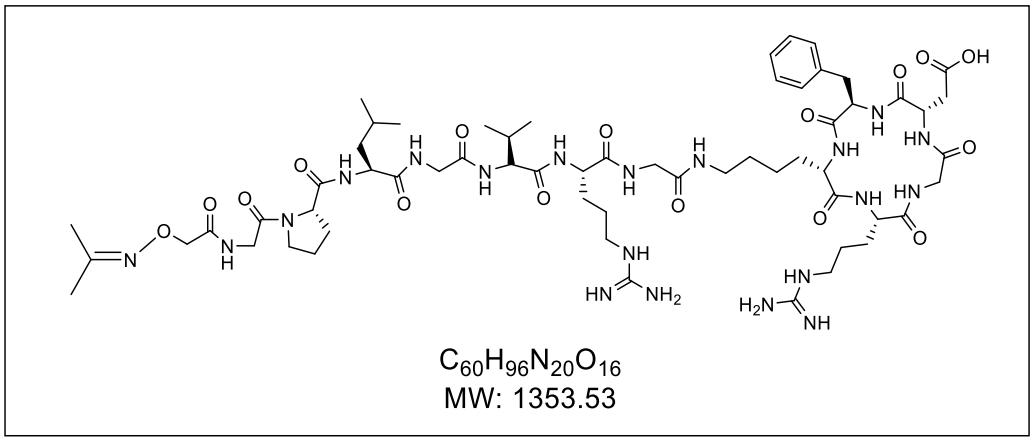

Compound **78** (31 mg, 0.035 mmol, 1 equiv.) and BOP (14.2 mg, 0.032 mmol, 0.9 equiv.) were dissolved in DMF (600 µL). After this, *i*Pr_2EtN (16.5 µL, 0.0945 mmol, 2.7 equiv.) was added and the mixture was stirred for 20 minutes. Then, a solution of *cyclo*[RGDfK] **46** (14.6 mg, 0.0175 mmol, 0.5 equiv.) in DMF (800 µL) was added and the reaction was stirred during 3 hours. The crude is purified by preparative HPLC [Gradient: 95% (H_2O + 0.1% CF_3COOH) / 5% (CH_3CN + 0.1% CF_3COOH) to 50% (H_2O + 0.1% CF_3COOH) / 50% (CH_3CN + 0.1% CF_3COOH) in 45 min]. Yield: 24.8 mg (89%). HRMS (ESI+): *m/z* calcd. for $[C_{60}H_{97}N_{20}O_{16}]^+$: 1353.731 $[M + H]^+$; found: 1353.743; *m/z* calcd. for $[C_{97}H_{98}N_{20}O_{16}]^{2+}$: 677.373 $[M + 2H]^{2+}$; found: 677.371; *m/z* calcd. for $[C_{97}H_{97}N_{20}O_{16}Na]^{2+}$: 688.364 $[M + H + Na]^{2+}$; found: 688.363.

*Dau=Aoa-GPLGVRG-cyclo[RGDfK] (**71**)*

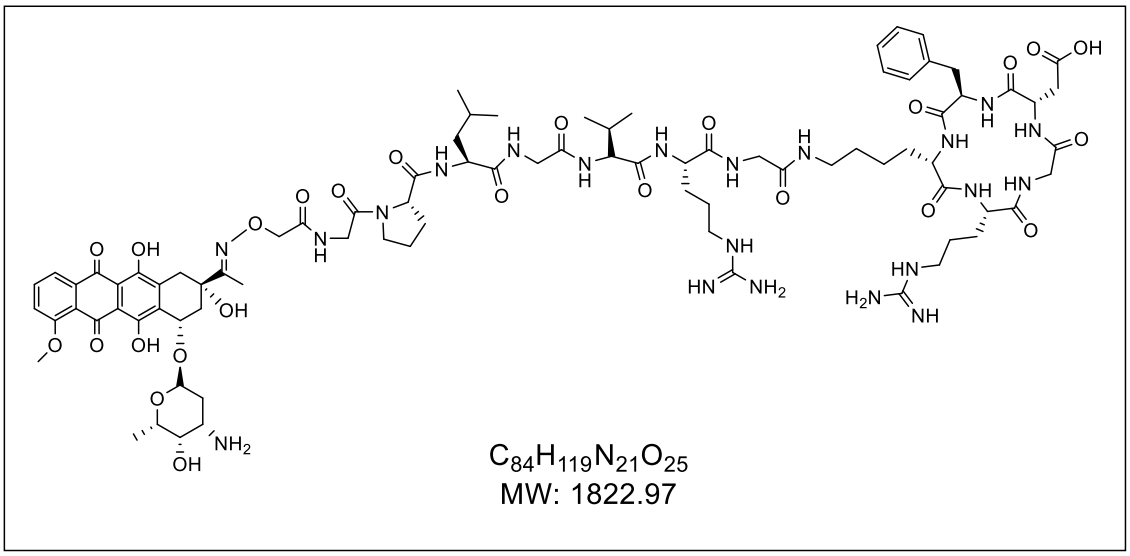

Compound **79** (14 mg, 0.0088 mmol, 1 equiv.) was dissolved in NH_4OAc buffer (3 mL) and then *O*-methyloxylamine hydrochloride (15.7 mg, 0.176 mmol, 20 equiv.) was added. The reaction was stirred for 2 hours and then purified by semipreparative HPLC [Gradient: 95% (H_2O + 0.1% CF_3COOH) / 5% (CH_3CN + 0.1% CF_3COOH) to 50% (H_2O + 0.1% CF_3COOH) / 50% (CH_3CN + 0.1% CF_3COOH) in 45 min]. The unstable deprotected intermediate was evaporated under high vacuum and used directly in the following reaction. The compound was redissolved in NH_4OAc buffer and then daunomycin (15 mg, 0.028 mmol, 3.2 equiv.) was added. The mixture was stirred over two nights and then purified by semipreparative HPLC [Gradient: 95% (H_2O + 0.1% CF_3COOH) / 5% (CH_3CN + 0.1% CF_3COOH) to 50% (H_2O + 0.1% CF_3COOH) / 50% (CH_3CN + 0.1% CF_3COOH) in 45 min]. Yield: 7.9 mg (41% over two steps). MS (ESI +): *m/z* calcd. for HRMS (ESI+): *m/z* calcd. for $[C_{84}H_{121}N_{21}O_{25}]^{2+}$: 911.942 $[M + 2H]^+$; found: 912.443.

Synthesis of *cyclo*[RGDfK]-GPLG-PTX (**73**)

*Fmoc-Gly-Pro-Leu-Gly-OH (**81**)*

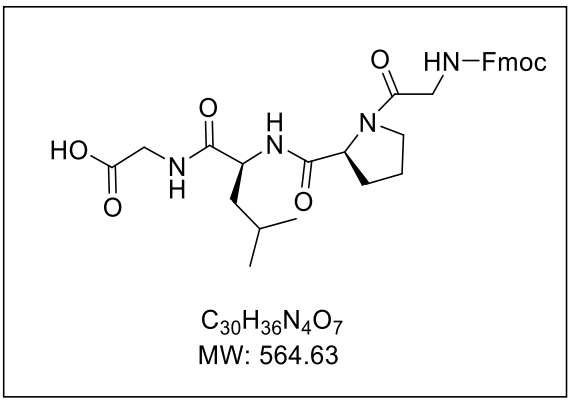

$C_{30}H_{36}N_4O_7$
MW: 564.63

The experimental protocol is described in the general procedure for SPPS.

^{1}H NMR (400 MHz, $CDCl_3$): *δ* 7.74 (d, *J* = 7.5 Hz, 2H), 7.57 (dt, *J* = 25.4, 12.8 Hz, 2H), 7.38 (t, *J* = 7.2 Hz, 3H), 7.33 – 7.27 (m, 2H), 6.30 (s, 1H), 5.70 (s, 3H), 4.53 (d, *J* = 18.7 Hz, 1H), 4.41 – 4.31 (m, 1H), 4.26 (m, 1H), 4.22 – 4.09 (m, 2H), 3.99 (d, *J* = 14.9 Hz, 1H), 3.90 – 3.69 (m, 3H), 3.48 (s, 1H), 2.12 (s, 2H), 2.00 (s, 2H), 1.80 (s, 1H), 1.60 (d, *J* = 7.1 Hz, 2H), 0.92 – 0.82 (m, 6H). MS (ESI+): *m/z* calcd. for $[C_{30}H_{37}N_4O_7]^+$: 565.3 [M + H]$^+$; found: 565.4.

*Fmoc-Gly-Pro-Leu-Gly-N-[4-(hydroxymethyl)phenyl] (**82**)*

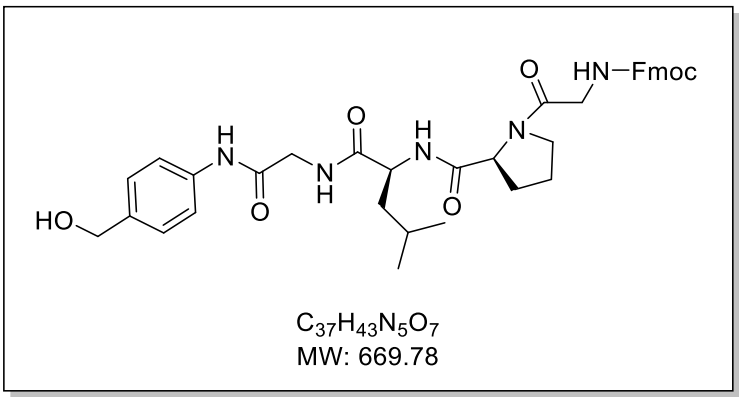

$C_{37}H_{43}N_5O_7$
MW: 669.78

Compound **81** (250 mg, 0.44 mmol, 1 equiv.) was dried under vacuum for 1 hour before using. After this, it was dissolved in CH_2Cl_2 (5 mL) and EEDQ (247 mg, 0.88 mmol, 2 equiv.) and 4-aminobenzyl alcohol (108.4 mg, 0.88 mmol, 2 equiv.) were added. The reaction is stirred overnight under argon conditions at r.t. The solvent is evaporated and

cold diethyl ether is added. The precipitate formed was filtered, dried and used without further purification. Yield: 270.4 mg (91%). MS (ESI+): *m/z* calcd. for $[C_{37}H_{44}N_5O_7]^+$: 670.3 $[M + H]^+$; found: 670.4.

*Fmoc-Gly-Pro-Leu-Gly-N-[4-[[[(4-nitrophenoxy)carbonyl]oxy]methyl]phenyl] (**83**)*

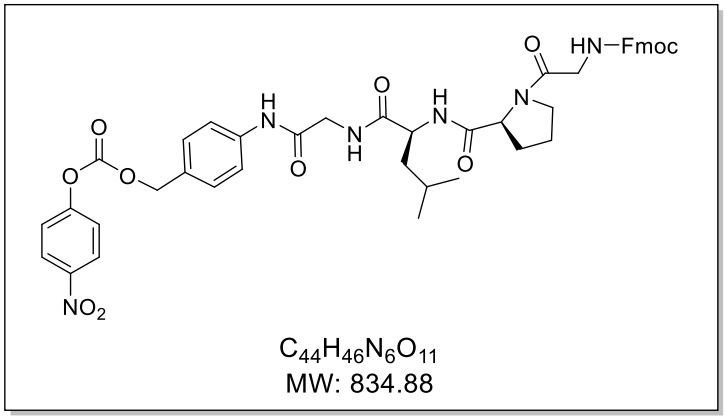

$C_{44}H_{46}N_6O_{11}$
MW: 834.88

Compound **82** (50 mg, 0.075 mmol, 1 equiv.) and 4-nitrophenyl choloroformate (30 mg, 0.15 mmol, 2 equiv.) were dissolved in CH_2Cl_2 (2.1 mL). Then, pyridine (20 µL, 0.187 mmol, 2.5 equiv.) was added and the reaction was stirred overnight under argon conditions. The mixture was extracted with a 1 M aqueous solution of $KHSO_4$ (2 ×) and brine (1 ×). The organic phase was dried over Na_2SO_4, concentrated and purified by flash chromatography (eluent: 9.5:0.5 CH_2Cl_2/MeOH) to afford pure **83**. Yield: 45 mg (72%). MS (ESI+): *m/z* calcd. for $[C_{44}H_{47}N_6O_{11}]^+$: 835.3 $[M + H]^+$; found: 835.3.

*Fmoc-Gly-Pro-Leu-Gly-N-[4-[[[(N-(Boc)-N,N'-dimethylethylenediamine)carbonyl]oxy]methyl]phenyl] (**84**)*

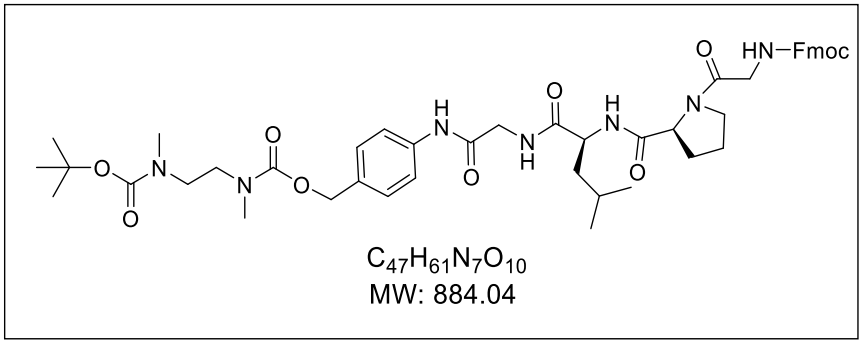

$C_{47}H_{61}N_7O_{10}$
MW: 884.04

Compound **83** (331 mg, 0.396 mmol, 1 equiv.) was dissolved in CH_2Cl_2 (9 mL) and cooled to 0 ºC. Then, a solution of *N*-Boc-*N,N'*-dimethylethylenediamine (162 µL, 0.792 mmol,

2 equiv.) and *i*Pr_2Net (172 µL, 0.99 mmol, 2.5 equiv.) in CH_2Cl_2 (9 mL) was added. The reaction was allowed to reach room temperature and stirred overnight. The mixture was extracted with 1 M aqueous solution of $KHSO_4$ (2 ×) and saturated 5% aqueous solution of $NaHCO_3$ (2 ×). The organic phase was dried over Na_2SO_4, concentrated and purified by flash chromatography (eluent: 9.5:0.5 CH_2Cl_2/MeOH) to afford pure **84**. Yield: 301 mg (86%). MS (ESI+): *m/z* calcd. for $[C_{47}H_{62}N_7O_{10}]^+$: 884.5 $[M + H]^+$; found: 884.4.

*(Hemiglutarate)-Gly-Pro-Leu-Gly-N-[4-[[[(N-(Boc)-N,N'-dimethylethylenediamine)carbonyl]oxy]methyl]phenyl] (**85**)*

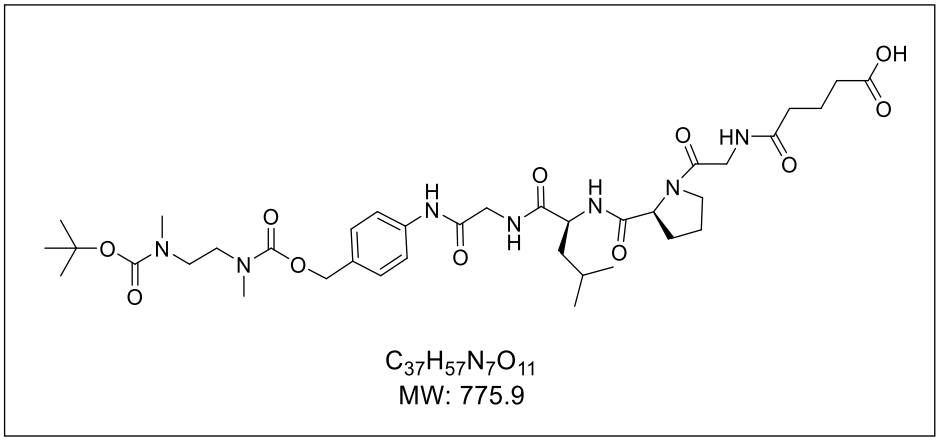

$C_{37}H_{57}N_7O_{11}$
MW: 775.9

Compound **84** (405 mg, 0.458 mmol, 1 equiv.) was dissolved in CH_2Cl_2 (4.6 mL) and the mixture was cooled to 0 ºC under argon. Piperidine (226 µL, 2.29 mmol, 5 equiv.) was added and the reaction was stirred for 3 h. The crude was extracted with 5% aqueous solution of $NaHCO_3$ (3 ×). The organic phase was dried over Na_2SO_4, concentrated, dried under vacuum for 2 h and used in the following step without further purification. The crude free amine (303 mg, 0.458 mmol, 1 equiv.) and DMAP (15.8 mg, 0.12 mmol, 0.25 equiv.) were dissolved in CH_2Cl_2 (5.3 mL) and cooled to 0 ºC under argon atmosphere. Then, *i*Pr_2NEt (338 µL, 1.94 mmol, 3.75 equiv.) is added followed by glutaric anhydride (147 mg, 1.29 mmol, 2.5 equiv.) dissolved in CH_2Cl_2/DMF (1.3 mL/2 mL). The reaction was kept a few minutes at 0 ºC and then it was allowed to reach r.t. and stirred overnight. The solvents are evaporated and the mixture is redissolved in CH_2Cl_2. The mixture is extracted with with 1 M aqueous solution of $KHSO_4$ (2 ×) and brine (1 ×). The organic phase was dried over Na_2SO_4, concentrated and purified by flash chromatography (eluent: 9:1 CH_2Cl_2/MeOH + 0.2% AcOH). Yield: 220 mg (62%) over two steps. MS (ESI+): *m/z* calcd. for $[C_{37}H_{58}N_7O_{11}]^+$: 776.4 $[M + H]^+$; found: 776.4.

*Cyclo[RGDfK]–Gly-Pro-Leu-Gly-N-[4-[[[(N-(Boc)-N,N'-dimethylethylenediamine)carbonyl]oxy]methyl]phenyl] (**86**).*

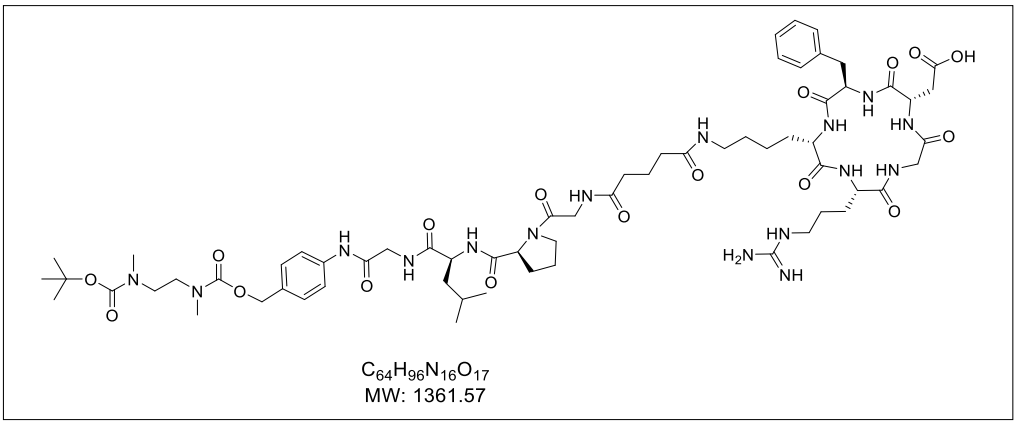

Compound **85** (17.4 mg, 0.022 mmol, 1 equiv.) and BOP (8.9 mg, 0.0202 mmol, 0.9 equiv.) were dissolved in DMF (500 µL) and then *i*Pr_2Net (10.3 µL, 0.0549 mmol, 2.7 equiv.) was added (pH = 6-7). The mixture was stirred at r.t. for 20 minutes and after *cyclo*[RGDfK] **46** (9.14 mg, 0.011 mmol, 0.5 equiv.) dissolved in DMF (570 µL) was added. The mixture was stirred for 3 hours and then it was purified directly by preparative HPLC [Gradient: 95% (H_2O + 0.1% CF_3COOH) / 5% (CH_3CN + 0.1% CF_3COOH) to 50% (H_2O + 0.1% CF_3COOH) / 50% (CH_3CN + 0.1% CF_3COOH) in 45 min]. Yield: 5.2 mg (32%). MS (ESI+): *m/z* calcd. for $[C_{64}H_{97}N_{16}O_{17}]^+$: 1361.7 $[M + H]^+$; found: 1361.9.

Cyclo[RGDfK]-GPLG-PTX (**73**)

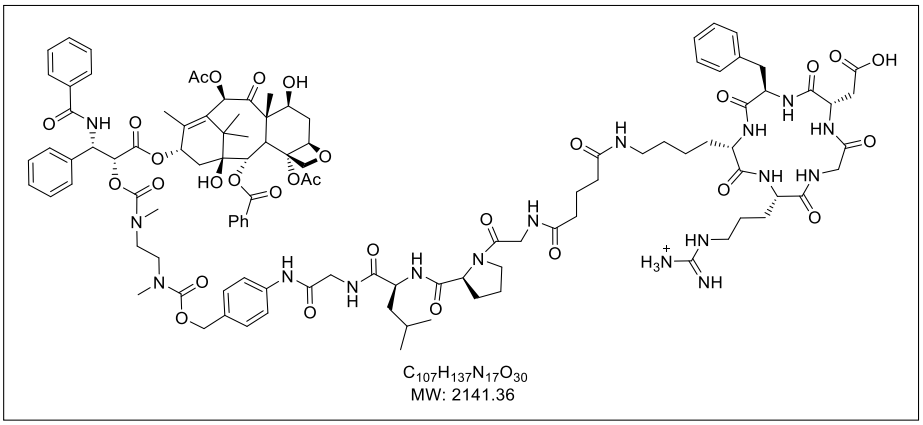

A half volume of TFA was added to a 0.03 M solution of intermediate **86** in CH_2Cl_2 and the reaction was stirred at r.t. for 1 h. The solvent was evaporated under vacuum to afford the amine TFA salt. The crude was freeze-dried and used without further purification. The resulting TFA salt (3.06 mg, 0.00206 mmol, 1 equiv.) and and 2'-(4-nitrophenoxycarbonyl)paclitaxel **60** (42 mg, 0.0041mmol, 2 equiv.) were dissolved in DMF (149 µL) and cooled to 0 ºC under nitrogen atmosphere. *i*Pr_2NEt (1.79 µL, 0.0103 mmol, 5 equiv.) was added and the mixture was allowed to reach r.t. and stirred over two nights. The crude was concentrated, and the residue was purified by semipreparative HPLC [Gradient: 95% (H_2O + 0.1% CF_3COOH) / 5% (CH_3CN + 0.1% CF_3COOH) to 50% (H_2O + 0.1% CF_3COOH) / 50% (CH_3CN + 0.1% CF_3COOH) in 45 min]. Yield: 0.3 mg (6%). MS (ESI+): *m/z* calcd. for $[C_{107}H_{138}N_{17}O_{30}]^+$: 2141.0 $[M + H]^+$; found: 2141.6.

Synthesis of conjugates containing the β-glucuronide linker (88 and 89)

(2*S*,3*R*,4*S*,5*S*,6*S*)-2-(4-formyl-2-nitrophenoxy)-6-(methoxycarbonyl)tetrahydro-2H-pyran-3,4,5-triyl triacetate (**92**)

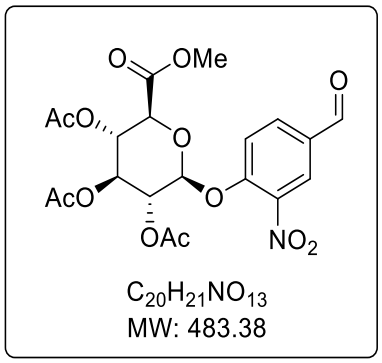

$C_{20}H_{21}NO_{13}$
MW: 483.38

To a solution of 4-hydroxy-3-nitrobenzaldehyde (5 g, 29.6 mmol, 1 equiv.) and acetobromo-α-D-glucuronic acid methyl ester (8.5 g, 31.3 mmol, 1.1 equiv.) in CH_3CN (100 mL), molecular sieves (10 g) and Ag_2O (18 g) were added. The reaction was stirred under argon overnight and then filtrated and concentrated under vacuum. The crude was diluted in H_2O (100 mL) and washed with ethyl acetate (2 x 200 mL). The organic phase was dried over $MgSO_4$, concentrated and purified by automatic chromatography (gradient: from 100% CH_2Cl_2/ 0% CH_2Cl_2:CH_3OH 9:1 to 50% CH_2Cl_2/ 50% CH_2Cl_2:CH_3OH 9:1 in 27 minutes). Yield: 9.33 g (65%). ^{1}H NMR (500 MHz, $CDCl_3$) *δ* 9.97 (s, 1H), 8.31 (d, *J* = 2.0 Hz, 1H), 8.08 (dd, *J* = 8.7, 2.1 Hz, 1H), 7.50 (d, *J* = 8.6 Hz, 1H), 5.43 – 5.39 (m, 2H), 5.34 – 5.26 (m, 2H), 4.33 (d, *J* = 8.5 Hz, 1H), 3.70 (s, 3H), 2.12 (d, *J* = 6.8 Hz, 3H), 2.06 (t, *J* = 6.0 Hz, 6H); ^{13}C NMR (126 MHz, $CDCl_3$) *δ* 188.73, 170.03, 169.37, 169.20, 166.76, 153.39, 141.20, 134.41, 131.54, 126.81, 118.81, 98.63, 72.75, 70.26, 69.82, 68.22, 53.22, 20.70, 20.66, 20.65.

(2*S*,3*R*,4*S*,5*S*,6*S*)-2-(4-(hydroxymethyl)-2-nitrophenoxy)-6 (methoxycarbonyl)tetrahydro-2H-pyran-3,4,5-triyl triacetate (**93**)

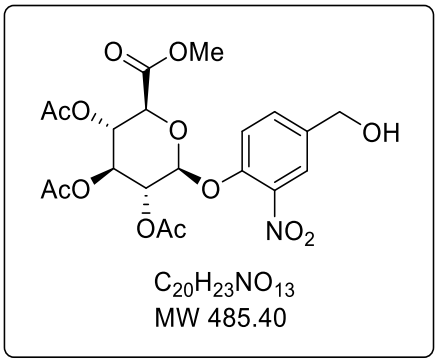

$C_{20}H_{23}NO_{13}$
MW 485.40

$NaBH_4$ (1.23 g, 32.5 mmol, 1.7 equiv.) was added to a solution of **92** (9.21 g, 19 mmol, 1 equiv.) in *i*PrOH/$CHCl_3$ (37 mL/135 mL) under argon conditions. The reaction was stirred at 0 ºC for 2 hours and a half. The crude mixture was quenched with water and later diluted with ethyl acetate and washed with ammonium hydroxide solution and brine. The organic phase was dried over $MgSO_4$, concentrated and purified by automatic chromatography (gradient: from 100% CH_2Cl_2/ 0% CH_2Cl_2:CH_3OH 9:1 to 0% CH_2Cl_2/ 100% CH_2Cl_2:CH_3OH 9:1 in 27 minutes). Yield: 5.71 g (62%). ^{1}H NMR (500 MHz, $CDCl_3$) δ 7.79 (d, *J* = 2.0 Hz, 1H), 7.52 (dd, *J* = 8.5, 2.1 Hz, 1H), 7.35 (d, *J* = 8.5 Hz, 1H), 5.35 – 5.25 (m, 3H), 5.18 (d, *J* = 6.9 Hz, 1H), 4.71 (d, *J* = 4.5 Hz, 2H), 4.22 – 4.19 (m, 1H), 3.73 (d, *J* = 6.4 Hz, 3H), 2.18 (d, *J* = 4.5 Hz, 1H), 2.11 (s, 3H), 2.05 (d, J = 3.4 Hz, 6H); ^{13}C NMR (126 MHz, $CDCl_3$) δ 170.01, 169.32, 169.30, 166.70, 148.10, 141.22, 137.36, 131.90, 123.15, 120.16, 99.84, 72.46, 71.10, 70.15, 68.71, 63.37, 53.03, 20.55, 20.51, 20.47.

(2*S*,3*R*,4*S*,5*S*,6*S*)-2-(2-amino-4-(hydroxymethyl)phenoxy)-6-(methoxycarbonyl)tetrahydro-2H-pyran-3,4,5-triyl triacetate (**94**)

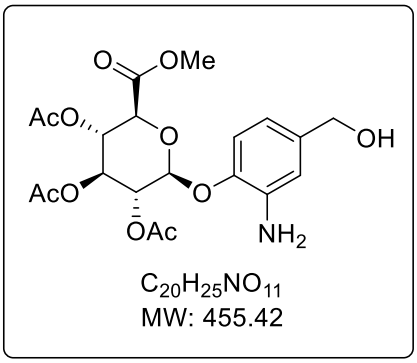

$C_{20}H_{25}NO_{11}$
MW: 455.42

Compound **93** (5.71 g, 11.8 mmol, 1 equiv.) was dissolved in ethyl acetate (80 mL), EtOH (180 mL) and MeOH (40 mL) and then a spatula of Pd catalyst was added under argon. After this, H_2 was added. The reaction was stirred overnight at room temperature. The catalyst was filtered with celite and concentrated under vacuum. The crude was used without further purification. Yield: 5.2 g (97%). ^{1}H NMR (500 MHz, CDCL3) δ 6.88 (d, *J* = 8.2 Hz, 1H), 6.71 (d, *J* = 1.8 Hz, 1H), 6.63 (dd, *J* = 8.2, 1.9 Hz, 1H), 5.38 – 5.24 (m, 3H), 4.99 (t, *J* = 10.3 Hz, 1H), 4.53 (s, 2H), 4.13 (t, *J* = 12.0 Hz, 1H), 3.76 (d, *J* = 14.7 Hz, 3H), 3.04 (s, 2H), 2.11 – 1.99 (m, 9H); ^{13}C NMR (126 MHz, $CDCl_3$) δ 169.99, 169.63, 169.37, 166.78, 143.67, 137.80, 137.30, 116.70, 116.50, 114.46, 100.52, 72.49, 71.59, 70.93, 69.22, 64.93, 52.98, 20.72, 20.57, 20.45.

Synthesis of *cyclo*[DKP-RGD]-β-glucuronide-MMAE (**88**)

Fmoc-(2*S*,3*R*,4*S*,5*S*,6*S*)-2-(2-amino-4-(hydroxymethyl)phenoxy)-6-(methoxycarbonyl)tetrahydro-2H-pyran-3,4,5-triyl triacetate (**94b**)

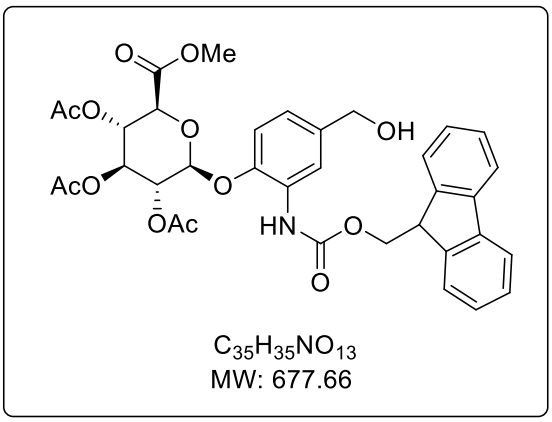

Compound **94** (200 mg, 0.44 mmol, 1 equiv.) was dissolved in CH_2Cl_2 (12 mL) and *i*Pr_2NEt (115 µL, 0.66 mmol, 1.5 equiv.) and DMAP (13.4 mg, 0.11 mmol, 0.25 equiv.) were added. Then, Fmoc-OSu (178 mg, 0.53 mmol, 1.2 equiv.) was added and the reaction was stirred under argon for 3 hours. The reaction mixture was washed with a 1 M aqueous solution of $KHSO_4$ (2 ×) and brine (1 ×). The organic phase was dried over $MgSO_4$, concentrated and purified by automatic chromatography (eluent: 9.8:0.2 CH_2Cl_2/MeOH). Yield: 66 mg (22%). MS (ESI+): *m/z* calcd. for $[C_{35}H_{36}NO_{13}]^+$: 678.22 $[M + H]^+$; found: 678.17; *m/z* calcd. for $[C_{35}H_{35}NO_{13}Na]^+$: 700.20 $[M + Na]^+$; found: 700.25.

Fmoc-(2*S*,3*R*,4*S*,5*S*,6*S*)-2-(2-amino-4-((((4-nitrophenoxy)carbonyl)oxy)methyl)phenoxy)-6-(methoxycarbonyl)tetrahydro-2H-pyran-3,4,5-triyl triacetate (**95**)

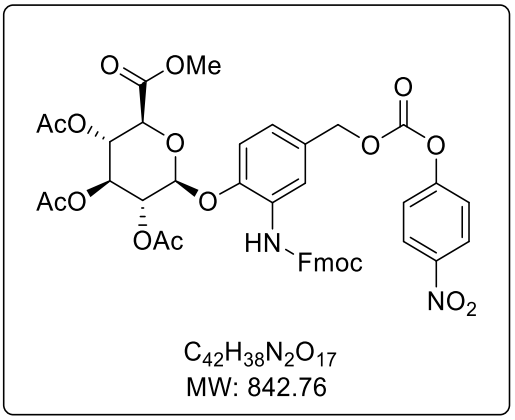

Compound **94b** (66 mg, 0.097 mmol, 1 equiv.) was dissolved in THF (2.9 mL) and then pyridine (19.6 µL, 0.242 mmol, 2.5 equiv.) was added. The reaction was stirred at 0 ºC under argon conditions. Then, 4-nitrophenylchloroformate (39.3 mg, 0.195 mmol, 2 equiv.) was added and the reaction is stirred at room temperature for 3 hours. The mixture is diluted in CH_2Cl_2 (40 mL) and washed with an aqueous solution of citric acid (2 x 20 mL) and brine (1 x 20 mL). The organic phase was dried over $MgSO_4$, concentrated and purified by automatic chromatography (eluent: 4:6 hexane/ethyl acetate). Yield: 34 mg (42%). MS (ESI+): *m/z* calcd. for $[C_{42}H_{38}N_2O_{17}Na]^+$: 865.21 [M + Na]$^+$; found: 865.17.

MMAE-Fmoc-(2*S*,3*R*,4*S*,5*S*,6*S*)-2-(2-amino-4-(hydroxymethyl)phenoxy)-6-(methoxycarbonyl)tetrahydro-2H-pyran-3,4,5-triyl triacetate (**95b**)

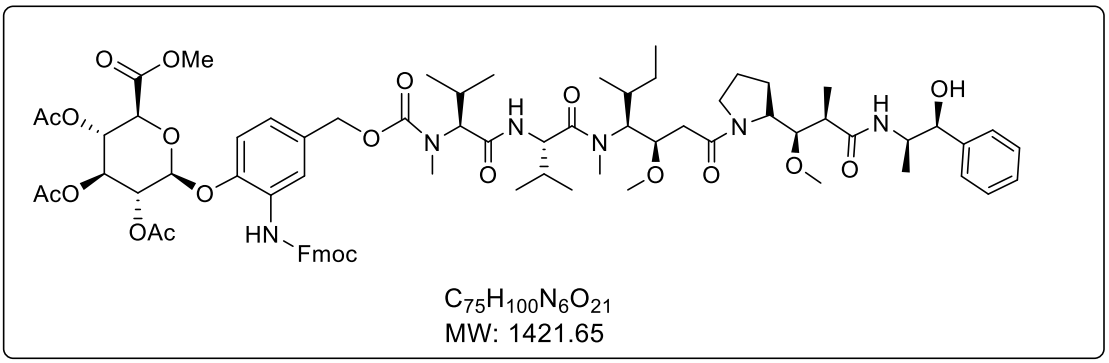

$C_{75}H_{100}N_6O_{21}$
MW: 1421.65

Compound **95** (15 mg, 0.0178 mmol, 1.5 equiv.), MMAE (8.5 mg, 0.0119 mmol, 1 equiv.) and HOBt (0.32 mg, 0.00238 mmol, 0.2 equiv.) were dissolved in DMF (340 µL) at 0 ºC. Then, pyridine (12 µL, 0.149 mmol, 12.5 equiv.) and *i*Pr_2NEt (4.1 µL, 0.0238 mmol, 2 equiv.) were added. The reaction was stirred at room temperature under argon 2 hours. The solvent was evaporated and a preparative HPLC was carried out [Gradient: 95% (H_2O + 0.05% CF_3COOH) / 5% CH_3CN to 50% (H_2O + 0.05% CF_3COOH) / 50% CH_3CN in 1 min and then from 50% (H_2O + 0.05% CF_3COOH) / 50% CH_3CN to 100% CH_3CN in 14 mins]. Yield: 12.06 mg (71%). MS (ESI+): *m/z* calcd. for $[C_{75}H_{100}N_6O_{21}Na]^+$: 1443.68 $[M + Na]^+$; found: 1443.67.

MMAE-β-glucuronide (**96**)

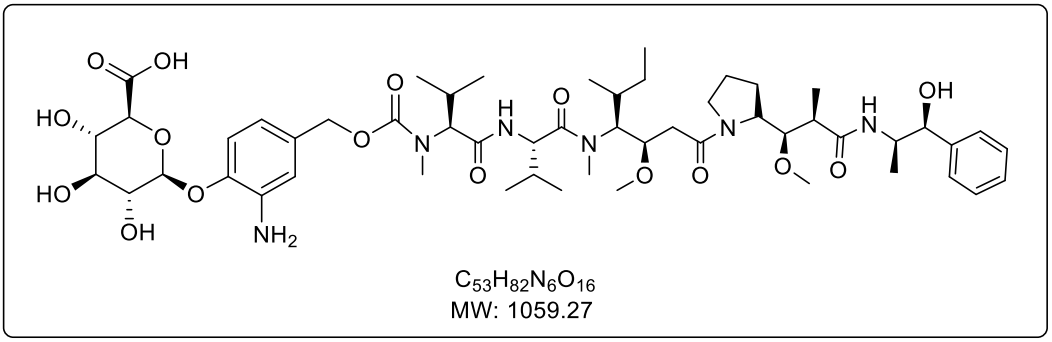

$C_{53}H_{82}N_6O_{16}$
MW: 1059.27

Compound **95b** (10 mg, 0.007 mmol, 1 equiv.) was dissolved in MeOH (250 µL) and cooled at – 20 ºC in acetone/dry ice. After this, LiOH (1.35 mg, 0.066 mmol, 8 equiv.) dissolved in H_2O (250 µL) was added and the reaction was stirred 2 hours at 0 ºC. The purificacion was carried out in preparative HPLC was carried out [Gradient: 95% (H_2O +

0.05% CF_3COOH) / 5% CH_3CN to 100% CH_3CN in 15 min]. Yield: 3.42 mg (46%). MS (ESI+): *m/z* calcd. for $[C_{53}H_{82}N_6O_{16}Na]^+$: 1081.57 $[M + Na]^+$; found: 1081.58.

MMAE-β-glucuronide-hemiglutarate-*N*-hydroxysuccinimidyl (**97**)

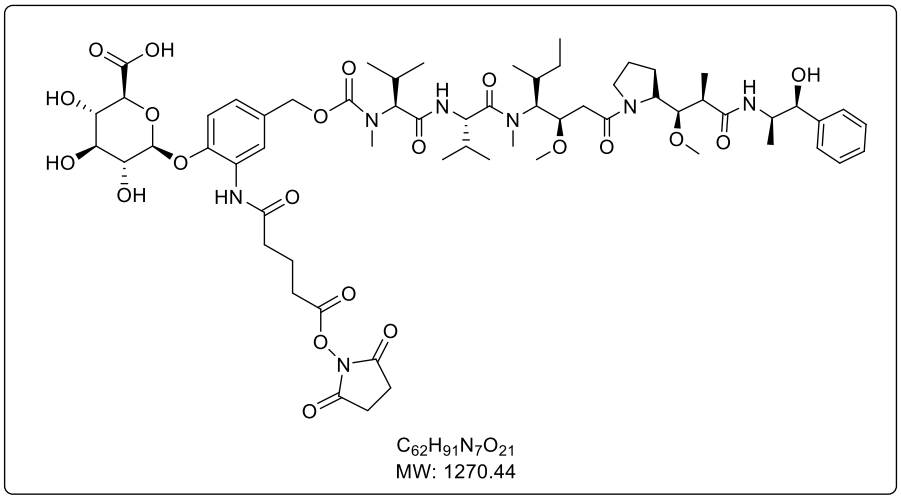

Compound **96** (3.62 mg, 0.0034 mmol, 1 equiv.) was dissolved in DMF under argon conditions. Then, Di(succinimidyl)glutarate (5.58 mg, 0.0171mmol, 5 equiv.), *i*Pr_2NEt (pH 8-10) and DMAP (0.415 mg, 0.0034 mmol, 1 equiv.) were added and the reaction was stirred at 50 ºC for 6 hours. The purification was carried out in preparative HPLC was carried out [Gradient: 95% (H_2O + 0.05% CF_3COOH) / 5% CH_3CN to 30% (H_2O + 0.05% CF_3COOH) / 70% CH_3CN in 15 min and 100% CH_3CN in 3 mins]. Yield: 1.44 mg (33%). MS (ESI+): *m/z* calcd. for $[C_{62}H_{92}N_7O_{21}]^+$: 1270.63 $[M + H]^+$; found: 1270.33; *m/z* calcd. for $[C_{62}H_{91}N_7O_{21}Na]^+$: 1292.62 $[M + Na]^+$; found: 1292.5.

MMAE-β-glucuronide-*cyclo*[DKP-RGD] (**88**)

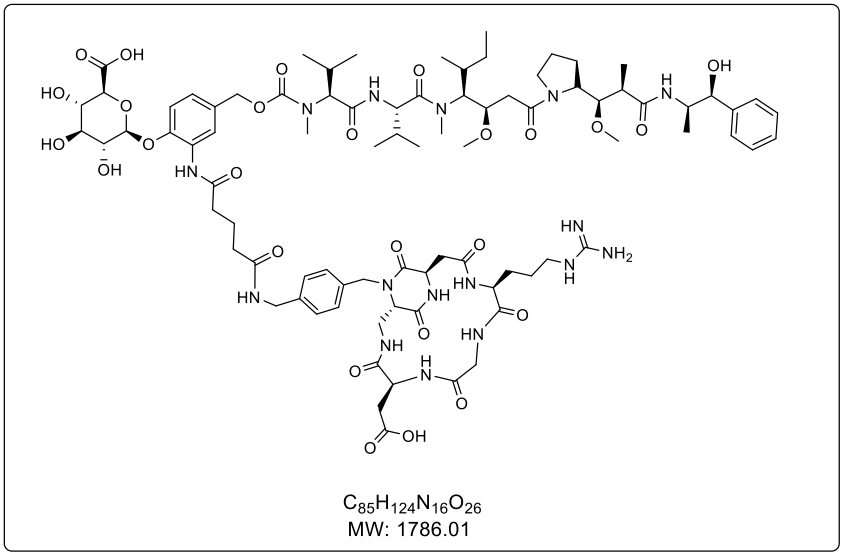

Cyclo[DKP-RGD]-CH_2NH_2 **32** (3.09 mg, 0.0036 mmol, 1 equiv.) was dissolved in Phosphate Buffer (100 µL, pH= 7.5) and the pH adjusted to 7.3-7.6. Then, this mixture was added to a solution of compound **97** in DMF (100 µL) at 0 ºC and the reaction was stirred 3 hours. The pH was kept between 7.3-7.6 all the time. The purificacion was carried out in preparative HPLC was carried out [Gradient: 95% (H_2O + 0.05% CF_3COOH) / 5% CH_3CN to 100% CH_3CN in 15 mins]. Yield: 0.84 mg (26%). MS (ESI+): *m/z* calcd. for $[C_{85}H_{125}N_{16}O_{26}Na]^{2+}$: 904.44 $[M + H + Na]^{2+}$; found: 904.50; *m/z* calcd. for $[C_{85}H_{124}N_{16}O_{26}Na_2]^{2+}$: 915.44 $[M + 2Na]^{2+}$; found: 915.92; *m/z* calcd. for $[C_{85}H_{123}N_{16}O_{26}]^{-}$: 1783.88 $[M - H]^{-}$; found: 1784.83.

Synthesis of *cyclo*[DKP-RGD]-PEG-4-β-glucuronide-MMAE (**89**)

4-pentyonyl-(2*S*,3*R*,4*S*,5*S*,6*S*)-2-(2-amino-4-(hydroxymethyl)phenoxy)-6-(methoxycarbonyl)tetrahydro-2H-pyran-3,4,5-triyl triacetate (**98**)

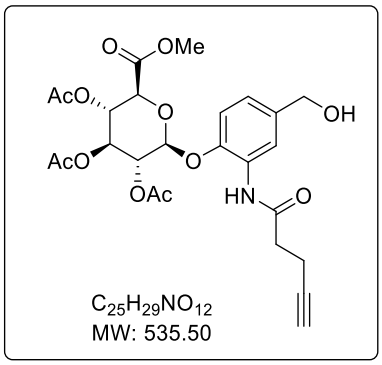

4-pentynoic acid (32.4 mg, 0.33 mmol, 1.5 equiv.) was dissolved in DMF (7.5 mL) and preactivated with HATU (142.2 mg, 0.374 mmol, 1.7 equiv.), HOBt (50.53 mg, 0.374 mmol, 1.7 equiv.) and *i*Pr_2NEt (153 µL, 0.88 mmol, 4 equiv.) for 20 minutes. Then, compound **94** (100 mg, 0.22 mmol, 1 equiv.) dissolved in DMF (3 mL) was added and the pH adjusted to 8-9 with *i*Pr_2NEt. The reaction mixture was washed with a 1 M aqueous solution of $KHSO_4$ (2 ×) and brine (1 ×). The organic phase was dried over $MgSO_4$, concentrated and purified by automatic chromatography (gradient: from 100% CH_2Cl_2/ 0% CH_3OH to 95% CH_2Cl_2/ 5% CH_3OH in 12 minutes). Yield: 40 mg (34%). MS (ESI+): *m/z* calcd. for $[C_{25}H_{29}NO_2Na]^+$: 558.16 $[M + Na]^+$; found: 558.17; MS (ESI-): *m/z* calcd. for $[C_{25}H_{28}NO_2]^-$: 534.14 $[M - 1H]^-$; found: 533.92.

4-pentyonyl-(2*S*,3*R*,4*S*,5*S*,6*S*)-2-(2-amino-4-((((4-nitrophenoxy)carbonyl)oxy)methyl)phenoxy)-6-(methoxycarbonyl)tetrahydro-2H-pyran-3,4,5-triyl triacetate (**98b**)

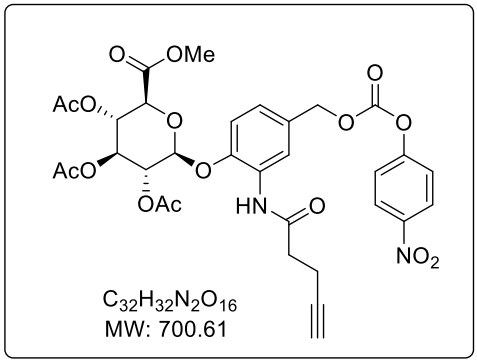

Compound **98** (30 mg. 0.056 mmol, 1 equiv.) was dissolved in THF (1.6 mL) and cooled at 0 ºC. Then, pyridine (11.3 µL, 0.14 mmol, 2.5 equiv.) and 4-nitrophenyl chloroformate (22.6 mg, 0.112 mmol, 2 equiv.) were added. The reaction was stirred under argon conditions at room temperature for 2 hours. The reaction mixture was washed with a 1 M aqueous solution of $KHSO_4$ (2 ×) and brine (1 ×). The organic phase was dried over $MgSO_4$, concentrated and purified by automatic chromatography (gradient: from 100% hexane/ 0% ethyl acetate to 45% hexane/ 55% ethyl acetate in 12 minutes). Yield: 20 mg (51%). MS (ESI+): *m/z* calcd. for $[C_{32}H_{32}N_2O_{16}Na]^+$: 723.16 $[M + Na]^+$; found: 723.17 ; MS (ESI-): *m/z* calcd. for $[C_{32}H_{31}N_2O_{16}]^-$: 699.17 $[M - 1H]^-$; found: 698.92.

MMAE-4-pentyonyl-(2*S*,3*R*,4*S*,5*S*,6*S*)-2-(2-amino-4-(hydroxymethyl)phenoxy)-6-(methoxycarbonyl)tetrahydro-2H-pyran-3,4,5-triyl triacetate (**99**)

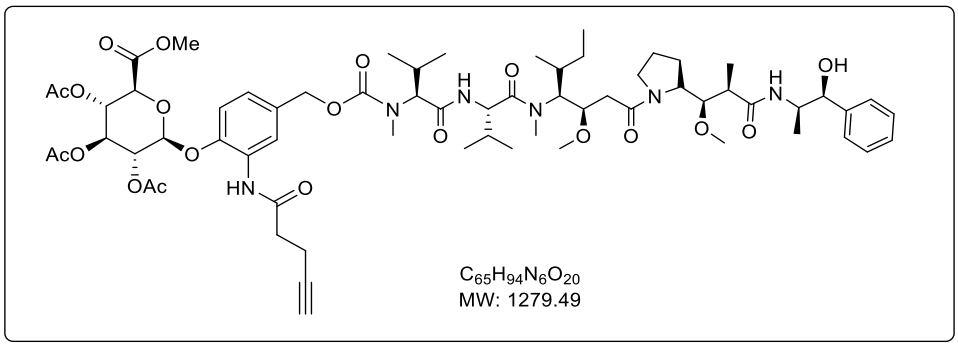

Compound **98b** (20 mg, 0.029 mmol, 1.5 equiv.), MMAE (13.7 mg, 0.019 mmol, 1 equiv.) and HOBt (0.5 mg, 0.0038 mmol, 0.2 equiv.) were dissolved in DMF (550 µL) at 0 ºC. Then, pyridine (19.3 µL, 0.24 mmol, 12.7 equiv.) and *i*Pr_2NEt (6.6 µL, 0.038 mmol, 2

equiv.) were added and the reaction was stirred at room temperature under argon conditions for 2 hours. The solvent was evaporated and the mixture was purified by automatic chromatography (gradient: from 100% CH_2Cl_2/ 0% CH_3OH to 95% CH_2Cl_2/ 5% CH_3OH in 13 minutes). Yield: 14 mg (58%). MS (ESI+): *m/z* calcd. for $[C_{65}H_{94}N_6O_{20}Na]^+$: 1301.64 $[M + Na]^+$; found: 1301.58.

MMAE-β-glucuronide-alkyne (**100**)

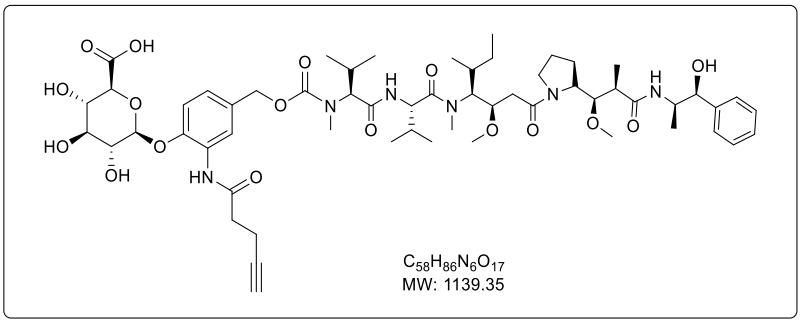

Compound **99** (3 mg, 0.0023 mmol, 1 equiv.) was dissolved in MeOH (100 µL) and cooled at – 20 ºC in acetone/dry ice. After this, LiOH (0.45 mg, 0.019 mmol, 8 equiv.) dissolved in H_2O (100 µL) was added and the reaction was stirred 2 hours at 0 ºC. The purificacion was carried out in preparative HPLC was carried out [Gradient: 95% (H_2O + 0.05% CF_3COOH) / 5% CH_3CN to 100% CH_3CN in 15 mins]. Yield: 6.06 mg (62 %). MS (ESI+): *m/z* calcd. for $[C_{58}H_{86}N_6O_{20}Na]^+$: 1161.59 $[M + Na]^+$; found: 1161.89; MS (ESI-): *m/z* calcd. for $[C_{58}H_{85}N_6O_{20}]^-$: 1137.6 $[M - 1H]^-$; found: 1137.95.

MMAE-β-glucuronide-PEG-4-*cyclo*[DKP-RGD] (**89**)

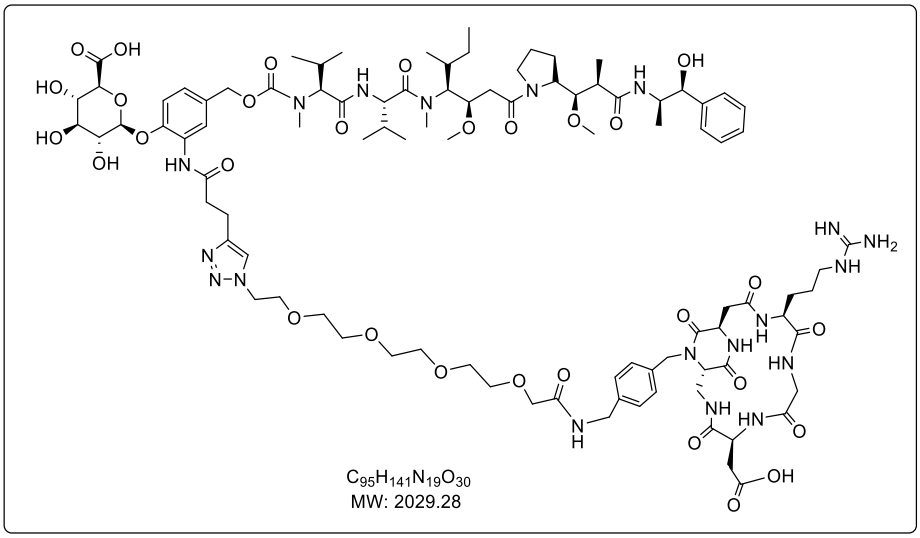

Compound **100** (5.24 mg, 0.0046 mmol, 1.5 equiv.) and N_3-PEG-4-*cyclo*[DKP-RGD] **51b** (3.08 mg, 0.0031 mmol, 1 equiv.) were dissolved in a degassed mixture of H_2O/DMF (1:1). A degassed solution of $CuSO_4 \cdot 5\ H_2O$ (0.39 mg, 0.0016, 0.5 equiv.) and sodium ascorbate (0.37 mg, 0.0019 mmol, 0.6 equiv.) were added at room temperature and stirred overnight at 30 ºC. The solvents were evaporated and the mixture was purified in semipreparative HPLC [Gradient: 100% (H_2O + 0.1% CF_3COOH) / 0% (CH_3CN + 0.1% CF_3COOH) to 0% (H_2O + 0.1% CF_3COOH) / 100% (CH_3CN + 0.1% CF_3COOH) in 20 min]. Yield: 5.27 mg (84%). MS (ESI+): *m/z* calcd. for $[C_{95}H_{143}N_{19}O_{30}]^{2+}$: 1015.01 $[M + 2H]^{2+}$; found: 1015.81; *m/z* calcd. for $[C_{95}H_{144}N_{19}O_{30}]^{3+}$: 677.01 $[M + 3H]^{3+}$; found: 677.75.

Appendix of HPLC traces of the final compounds

HPLC traces of the final compounds

The purity evaluation of *cyclo*[DKP-RGD]-β-glucuronide-MMAE (**88**) was carried out in Phenomenex Luna C-18(2) column 10 µm, 250 × 21.2 mm, with precolumn at 30 mL/min flow rate. In the rest of the cases, the Dionex Ultimate 3000 equipped with Dionex RS Variable Wavelength Detector (semipreparative column: Atlantis Prep T3 OBDTM 5 µm 19 × 100 mm; flow 15 ml/min) was used.

Cyclo[RGDfK] (**46**)

Gradient: 100% (H_2O + 0.1% CF_3COOH) / 0% (CH_3CN + 0.1% CF_3COOH) to 0% (H_2O + 0.1% CF_3COOH) / 100% (CH_3CN + 0.1% CF_3COOH) in 14 min; t_R (product): 6 min.

Purity: 100%.

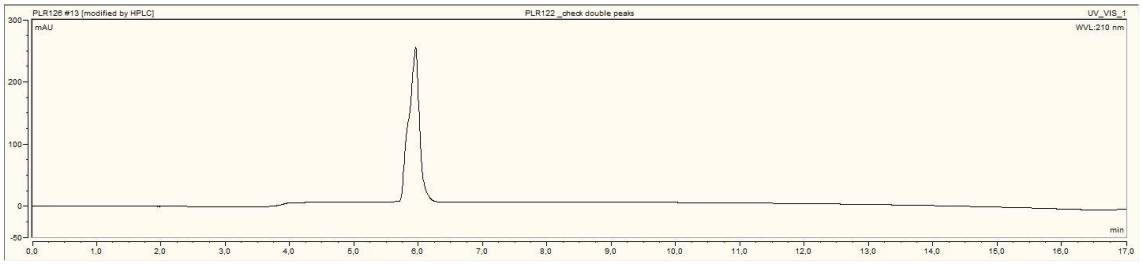

Cyclo[DKP-RGD]-GFLG-PTX (**37**)

Gradient: 100% (H_2O + 0.1% CF_3COOH) / 0% (CH_3CN + 0.1% CF_3COOH) to 0% (H_2O + 0.1% CF_3COOH) / 100% (CH_3CN + 0.1% CF_3COOH) in 20 min; t_R (product): 12.5 min.

Purity: 99%.

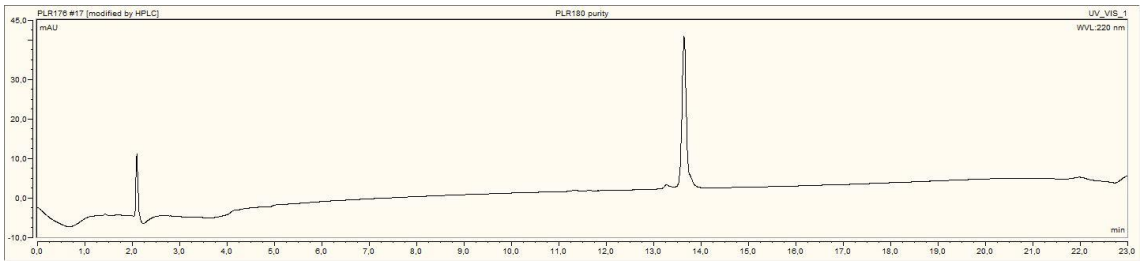

Cyclo[RGDfK]-GFLG-PTX (**38**)

Gradient: 100% (H_2O + 0.1% CF_3COOH) / 0% (CH_3CN + 0.1% CF_3COOH) to 0% (H_2O + 0.1% CF_3COOH) / 100% (CH_3CN + 0.1% CF_3COOH) in 20 min; t_R (product): 13 min.

Purity: 93%.

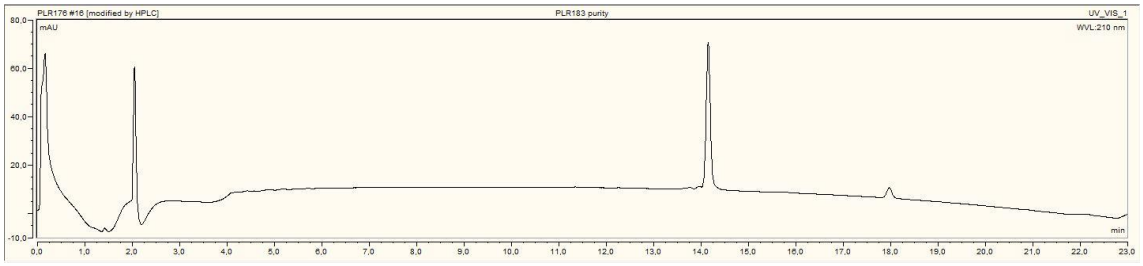

Cyclo[DKP-RGD]-PEG-4-GFLG-PTX (**39**)

Gradient: 100% (H_2O + 0.1% CF_3COOH) / 0% (CH_3CN + 0.1% CF_3COOH) to 0% (H_2O + 0.1% CF_3COOH) / 100% (CH_3CN + 0.1% CF_3COOH) in 20 min; t_R (product): 12.5 min.

Purity: 100%.

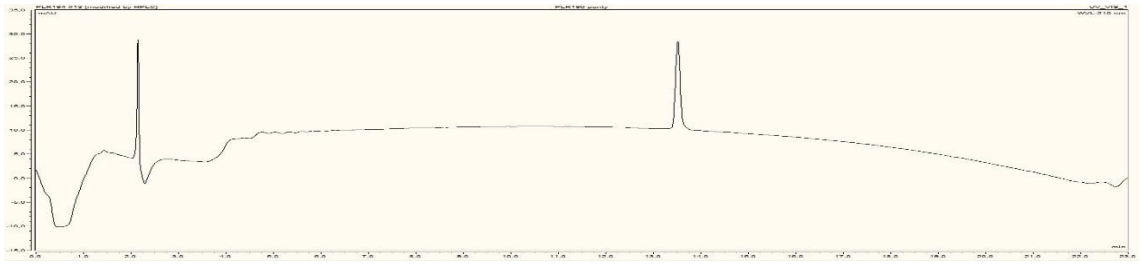

Cyclo[RGDfK]-PEG-4-GFLG-PTX (**40**)

Gradient: 100% (H_2O + 0.1% CF_3COOH) / 0% (CH_3CN + 0.1% CF_3COOH) to 0% (H_2O + 0.1% CF_3COOH) / 100% (CH_3CN + 0.1% CF_3COOH) in 20 min; t_R (product): 13 min.

Purity: 93%.

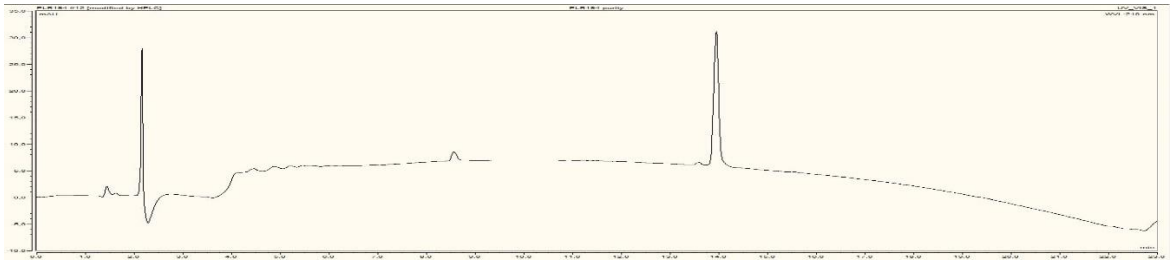

Cyclo[DKP-RGD]-Val-Ala-α-amanitin (**62**)

Gradient: 100% (H_2O + 0.1 % CF_3COOH)/0% (CH_3CN + 0.1% CF_3COOH) to 50% (H_2O + 0.1 % CF_3COOH)/50% (CH_3CN + 0.1% CF_3COOH) in 9 minutes; t_R: (product): 8.3 min Purity: 99.6%.

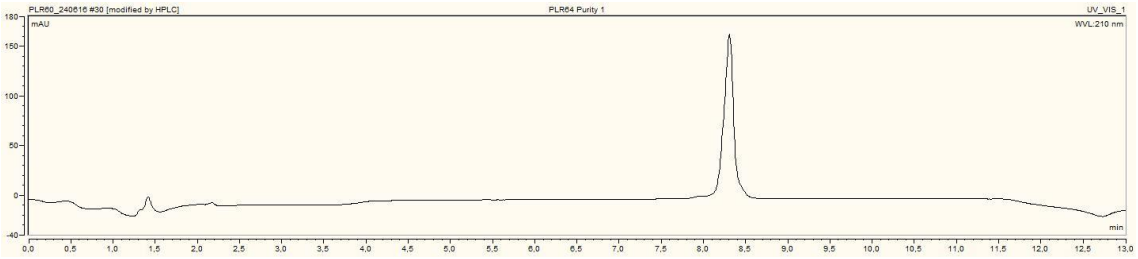

Cyclo[DKP-RGD]-uncleavable-α-amanitin (**63**)

Gradient: 100% (H_2O + 0.1 % CF_3COOH)/0% (CH_3CN + 0.1% CF_3COOH) to 50% (H_2O + 0.1 % CF_3COOH)/ 50% (CH_3CN + 0.1% CF_3COOH) in 9 minutes; t_R: (product): 8 min. Purity: 95%.

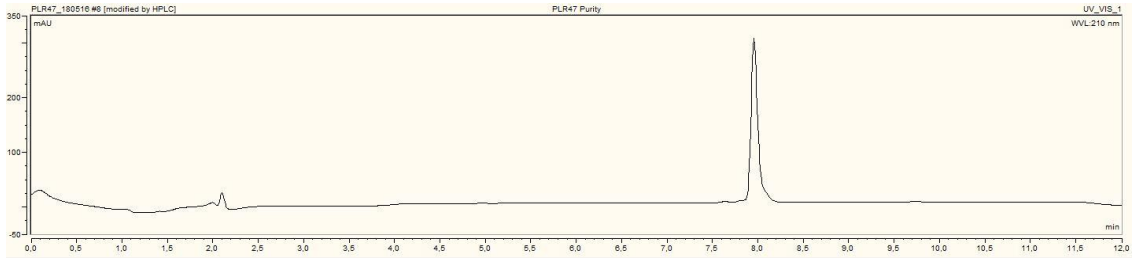

Dau=Aoa-GPLGVRG-cyclo[RGDfK] (**71**)

Gradient: 100% (H_2O + 0.1% CF_3COOH) / 0% (CH_3CN + 0.1% CF_3COOH) to 0% (H_2O + 0.1% CF_3COOH) / 100% (CH_3CN + 0.1% CF_3COOH) in 14 min; t_R (product): 7.9 min. Purity: 98.5%.

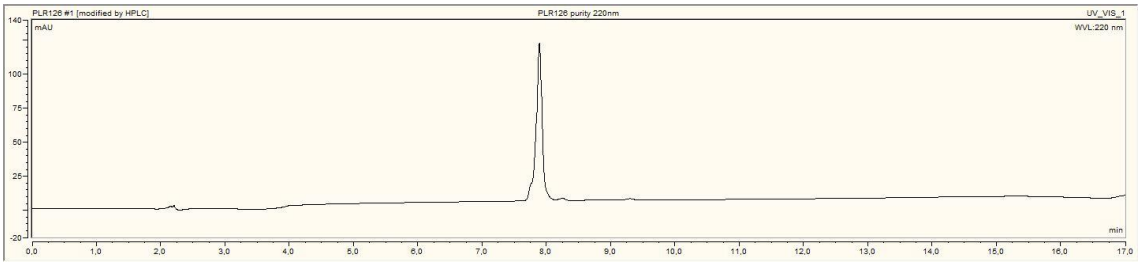

Cyclo[RGDfK]-GPLG-PTX (**73**)

Gradient: 100% (H_2O + 0.1% CF_3COOH) / 0% (CH_3CN + 0.1% CF_3COOH) to 0% (H_2O + 0.1% CF_3COOH) / 100% (CH_3CN + 0.1% CF_3COOH) in 14 min; t_R (product): 10.7 min. Purity: 85%.

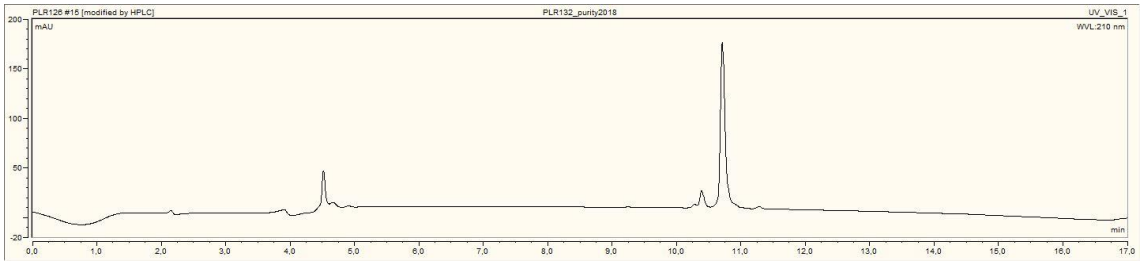

Cyclo[DKP-RGD]-β-glucuronide-MMAE (**88**)

Gradient: 95% (H_2O + 0.05 % CF_3COOH)/5% CH_3CN to 0% (H_2O + 0.05 % CF_3COOH)/100% CH_3CN in 15 mins, t_R (product): 8.5 min

Purity: 96%.

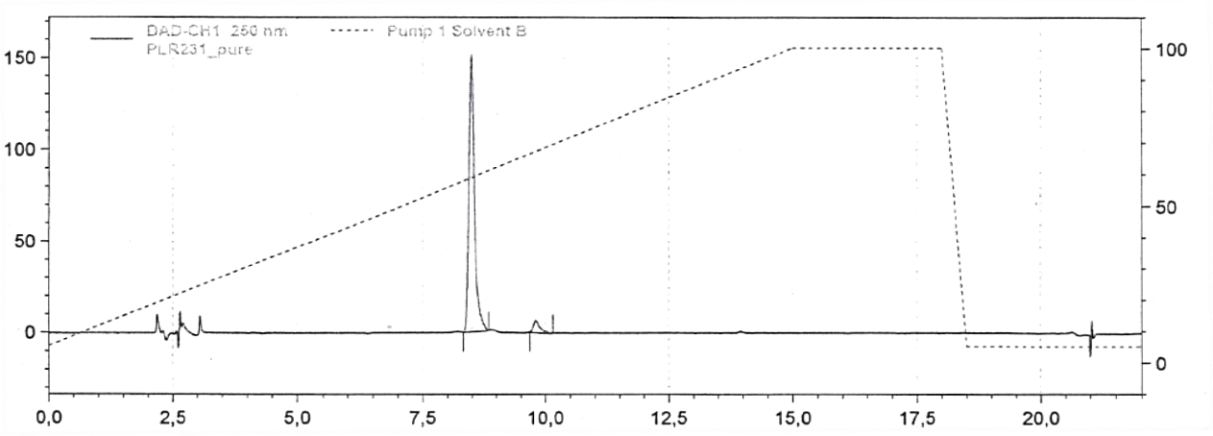

Cyclo[DKP-RGD]-PEG-4-β-glucuronide-MMAE (**89**)

Gradient: 100% (H_2O + 0.1% CF_3COOH) / 0% (CH_3CN + 0.1% CF_3COOH) to 0% (H_2O + 0.1% CF_3COOH) / 100% (CH_3CN + 0.1% CF_3COOH) in 20 min; t_R (product): 11.4 min. Purity: 94%.

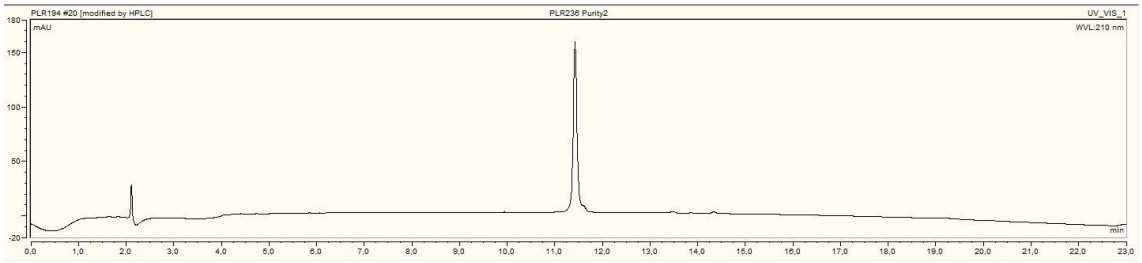

Appendix of ^{1}H NMR and ^{13}C NMR spectra

*Fmoc-Gly-Phe-Leu-Gly-OH (**48**)*

^{1}H NMR (400 MHz, DMSO)

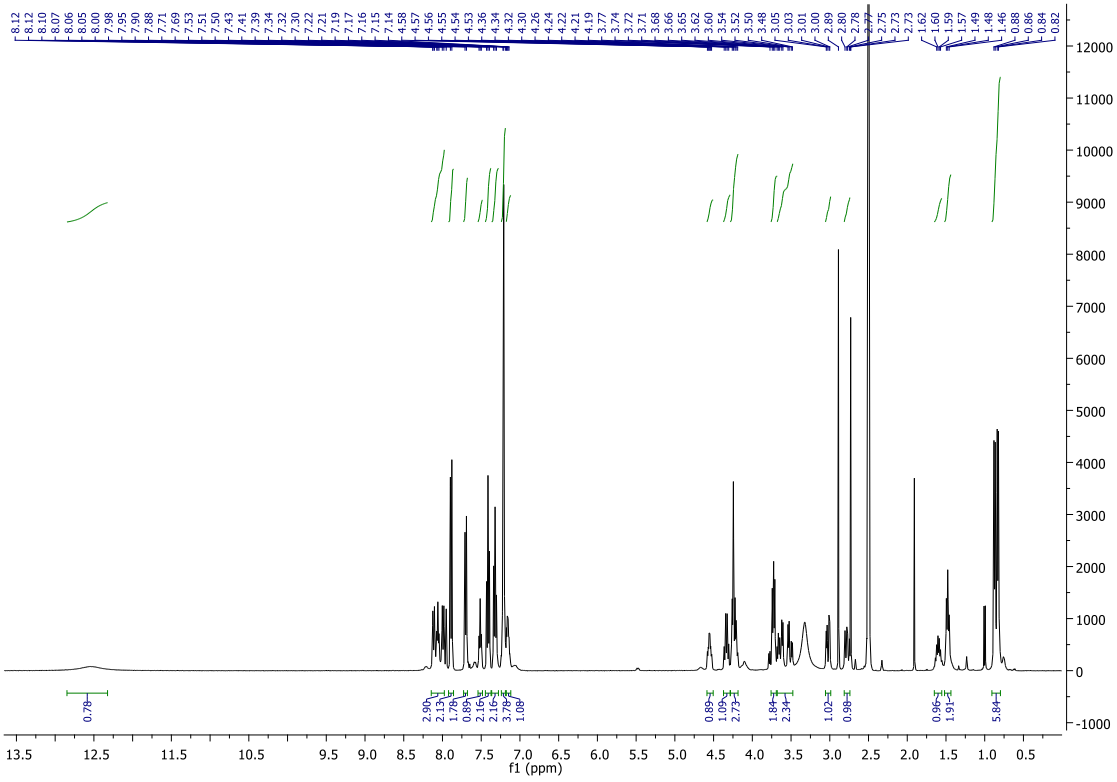

*Fmoc-Gly-Phe-Leu-Gly-N-[4-(hydroxymethyl)phenyl] (**52**)*

^{1}H NMR (400 MHz, DMSO)

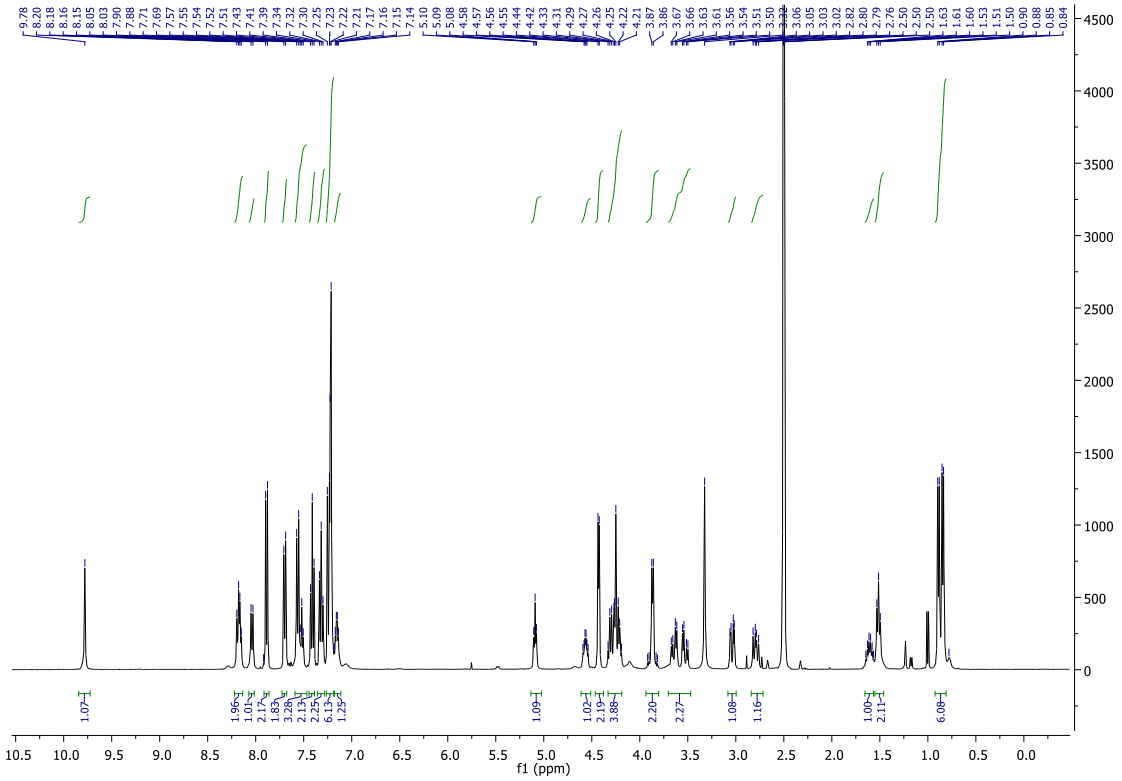

^{13}C NMR (101 MHz, DMSO)

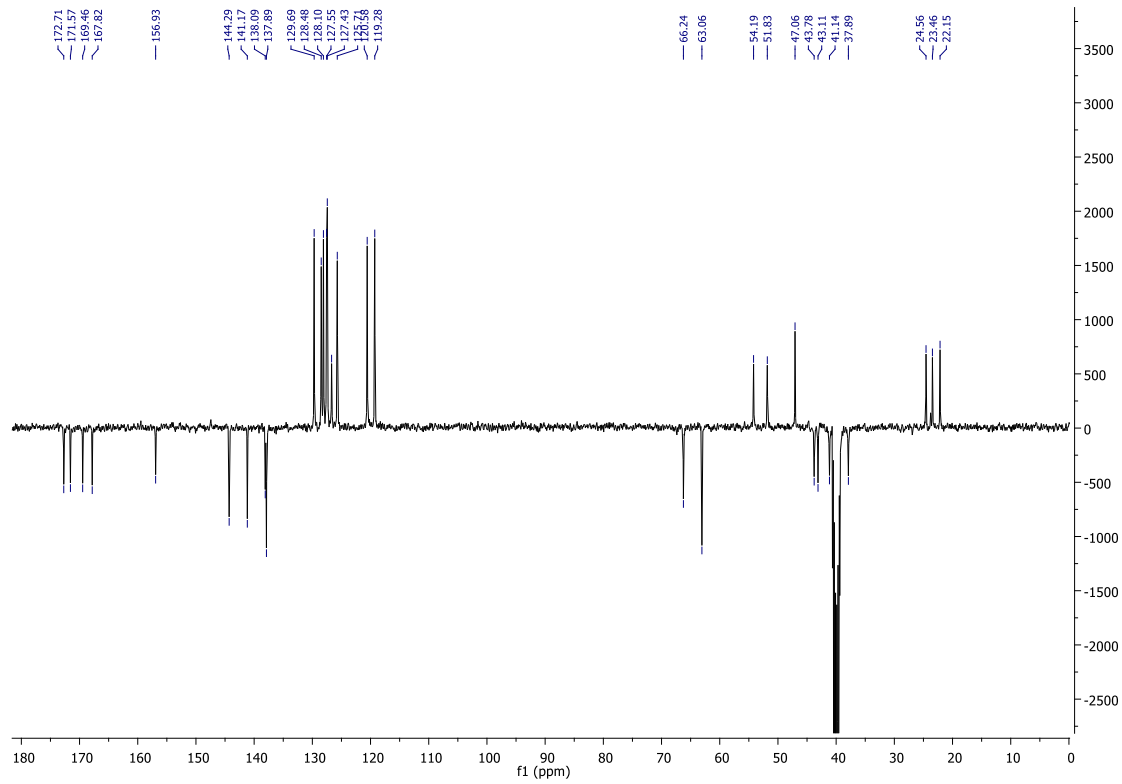

Fmoc-Gly-Phe-Leu-Gly-N-[4-[[[(4-nitrophenoxy)carbonyl]oxy]methyl]phenyl] (***53***)

^{1}H NMR (400 MHz, DMSO)

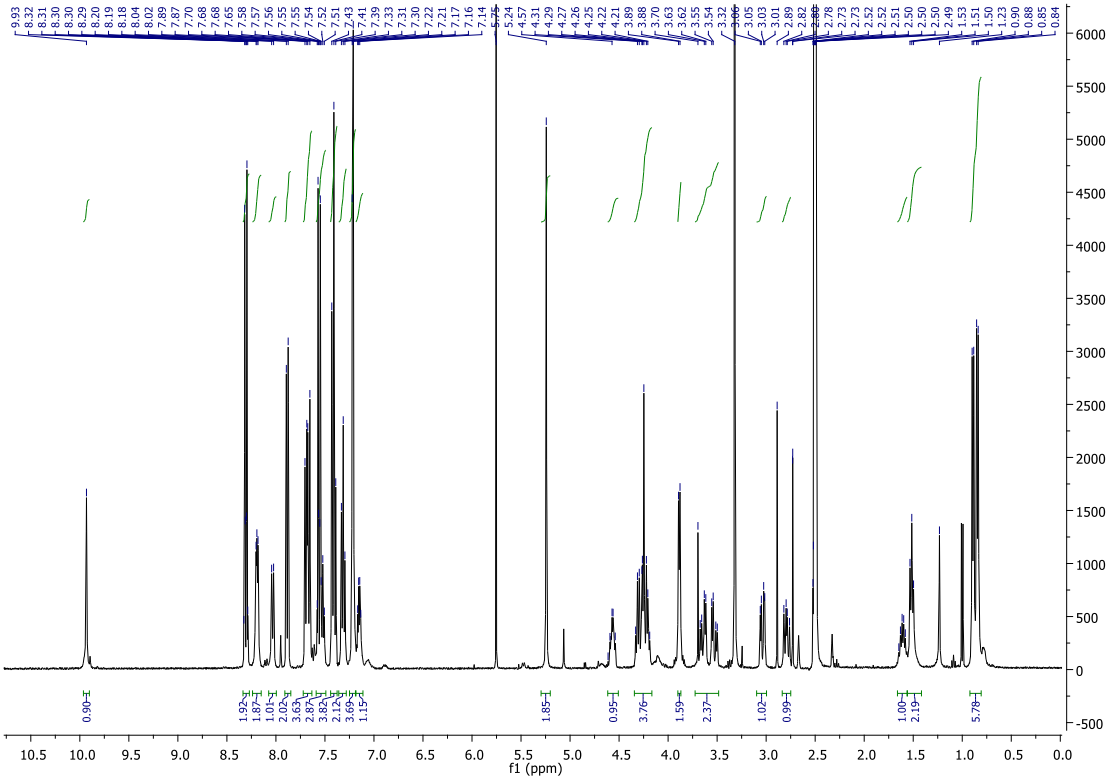

^{13}C NMR (101 MHz, DMSO)

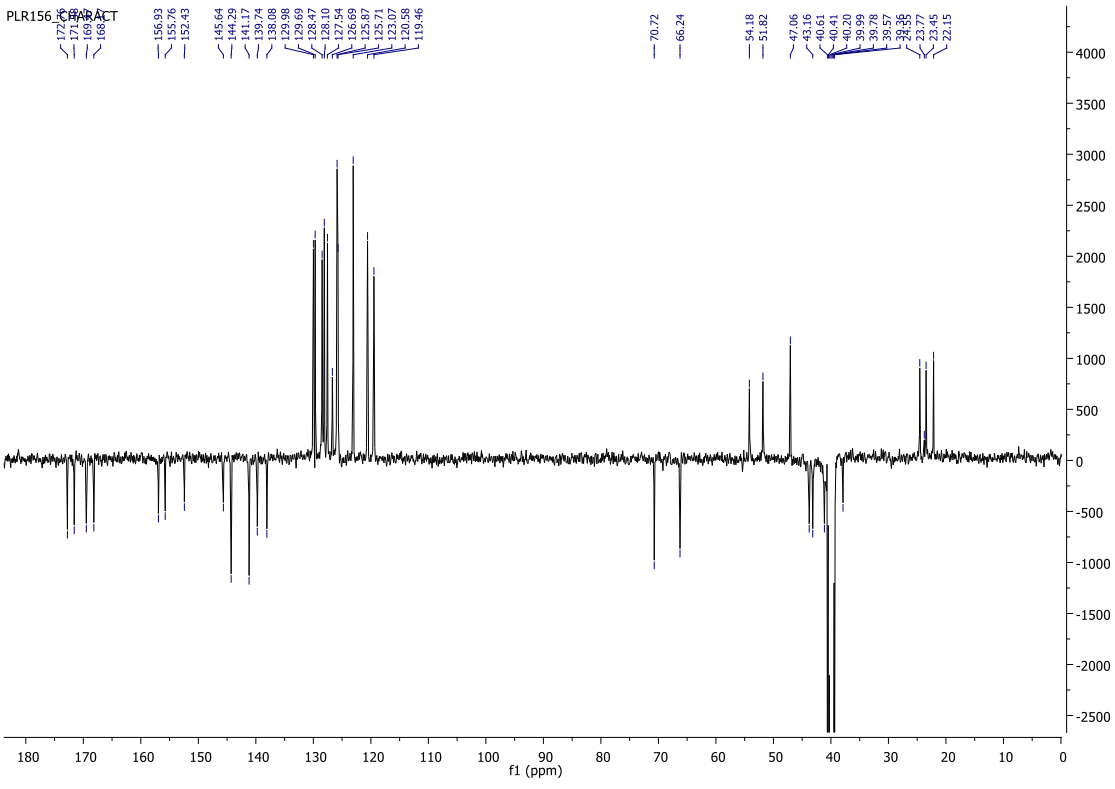

*Fmoc-Gly-Phe-Leu-Gly-N-[4-[[[(N-(Boc)-N,N'-dimethylethylenediamine)carbonyl]oxy]methyl]phenyl] (**54**)*

^{1}H NMR (400 MHz, DMSO)

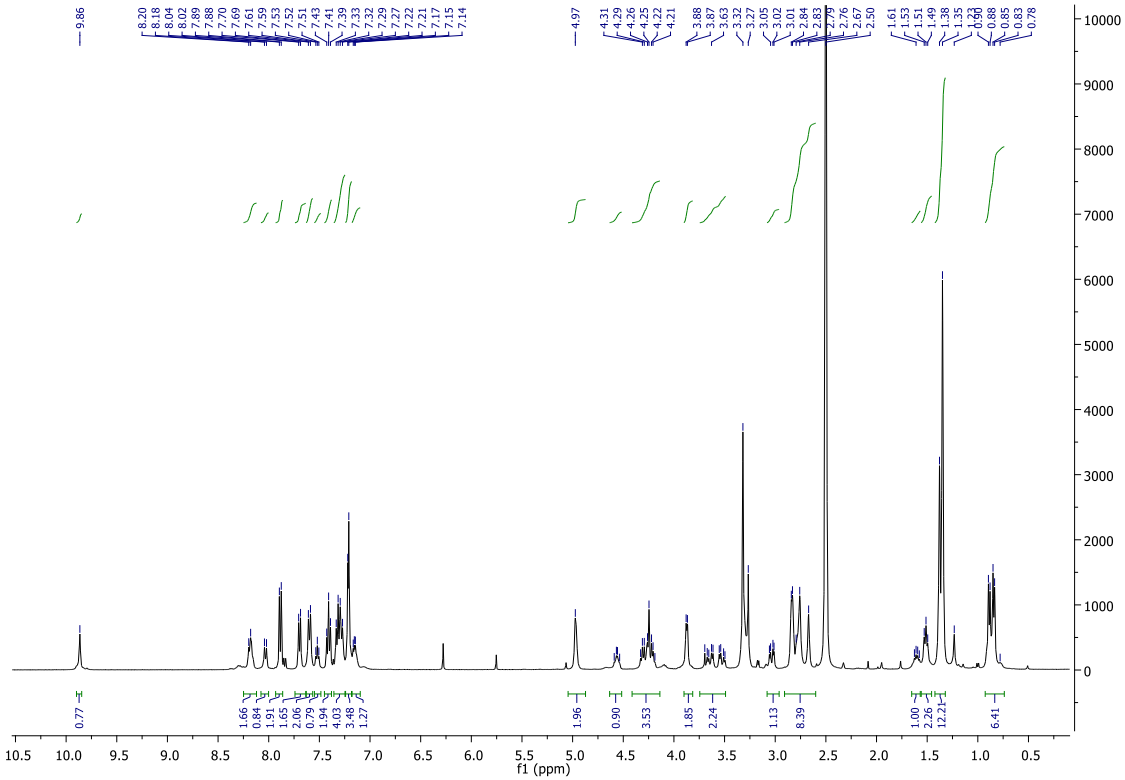

^{13}C NMR (101 MHz, DMSO)

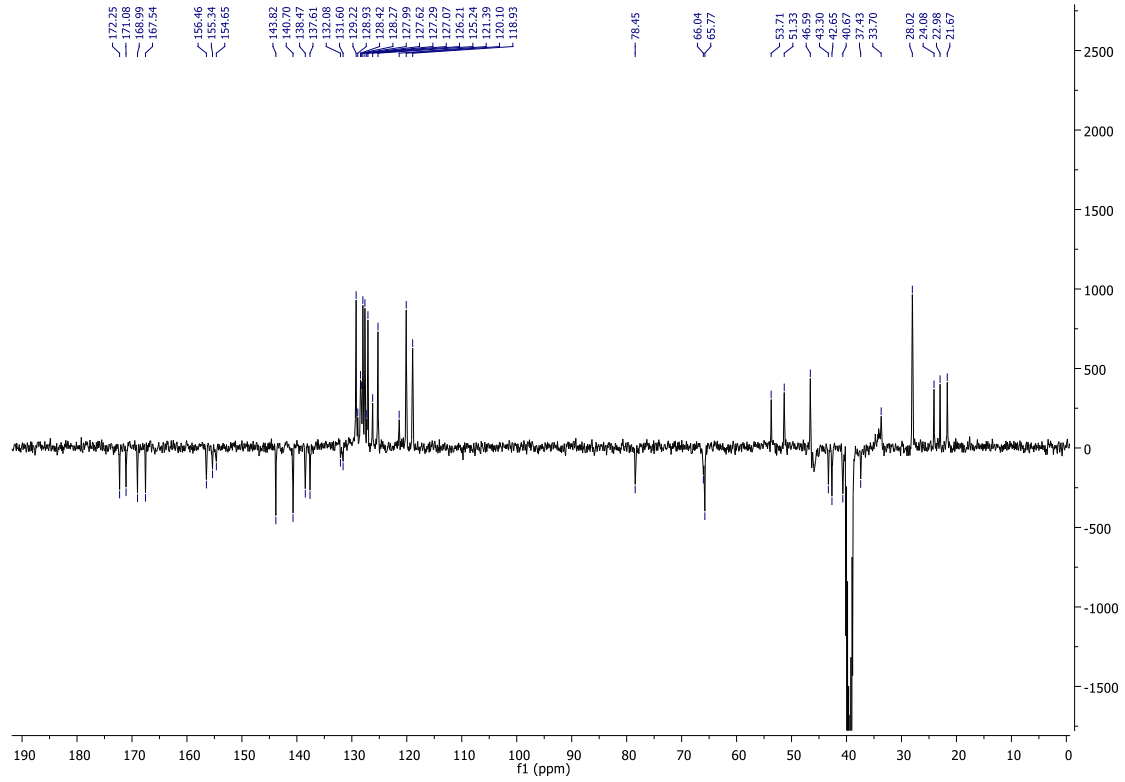

*(Hemiglutarate)-Gly-Phe-Leu-Gly-N-[4-[[[(N-(Boc)-N,N'-dimethylethylenediamine)carbonyl]oxy]methyl]phenyl] (**55**)*

^{1}H NMR (400 MHz, DMSO)

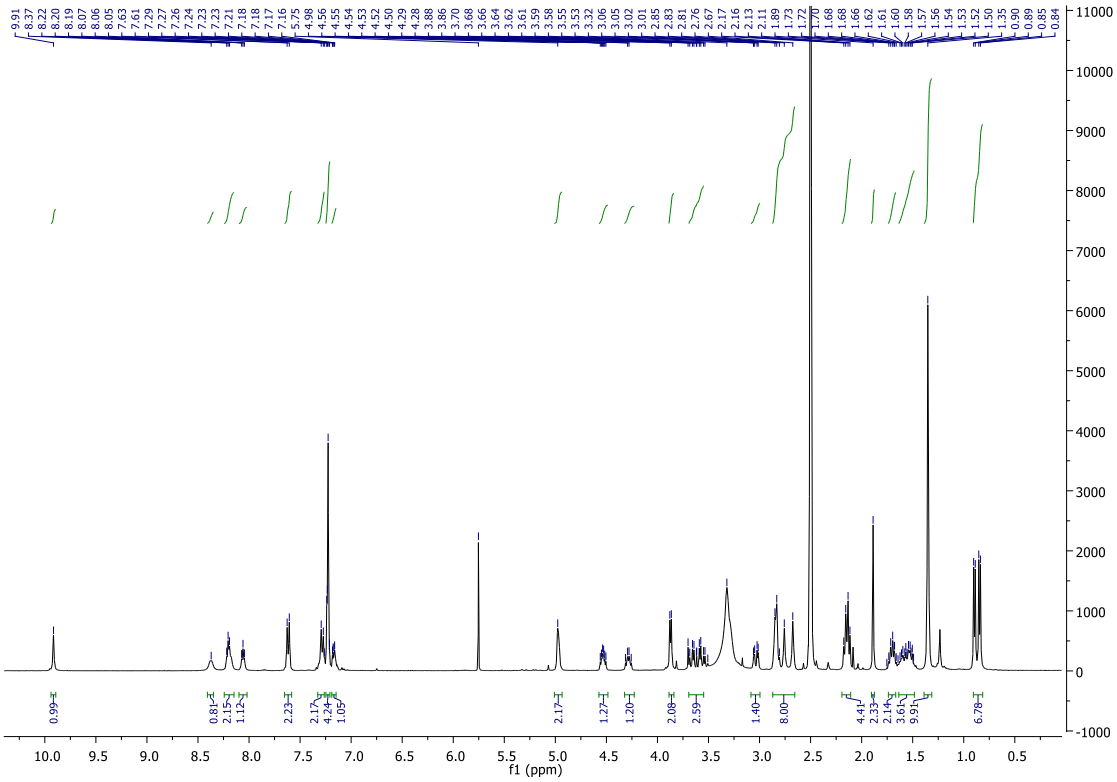

^{13}C NMR (101 MHz, DMSO)

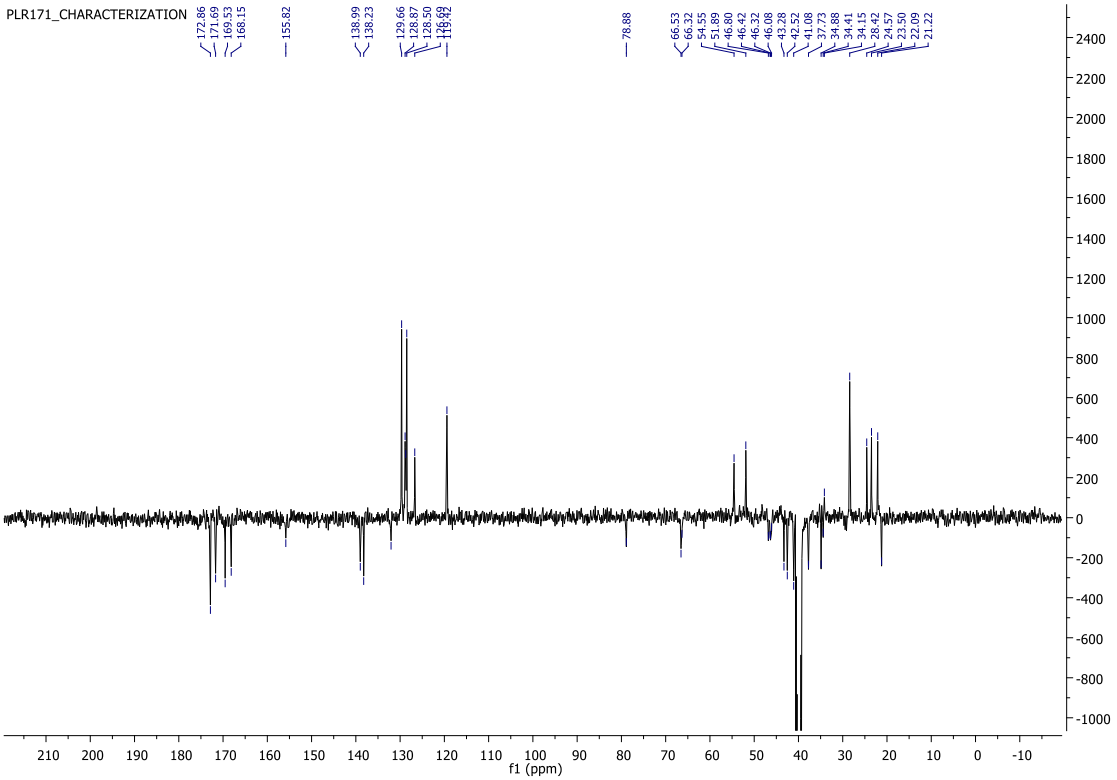

*Cyclo[RGDfK]-PEG-4-azide (**51a**)*

^{1}H NMR (400 MHz, DMSO)

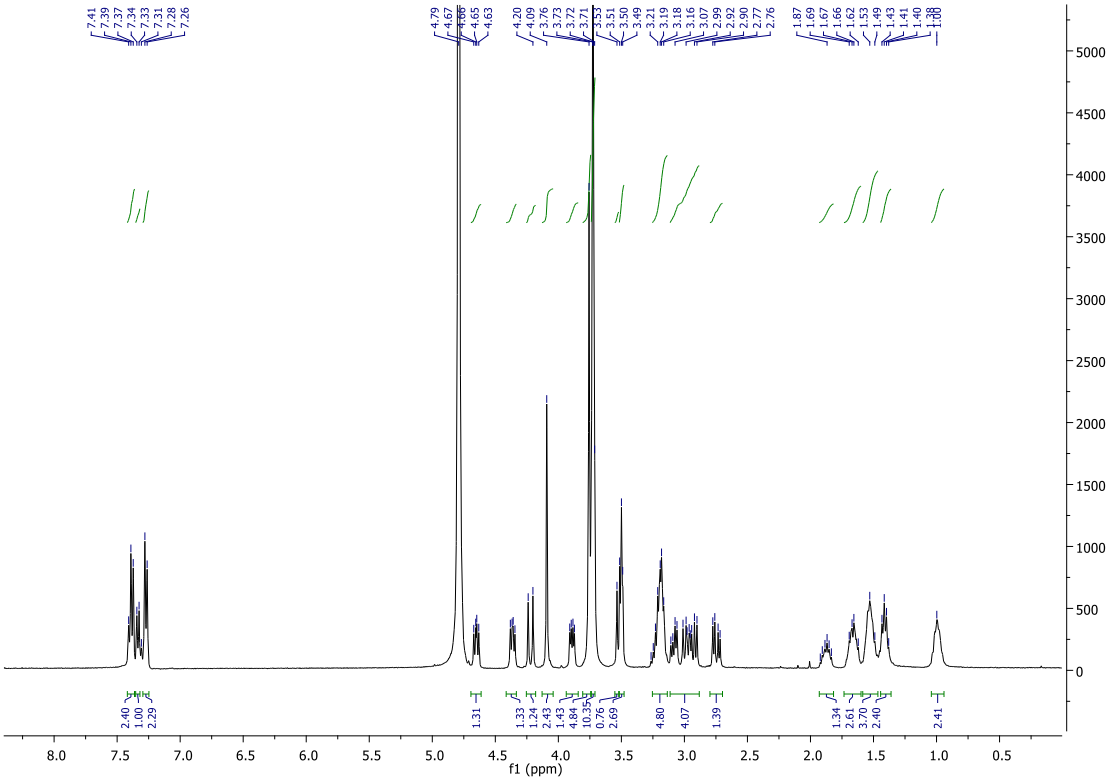

^{13}C NMR (101 MHz, DMSO)

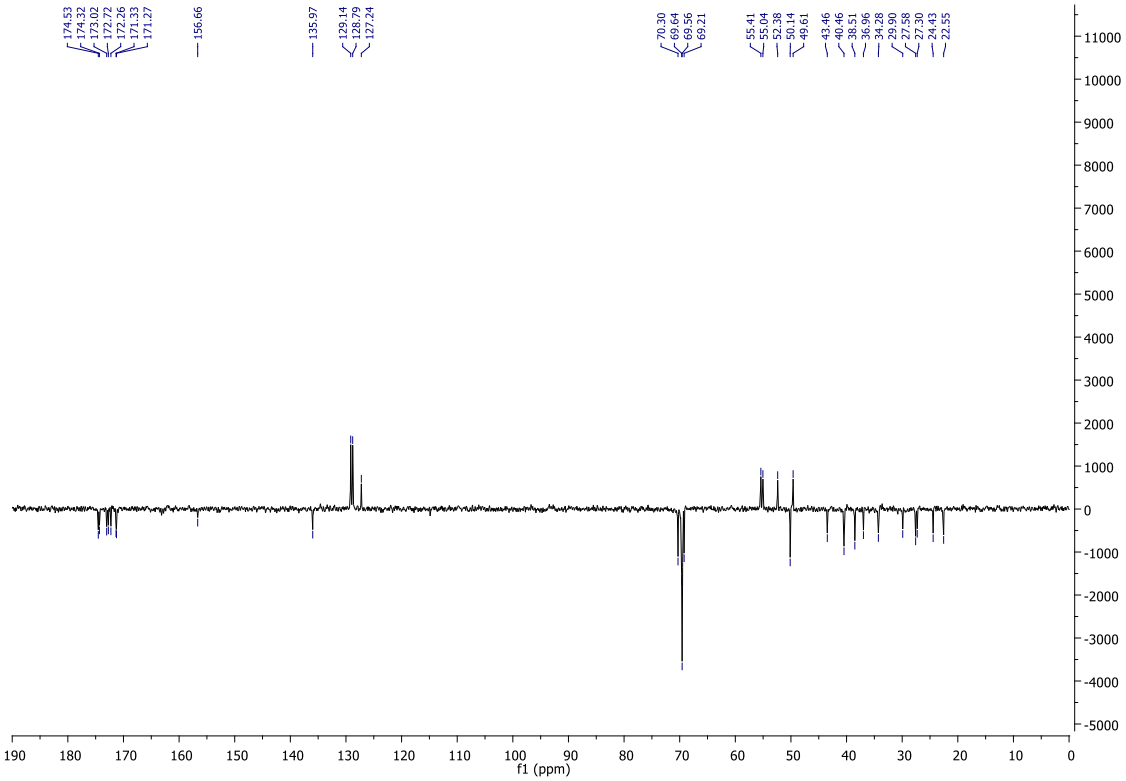

*4-((5S,8S)-8-benzyl-5-isobutyl-4,7,10,13-tetraoxo-3,6,9,12-tetraazaheptadec-16-ynamido)benzyl tert-butyl ethane-1,2-diylbis(methylcarbamate) (**57**)*

^{1}H NMR (400 MHz, DMSO)

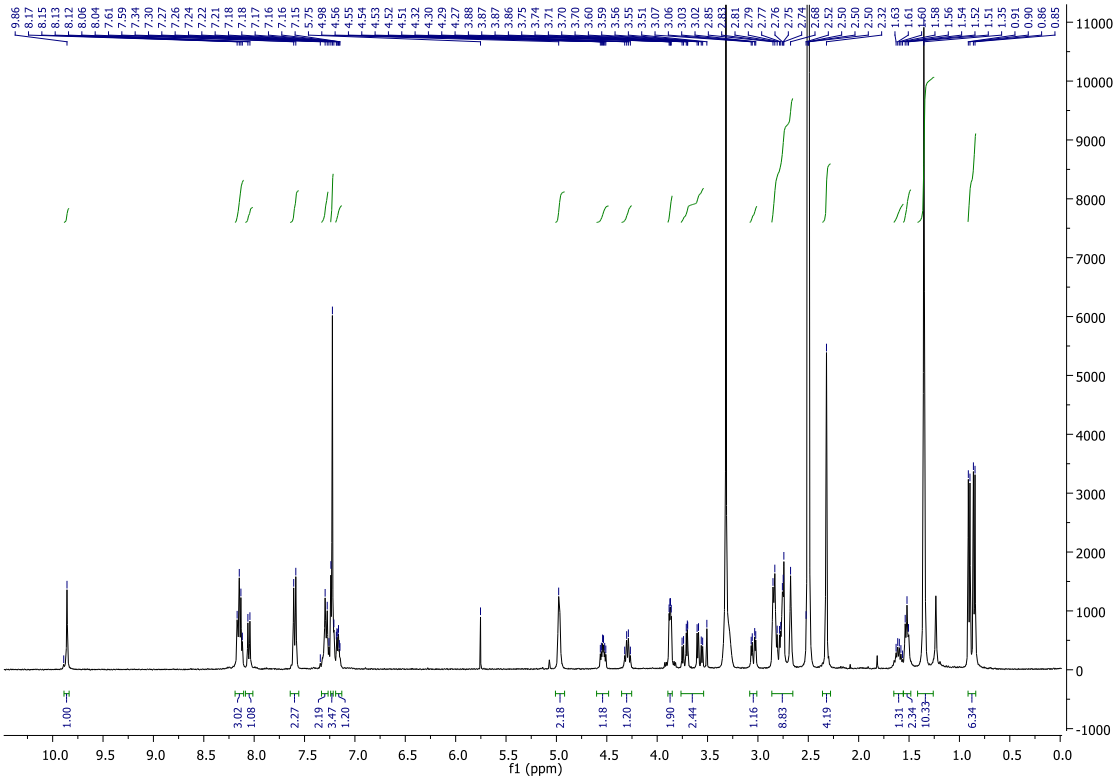

Hemiglutarate-aminohexyl-α-amanitin (**65a**)

^{1}H NMR (400 MHz, D_2O)

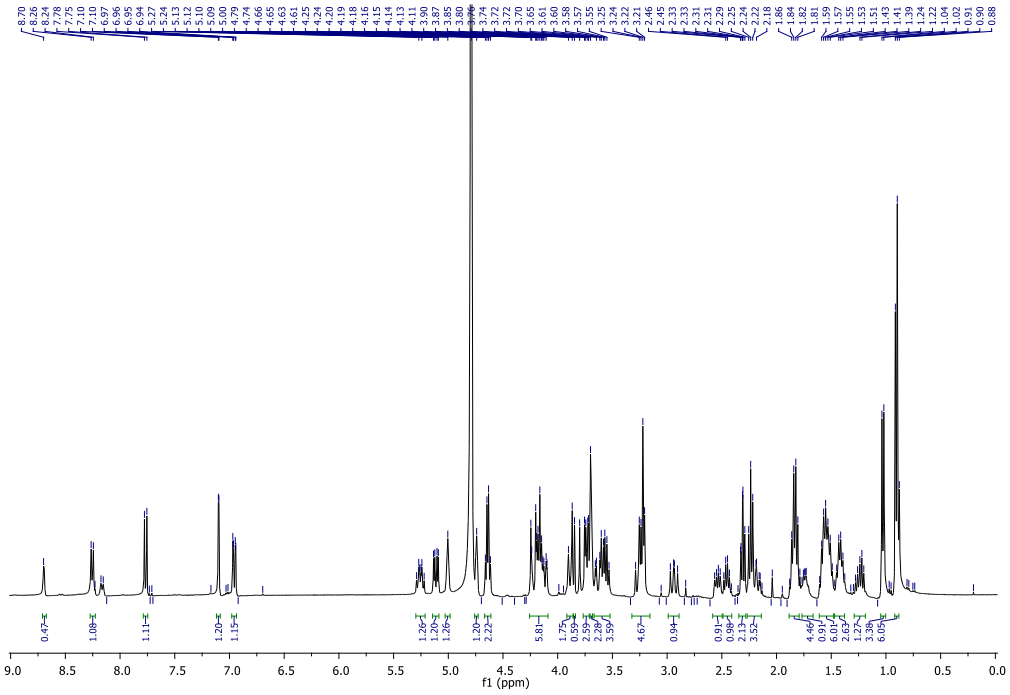

^{13}C NMR (101 MHz, D_2O)

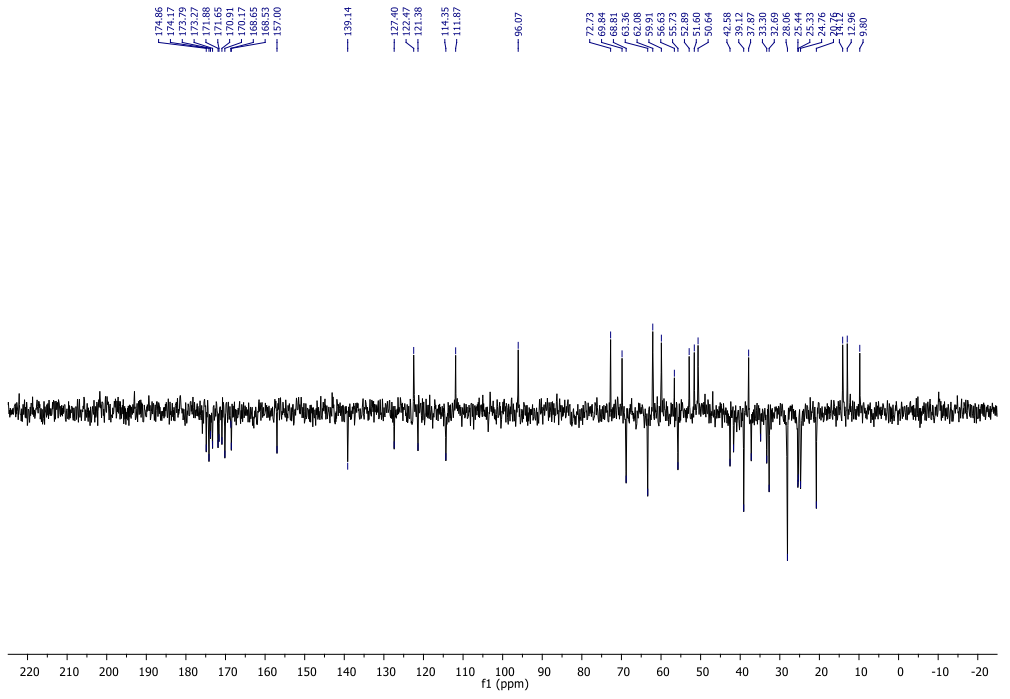

Cyclo[DKP-RGD]-uncleavable-α-amanitin (**63**)

^{1}H NMR (400 MHz, D_2O)

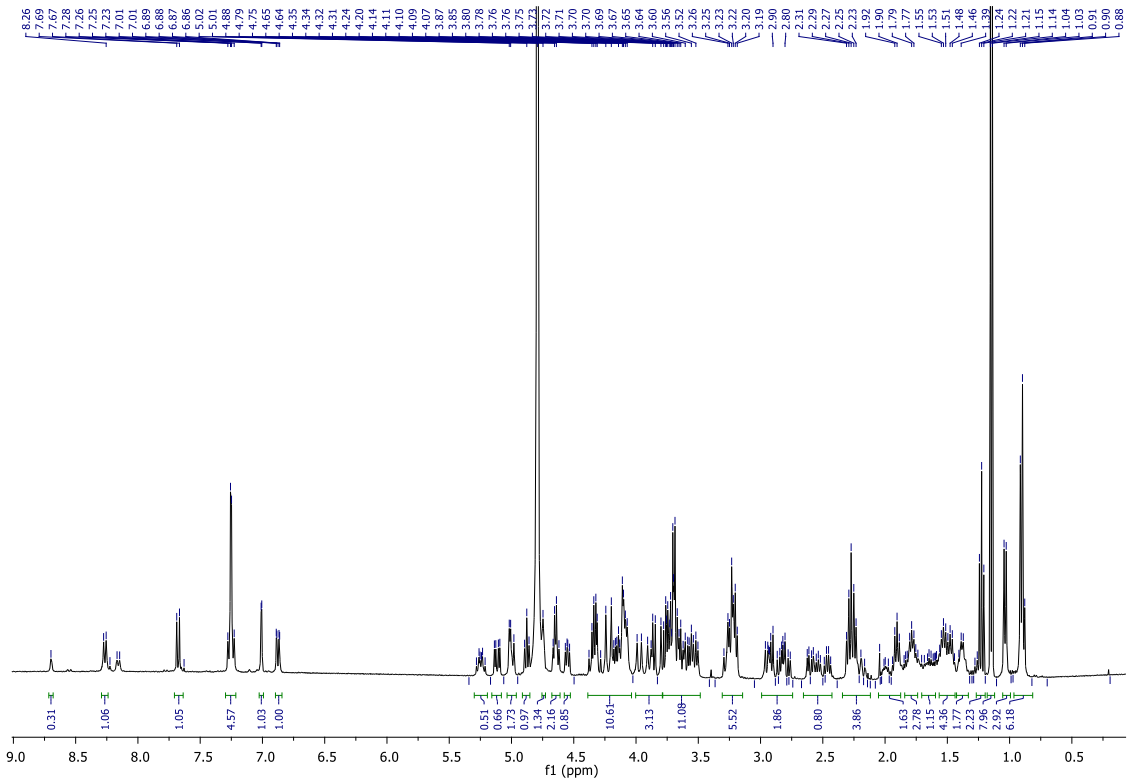

*Fmoc-Gly-Pro-Leu-Gly-OH (**81**)*

^{1}H NMR (400 MHz, $CDCl_3$)

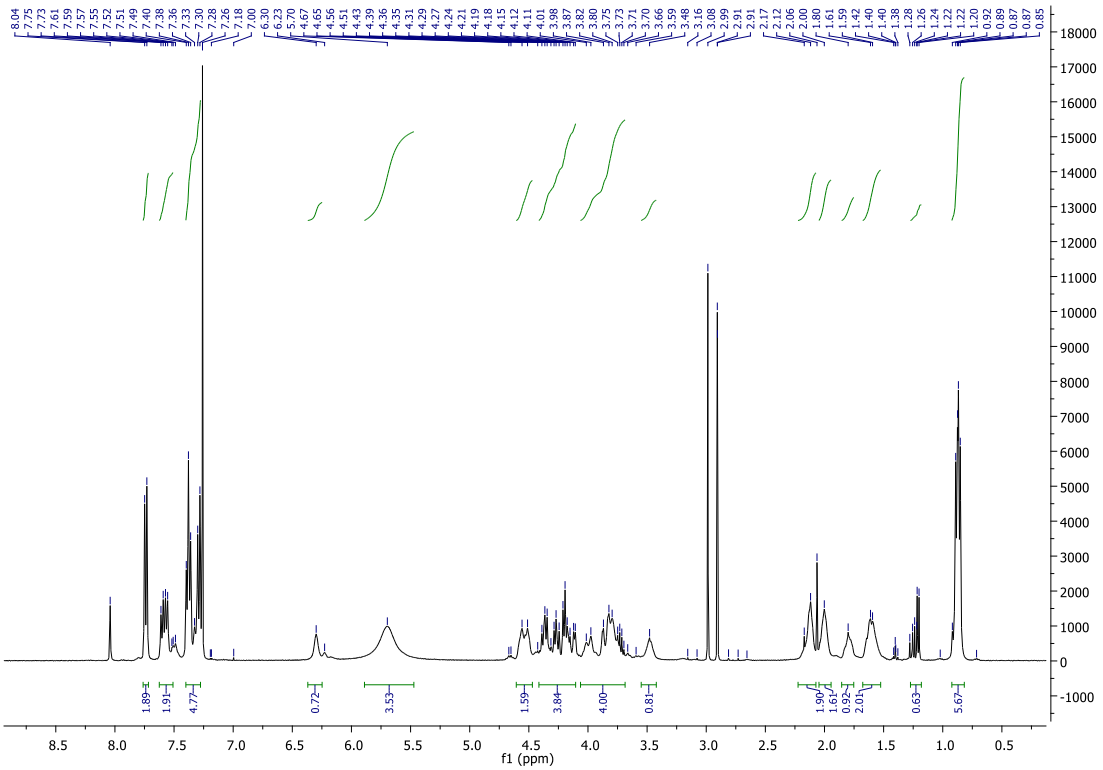

*(2S,3R,4S,5S,6S)-2-(4-formyl-2-nitrophenoxy)-6-(methoxycarbonyl)tetrahydro-2H-pyran-3,4,5-triyl triacetate (**92**)*

^{1}H NMR (500 MHz, $CDCl_3$)

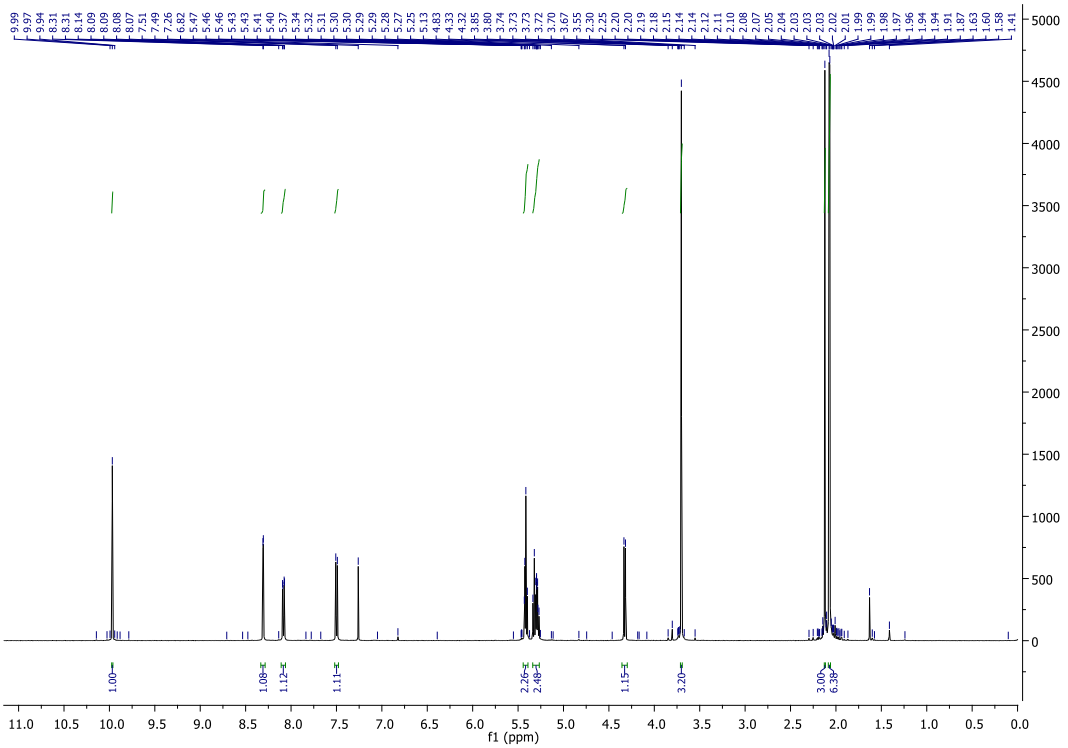

^{13}C NMR (126 MHz, $CDCl_3$)

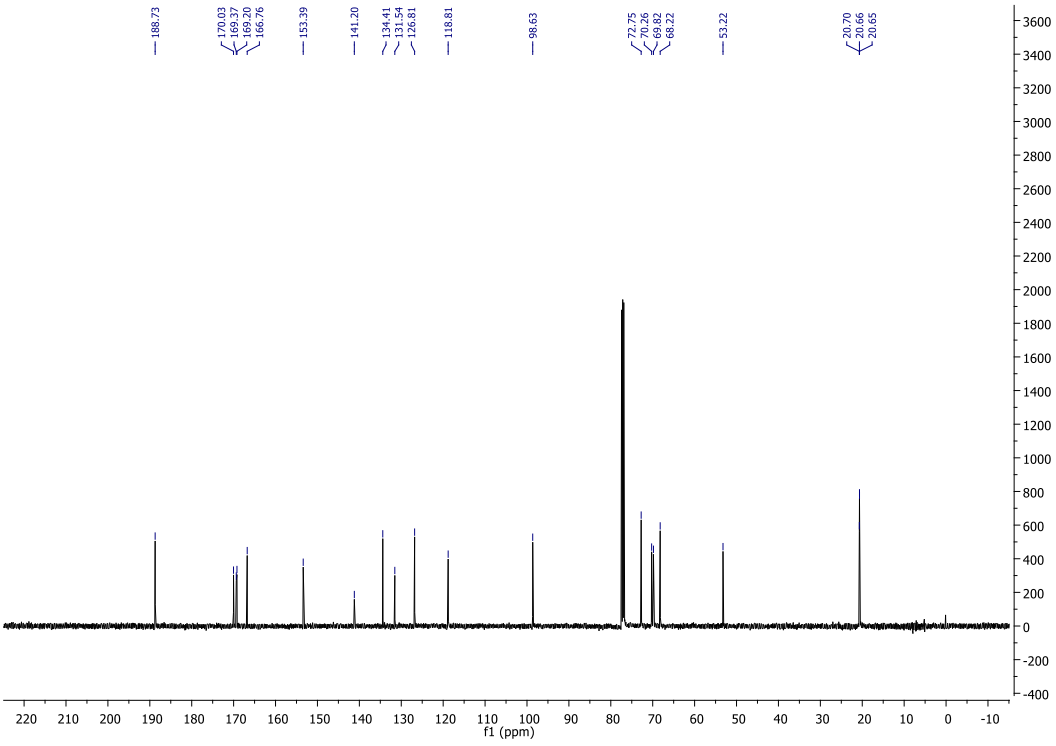

*(2S,3R,4S,5S,6S)-2-(4-(hydroxymethyl)-2-nitrophenoxy)-6 (methoxycarbonyl)tetrahydro-2H-pyran-3,4,5-triyl triacetate (**93**)*

^{1}H NMR (500 MHz, $CDCl_3$)

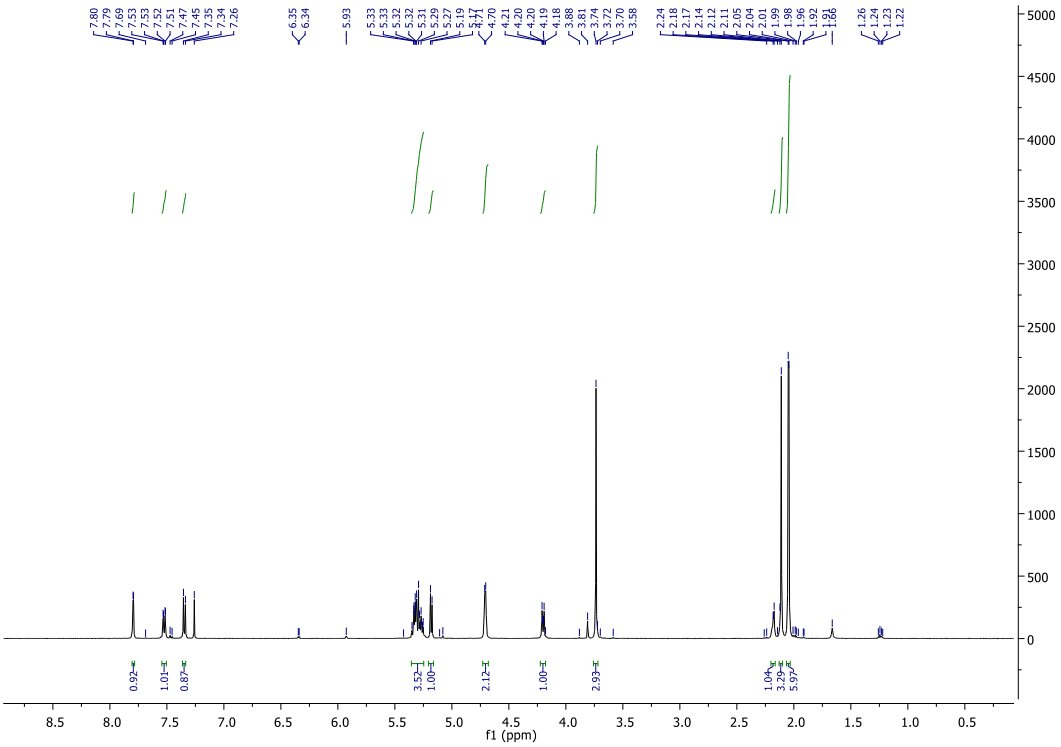

^{13}C NMR (126 MHz, $CDCl_3$)

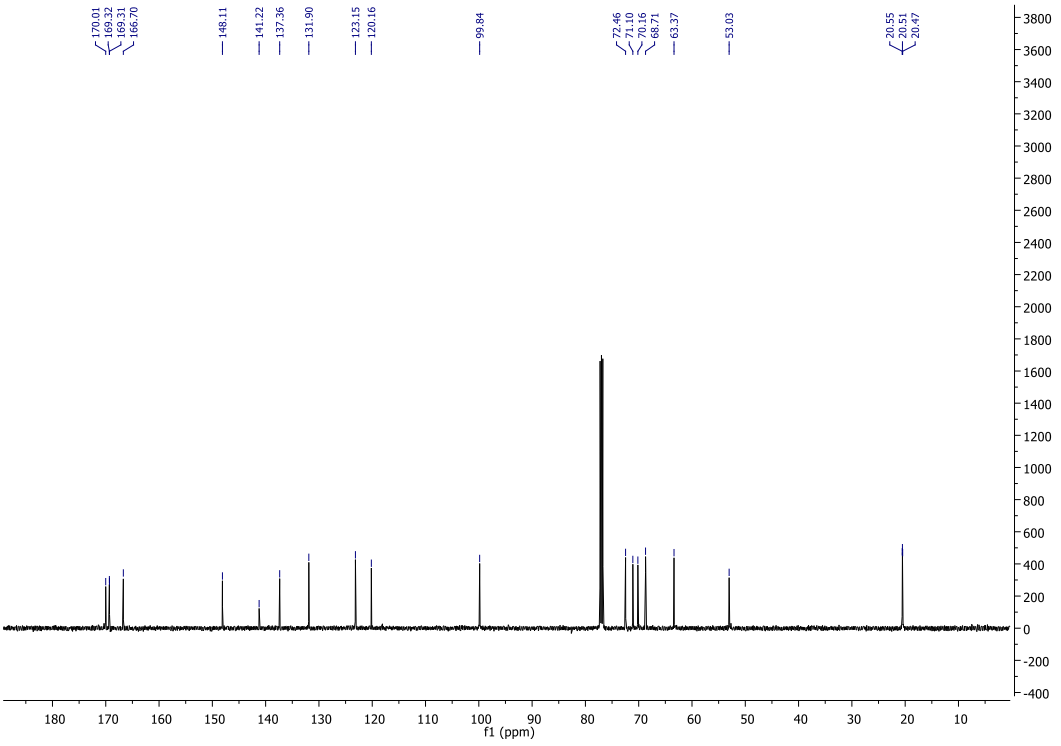

*(2S,3R,4S,5S,6S)-2-(2-amino-4-(hydroxymethyl)phenoxy)-6-(methoxycarbonyl)tetrahydro-2H-pyran-3,4,5-triyl triacetate (**94**)*

^{1}H NMR (500 MHz, $CDCl_3$)

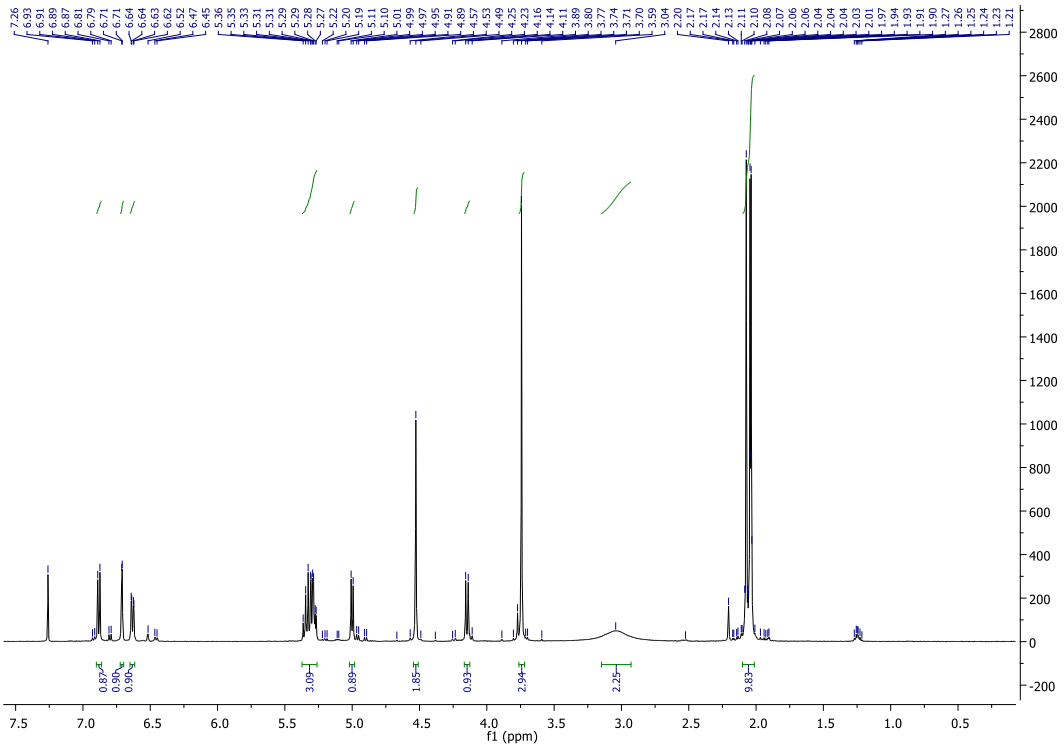

^{13}C NMR (126 MHz, $CDCl_3$)

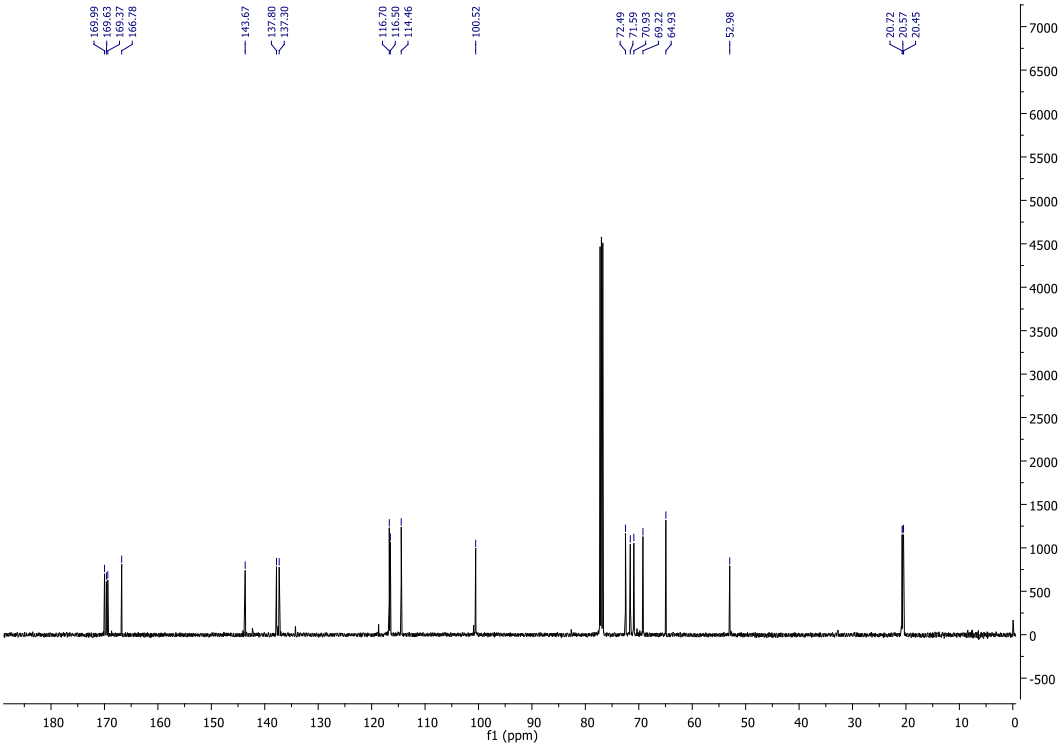

References

[1] a) V. T. DeVita and E. Chu, *Cancer Res.* **2008**, *68*, 8643-8653; b) J. A. McKnight, *Clin. Tech. Small Anim. Pract.* **2003**, *18*, 67-72.

[2] a) R. V. Chari, M. L. Miller, W. C. Widdison, *Angew. Chem. Int. Ed.* **2014**, *53*, 3796-3827; *Angew. Chem*. **2014**, *126*, 3872-3904; b) E. Dickens, S. Ahmed, *Surgery-Oxford International Edition* **2018**, *36*, 134-138.

[3] K. Cheung-Ong, G. Giaever, C. Nislow, *Chem. Biol.* **2013**, *20*, 648-659.

[4] S. Dasari, P. B. Tchounwou, *Eur. J. Pharmacol.* **2014**, *740*, 364-378.

[5] E. Mukhtar, V. M. Adhami, H. Mukhtar, *Mol. Cancer Ther.* **2014**, *13*, 275-284.

[6] S. Jain, L. T. Vahdat, *Clin. Cancer Res.* **2011**, *17*, 6615-6622.

[7] a) R. J. Motzer, B. I. Rini, R. M. Bukowski, B. D. Curti, D. J. George, G. R. Hudes, B. G. Redman, K. A. Margolin, J. R. Merchan, G. Wilding, *JAMA* **2006**, *295*, 2516-2524; b) G. D. Demetri, A. T. van Oosterom, C. R. Garrett, M. E. Blackstein, M. H. Shah, J. Verweij, G. McArthur, I. R. Judson, M. C. Heinrich, J. A. Morgan, *The Lancet* **2006**, *368*, 1329-1338.

[8] a) B. Escudier, T. Eisen, W. M. Stadler, C. Szczylik, S. Oudard, M. Siebels, S. Negrier, C. Chevreau, E. Solska, A. A. Desai, *N. Engl. J. Med.* **2007**, *356*, 125-134; b) J. M. Llovet, S. Ricci, V. Mazzaferro, P. Hilgard, E. Gane, J.-F. Blanc, A. C. de Oliveira, A. Santoro, J.-L. Raoul, A. Forner, *N. Engl. J. Med.* **2008**, *359*, 378-390.

[9] P. T. Wong, S. K. Choi, *Chem. Rev.* **2015**, *115*, 3388-3432.

[10] C. Chalouni, S. Doll, *J. Exp. Clin. Cancer Res.* **2018**, *37*, 20.

[11] G. Köhler, C. Milstein, *Nature* **1975**, *256*, 495 – 497.

[12] L. M. Nadler, P. Stashenko, R. Hardy, W. D. Kaplan, L. N. Button, D. W. Kufe, K. H. Antman, S. F. Schlossman, *Cancer Res.* **1980**, *40*, 3147-3154.

[13] T. J. Vaughan, J. K. Osbourn, P. R. Tempest, *Nat. Biotechnol.* **1998**, *16*, 535.

[14] Data taken from firstwordpharma.com (https://www.firstwordpharma.com/node/1132129)

[15] G. Casi, D. Neri, *J. Med. Chem* **2015**, *58*, 8751-8761.

[16] P. D. Senter, E. L. Sievers, *Nat. Biotechnol.* **2012**, *30*, 631.

[17] a) D. Hoelzer, *Curr. Opin. Oncol.* **2013**, *25*, 701-706; b) T. Nittoli, M. Kelly, F. Delfino, J. Rudge, A. Kunz, T. Markotan, J. Spink, Z. Chen, J. Shan, E. Navarro, *Biorg. Med. Chem.* **2018**, *26*, 2271-2279.

[18] N. Krall, J. Scheuermann, D. Neri, *Angew. Chem. Int. Ed.* **2013**, *52*, 1384-1402.

[19] P. A. Van Schouwenburg, G. M. Bartelds, M. H. Hart, L. Aarden, G. J. Wolbink and D. Wouters, *J. Immunol. Methods* **2010**, *362*, 82-88.

[20] M. De Graaf, E. Boven, D. Oosterhoff, I. Van der Meulen-Muileman, G. Huls, W. Gerritsen, H. Haisma, H. Pinedo, *Br. J. Cancer* **2002**, *86*, 811 – 818.

[21] A. Dal Corso, L. Pignataro, L. Belvisi, C. Gennari, *Curr. Top. Med. Chem.* **2016**, *16*, 314-329.

[22] a) I. R. Vlahov, H. K. R. Santhapuram, F. You, Y. Wang, P. J. Kleindl, S. J. Hahn, J. F. Vaughn, D. S. Reno, C. P. Leamon, *J. Org. Chem.* **2010**, *75*, 3685-3691; b) S. Ordanini, N. Varga, V. Porkolab, M. Thépaut, L. Belvisi, A. Bertaglia, A. Palmioli, A. Berzi, D. Trabattoni, M. Clerici, *Chem. Commun.* **2015**, *51*, 3816-3819

[23] a) R. Mahato, W. Tai and K. Cheng, *Adv. Drug Deliv. Rev.* **2011**, *63*, 659-670; b) P. López Rivas, I. Randelovic, A. Raposo Moreira Dias, A. Pinna, D. Arosio, J. Tóvári, G. Mező, A. Dal Corso, L. Pignataro, C. Gennari, *Eur. J. Org. Chem*. **2018**, 2902-2909 10.1002/ejoc.201800447.

[24] a) F. M. De Groot, W. J. Loos, R. Koekkoek, L. W. van Berkom, G. F. Busscher, A. E. Seelen, C. Albrecht, P. de Bruijn, H. W. Scheeren, *J. Org. Chem.* **2001**, *66*, 8815-8830; b) A. Alouane, R. Labruere, T. Le Saux, F. Schmidt and L. Jullien, *Angew. Chem. Int. Ed.* **2015**, *54*, 7492-7509.

[25] a) O. H. Aina, R. Liu, J. L. Sutcliffe, J. Marik, C.-X. Pan, K. S. Lam, *Mol. Pharm.* **2007**, *4*, 631-651; b) L. M. Mayr, D. Bojanic, *Curr. Opin. Pharmacol.* **2009**, *9*, 580-588.

[26] a) P. S. Low, W. A. Henne, D. D. Doorneweerd, *Acc. Chem. Res.* **2007**, *41*, 120-129; b) A. Gupta, C. D. Kaur, S. Saraf, S. Saraf, *J. Recept. Signal Transduct.* **2017**, *37*, 314-323.

[27] a) R. Morris, R. Joyrich, R. Naumann, N. Shah, A. Maurer, H. Strauss, J. Uszler, J. Symanowski, P. Ellis, W. Harb, *Ann. Oncol.* **2014**, *25*, 852-858; b) I. Vergote, C. P. Leamon, *Ther. Adv. Med. Oncol.* **2015**, *7*, 206-218; c) T. J. Herzog, E. Kutarska, M. Bidzinsk, J. Symanowski, B. Nguyen, R. A. Rangwala, R. W. Naumann, *Int. J. Gynecol. Cancer* **2016**, *26*, 1580-1585.

[28] a) M. M. Dcona, J. E. Sheldon, D. Mitra, M. C. Hartman, *Bioorg. Med. Chem. Lett.* **2017**, *27*, 466-469; b) S. a. Krajčovičová, T. s. Gucký, D. Hendrychová, V. r. Kryštof, M. Soural, *J. Org. Chem.* **2017**, *82*, 13530-13541; c) C. P. Leamon, J. A. Reddy, I. R. Vlahov, R. Dorton, A. Bloomfield, M. Vetzel, P. J. Klein, E. Westrick, L.-c. Xu, Y. Wang, *Cancer Chemother. Pharmacol.* **2017**, *79*, 1151-1160; d) L. Shan, X. Zhuo, F. Zhang, Y. Dai, G. Zhu, B. C. Yung, W. Fan, K. Zhai, O. Jacobson and D. O. Kiesewetter, *Theranostics* **2018**, *8*, 2018-2030.

[29] a) S. Maiti, N. Park, J. H. Han, H. M. Jeon, J. H. Lee, S. Bhuniya, C. Kang, J. S. Kim, *J. Am. Chem. Soc.* **2013**, *135*, 4567-4572; b) A. Pettenuzzo, R. Pigot, L. Ronconi, *Eur. J. Inorg. Chem.* **2017**, *2017*, 1625-1638.

[30] M. Volante, R. Rosas, E. Allia, R. Granata, A. Baragli, G. Muccioli, M. Papotti, *Mol. Cell. Endocrinol.* **2008**, *286*, 219-229.

[31] A. Höög, M. Kjellman, P. Mattsson, C. C. Juhlin, I. Shabo, *Clin. Genitourin. Cancer* **2018**.

[32] a) C. Kwok, O. Treeck, S. Buchholz, S. Seitz, O. Ortmann, J. Engel, *Target. Oncol.* **2015**, *10*, 365-373; b) C. Gründker, G. Emons, *Front. Endocrinol. (Lausanne)* **2017**, *8*, 187.

[33] a) C. Wang, Y. Ma, S. Feng, K. Liu, N. Zhou, *J. Pept. Sci.* **2015**, *21*, 569-576; b) M. Huo, Q. Zhu, Q. Wu, T. Yin, L. Wang, L. Yin, J. Zhou, *J. Pharm. Sci.* **2015**, *104*, 2018-2028.

[34] a) S. Dharap, B. Qiu, G. Williams, P. Sinko, S. Stein, T. Minko, *J. Controlled Release* **2003**, *91*, 61-73; b) B. Redko, E. Ragozin, B. Andreii, T. Helena, A. Amnon, S. Z. Talia, O. H. Mor, K. Genady, G. Gary, *Peptide Science* **2015**, *104*, 743-752.

[35] a) B. Kapuvári, R. Hegedüs, Á. Schulcz, M. Manea, J. Tóvári, A. Gacs, B. Vincze and G. Mező, *Invest. New Drugs* **2016**, *34*, 416-423; b) S. Schuster, B. Biri-Kovács, B. Szeder, V. Farkas, L. Buday, Z. Szabó, G. Halmos and G. Mező, *Beilstein J. Org. Chem.* **2018**, *14*, 756-771.

[36] a) S. Westphalen, G. Kotulla, F. Kaiser, W. Krauss, G. Werning, H. P. Elsasser, A. Nagy, K.-D. Schulz, C. Grundker, A. V. Schally, *Int. J. Oncol.* **2000**, *17*, 1063-1072; b) C. Gründker, P. Völker, F. Griesinger, A. Ramaswamy, A. Nagy, A. V. Schally, G. Emons, *Am. J. Obstet. Gynecol.* **2002**, *187*, 528-537; c) G. Emons, M. Kaufmann, G. Gorchev, V. Tsekova, C. Gründker, A. R. Günthert, L. C. Hanker, M. Velikova, H. Sindermann, J. Engel, *Gynecol. Oncol.* **2010**, *119*, 457-461; d) G. Emons, G. Gorchev, P. Harter, P. Wimberger, A. Stähle, L. Hanker, F. Hilpert, M. W. Beckmann, P. Dall, C. Gründker, *Int. J. Gynecol. Cancer* **2014**, *24*, 260 - 265; e) G. Emons, G. Gorchev, J. Sehouli, P. Wimberger, A. Stähle, L. Hanker, F. Hilpert, H. Sindermann, C. Gründker, P. Harter, *Gynecol. Oncol.* **2014**, *133*, 427-432.

[37] M. Ginj, H. Zhang, B. Waser, R. Cescato, D. Wild, X. Wang, J. Erchegyi, J. Rivier, H. R. Mäcke, *PNAS* **2006**, *103*, 16436-16441.

[38] H. R. Maecke, J. C. Reubi, *J. Nucl. Med.* **2011**, *52*, 841-844.

[39] a) A. Ghosh and W. D. Heston, *J. Cell. Biochem.* **2004**, *91*, 528-539; b) M. Kasoha, C. Unger, E.-F. Solomayer, R. M. Bohle, C. Zaharia, F. Khreich, S. Wagenpfeil and I. Juhasz-Böss, *Clin. Exp. Metastasis* **2017**, *34*, 479-490.

[40] a) F. Nan, T. Bzdega, S. Pshenichkin, J. T. Wroblewski, B. Wroblewska, J. H. Neale, A. P. Kozikowski, *J. Med. Chem.* **2000**, *43*, 772-774.; b) A. P. Kozikowski, F. Nan, P. Conti, J. Zhang, E. Ramadan, T. Bzdega, B. Wroblewska, J. H. Neale, S. Pshenichkin, J. T. Wroblewski, *J. Med. Chem.* **2001**, *44*, 298-301.

[41] a) S. A. Kularatne, K. Wang, H.-K. R. Santhapuram and P. S. Low, *Mol. Pharm.* **2009**, *6*, 780-789; b) S. A. Kularatne, Z. Zhou, J. Yang, C. B. Post and P. S. Low, *Mol. Pharm.* **2009**, *6*, 790-800.

[42] Q. Lv, J. Yang, R. Zhang, Z. Yang, Z. Yang, Y. Wang, Y. Xu, Z. He, *Mol. Pharm.* **2018**, *15*, 1842 – 1852.

[43] J. Roy, T. X. Nguyen, A. K. Kanduluru, C. Venkatesh, W. Lv, P. N. Reddy, P. S. Low and M. Cushman, *J. Med. Chem.* **2015**, *58*, 3094-3103.

[44] a) M. Wichert, N. Krall, *Curr. Opin. Chem. Biol.* **2015**, *26*, 48-54; b) M. Y. Mboge, B. P. Mahon, R. McKenna, S. C. Frost, *Metabolites* **2018**, *8*, 19; c) C. T. Supuran, V. Alterio, A. Di Fiore, K. D'Ambrosio, F. Carta, S. M. Monti, G. De Simone, *Med. Res. Rev.* **2018**, 1-38 https://doi.org/10.1002/med.21497

[45] The clinical trials can be followed here: a) SLC-0111: https://clinicaltrials.gov/ct2/show/study/NCT02215850; b) RENCAREX®: https://clinicaltrials.gov/ct2/show/NCT00087022

[46] N. Krall, F. Pretto, W. Decurtins, G. J. Bernardes, C. T. Supuran, D. Neri, *Angew. Chem. Int. Ed.* **2014**, *53*, 4231-4235.

[47] a) P.-C. Lv, J. Roy, K. S. Putt, P. S. Low, *Mol. Cancer Ther.* **2017**, *16*, 453-460; b) S. Cazzamalli, A. Dal Corso, F. Widmayer and D. Neri, *J. Am. Chem. Soc.* **2018**, *140*, 1617-1621.

[48] D. Matsuoka, H. Watanabe, Y. Shimizu, H. Kimura, M. Ono and H. Saji, *Bioorg. Med. Chem. Lett.* **2017**, *27*, 4876-4880.

[49] a) K.-C. Chen, K. Schmuck, L. F. Tietze, S. R. Roffler, *Mol. Pharm.* **2013**, *10*, 1773-1782; b) P. J. Burke, J. Z. Hamilton, T. A. Pires, J. R. Setter, J. H. Hunter, J. H. Cochran, A. B. Waight, K. A. Gordon, B. E. Toki and K. K. Emmerton, *Mol. Cancer Ther.* **2016**, *15*, 938-945; c) P. J. Burke, J. Z. Hamilton, S. C. Jeffrey, J. H. Hunter, S. O. Doronina, N. M. Okeley, J. B. Miyamoto, M. E. Anderson, I. J. Stone, M. L. Ulrich, *Mol. Cancer Ther.* **2017**, *16*, 116-123.

[50] A. Dal Corso, M. Caruso, L. Belvisi, D. Arosio, U. Piarulli, C. Albanese, F. Gasparri, A. Marsiglio, F. Sola, S. Troiani, B. Valsasina, L. Pignataro, D. Donati, C. Gennari, *Chem. Eur. J.* **2015**, *21*, 6921-6929

[51] a) E. Orbán, G. Mező, P. Schlage, G. Csík, Ž. Kulić, P. Ansorge, E. Fellinger, H. M. Möller, M. Manea, *Amino Acids* **2011**, *41*, 469-483; b) P. Zhang, A. G. Cheetham, L. Lin Lock, H. Cui, *Bioconjugate Chem*. **2013**, *24*, 604-613; c) C. Zhang, D. Pan, K. Luo, N. Li, C. Guo, X. Zheng, Z. Gu, *Polym. Chem.* **2014**, *5*, 5227 - 5235; d) I. Szabó, S. Bősze, E. Orbán, É. Sipos, G. Halmos, M. Kovács, G. Mező *J. Pept. Sci.* **2015**, *21*, 426-435.

[52] a) K. M. Bajjuri, Y. Liu, C. Liu, S. C. Sinha, *ChemMedChem* **2011**, *6*, 54-59; b) Y. Liu, K. M. Bajjuri, C. Liu, S. C. Sinha, *Mol. Pharm.* **2011**, *9*, 168-175.

[53] R. Yamada, M. B. Kostova, R. K. Anchoori, S. Xu, N. Neamati, S. Khan, *Cancer Biol. Ther.* **2010**, *9*, 192-203.

[54] Y. Chau, F. E. Tan, R. Langer, *Bioconjugate Chem.* **2004**, *15*, 931-941.

[55] F. Li, K. K. Emmerton, M. Jonas, X. Zhang, J. B. Miyamoto, J. R. Setter, N. D. Nicholas, N. M. Okeley, R. P. Lyon, D. R. Benjamin, *Cancer Res.* **2016**, *76*, 2710-2719.

[56] a) J. S. Desgrosellier, D. A. Cheresh, *Nat. Rev. Cancer* **2010**, *10*, 9. b) F. Danhier, A. Le Breton, V. r. Préat, *Mol. Pharm.* **2012**, *9*, 2961-2973.

[57] W. Guo and F. G. Giancotti, *Nat. Rev. Mol. Cell Biol.* **2004**, *5*, 816 - 826.

[58] M. Barczyk, A. I. Bolstad and D. Gullberg, *Periodontol. 2000* **2013**, *63*, 29-47.

[59] N. De Franceschi, H. Hamidi, J. Alanko, P. Sahgal and J. Ivaska, *J. Cell Sci.* **2015**, *128*, 839-852.

[60] M.-Y. Hsu, D.-T. Shih, F. E. Meier, P. Van Belle, J.-Y. Hsu, D. E. Elder, C. A. Buck and M. Herlyn, *Am. J. Pathol.* **1998**, *153*, 1435-1442.

[61] a) M. D. Pierschbacher, E. Ruoslahti, *Nature*, **1984**, *309*, 30-33; b) E. Ruoslahti, M. D. Pierschbacher, *Science*, **1987**, *238*, 491-497

[62] a) M. Aumailley, M. Gurrath, G. Müller, J. Calvete, R. Timpl, H. Kessler. *FEBS Lett.* **1991**, *291*, 50-54; b) R. S. McDowell, T. R. Gadek. *J. Am. Chem. Soc.* **1992**, *114*, 9245-9253; c) R. Pasqualini, E. Koivunen, E. Ruoslahti, *Nat. Biotech.* **1997**, *15*, 542-546.

[63] Gottschalk, K. E.; Kessler, H. *Angew. Chem. Int. Ed.* **2002**, *41*, 3767; *Angew. Chem.* **2002**, *114*, 3919 - 3774.

[64] Xiong, J. -P.; Stehle, T.; Zhang, R.; Joachimiak, A.; Frech, M.; Goodman, S. L.; Arnaout, M. A *Science* **2002**, *296*, 151 - 155.

[65] a) K. E. Gottschalk, H. Kessler, *Angew. Chem. Int. Ed.* **2002**, *41*, 3767-3774; *Angew. Chem.* **2002**, *114*, 3919-3927; b) L. Auzzas, F. Zanardi, L. Battistini, P. Burreddu, P. Carta, G. Rassu, C. Curti, G. Casiraghi, *Curr. Med. Chem.* **2010**, *17*, 1255-1299; c) T. G. Kapp, F. Rechenmacher, S. Neubauer, O. V. Maltsev, E. A. Cavalcanti-Adam, R. Zarka, U. Reuning, J. Notni, H.-J. Wester, C. Mas-Moruno, J. Spatz, B. Geiger, H. Kessler, *Sci Rep.* **2017**, *7*, 39805; d) A. S. M. Ressurreição, A. Vidu, M. Civera, L. Belvisi, D. Potenza, L. Manzoni, S. Ongeri, C. Gennari, U. Piarulli, *Chem. Eur. J.* **2009**, *15*, 12184-12188; e) M. Marchini, M. Mingozzi, R. Colombo, I. Guzzetti, L. Belvisi, F. Vasile, D. Potenza, U. Piarulli, D. Arosio, C. Gennari, *Chem. Eur. J.* **2012**, 18, 6195-6207; f) S. Panzeri, S. Zanella, D. Arosio, L. Vahdati, A. Dal Corso, L. Pignataro, M. Paolillo, S. Schinelli, L. Belvisi, C. Gennari, U. Piarulli, *Chem. Eur. J.* **2015**, *21*, 6265-6271.

[66] C. C. Suna, X. J. Qua, Z. H. Gao. *Anticancer Drugs* **2014**, *25*, 1107-1121.

[67] a) Reynolds, A. R.; Hart, I. R.; Watson, A. R.; Welti, J. C.; Silva, R. G.; Robinson, S. D.; Da Violante, G.; Gourlaouen, M.; Salih, M.; Jones, M. C.; Jones, D. T.; Saunders, G.; Kostourou, V.; Perron-Sierra, F.; Norman, J. C.; Tucker, G. C.; Hodivala-Dilke, K. M. *Nat. Med.* **2009**, *15*, 392 - 400; b) Alghisi, G. C.; Ponsonnet, L.; Rüegg, C. *PLoS ONE* **2009**, *4*, e4449.

[68] a) A. J. Beer, R. Haubner, M. Goebel, S. Luderschmidt, M. E. Spilker, H.-J. Wester, W. A. Weber and M. Schwaiger, *J. Nucl. Med.* **2005**, *46*, 1333-1341; b) J. Shi, F. Wang and S. Liu, *Biophysics reports* **2016**, *2*, 1-20.

[69] M. Yoshimoto, K. Ogawa, K. Washiyama, N. Shikano, H. Mori, R. Amano, K. Kawai, *Int. J. Cancer* **2008**, *123*, 709-715.

[70] A. M. Mozid, M. Holstensson, T. Choudhury, S. Ben-Haim, R. Allie, J. Martin, A. J. Sinusas, B. F. Hutton and A. Mathur, *Nucl. Med. Commun.* **2014**, *35*, 839-848.

[71] P. Caswell, J. Norman, *Trends Cell Biol.* **2008**, *18*, 257-263.

[72] P. T. Caswell, S. Vadrevu, J. C., *Nat. Rev. Mol. Cell Biol.* **2009**, *10*, 843-853.

[73] W. Arap, R. Pasqualini, E. Ruoslahti, *Science* **1998**, *279*, 377-380.

[74] M. Pilkington-Miksa, D. Arosio, L. Battistini, L. Belvisi, M. De Matteo, F. Vasile, P. Burreddu, P. Carta, G. Rassu, P. Perego, *Bioconjugate Chem.* **2012**, *23*, 1610-1622.

[75] Y. Liu, K. M. Bajjuri, C. Liu, S. C. Sinha, *Mol. Pharm.* **2011**, *9*, 168-175.

[76] R. Fanelli, L. Schembri, U. Piarulli, M. Pinoli, E. Rasini, M. Paolillo, M. C. Galiazzo, M.

Cosentino, F. Marino, *Vasc. Cell* **2014**, *6*, 11.

[77] R. Colombo, M. Mingozzi, L. Belvisi, D. Arosio, U. Piarulli, N. Carenini, P. Perego, N. Zaffaroni, M. De Cesare, V. Castiglioni, E. Scanziani, C. Gennari, *J. Med. Chem.* **2012**, *55*, 10460-10474.

[78] a) A. Pina, A. Dal Corso, M. Caruso, L. Belvisi, D. Arosio, S. Zanella, F. Gasparri, C. Albanese, U. Cucchi, I. Fraietta, A. Marsiglio, L. Pignataro, D. Donati, C. Gennari, *ChemistrySelect* **2017**, *2*, 4759 – 4766.

[79] A. D. Wong, M. A. DeWit, E. R. Gillies, *Adv. Drug Deliv. Rev.* **2012**, *64*, 1031-1045.

[80] F. M. de Groot, L. W. van Berkom and H. W. Scheeren, *J. Med. Chem.* **2000**, *43*, 3093-3102.

[81] a) S. Ordanini, N. Varga, V. Porkolab, M. Thepaut, L. Belvisi, A. Bertaglia, A. Palmioli, A. Berzi, D. Trabattoni, M. Clerici, F. Fieschi, A. Bernardi, *Chem. Commun.* **2015**, *51*, 3816-3819; b) A. Raposo Moreira Dias, A. Pina, A. Dal Corso, D. Arosio, L. Belvisi, L. Pignataro, M. Caruso and C. Gennari, *Chem. Eur. J.* **2017**, *23*, 14410-14415; c) R. Böttger, D. Knappe, R. Hoffmann, *J. Controlled Release* **2018.** Doi: 10.1016/j.jconrel.2018.05.001

[82] A. Dal Pozzo, E. Esposito, M. Ni, L. Muzi, C. Pisano, F. Bucci, L. Vesci, M. Castorina and S. Penco, *Bioconjugate Chem.* **2010**, *21*, 1956-1967.

[83] P. Rejmanová, J. Pohl, M. Baudyš, V. Kostka and J. Kopeček, *Makromol Chem* **1983**, *184*, 2009-2020.

[84] V. Omelyanenko, C. Gentry, P. Kopečková and J. Kopeček, *Int. J. Cancer* **1998**, *75*, 600-608.

[85] Y.-J. Cheng, G.-F. Luo, J.-Y. Zhu, X.-D. Xu, X. Zeng, D.-B. Cheng, Y.-M. Li, Y. Wu, X.-Z. Zhang, R.-X. Zhuo, F. He, *ACS applied materials & interfaces* **2015**, *7*, 9078-9087.

[86] R. Haubner, R. Gratias, B. Diefenbach, S. L. Goodman, A. Jonczyk and H. Kessler, *J. Am. Chem. Soc.* **1996**, *118*, 7461-7472.

[87] Y. Meyer, J.-A. Richard, B. Delest, P. Noack, P.-Y. Renard and A. Romieu, *Org. Biomol. Chem.* **2010**, *8*, 1777-1780.

[88] a) S. L. Goodman, H. J. Grote, C. Wilm, *Biol. Open* **2012**, *1*, 329-340; b) N. V. Currier, S. E. Ackerman, J. R. Kintzing, R. Chen, M. F. Interrante, A. Steiner, A. K. Sato, J. R. Cochran, *Mol. Cancer Ther*. **2016**, *15*, 1291-1300.

[89] S. Block, R. Stephens, A. Barreto, W. Murrill, *Science* **1955**, *121*, 505-506.

[90] K. Matinkhoo, A. Pryyma, M. Todorovic, B. O. Patrick and D. M. Perrin, *J. Am. Chem. Soc.* **2018**. DOI: 10.1021/jacs.7b12698

[91] T. Wienland and H. Faulstich, *Experientia* **1991**, *47*, 1186-1193.

[92] J. Anderl, H. Echner and H. Faulstich, *Beilstein J. Org. Chem.* **2012**, *8*, 2072 - 2084.

[93] a) K. Letschert, H. Faulstich, D. Keller and D. Keppler, *Toxicol. Sci.* **2006**, *91*, 140-149;

[94] M. T. Davis, J. F. Preston, *Science* **1981**, *213*, 1385-1388.

[95] G. Moldenhauer, A. V. Salnikov, S. Lüttgau, I. Herr, J. Anderl and H. Faulstich, *J. Natl. Cancer Inst.* **2012**, *104*, 622-634.

[96] A. Moshnikova, V. Moshnikova, O. A. Andreev, Y. K. Reshetnyak, *Biochemistry* **2013**, *52*, 1171–1178.

[97] L. Zhao, J-P. May, A. Blanc, D-J. Dietrich, A. Loonchanta, K. Matinkhoo, A. Pryyma, D-M. Perrin, *ChemBioChem* **2015**, *16*, 1420-1425.

[98] a) A. S. M. da Ressurreição, A. Vidu, M. Civera, L. Belvisi, D. Potenza, L. Manzoni, S. Ongeri, C. Gennari and U. Piarulli, *Chem. Eur. J.* **2009**, *15*, 12184-12188; b) M. Marchini, M. Mingozzi, R. Colombo, I. Guzzetti, L. Belvisi, F. Vasile, D. Potenza, U. Piarulli, D. Arosio and C. Gennari, *Chem. Eur. J.* **2012**, *18*, 6195-6207; c) M. Mingozzi, A. Dal Corso, M. Marchini, I. Guzzetti, M. Civera, U. Piarulli, D. Arosio, L. Belvisi, D. Potenza and L. Pignataro, *Chem. Eur. J.* **2013**, *19*, 3563-3567; d) S. Panzeri, S. Zanella, D. Arosio, L. Vahdati, A. Dal Corso, L. Pignataro, M. Paolillo, S. Schinelli, L. Belvisi and C. Gennari, *Chem. Eur. J.* **2015**, *21*, 6265-6271.

[99] a) T. Meyer, J. Marshall and I. Hart, *Br. J. Cancer* **1998**, *77*, 530 - 536; b) Z. Liu, Y. Yan, S. Liu, F. Wang and X. Chen, *Bioconjugate Chem.* **2009**, *20*, 1016-1025; c) T. Lautenschlaeger, J. Perry, D. Peereboom, B. Li, A. Ibrahim, A. Huebner, W. Meng, J. White and A. Chakravarti, *Radiation oncology* **2013**, *8*, 246; d) K. C. Kwon, H. K. Ko, J. Lee, E. J. Lee, K. Kim and J. Lee, *Small* **2016**, *12*, 4241-4253.

[100] a) S. Y. Bai, N. Xu, C. Chen, Y. l. Song, J. Hu, C. X. Bai, *Clin. Respir. J.* **2015**, *9*, 457-467.

[101] a) T. G. Kapp, F. Rechenmacher, S. Neubauer, O. V. Maltsev, E. A. Cavalcanti-Adam, R. Zarka, U. Reuning, J. Notni, H.-J. Wester, C. Mas-Moruno, *Sci. Rep.* **2017**, *7*, 39805; b) M. Civera, D. Arosio, F. Bonato, L. Manzoni, L. Pignataro, S. Zanella, C. Gennari, U. Piarulli, L. Belvisi, *Cancers* **2017**, *9*, 128.

[102] a) A. H. Staudacher, M. P. Brown, *Br. J. Cancer* **2017**, *117*, 1736 - 1742; b) R. Raavé, T. H. van Kuppevelt, W. F. Daamen, *J. Controlled Release* **2018**, *274*, 1-8.

[103] G. Casi, D. Neri, *Mol. Pharm.* **2015**, *12*, 1880-1884.

[104] J. L. Crisp, E. N. Savariar, H. L. Glasgow, L. G. Ellies, M. A. Whitney and R. Y. Tsien, *Mol. Cancer Ther.* **2014**, *13*, 1514-1525.

[105] Y.-h. Yang, H. Aloysius, D. Inoyama, Y. Chen, L.-q. Hu, *Acta Pharm. Sin. B* **2011**, *1*, 143-159

[106] A. H. Said, J.-P. Raufman, G. Xie, *Cancers (Basel)* **2014**, *6*, 366-375.

[107] a) Y. Chau, F. E. Tan, R. Langer, *Bioconjugate Chem.* **2004**, *15*, 931-941; b) R. Yamada, M. B. Kostova, R. K. Anchoori, S. Xu, N. Neamati, S. Khan, *Cancer Biol. Ther.* **2010**, *9*, 192-203.

[108] P. C. Brooks, S. Strömblad, L. C. Sanders, T. L. von Schalscha, R. T. Aimes, W. G. Stetler-Stevenson, J. P. Quigley, D. A. Cheresh, *Cell* **1996**, *85*, 683-693.

[109] a) P. C. Baciu, E. A. Suleiman, E. I. Deryugina, A. Y. Strongin, *Exp. Cell Res.* **2003**, *291*, 167-175; b) R. E. Nisato, G. Hosseini, C. Sirrenberg, G. S. Butler, T. Crabbe, A. J. Docherty, M. Wiesner, G. Murphy, C. M. Overall, S. L. Goodman, *Cancer Res.* **2005**, *65*, 9377-9387. c)H. Sil, A. Chatterjee, *J. Cancer Ther.* **2015**, *6*, 793.

[110] a) E. I. Chen, S. J. Kridel, E. W. Howard, W. Li, A. Godzik, J. W. Smith, *J. Biol. Chem.* **2002**, *277*, 4485-4491; b) A. Suarato, F. Angelucci, M.Caruso, A. Scolaro, D. Volpi, M. Zamai, Polymeric conjugates of antitumor agents. WO Patent WO2002007770A2, January 31, 2002.

[111] a) N. Li, C. Guo, Z. Duan, L. Yu, K. Luo, J. Lu, Z. Gu, *J. Mater. Chem. B* **2016**, *4*, 3760-3769; b) D. Guarnieri, M. Biondi, H. Yu, V. Belli, A. P. Falanga, M. Cantisani, S. Galdiero, P. A. Netti, *Biotechnol. Bioeng.* **2015**, *112*, 601-611; c) X. Zhao, S. Zhou, D. Wang, W. He, J. Li, S. Zhang, *Int. J. Clin. Exp. Med.* **2016**, *9*, 13584-13594; d) C. Huang, X. Yi, D. Kong, L. Chen, G. Min, *Oncotarget* **2016**, *7*, 52230 - 52238.

[112] a) S. Netzel-Arnett, Q. X. Sang, W. G. Moore, M. Navre, H. Birkedal-Hansen, H. E. Van Wart, *Biochemistry* **1993**, *32*, 6427-6432; b) T. Xia, K. Akers, A. Z. Eisen and J. L. Seltzer, *Biochim. Biophys. Acta* **1996**, *1293*, 259-266.

[113] a) Z.-H. Peng, J. i. Kopeček, *J. Am. Chem. Soc.* **2015**, *137*, 6726-6729; b) L. Shi, Y. Hu, A. Lin, C. Ma, C. Zhang, Y. Su, L. Zhou, Y. Niu, X. Zhu, *Bioconjugate Chem.* **2016**, *27*, 2943-2953; c) N.-Q. Shi, X.-R. Qi, *ACS Appl. Mater. Interfaces* **2017**, *9*, 10519-10529.

[114] a) G. Y. Lee, K. Park, S. Y. Kim, Y. Byun, *Eur. J. Pharm. Biopharm.* **2007**, *67*, 646-654; b) P. Kele, G. Mezö, D. Achatz and O. S. Wolfbeis, *Angew. Chem. Int. Ed.* **2009**, *48*, 344-347.; c) W. Ke, J. Li, K. Zhao, Z. Zha, Y. Han, Y. Wang, W. Yin, P. Zhang, Z. Ge, *Biomacromolecules* **2016**, *17*, 3268-3276.

[115] a) C. Bremer, C.-H. Tung, R. Weissleder, *Nat. Med.* **2001**, *7*, 743 - 748.

[116] a) J. Kalia, R. T. Raines, *Angew. Chem.* **2008**, *120*, 7633-7636; b) S. Schuster, B. Biri-Kovács, B. Szeder, V. Farkas, L. Buday, Z. Szabó, G. Halmos, G. Mező, *Beilstein J. Org. Chem.* **2018**, *14*, 756 - 771.

[117] a) D. Weyel, H. Sedlacek, R. Müller, S. Brüsselbach, *Gene Ther.* **2000**, *7*, 224 - 231; b) K.-C. Chen, K. Schmuck, L. F. Tietze, S. R. Roffler, *Mol. Pharm.* **2013**, *10*, 1773-1782.

[118] a) B. Sperker, J. T. Backman, H. K. Kroemer, *Clin. Pharmacokinet.* **1997**, *33*, 18-31; b) Q. Shi, G. Haenen, L. Maas, V. Arlt, D. Spina, Y. R. Vasquez, E. Moonen, C. Veith, F. Van Schooten, R. Godschalk, *Arch. Toxicol.* **2016**, *90*, 2261-2273.

[119] M. d. Graaf, E. Boven, H. W. Scheeren, H. J. Haisma, H. M. Pinedo, *Curr. Pharm. Des.* **2002**, *8*, 1391-1403.

[120] a) E. Bakina, Z. Wu, M. Rosenblum, D. Farquhar, *J. Med. Chem.* **1997**, *40*, 4013-4018; b) A. Kamal, V. Tekumalla, P. Raju, V. Naidu, P. V. Diwan, R. Sistla, *Bioorg. Med. Chem. Lett.* **2008**, *18*, 3769-3773; c) Y.-L. Leu, C.-S. Chen, Y.-J. Wu, J.-W. Chern, *J. Med. Chem.* **2008**, *51*, 1740-1746; d) Y. Gu, G. J. Atwell, W. R. Wilson, *Drug Metab. and Dispos.* **2010**, *38*, 498-508.

[121] a) Y. Jin, X. Tian, L. Jin, Y. Cui, T. Liu, Z. Yu, X. Huo, J. Cui, C. Sun, C. Wang, *Anal. Chem.* **2018**, *90*, 3276-3283; b) V. Herceg, S. Adriouach, K. Janikowska, E. Allémann, N. Lange, A. Babič, *Bioorg. Chem.* **2018**, *78*, 372-380.

[122] S. C. Jeffrey, J. De Brabander, J. Miyamoto, P. D. Senter, *ACS Med. Chem. Lett.* **2010**, *1*, 277-280.

[123] B. Renoux, T. Legigan, S. Bensalma, C. Chadéneau, J.-M. Muller, S. Papot, *Org. Biomol. Chem.* **2011**, *9*, 8459-8464.

[124] a) S. C. Jeffrey, J. B. Andreyka, S. X. Bernhardt, K. M. Kissler, T. Kline, J. S. Lenox, R. F. Moser, M. T. Nguyen, N. M. Okeley, I. J. Stone, *Bioconjugate Chem.* **2006**, *17*, 831-840; b) Y. Z. Kim, Y. S. Oh, J. Chae, H. Y. Song, C.-W. Chung, Y. H. Park, H. J. Choi, K. E. Park, H. Kim, J. Kim, J. Y. Min, S. M. Kim, B. S. Lee, D. H. Woo, J. E. Jun, S. I. Lee, Conjugates comprising self-immolative groups and methods related threto, WO patent WO2017089890A1, June 1, 2017; c) P. J. Burke, J. Z. Hamilton, T. A. Pires, J. R. Setter, J. H. Hunter, J. H. Cochran, A. B. Waight, K. A. Gordon, B. E. Toki, K. K. Emmerton, *Mol. Cancer Ther.* **2016**, *15*, 938-945; d) R. V. Kolakowski, K. T. Haelsig, K. K. Emmerton, C. I. Leiske, J. B. Miyamoto, J. H. Cochran, R. P. Lyon, P. D. Senter and S. C. Jeffrey, *Angew. Chem.* **2016**, *128*, 8080-8083; e) P. J. Burke, J. Z. Hamilton, S. C. Jeffrey, J. H. Hunter, S. O. Doronina, N. M. Okeley, J. B. Miyamoto, M. E. Anderson, I. J. Stone and M. L. Ulrich, *Mol. Cancer Ther.* **2017**, *16*, 116-123.

[125] S. C. Jeffrey, M. T. Nguyen, R. F. Moser, D. L. Meyer, J. B. Miyamoto and P. D. Senter, *Bioorg. Med. Chem. Lett.* **2007**, *17*, 2278-2280.

[126] F. Castro, W. G. Dirks, S. Fähnrich, A. Hotz-Wagenblatt, M. Pawlita, M. Schmitt, *Int. J. Cancer* **2013**, *132*, 308–314.

[127] M. Schmitt, M. Pawlita, *Nucleic Acids Res.* **2009**, *37*, e119.

Acknowledgements

First of all, I would like to thank my supervisor, Prof. Cesare Gennari, for giving me the opportunity to join this interesting and multidisciplinary project, which has extensively contributed to my scientific education and has impacted so much into my development as a person.
I want to specially thank Dr. Luca Pignataro for all the support, patience and help during these three years and for finding always a bit of time to answer to all my questions, even if you were always busy.
I would like also to acknowledge Prof. Laura Belvisi, Prof. Umberto Piarulli and Dr. Daniela Arosio for their scientific contribution and their kindness during all this time.

I would like to mention to all the Magicbullet members (PIs), who gave good and useful advises during all the Network Meetings. I would like to particulary acknowledge Prof. Gábor Mező and Dr. Müller for their supervision during my secondments in ELTE (Budapest) and HDP, respectively.
Furthemore, I would like to warmly thank to all my colleagues of the Network, but specially to those which whom I spent more time and/or developed a deeper friendship: Francesca, Barbara, Lizeth and Clémence, thank you very much for so many good moments! Eduard, compañero de *"pailanismo"*, solo espero que poco a poco vayamos aprendiendo a ser un poquito menos tontos…jeje. Andrea, thank you very much for your support in Budapest, specially in the last period, which we both know that was one of the most complicated moments of my PhD...I would be always grateful for that! I would like to say my warmest and deepest thank you to my very good friends Ivan and his (our) beautiful and amazing Anna. You guys are two of the most wonderful, good and pure hearted people I have ever met, and I feel extremely lucky to count you between my friends. The doors of my home will be always open for you and I wish you the most exciting, happy and fulfilled life possible, you deserve it!

I would like to thank to all my colleagues of the lab (Gennari's group): in these three years I grew up with you both as a person as a scientist. You all had a beautiful impact in my life, even if we spent just a few months together. We shared a lot of desperation and joy moments and, for this reason, you will always have an important place in my memory! I would like to give specially mention to: Dennis and Marc (I missed you a lot!), Alberto (I find it very poetic that I started and finished my PhD with you...and thank you very much for the effort of correcting this thesis!), Arianna (it has not always been easy

between us, but I am happy that we were able to find an equilibrium!) and Simone Grosso (for all the affection and the beautiful words that you have dedicated me during the time in the lab and also after that).
Thank you very much to my colleague in the *"sufferings"* and ex-flatmate André. It was hard, but we made it! Thank you for making me laugh so much and don't forget: paper is paper and broken is cool. You will miss me, I'm sure :P
I would like to thank to the two people with whom I developed a stronger friendship in these three years: Mattia, thank you very much for all the support in many different bad moments! You are a really great and good-hearted person! I really consider you as a friend and I hope that you keep being as you are. I will miss you a lot...but I hope that we will manage to see each other every once in a while! Anyway, you know that you can always contact me by e-mail, hehe.
Serena, I'm sad that we found each other just in the last year of my PhD and that we were apart many months! I appreciate you a lot and I hope that everything will be great and that you also will visit me in Spain :)

I would like to thank also to the colleagues of the the corridor (Bernardi's group), for all the lunch times, coffees laughs, jokes and beautiful moments. Thank you very much to Laura for sharing the frustrating thesis writing period!

Me gustaría agradecer a Nuria, Adriana, Alberto F. Boo y su novia Antía, mis amigos "más antiguos", por tenerme siempre presente aún si vivimos a muchos kilómetros y hablamos solo de pascuas en ramos…

A mis amigos *"Compostelanos"* (sí, os voy a nombrar a todos, jeje): Didi, Cara, Meuge, Mariana, Meijo, Manu, Raquel, Víctor, Óscar. Ay queridos míos, que os voy a decir que no sepáis ya, si sois mi segunda familia. Con nuestros buenos momentos y nuestras peleas, como todas las familias! Compartiendo siempre lo bueno y, sobre todo, lo malo. Muchísimas gracias por estar ahí desde hace muchos años. Gracias por estar ahí a pesar de la distancia, gracias por estar ahí siempre. Vosotros mejor que nadie sabeis lo difíciles que han sido estos tres años, y teneros a vosotros cerca, aunque fuera a través de la pantalla del móvil, ha sido un regalo y una maravilla! Gracias por vuestro cariño a pesar de todo!

Por último, y de forma especial, me gustaría dar infinitas gracias a mi familia. Gracias a mi hermano David por todas las imágenes y publicaciones chorras que nos hemos

enviado durante todo este tiempo (jeje) y por no ir ningún domingo a misa, como yo! :) A veces nos cuesta llevarnos bien, pero al fin y al cabo…aquí me tienes para todo! Zaida, para la defensa de mi tesis prometo maquillarme ;P.

Quiero agradecer a mi tío Fran y su mujer Paula por todo el cariño demostrado desde siempre, pero de forma especial en los malos momentos, y por ser siempre un apoyo y hacer todo lo que está en vuestras manos por mí.

A mi madre…una tesis doctoral entera, llena de agradecimientos, no sería suficiente para darte las gracias. Eres la persona más generosa y comprensiva que existe, la forma en la que aceptas y apoyas las decisiones y los caminos que tomamos los demás me parece de una bondad infinita, fuera de lo común. Eres una personal realmente especial, admiro la forma en la que has podido afrontar la vida que te ha tocado sin perder nunca esa forma de hacer las cosas con cariño y sensibilidad. Muchísimas gracias por todo el amor y el apoyo incondicional, no solo durante estos tres años, sino siempre!

A meu pai, o "físico-albañil", unha das persoas máis especiais (no bo sentido) que coñezo. Gracias polas túas palabras, cheas de sabiduría e boas reflexións e polos bos consellos durante os malos momentos pasados aquí e durante as conversas por teléfono nesa época. Gracias tamén pola complicidade, sobre todo para darlle sorpreas a mamá! Gracias por ser un referente de honestidade e sinceridade, aínda que iso acarree moitas consecuencias negativas. Gracias tamén por inspirarme para estudiar unha carreira e, sobre todo, para estudiar unha carreira de ciencias. Dende logo, os xenes científicos que teño, son teus!

No quiero acabar estos agradecimientos sin mencionar con todo el cariño del mundo a mis abuelos, ejemplos de lucha, fuerza y superación hasta el final! ¡Va por vosotros!